Ligno cellulosic materials for energy storage

POLITECNICO DI TORINO

Materials Science and Technology

PhD Thesis

Ligno-cellulosic materials for energy storage

Supervisor

Roberta Bongiovanni

Candidate

Annalisa Chiappone

March 2012

Contents

Preface 1

CHAPTER I

LITHIUM BATTERIES 5

I.1. Introduction to the energy storage systems *5*

I.2 Lithium Batteries *7*

I.3 Lithium Batteries Materials *12*

I.3.1 Electrodes 12

I.3.1.1Anode 12

I.3.1.2 Cathode 16

I.3.2 Electrolytes 19

I.3.2.1 Liquid electrolytes 20

I.3.2.2 Ionic Liquids as electrolytes 23

I.3.2.3 Polymer electrolytes 24

I.4 UV radiation in Lithium batteries *33*

I.5 Cellulose and Paper in Li batteries *37*

SECTION A 43

I.A.1 Photopolymerisation process *43*

I.A.2 Photopolymerisation mechanism *47*

I.A.2.1 Radical photopolymerization 47

I.A.2.2 Cationic photopolymerization 49

I.A.3 Grafting for polymer surface modification *51*

SECTION B 55

I.B.1 Wood and fibers structures *55*

I.B.2 Cellulose *58*

I.B.3. Short fibers *59*

I.B.3.1 Whiskers 59

I.B.3.2 Microfibrils 60

I.B.4 Paper *61*

I.B.5 Cellulose modifications *66*

I.B.5.1 Radiation chemistry of cellulose 67

References *69*

CHAPTER II

COMPOSITE POLYMER ELECTROLYTES USING CELLULOSE MICROFIBRILS AS A REINFORCEMENT 87

SECTION A - MFC reinforced gel polymer electrolytes *89*

II.A.1. Materials and methods 89

II.A.2. Results 94

II.A.3.Conclusion 108

SECTION B - MFC reinforced solid polymer electrolytes *109*

II.B.1. Materials and methods 109

II.B.2 Results 111

II.B.3.Conclusion 120

References 122

CHAPTER III

TOWARDS FEASIBLE GEL-POLYMER ELECTROLYTES 124

III.1 Materials and methods 126

III.2. Results 138

2.1 GPCE synthesis and structure 139

2.2 GPCE electrochemical properties 152

2.4 Mechanical properties 159

2.5 Strategies for increasing the ionic conductivity 169

III.3. Conclusions 180

References 182

CHAPTER IV

IMPROVED GEL POLYMER-CELLULOSE ELECTROLYTES .....

New process of fabrication including polymer-cellulose bonding by UV-grafting methods 184

SECTION A

POLYMER-CELLULOSE BONDING: In situ grafting by Benzophenone..... 186

IV.A.1. Materials and methods 186

IV.A.2 Results 193

2.1 Synthesis of the membranes 193

2.2 Improving the GPE membrane by grafting 196

2.3 Improvement of the electrochemical behaviour using additives 203

2.4 Swelling procedure 209

VI.A.3 Conclusion 209

SECTION B

POLYMER-CELLULOSE BONDING: Two steps grafting by Benzophenone 211

IV.B.1. Materials and methods 212

VI.B.2. Results 214

2.1 Handsheets modification 214

2.2 Preparation of the membranes 220

2.3 Characterization of the GPEs 221

2.4 Swelling method 229

IV. B. 3. Conclusion 229

SECTION C

POLYMER-CELLULOSE BONDING: In situ grafting of Glycidyl Acrylate..... 230

VI.C.1. Materials and methods 230

VI.C.2. Results 233

2.1 Membrane preparation..... 233

2.2 Characterisation of the GPEs 239

2.3 Study on the grafting of GA 244

VI.C.3 Conclusion 255

References 256

Conclusions..... 258

APPENDIX A

COMPLETE RESULTS ON THE REFINING SERIES (Chapter III) 262

APPENDIX B

ELECTROCHEMICAL CELLS GLOSSARY..... 269

Acknowledgements.....272

Preface

The constantly increasing production of a large variety of portable consumer electronic devices and the urgent request of replacement of polluting, internal combustion cars with more efficient, controlled emissions vehicles, such as hybrid vehicles or, ideally, electric vehicles require the development of new reliable and safe power sources.

Furthermore the continuous decrease of the oil resources and the growing concern on the climate changes call, with constantly increasing urgency, for a larger use of green, alternative energy sources, such as solar and wind. But wind does not blow on command and the sun does not always shine thus, this discontinuity in operation leads to the need of suitable storage systems to efficiently run renewable energy plants.

It is evident that a new energy economy has to emerge, and it must be based on a cheap and sustainable energy supply. Lithium ion batteries, due to their high-energy efficiency, appear as ideal candidates for this purpose. Although these batteries are well established commercial products, further research and development is required to improve their performance to meet the market requirements. In particular, enhancement in safety, cost, and energy density are needed. A big portion of the R&D studies are nowadays devoted to the search for optimal materials both for the electrodes and the electrolyte of the battery: as far as the electrolyte is concerned, the main goal is to replace the liquid electrolyte with a solid one. The passage to a solid configuration gives concrete promise of increasing cell safety and reliability and, at the same time, of offering modularity in design and ease of handling.

Behind the optimization of existing batteries a big effort in this research field is the transformation of current batteries into a light, flexible, portable device. If integrated structures containing the three essential components (electrodes, spacer, and electrolyte) of the electrochemical cells can be made

mechanically flexible, it would enable these to be embedded into various functional devices in a wide range of innovative products such as smart cards, displays, and implantable medical devices.

In the fabrication of such a device the exploitation of cellulose as a flexible material and at the same time the exploitation of the papermaking and printing techniques for the development of paper electrodes and electrolytes and, in a future, of the full paper battery, is under consideration. This will open the way to a reinvestment of the paper technologies in a high tech field such as the Lithium based batteries.

Paper industry, as a matter of fact, is in Europe an important manufacturing industry but the economic change together with the development of electronics highly threaten the role and the surviving of such an activity. In this context grows the urgent need for higher value-added paper products and the conversion of the traditional paper industry, as well as its satellite industries, such as printing and converting. Introducing paper into new products with more profitable markets is crucial.

In this context the research work of the present thesis has been developed in collaboration with the "*Centre Technique du Papier* "(CTP) in Grenoble (Fr).

The work has been focused on the use of cellulose in the form of handsheet or microfibrils for the production of innovative electrolyte membranes to be used in Li-based batteries.

Two research lines have been followed:

1- Development of composite membranes based on cellulose microfibrils and a polymeric matrix obtained by photopolymerisation of reactive oligomers.
2- Development of multilayered membranes made of cellulose handsheet and polymeric layers obtained by photopolymerisation of reactive oligomers.

Both the research lines adopt the photopolymerisation process for developing the membranes. In particular using multifunctional monomers, highly cross-

linked polymer membranes are obtained which can be successfully used as gel or solid polymer electrolytes.

The process is well established in many industrial fields such as ink and coatings, optical and electronics being fast, low cost and versatile. In fact a fully cured polymer is obtained in seconds at room temperature irradiating a proper mixture of reactive molecules and photoinitiator. In view of preparing lithium batteries membranes, along with the reactive molecules, Li-salts and a proper solvent can be added. Alternatively the solid UV cured membranes can be swelled in a second step by the lithium salt solution.

The works developed will be described in this thesis starting from an introduction that gives the general information needed to follow the discussions.

Therefore the first chapter summarizes the state of the art in the domain of lithium batteries materials with a special interest toward the materials for the electrolyte.

After a short introduction on Lithium batteries, their development and functioning, the different components of a battery are presented and an explanation of the materials relevant to the Li-ion battery technology during recent years and for the next future is reviewed. The state of the art of the use of the UV curing technique for lithium batteries is reported followed by an overview of the cellulose-based materials and component currently used in the Lithium batteries field.

The chapter is then completed by two more sections: the first explains the fundamentals about the general photoreactions of the photo-polymerisation process. The second section gives basic information for the understanding of the paper and cellulose fibers characteristics, explaining their relation with the origin of the raw material and with the common industrial treatments.

The experimental activity is described in Chapters II, III and IV.

CHAPTER II demonstrates the possibility of producing gel and solid electrolytes based on polymeric composites obtained by photopolymerization and reinforced by cellulose microfibrils (MFC).

In CHAPTER III in view of adapting the paper technology of papermaking to high tech fabrication of flexible devices, cellulose handsheets have been used to obtain a multilayer membrane. Gel polymer salt-in electrolytes reinforced with the different papers have then been produced by impregnating the paper sheets with a rective oligomer mixture containing the Lithium salt and photopolymerizing it. The membranes were tested in terms of ionic conductivity and tensile resistance in order to understand the influence of the paper characteristics on the functioning of the electrolyte. Various handsheets have been prepared by varying the nature of the fibers or the treatments done on them and also by adding various kinds of filler.
In CHAPTER IV the activities were addressed to modify the process of fabrication described in Chapter III in order to introduce the Lithium salt in a separate production step. In fact manipulating Li solutions requires an inert atmosphere, total absence of water, therefore from an industrial point of view the production of the membranes first and then the salt addition in a dedicated step is clearly preferred. Introduction of the salt means the swelling of reinforced polymer membranes in a liquid electrolyte, and this process usually affects the adhesion between the polymer and the cellulose reinforcement. Therefore, for enabling the swelling procedure, the improvement of the interface between the polymer and the cellulose was attempted by introducing covalent bonds through different grafting processes.

In each chapter there is the description of the new materials and processes, the mechanical characteristics and the electrochemical performances. The thesis proposes a series of new electrolytes most of which show electrochemical performances similar or even superior to the present polymeric electrolytes described in the literature. Most of the UV cured membranes both containing MFC and handsheets assure also good mechanical resistance. The perspective of application in real is feasible and the development of fully flexible devices can follow.

CHAPTER I

LITHIUM BATTERIES

I.1. Introduction to the energy storage systems

Energy consumption and production that rely on the combustion of fossil fuels is forecast to have a severe future impact on world economics and ecology. The present economy based on this kind of fuel is already at a serious risk due to a series of factors, such as the continuous increase in the demand for oil, the depletion of non-renewable resources and the dependency on politically unstable oil producing countries. Another worrying problem linked to the present fossil fuel energy economy is associated with CO_2 emissions, which have increased at a constant rate, with a dramatic jump in the last 30 years, the CO_2 level has almost doubled passing from 1970 to 2005.[1]

Accordingly, investments for the exploitation of renewable energy resources are increasing worldwide, with particular attention to wind and solar power energy plants (REPs), which are the most mature technologies. The intermittence of these resources requires high efficiency energy storage systems. [2]

Electrochemical energy production and storage is under serious consideration as an alternative energy and power source, as long as this energy consumption is designed to be more sustainable and more environmentally friendly. Systems for electrochemical energy storage and conversion include batteries, fuel cells, and electrochemical capacitors (ECs). Although the

energy storage and conversion mechanisms are different, there are "electrochemical similarities" of these three systems.

A plot that compares the power and energy capabilities of the three systems (Figure 1) discloses that fuel cells can be considered to be high-energy systems, whereas supercapacitors are considered to be high-power systems.

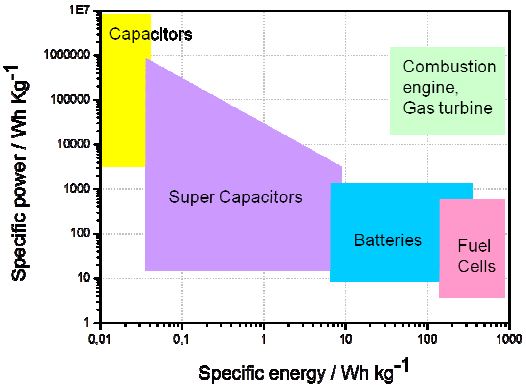

FigureI.1. Comparison in terms of specific power and specific energy of different energy storage system[3]

Batteries have intermediate power and energy characteristics. There is some overlap in energy and power of supercapacitors, or fuel cells, with batteries. Indeed, batteries with thin film electrodes exhibit power characteristics similar to those of supercapacitors. Figure 1 also shows that no single electrochemical power source can match the characteristics of the internal combustion engine.

In comparison to supercapacitors and fuel cells, batteries have found the most application markets and have now an established market position.[3]

Even if batteries are inherently simple in concept their development has progressed much more slowly than other areas of electronics. This is because of the lack of suitable electrode materials and electrolytes, together with difficulties in mastering the interfaces between them. All batteries are composed of two electrodes connected by an ionically conductive material called an electrolyte. The two electrodes have different chemical potentials, dictated by the chemistry that occurs at each. The amount of electrical energy per mass or volume that a battery can deliver is a function of the cell's voltage and capacity, which are dependent on the chemistry of the system.

Another important parameter is power, which depends partly on the battery's engineering but crucially on the chemicals the battery contains. Hundreds of electrochemical couples were proposed, the most notable primary battery being Zn–MnO_2, with lead–acid and Ni–Cd being the most common secondaries.(4)

The stored energy content of a battery can be maximized by having a large chemical potential difference between the two electrodes; by making the mass (or volume) of the reactants per exchanged electron as small as possible; by ensuring that the electrolyte is not consumed in the chemistry of the battery.

This final condition was not true for the three principal battery technologies developed in the twentieth century, but holds for the more recent Ni–MH and lithium-ion batteries. One of the key elements of these two batteries is that the same ion (H+ for Ni–MH and Li+ for lithium-ion batteries) participates at both electrodes, being reversibly inserted and extracted from the electrode material, with the concomitant addition or removal of electrons.(5)

I.2 Lithium Batteries

The concept of electrochemical cell has been spread at the end of the eighteenth century thanks to the works of Luigi Galvani and of Alessandro Volta.(6)

One of the first developed batteries was the engine proposed by the French engineer Georges-Lionel Leclanché in 1866, its battery was based on a zinc rod negative electrode (anode) and a manganese oxide–carbon mixture as positive electrode (cathode) immersed in an aqueous ammonium chloride solution. It is interesting to notice that the Leclanché cell concept is still exploited in the consumer primary batteries commonly known as carbon–zinc and alkaline cells which show innovations in the materials but the same functioning principles developer 150 years ago.

In the same period other key steps in the battery evolution were marked by the French Scientist Gaston Plantè who in 1869 invented the lead–acid rechargeable battery and by the Swedish engineer Waldmar Jungner with the

discovery in 1901 of the rechargeable nickel–cadmium battery. These devices, even if improved by innovations in construction design and in materials packaging, are also the bases of today's commercial batteries, addressed to important applications, such as power supply for car ignition and for portable tools.

Since those years until 1960 the battery field has not seen much innovation being the devices previously developed sufficient to meet the requirements of at the time technology. In the late 1960s the situation drastically changed, the need of portable energy devices increased because of many factors such as the progress of the implantable medical devices, the request of high-energy and high-power sources for military purposes and the explosion of the consumer electronic market.

The need of new and higher performing devices was evident, the breakthrough arrived with the development of new concept batteries exploiting lithium as one of the electrode material.

Among the various existing technologies, lithium batteries are considered as the most competitive power source because of their high volumetric energy density and gravimetric energy density, superior power capability and design flexibility. Figure 2 shows the comparison of the volumetric and gravimetric energy density with other batteries.(7)

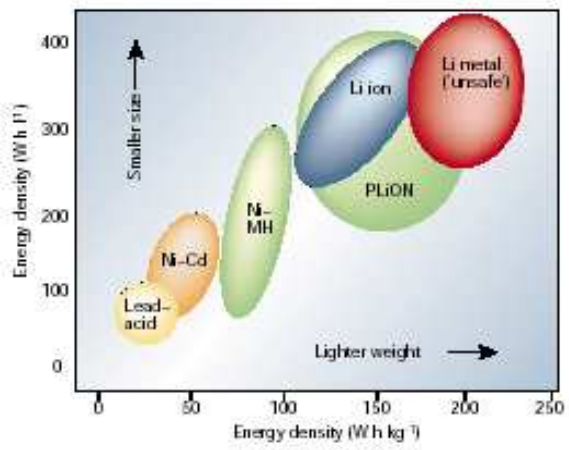

Figure I.2. Comparison of the volumetric and gravimetric energy density with other batteries(7)

This explains why they receive most attention at both fundamental and applied levels. The chances of finding a practical new battery system with a significant higher energy density in the next 10 years are extremely small. There is simply no such concept being presently studied at research level, as was the case for many years for rechargeable lithium battery. Lithium battery has however been in constant evolution since its beginning, and will continue to evolve. [8]

Due to its electrochemical equivalent, the highest among all metals, lithium can assure theoretical specific capacity much higher than zinc, i.e., 3,860 $Ahkg^{-1}$ versus 820 $Ahkg^{-1}$. Lithium metal is not compatible with water thus, its use required moving from the common aqueous electrolytes to more electrochemically stable organic electrolytes, generally formed by a solution of lithium salt in a carbonate organic solvent (e.g., propylene carbonate, ethylene carbonate) or in a mixture of them. [6]

Clearly, moving from zinc-based to a lithium-based battery, a considerable increase in energy density could be obtained. A battery combining a lithium metal anode with an iodine-based cathode (lithium–iodine battery)[9] was developed, it provided a practical energy density of about 250 Wh kg^{-1}, almost five times higher than that of the zinc–mercury oxide. The success of the lithium–iodine battery highlighted the potentiality of lithium and opened the route for the development of a series of new batteries meeting the requests of many different applications.

Considerable impulse to the lithium battery evolution was triggered by military demands for power sources characterized by high energy and, particularly high power. [6]

Another key driving force for lithium battery development in the 1970s was the diffusion of consumer electronics that brought into the market a series of popular devices such as electronic watches, toys, and cameras. These devices required batteries capable of providing a good powering operation with a small volume size and a contained price. In 1970 SANYO Inc. Commercialized the first lithium battery containing Li-MnO_2 as cathode and

lithium metal as anode fabricated in a coin-type cell version that well fitted into the device case [10]. This battery had a high potential of 3 V.

All the batteries fabricated in the initial stage of the lithium battery technology were of the primary type. The success of these batteries stimulated an obvious interest for moving to secondary, rechargeable systems.

Many cathode- active materials were studied. For example, already in 1985 rechargeable battery based on lithium metal anode and molybdenum sulphide cathode (Li insertion electrode) had been developed unfortunately this battery system was abandoned owing safety problems. Lithium batteries composed of a Li metal anode and a commonly used electrolyte showed the thermal runaway of the systems, which can lead to their explosion; this was almost inevitable in abuse cases such a short circuit, overheating and overcharging.

Even if batteries based on lithium metal were the most performing ones a solution to these safety issues needed to be found. To circumvent the problems surrounding the use of lithium metal principally two ways have been followed: modification of the negative electrode or modification of the electrolyte. [4]

The first approach involved substituting metallic lithium for new materials. Active compounds with good reversibility for the Li intercalation/deintercalation and low charge/discharge voltage were used as anode materials instead of Li metal. Extensive studies on carbon material were carried on and in 1991 a battery constituted by a carbon anode and $LiCoO_2$ (layered lithium cobalt oxide) cathode was mass-produced and commercialized by Sony Inc. This Li-ion battery was capable of high performances as well as high voltage of 4V. The Li-ion technology had started. [8]

The second approach involved replacing the liquid electrolyte by a polymer electrolyte, leading to the so called Li solid (or gel) polymer batteries. Polymer electrolytes were then studied for both Li metal an Li ion technologies.[7]

Electrodes and electrolytes developed since the birth of the lithium technology will be discussed in further chapters.

A typical lithium battery consists of two electrodes, one positive and one negative, and an electrolyte, as depicted in Figure 3 [7].

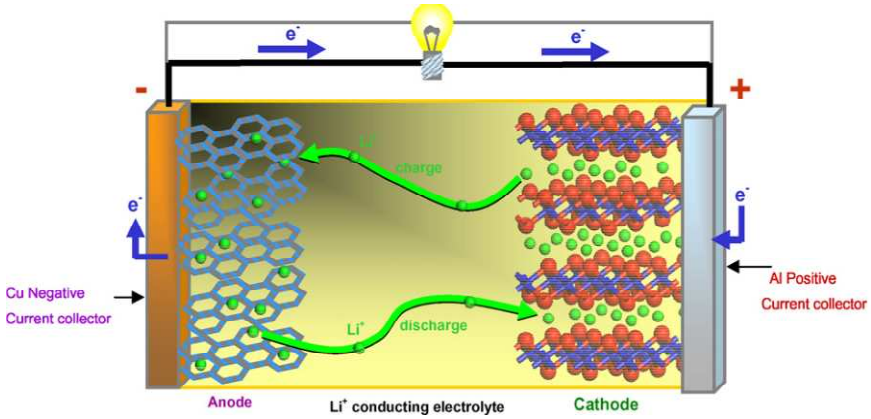

Figure I. 3. Schematic illustration of the discharge and charge processes of a lithium rechargeable battery[8]

Current collector foils, supporting the active electrode material, are also necessary. The porous electrodes contain the chemical compounds that react and produce current. Those are mixed electronic/ionic conductors and work like a host framework into which mobile ions (in this case lithium ions) may be reversibly inserted or extracted by electrochemical reaction. The electrolyte, in the case of liquid electrolytes, consists of a salt (e.g. $Li+PF_6$) dissociated in an organic mixture of cyclic (e.g. ethylene carbonate) and linear (e.g. dimethyl carbonate, diethyl carbonate, ethyl methyl carbonate) carbonates. Many organic solvents and all the aqueous ones, can not be used because their thermodynamic and/or potential windows of electrochemical stability are not wide enough.[11] Li salt can also be trapped in a dry or gel polymer matrix. The electrolyte has two main roles: it serves as the interconnecting media between the electrodes, transporting reacting species between the electrodes as an ionic current, and it keeps the electrodes from electrically short-circuiting.

During discharge, an oxidation reaction occurs at the negative electrode and a reduction reaction occurs at the positive electrode. A lithium ion diffuses to the surface of the active negative electrode, it electrochemically reacts and it

is transferred into the electrolyte. The lithium ion is then transported across the electrolyte and it electrochemically reacts at the surface of the active positive electrode and diffuses into the centre of this one. The charge compensating electrons flow through the external load in order to close the circuit. These series of steps are reversed during charging. An example of the reaction for the negative (assuming carbon-based) and positive electrode (assuming metal oxide-based) can be written as:

$$Li_yC_6 \longleftrightarrow yLi^+ + ye^- + C_6, \quad \text{and}$$
$$Li_xMO_2 + zLi^+ + ze^- \longleftrightarrow Li_x + zMO_2,$$

respectively. Essentially, the basic electrochemistry involves only the transfer of lithium cations between the two insertion electrodes, hence the name 'rocking chair' battery. [12]

I.3 Lithium Batteries Materials

I.3.1 Electrodes

I.3.1.1Anode

As mentioned before, lithium metal has been the first material to be used as an anode, primary cells using lithium metal were produced for more than two decades. Even if this material has extremely attracting characteristics, some operational faults, including fire incidents, led to the rapid conclusion that there were some problems linked to this kind of anode. Because of its very high reactivity, in fact, lithium metal easily reacts with the electrolyte with the formation of a passivation layer on its surface. The layer, usually called solid electrolyte interface (SEI)[4] is permeable to lithium ions, thus allowing the ongoing of the discharge process; however, after a prolonged deposition/dissolution cycling, irregularities on the SEI surface may lead to uneven lithium deposition with dendrite formation that eventually grew to

short the cell. In extreme cases, these uncontrolled events gave rise to overheating effects with thermal runaway and explosions. [6]

Research turned than on carbonaceous materials that could be used as "lithium sink" at the anode. Carbon forms small particles of graphitic layered structure and built highly porous agglomerates for those structures. Lithium ion can be intercalated, more or less, into most kinds of carbon; the resulting lithiated material shows extremely negative electrochemical potential which is comparable to the one of the lithium metal electrode. The reversible intercalation/deintercalation reaction overcome the problem of dendrite formation.[11] Usually the carbon anodes combined with non aqueous electrolytes and lithium-transition metal oxides (eg. $LiCO_2$) as cathode give a 4V class battery. [8] The idea of using insertion materials at both electrodes started the "rocking chair" batteries era.

Graphite has a relatively high specific capacity and good cylability that's why it has been the first and it is still now the most used material for the anode in commercially available Li-ion batteries. Electrochemical lithium intercalation properties of carbonaceous materials greatly depends on the crystallinity, morphology and orientation of crystallites. Many kinds of carbonaceous materials, from crystalline to strongly disordered carbon, have been testes over the past decades. [13]

The electrochemical performances of carbon negative electrodes improve continuously, a way to increase those performances is to modify carbon material both chemically (pyrolitic processing) or physically (mechanical milling). Reversible capacities of around 450 mAh g^{-1} are now being reached, compared with a practical value of 350 mA h g^{-1} for graphite (372 mA h g^{-1} for the end compound LiC_6). Many interesting studies have been developed also using Carbon Nano Tubes. [12]

In parallel, many alternative materials have also been studied in order to find possible anodes with both larger capacities and slightly more positive intercalation voltages compared to Li/Li+, hoping to minimize any risks of

high-surface-area lithium plating at the end of fast recharge, thing that could lead to safety problems.

Lithium transition-metal nitrides were between the most promising materials and, above all, $Li_{3-x}Co_xN$ but unfortunately its use is constrained by the restrictive manufacturing requirements for handling such moisture-sensitive negative electrodes. [14,15]

The use of composite negative electrodes has also been investigated. The basis behind this idea was the use of a 'buffer matrix' to compensate for the expansion of the reactants, so preserving the electrical pathway. Initially, such a buffer action was achieved by mixing two or more metals to form alloys that reacted at different potentials so that the electrochemically active phases were imbedded in a non-electrochemically active matrix.[16,17] In 1997 a new amorphous tin composite oxide (ATCO) was proposed with the new Li-ion device named STALION. This electrode reacts reversibly with Li at about 0.5 V, and has a specific capacity twice that of graphite. However, the STALION cell was never commercialized because it also had problems of cyclabilty and capacity loss during the first cycle. [18]

Other investigations [19] on the Sn–Fe–C system, have also revealed an interesting low-voltage reversible reactivity in composite materials developed as negative electrodes even if they presented initial irreversibility and short-lived capacities. In this case the cycling performance was improved at the expense of the electrode electrochemical capacity.

Li alloys (e.g. Li-Si and Li-Sn) have also been studied. Those alloys present good behaviour in terms of gravimetric capacity but they have problems in cycleability showing during tests disintegration and a loss of electrical contacts between particles. A partial solution of this problem can be the reduction of the size of alloy particles and the production of nanostructured materials that can increase the tolerance to stress cracking. [20]

Intermetallic alloys (eg. Cu_6Sn_5, InSb and Cu_2Sb) that show a strong structural relationship to their lithiated products, (Li_2CuSn and Li_3Sb for the Sn and Sb compounds), [21] partially solved the problem linked to alloy expansion. InSb and Cu_2Sb electrodes are particularly interesting because

they operate through a reversible process of lithium insertion and metal extrusion, with an invariant face-centred-cubic Sb array that gives a stable host frameworks to ions with low expansion in volume (4%). But even if those materials are interesting and fascinating, they still suffer from poor cyclability, particularly upon the initial cycle; nevertheless, the approach deserves further study. [7]

Subsequently, starting from the behavior of the transition-metal vanadates M–V–O[22] that has large capacity at low potential, the reactivity of Li-metal oxide was reinvestigated[23]. It was found a Li electrochemical activity for well known oxides, but these did not react with Li according to the classical processes of Li insertion–deinsertion or Li alloying.

For instance, MO-type compounds (where M is Co, Ni, Fe, Cu or Mn), having a rocksalt structure and containing metal elements (M) that do not alloy with Li, exhibited capacities two to three times those of carbon with 100% capacity retention for up to 100 cycles. The mechanism of Li reactivity differs from the classical Li insertion/deinsertion or Li-alloying processes, and involves the formation and decomposition of Li_2O, accompanying the reduction and oxidation of metal nanoparticles (in the range 1–5 nanometres) respectively. Remaining issues relate to a problem of surface, with the chemical reactivity being enhanced as the particle size becomes smaller.

Research for new anode materials is now addressed to titanium oxides. In this range of materials, anatase titanium oxide TiO_2 (TO) [24] and lithium titanium oxide, $Li_4Ti_5O_{12}$ (LTO) [25] are attractive negative electrodes for advanced lithium ion batteries. The lithium insertion potential of these oxides is between 1.2V and 2.0V vs. Li, i.e. within the stability window of common organic electrolytes. It has been observed that also the electrochemical performance of TO strongly depends on the particles' morphology; consequently, the research on this material is focused on fabrication process suitable to produce it in nanosized or nanotextured forms.

These findings open new avenues of research aimed at capitalizing on the beneficial effect that particle-size confinement could have within the field of

electrochemistry. These and related nanocluster systems under development hold much promises for future developments. [24, 5]

I.3.1.2 Cathode

The materials to be used as cathode in a lithium battery has to be chosen in function of the kind of battery: rechargeable Li metal or Li-ion devices. For rechargeable Li batteries that use Li-metal as the negative electrode, the positive electrode does not need to be lithiated before cell assembly. Instead, for Li-ion batteries using empty (no Li) carbon negative electrodes, the positive one must act as a source of Li, which means that air-stable Li-based intercalation compounds are needed. [7, 26]

Almost all of the research and commercialization of cathode materials has been developed on two classes of materials. The first contains layered compounds with an anion close-packed lattice in which alternate layers between the anion sheets are occupied by a redox-active transition metal and lithium then inserts itself into the essentially empty remaining layers. This structure is shown in Figure 4. This group is exemplified by first $LiTiS_2$, followed by $LiCoO_2$, $LiNi_{1-y}Co_yO_2$, and today $LiNi_yMn_yCo_{1-2y}O_2$. The spinels may be considered as a special case where the transition-metal cations are ordered in all the layers.

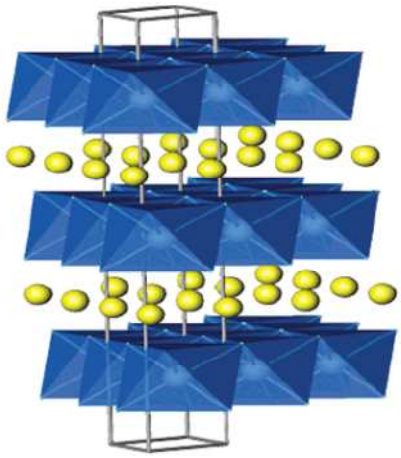

Figure I. 4. Layered structure of $LiTiS_2$, $LiVSe_2$, $LiCoO_2$, $LiNiO_2$, and $LiNi_yMn_yCo_{1-2y}O_2$, showing the lithium ions between the transition-metal oxide/sulfide sheets. The actual stacking of the metal oxide sheets depends on the transition metal and the anion[27]

The materials in the second group have more open structures, like many of the vanadium oxides, the tunnel compounds of manganese dioxide, and most recently the transition-metal phosphates, such as the olivine $LiFePO_4$.

The first group will have an inherent advantage in energy stored per unit of volume thanks to their compact lattice, but some in the second group, such as $LiFePO_4$, are potentially much lower cost. The following discussion will centre predominantly on these two classes of materials. [27]

Nowadays, although rechargeable Li-SPE (solid-polymer-electrolyte) cells mainly use Li-free V_2O_5 or its derivatives as the positive electrode, $LiCoO_4$ is most widely used in commercial Li-ion batteries, deintercalating and intercalating Li around 4 V. [7]

Goodenough in 1980[28] recognized that in $LiCoO_2$ the lithium could be easily removed electrochemically, thus making it a viable cathode material. $LiCoO_2$ presents the oxygen atoms in a cubic close-packed arrangement. On complete removal of the lithium, the oxygen layers rearrange themselves to give hexagonal close packing of the oxygen in CoO_2. Between these composition limits several phases are formed with varying degrees of distortion of the oxygen lattice [6].

Different spinel lithiated compounds were also studied (e.g. $Li_{0.5}CoO_2$[29], layered $LiNiO_2$[30]) but these have not been too developed for commercial applications for safety reasons.

To circumvent these safety and capacity issues it was tried to stabilize the layered structural framework of $LiCoO_2$ by an electrochemically inert di-, tri- or tetravalent cationic substitute for Ni or Co (Al, Ga, Mg or Ti)[31,27].

Another line of investigation has developed studies on layered $LiMnO_2$. These materials exhibit a capacity of 190 mA h g^{-1} (larger than that expected from the full oxidation of Mn3+ to Mn4+) with little capacity fading upon cycling, among the "$LiMO_2$ electrodes" the one using manganese as metal would be the most attractive for ecological and economical reasons; [32, 33] it presents lower capacity than $LiCoO_2$ but has an advantage in terms of cost and it is, non-toxic and from abundant material sources. Additionally, it has long been recognized as a potential alternative cathode, its implementation has been

delayed because of limited cycling and storage performances at elevated temperatures, although these hurdles were overcome recently by synthesizing dually substituted $LiMn_{2-x}Al_xO_{4-y}F_y$ spinel phases, and by altering their surface chemistry. [34]

Other alternative materials have been intensively studied; the olivine structure resulted to be one of the most promising and, as part of this intensive search, lithium iron phosphate ($LiFePO_4$) among all, turned out to be a possible candidate for the production of cathode for lithium rechargeable batteries. $LiFePO_4$ has become of great interest as storage cathode for rechargeable lithium batteries because of its high energy density, low raw materials cost, environmental friendliness, high thermal stability at fully charged state and safety than conventional materials. $LiFePO_4$ has a high lithium intercalation voltage (about 3.5 V relative to lithium metal), high theoretical capacity (170 mAh/g), ease of synthesis and stability when used with common organic electrolyte systems. [35]

Olivines are oxyanion scaffolded structures, built from corner-sharing MO_6 octahedra (where M is Fe, Ti, V or Nb) and XO_4^{n-1} tetrahedral anions (where X is S, P, As, Mo or W). Polyoxyanionic structures possess M–O–X bonds; altering the nature of X will change (through an inductive effect) the iono-covalent character of the M–O bonding[33]. With the use of the phosphate polyanions PO_4^{3-}, the Fe^{3+}/Fe^{2+} redox couples lie at higher potentials than in the oxide form.

Many efforts have been made to prepare this material since it was discovered that $LiFePO_4$ could be used as a cathode material in lithium secondary batteries. One of the main drawbacks observed during the development of this cathode was the poor electronic conductivity, and this limitation had to be overcome through various materials processing approaches, including the use of carbon coatings, mechanical grinding or mixing, and low-temperature synthesis routes to obtain tailored particles. [36, 37, 38]

Similar structures XO_4^{n-} entities (where X is Si, Ge) are now receiving renewed attention with respect to their electrochemical performance as electrode materials. [39]

Even if numerous classes of insertion–deinsertion materials were synthesized over the past 20 years, no real gain in capacity was achieved.

One possible way to achieve higher capacities is to design materials in which the metal-redox oxidation state can change reversibly by two units (M*n*+2/M*n*), while preserving the framework structure, and having molecular masses similar to those of the presently used 3*d* metal-layered oxides (for example, $LiCoO_2$). Inserting more than one Li ion per transition metal is feasible with a few V-based oxides. In principle, except for coordination number requirements, in effect, there is no obvious reason why this should not happen with other early transition metals. [6]

Another way to improve electrode capacities is to modify the morphology or texture of the electrode material to obtain porous and high-surface-area composite electrodes. In fact for example, V_2O_5 aerogels, which are mesoporous materials in which nanometre-sized domains are networked through a continuous, highly porous volume of free space, the interconnected porosity provides both molecular accessibility and rapid mass transport via diffusion, giving electroactive capacities up to 100% greater than polycrystalline non-porous V_2O_5 powders and superior power rate capabilities compared to usual powders[40] . Nanostructured materials, such as aerogels, create new opportunities not only at the applied level, but also at the fundamental level where some elementary questions, such as the exact mechanism governing these large capacities, remain unanswered.

I.3.2 Electrolytes

The electrolyte constitutes the third key component of a battery. The choice of the electrolyte is crucial for the battery behaviour, and it is based on criteria that differ depending on whether we are dealing with polymer or liquid-based Li-ion rechargeable batteries.

Working with a highly oxidizing (>4V versus Li/Li+) positive electrode material for Li-ion batteries requires electrolyte combinations that operate well outside their window of thermodynamic stability (3.5 V), this is the

reason why early workers in the field ignored very positive cathode materials. The electrolyte stability is kinetically controlled, enabling also the use of non-aqueous electrolytes at potentials as high as 5.5 V . Similarly, the use of a solid rather than a liquid electrolyte adds further selection criteria linked to the electrochemical stability of the solid, typically a polymer.[41-43]

Under the ideal conditions, the selected electrolyte, in addition of providing a high ionic conductivity, should also induce the creation the best morphology for the protecting film over the negative (carbon) anode and sustain the high operational voltage of the positive (lithium metal oxide) cathode.

I.3.2.1 Liquid electrolytes

The first electrolytes that has been used in the Li battery production is the solution of $LiPF_6$ in a propylene carbonate (PC)-diethyl carbonate (DEC) mixture[4]. Latest developments tend to exclude PC since this solvent induces exfoliation phenomena in the carbonaceous anodes, due to the intercalation of solvated lithium into the graphene layers, gas release in the carbon structure and large irreversible capacity. Most commonly $LiPF_6$ solutions in ethylene carbonate (EC)- dimethylcarbonate (DMC) have been used for the lithium ion battery commercial fabrication. These solutions have a high ionic conductivity (i.e. 10 mS cm^{-1}), a good electrochemical stability (extending to 5.1 V vs. Li) and they favour the formation of a dense and uniform film on the graphite electrode [42] as the ideal electrolyte should do.

In low molecular weight solvent used as conventional liquid electrolytes, solvation of lithium ions depends mainly on the number of molecules that may pack around a lithium ion. The most common solvents used in lithium batteries are summarized in the following table:

Solvent name and abbrev.	*Stuctural fomula*	*Melting point* (°C)	*Boiling point* (°C)	*Dielectric constant,* ε
Ethylene carbonate, **EC**	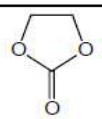	39-40	248	89.6 (40°C)
Propylene carbonate, **PC**	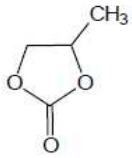	-49	240	64.4
Dimethyl carbonate, **DMC**	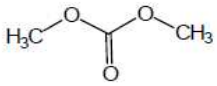	4.6	91	3.12
Diethyl carbonate, **DEC**	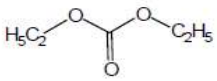	-43	126	2.82
2-Methyl-tetra hydrofuran, **2Me-THF**	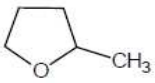	-137	79	6.29
Dimethoxy ethane, **DME**		-58	85	7.20
γ-Butyro lactone, **γ-BL**	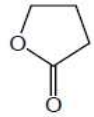	-43	204	39.1

Table I.1. Structure and properties of some solvents used for lithium battery electrolytes[44,45]

Different lithium salts, in alternative to $LiPF_6$ have also been studied in order to reduce the toxicity of the electrolyte; in general an ideal solute should possess the following minimal requirements:

1. It should be able to dissolve and dissociate in the non-aqueous media.
2. The solvated ions (lithium) should be able to move in the media with high mobility.
3. The anion should be inert to electrolyte solvents
4. Both cations and anions should be non-reactive towards the cell components such as separators, electrode substrate.
5. The anion should be non-toxic.

Because of the small ionic radius of the lithium ion, simple salts of lithium fail to meet the minimum solubility requirement in low dielectric media (e.g. LiCl, LiF).

The most used lithium salts are:

- Lithium perchlorate ($LiClO_4$) which has high ionic conductivity (9.0 $mScm^{-1}$ EC/DMC at 20°C) and high anodic stability (5.1V on a spinel cathode) but the high oxidation state of chlorine (VII) in perchlorate makes it strong oxidants and reacts violently with organic species at high temperature.

- Lithium tetrafluoroborate ($LiBF_4$) which is less toxic than many other salts, it has a higher safety than $LiClO_4$ and shows good performance not only above 50°C but also at low temperatures as well. Although BF^{4-} has highest mobility its dissociation constant is smaller than those of $LiAsF_6$ and $LiPF_6$.

- Lithium hexafluoroarsenate ($LiAsF_6$). It is stable up to 4.5V, and it has a long-term cycling, unfortunately $LiAsF_6$ is toxic and expensive.

-Lithium trifluoromethanesulfonate ($LiCF_3SO_6$) in which the acid strength is increased due to the stabilization of anions by the strongly electron-withdrawing groups. This salt is hermally stable, non-toxic and insensitive to moisture as compared with $LiPF_6$ and $LiBF_4$ however it offers low ionic conductivity in non-aqueous media.

- LiBETI and LiTFSI (LiIm) salts are novel acids based on an imide anion stabilized by two trifluoromethanesulfonyl (triflic) groups.

These LiIm were proved to be safe, thermally stable and highly conducting, LiBETI melts at 236°C without decomposition and does not decompose below 360 ° C. It can perform more than 1000 deep discharge with $LiNiO_2$ / petroleum coke as carbon. Despite these merits these salts have never been commercialized because it caused severe corrosion on aluminum current collector.

- Lithium hexafluorophosphate ($LiPF_6$). It has lower conductivity than $LiAsF_6$ and lower ionic mobility than LiIm, lower thermal stability and lower anodic stability than $LiAsF_6$ and $LiSbF_6$. In spite of these disadvantages it has been commercialized because of its multifaceted property. In fact even at room temperature, equilibrium exists:

$$LiPF_6\,(s) \leftrightarrow LiF(s)+PF_5(g)$$

P-F bond is labile towards the hydrolysis by even trace amounts of moisture in non-aqueous electrolytes. [43-46]

A liquid electrolyte needs a third component, a separator, that plays a key role, its main function is to keep the positive and negative electrodes apart and at the same time to allow rapid transport of ionic charge carriers (minimal ionic resistance).

A separator must have mechanical and dimensional stability and uniform thickness, it must be readily wetted by electrolyte and work as an electronic insulator.

In most of the batteries nonwoven fabrics or micro-porous polymer membranes are used. Nonwoven separators are textile products and are manufactured directly from fibers. [47]

Liquid electrolyte are still the most used in Li-ion batteries at a commercial level but many problems concerning safety and ecology are linked to their use; considerable effort is underway to improve the safety and reliability of the Li battery electrolytes, including: (i) additives to build-up stable SEI and/or enhance its thermal stability; (ii) redox shuttles to protect from overcharge, (iii) shut-down separators to prevent thermal runaway and (iv) search for the possible use at large scale of different lithium salts [2].

I.3.2.2 Ionic Liquids as electrolytes

Taking about electrolytes it is necessary to mention room temperature ionic liquids (RTIL) since they are nowadays gaining notoriety for their use as green solvents, a big portion of R&D is focusing on them and they are also finding wide application in electrolytes for electrochemical mechanical actuators, electrochromic windows and numerical displays with conducting polymers, dye-sensitized solar cells, light-emitting electrochemical cells and other devices. [48-55].

The works developed in this thesis do not involve the use of RTILs, therefore just a definition and a fast description of this kind of materials will be given in this pharagraph.

Common solutions of electrolytes are obtained by dissolution of salts in molecular solvents. Such systems consist of solvated ions, their charged or neutral combinations and solvent molecules. On the other hand, a salt may be melted down, or in other words 'liquified', by providing to the system a heat to counterbalance the salt lattice energy. Such a system, called molten salts or ionic liquid (IL), consists of ions and their combinations and is free of any molecular solvent. Relatively high melting points of many salts determine the temperature range of classical ionic liquids. These temperatures can be lowered by the addition of other salts forming a eutectic. Even in such a case considerable heat is necessary to maintain the system in the liquid state. On the other hand, salts having a low melting point are liquid at room temperature, or even below, and form the new class of liquids usually called room temperature ionic liquids (RTIL).[56]

Such a kind of material can be used as solvent for the production of electrolytes, batteries filled with this do not contain any volatile components and therefore, they are not flammable. Room temperature ionic liquids, being usually quaternary ammonium salts, are characterized by negligible vapour pressure, which makes them inflammable. In addition, they show a broad electrochemical stability window, generally >4 V, which is necessary for the application in lithium ion batteries with high energy cathodes. While the RTILs based on quaternary ammonium cations cannot be directly applied in any known type of primary or secondary batteries, it is possible to dissolve a lithium salt [Li+][X−] in ionic liquids [A+][X−], with the formation of a new "doped" ionic liquid [Li+]m[A+]n[X−]m+n, consisting of two cations and exploitable in lithium batteries[57, 58]. The doped ILs may then be incorporated into a flexible, thin membrane to form a battery electrolyte. [59]

I.3.2.3 Polymer electrolytes

The most recent development in the lithium ion battery technology is directed to the replacement of the liquid electrolyte with a polymer membrane capable of operating both as the separator and as the electrolyte, in order to produce

batteries having an overall polymer structure and to increase the safety of the systems. This is an appealing concept since it provides the prospect of a favourable combination of high energy and long life, which are typical of the lithium ion process, with reliability and easy processability, which are typical of the plastic configuration. [60]

Polymer electrolyte may generally be defined as a membrane that possesses transport properties comparable with that of common liquid ionic solutions. [61]

The study of polymer electrolytes has been extensively developed in the last decades as this kind of electrolyte finds applications not only in lithium batteries but also, in other electrochemical devices such as super capacitors and electrochromic devices, etc.

A polymer membrane has to be preferred to its liquid counter parts considering a series of advantages that it presents. These advantages include no internal shorting, leakage of electrolytes and non-combustible reaction products at the electrode surface existing in the liquid electrolytes. [13]

The requisites for a polymer electrolyte for lithium batteries are: high ionic conductivity at ambient and subambient temperatures, good mechanical strength, appreciable transference number, thermal and electrochemical stabilities, and better compatibility with electrodes. The polymer electrolyte should allow good cycle lives at low temperatures and must withstand the internal pressure build up during the battery operations.

In principle, it should be possible to form a polymer electrolyte battery by sandwiching the electrolyte between a lithium metal (or a composite carbon) anode and a composite cathode. [61]

The development of polymer electrolytes has gone through three stages (i) dry solid-state polymer, (ii) gel/plasticized polymer electrolyte systems, and (iii) polymer composites.

I.3.2.2.1 Solid polymer electrolytes

The very first example of “dry solid” polymer electrolyte is the poly(ethylene oxide) (PEO) based system [61]. This system does not possesses any organic

liquid and thus the polymer host is used as solid solvent for the lithium salt since heteroatoms (-O-) of polymer chains acting as electron donors are able to coordinate Li ions. In high molecular weight polymers, for the solvation, not only the DN is important but also the conformation of polymer chains. Lithium ions are more likely to be coordinated by heteroatoms on the same chain with the possibility of some coordination by neighbouring atoms; the chain must wrap around the lithium ions without excessive strain. Taking polyether as an example, it was found that $(–CH_2\text{-}CH_2\text{-}O)_n$ provides just the right space for maximum solvation and $(\text{-}CH_2\text{-}O)_n$ and $(\text{-}CH_2–CH_2\text{-}CH_2\text{-}O)_n$ are much weaker solvent. Accordingly PEO would be the most favourable basic units for polymer electrolytes and PEO chains would form a helix coil structure, in which lithium ions are solvated stably. From this point of view PEO based matrices have been the most used for polymer electrolytes [4].

Many studies were developed on ion mobility showing that it takes place principally in the amorphous phase of polymers and it is associated with local structural relaxations related to the glass transition. The ion transport is linked to the local segmental motion of the polymer in which the local environment remains liquid like for the lithium ion. [62]

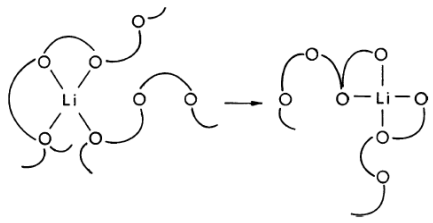

Figue I.5. Cartoon of ion motion in a polymer host [63]

The solid electrolytes commonly exhibit conductivities which range from 10^{-8} to 10^{-4} S cm^{-1} at temperatures between 40 and 100°C, which excludes practical applications at ambient temperature. This obstacle originates from, first, the high degree of crystallinity at room temperature in these complexes and, second, the low solubility of salt in the amorphous phase. [64]

Therefore many studies focused on suppression crystallisation and decrease of Tg of polymer chains were developed.

As first alternative PPO has been investigated since it was shown that it forms amorphous complexes with lithium salts; this has been the focus of a large number of studies [65, 66]. Some of the developed PPO-based electrolytes has higher ionic conductivity than PEO ones, but they cannot generate a high concentration of carrier ions around room temperature under a certain degree of lithium salt concentration. Thus the attempts to improve solid polymer electrolytes shifted to the suppressing the crystallisation of PEO-based electrolytes.

In order to reduce the crystallinity at room temperatures and hence the glass transition temperature new structures were synthesized, resulting into graft polymers, block copolymers, and cross-linked polymer networks. [67-69]

In most of the cases, PEO chain was used as the main polymer chain onto which the structural modifications were made. [70, 71]

It was observed that cross linking PEO by chemical reaction gives the polymer a rubber-like texture and large amorphous phase which enhances its ionic conductivity when a lithium salt is added and also prevents the material from creeping.[73, 73] Also radiation[74] cross linking have been used to produce amorphous and mechanical stable matrices.

Polymers containing oligo-oxyethylene side chains, acting as lithium salt complexing sites, attached to main chain polymer backbones were synthesized.

Recently, amorphous, up to comb polymers based on methyl vinyl ethermaleic anhydride copolymer containing oligo-oxyethylene and stable up to 140°C were prepared by Ding et al. [75] Flexible polymers such as polysiloxanes[76] and polyphosphazenes[77] with different lengths and mixtures of etheric side chains were also used as polymer backbones.

The limitations observed in the ionic conductivity of the amorphous polymers forced the investigation on other kind of electrolytes, Gadjourova et al[78] reported for instance the first ion conducting crystalline polymer electrolyte in which pairs of PEO chain fold to form tunnels in which Li ions can migrate. The ionic conductivity of this first attempt was too low but in other crystalline modified systems it raised up of about 3 orders of magnitude. [79]

Nevertheless the most developed solutions to get higher ionic mobility were adding ceramic fillers (composite polymer electrolytes) and introducing plasticizer (gel polymer electrolytes). [4]

I.3.2.2.2 Composite polymer electrolytes

Recent studies revealed that the composite polymer electrolytes (CPE) alone can offer lithium polymer batteries with improved electrolyte/electrode compatibilities and safety hazards[7]. One of the most promising ways to improve the morphological and electrochemical properties of polymer electrolytes is addition of ceramic fillers. The highly conducting ceramic fillers, zeolites, ionites, as well as electrically neutral ceramic fillers have been investigated. [80, 81]

It has been shown that the addition of fillers improves the conductivity of polymer hosts and their interfacial properties in contact with the lithium electrode. Inorganic fillers limit the crystallinity increasing ionic conductivity. Particle size and the characteristics of the ceramic fillers play a vital role on the electrochemical properties of the electrolytes. In general, this kind of additives for the polymer matrix are broadly classified into two categories:

- active
- passive

Materials belonging to the first class (e.g. Li_2N, $LiAl_2O_3$) participate in conduction process while passive materials that are inorganic fillers such as Al_2O_3, SiO_2, MgO are not involved in the lithium transport process. [82] The selection of fillers between active and passive components is arbitrary. Weston and Steele in 1982[80] first demonstrated that incorporating inert filler (α-alumina) in the PEO system the mechanical strength and the ionic conductivity were significantly enhanced. Many studies were then developed on PEO and PEO blend systems incorporating alumina. [83] In order to understand the role of the filler in the polymer electrolyte functioning, the specific interactions involved between the surface groups of the ceramic particles and both the PEO segments and the lithium salt anions were

interpreted in terms of Lewis acid–base interactions by Wieczorek et al. [84] According to this study the Lewis acid groups of the ceramics (e.g., the –OH groups on the Al_2O_3 surface) could compete with the Lewis–acid lithium cations for the formation of complexes with the PEO chains, as well as with the anions of the added LiX salt. [85]

The contribution by Al_2O_3 thus depends on whether it is acidic, basic and neutral, different surface group arrangements are observed. In the acidic case the –OH groups at the alumina surface prefers to interact (via hydrogen bonding) with the lithium salt anion and the PEO segments, causing an increase in salt dissociation and in the local PEO amorphous phase fraction and, consequently, in ionic conductivity. In the neutral case the interactions with the lithium salt anion and the PEO segments are weaker, with less important enhancement in ionic conductivity. Finally, in the case of basic Al_2O_3 no macroscopic changes of ionic transport properties with respect to ceramic-free polymer electrolytes are expected. The extent of structural modifications induced by the ceramics should be increasing according to the following sequence Al_2O_3 acidic > Al_2O_3 neutral > Al_2O_3 basic.

It has also been observed that the quantity of filler content influences the ionic conductivity. At low concentration levels, the dilution effect, which tends to depress the conductivity, is in competition with the specific interactions of the ceramic surface, which, as seen, promote fast ion transport resulting in a progressive enhancement of the conductivity. But at high filler content, the dilution effect predominates and the conductivity decays. Thus, a maximum in the conductivity versus composition curve is expected, generally occurring around 8-10 weight percent. [86] The enhancements in conductivity in the temperature range above crystallization temperature of PEO region, where the polymer is in its amorphous state is precise evidence of a promoting effect resulting from specific interactions at the surface of the ceramics. Further studies[87] showed that by adding higher quantities of inert filler (up to 30% wt) the mechanical properties of the membranes can be improved but the ionic conduction does not see any enhancement.

There have been lot of studies to understand the effect of solid fillers. The quantity of filler, the size, type, nature etc. also ceramic fillers organically modified have been studied. All kinds have been studied by different research groups. The most studies ceramic fillers include: SiO_2, γ-$LiAlO_2$, ferroelectric materials ($BaTiO_3$, $PbTiO_3$, $LiNbO_3$), MgO, TiO_2, ZrO_2, SiC, zeolites and many more. [88-92] Every material had its peculiarities and influenced the final properties. In every case either conductivity and/or mechanical property are improved along with some improvements in transport characteristics.

I.3.2.2.3 Gel polymer electrolytes

The second way of increasing the poor ionic conductivity of solid polymer electrolytes is the addition of a plasticizer, the obtained matrix is called "gel polymer electrolyte" (GPE) or "plasticized polymer electrolyte" which is neither liquid nor solid or conversely both liquid and solid. Gels possess both cohesive properties of solids and the diffusive property liquids[61]. Nowadays GPEs are closer to application than solid polymer electrolytes because they can match together good electrochemical performances and reduced safety risks. The use of solvents clearly limits the mechanical properties of the GPEs but this problem can be more easily overcome than the one liked to conductivity. Chemical or physical cross-linking is often adopted to improve the dimensional stability of the gel materials.

Typical examples of plasticizers used to improve the conductivity are organic solvent such as PC, EC, DEC etc. In these gelled electrolytes organic solvent are the major responsible for ionic transport, however in this case the safety problem associated with the use of volatile organic solvents essentially remains.

The use of small quantities of non-or low- volatile oligomer as plasticizer would reduce such safety issue to a level sufficient for practical use. It was shown that the addition of poly(ethylene glycol) (PEG) with low molecular weights to PEO polymers gave high ionic conductivity without loss of thermal stability.[4]

Ito [93] et al in 1987 observed that the conductivity increases with decreasing molecular weight of PEG and with increasing PEG content. The conductivity enhancement at room temperature can be attributed to the increase in the amorphous regions responsible for the ionic conduction.

Gel polymer electrolytes can be classified into two categories according to their structures as follows: one is homogeneous GPE in which polymer matrix and solvent are uniformly mixed to form a single phase composite, the other is GPE with phase separation in which a solvent is maintained in a porous polymer matrix.

To date, several polymer hosts have been developed and characterized that include poly(ethylene oxide) (PEO), poly(propylene oxide) (PPO), poly(acrylonitrile) (PAN), poly(methyl methacrylate) (PMMA), poly(vinylidene fluoride) (PVdF), poly(vinyl chloride) (PVC), poly(vinylidene fluoride-hexafluoro propylene) (PVdF-HFP), etc.[61] each one having advantages and limiting features for the effective application.

The most common polymer host are summarized in the following table:

Polymer host	**Repeat unit**	**Glass transition temperature T_g (°C)**	**Melting point Tm (°C)**
Poly (ethylene oxide)	$-(CH_2CH_2O)_n-$	-64	65
Poly (propylene oxide)	$-(CH(-CH_3)CH_2O)_n-$	-60	amorphous
Poly (acylonitrile)	$-(CH_2CH(-CN))_n-$	125	317
Poly (methyl methacrylate)	$-(CH_2C(-CH_3)(-COOCH_3)_n-$	105	-
Poly (Vinylidene fluoride)	$-(CH_2CF_2)_n-$	-40	171
Poly (vinyl chloride)	$-(CH_2CHCl)_n-$	85	-

Table I.2. Polymer hosts generally studied[61]

Only a brief discussion about the most popular polymer used in GPE membranes will be developed in the following paragraphs:

As first PEO gelled electrolytes have been investigated in presence of various salts and plasticizers, the most important observation to be done is that the addition of an organic solvent is able to improve ionic conductivity of the

resulting GPE up to 10^{-3} Scm^{-1}.[13] Many works and review papers document the development and general characteristics of many plasticized PEO based or blend polymer electrolytes. [61,94-106]

Among the polymer studied the PAN based electrolytes[107-114] offer a homogenous, hybrid electrolyte films in which the salt and the plasticizer are molecularly dispersed. However, despite the several advantages shown by PAN-based electrolytes, like high ionic conductivity of the order of 10^{-3} Scm^{-1} at 20°C and good electrochemical stability of 4.5 V, its poor compatibility with lithium metal anode offsets from practical applications. Other studies clearly revealed that the lithium electrode undergoes serious passivation when in contact with PAN-based electrodes and affects cyclability and eventually leads to safety hazards.[61]

GPE based on PMMA have also been investigated whit different plasticizer[115-120], it was shown that electrochemical stability window depends on the polymer host and lithium salt complexed. In particular Scrosati and Appetecchi[120] showed that improvement in lithium cyclability are obtained when passing from PAN-based to PMMA-based media.

However the voltammetric results and the efficiency tests revealed a consistent fraction of lithium is lost upon cycling and thus a large excess of lithium would be required eventually to assure an acceptable life to the battery. On the other hand the this kind of membrane has good transport properties which motivate a great interest.

Because of its properties PVdF has been widely used as a polymer host for lithium battery applications[121-124]. It is recognized that the PVDF polymer constitutes a two-phase separated gel composed of the swollen polymer chains and the solution retained in the cavities of the porous polymer. PVdF based polymer electrolytes are highly anodically stable due to the presence of strong electron-withdrawing functional group (–C–F) and the polymer itself has a dielectric constant ($\varepsilon = 8.4$) which helps for greater dissolution of lithium salts and subsequently supports high concentration of charge carriers. Gel electrolytes prepared using PVdF exhibits good dimensional stability, mechanical properties and they are easy to handle. The earlier report

indicates that a homogenous hybrid film can be obtained with PVdF when EC and or PC with lithium salt of proper proportions are added. This kind of polymer is nowadays the most used in GPE[122]. Although, the PVdF-based electrolytes offer excellent electrochemical properties, it has also been shown that this fluorinated polymer is not stable towards lithium leading to poor interfacial properties between lithium and fluorine

Many others polymer or polymer blends have been developed and studied as hosts for gelled electrolytes such as PEGDMA[125], PVC[126], PVdF-HPF[127,128] etc.[61]

GPEs developed till now have, in conclusion, excellent electrochemical properties combined with a satisfactory mechanical behaviour, however they always need the presence of a substrate.

I.4 UV radiation in Lithium batteries

As mentioned, Gel Polymer Electrolytes can have poor mechanical strength. The strategies for improving mechanical properties are commonly based either on promoting crystallisation or by introduction of fillers or by cross-linking. Considering the application as electrolytic membrane, crystallisation is not advisable because it hinders ionic conduction. Examples of composites membranes have been previously discussed, the quantities of fillers normally used are not high enough to strongly influence mechanical modulus and resistance of the polymer. Cross-linking is a versatile pathway, as the process can be induced in different way (thermally, photo-chemically, in the presence of co-reactants or catalyst), can be applied to many matrices (i.e. many of the linear polymers mentioned before) and can be controlled to give appropriate cross-linking density therefore tailoring the final properties of the network by changing its architecture. [129] Photochemical reactions will be described in *Chapter I Section A.*

Many examples of the use of UV radiation for the production of crosslinked gel polymer electrolytes are reported in literature.

UV has been used either for the simple crosslinking of macromolecules already polymerized or for the photopolymerization of monomers with the production of thermoplastic networks.

In 2007 Elmer and Jannasch[130] prepared a self supported mixed matrix membrane containing an immiscible blend of polymethacrylates having poly(ethylene carbonate co ethylene oxide) side chains (PMA-PEC-EO) with poly(vinylidenefluoride-co-hexafluoropropylene) (PVDF-HFP). The blend of polymers containing lithium bis(trifluorosulfonyl)imide (LiTFSI) salt and a UV initiator was cast and irradiated with UV light to polymerise the methacrylate units.

UV irradiation was also used to promote a sol-gel *in situ* synthesis of silica particles for the preparation of mixed matrix silica/poly(ethylene oxide) (PEO)-immobilized electrolyte membranes.[131] During the silica synthesis the system is able to develop the UV polymerisation of the macro-monomers in one step enabling the simultaneous formation of the polymer network and the inorganic nano particles.

Many different polymers cross-linked after polymerisation by a UV induced process are described in patents. [132, 133]

A cross-linked polyurethane acrylate was prepared by end capping 2,6-toluene diisocyanate/poly(ethylene glycol) based prepolymer with hydroxybutyl methacrylate. Significant interactions between lithium ions and soft/hard segments of the polymer were observed, when complexed with $LiClO_4$. The membrane showed high electrochemical stability window and better compatibility with lithium metal. [134]

Kim et al sintetized polyether urethane acrylate (PEUA)–$LiCF_3SO_3$ -based polymer electrolytes by prepolymerizing different kinds of polyether, with different diisocyanates and the caprolac-tone-modified hydroxyethyl acrylate. using the catalyst dibutyltin dilaurate by stepwise addition reaction. Lithium triflate $LiCF_3SO_3$ was dissolved in the prepolymers, and a plasticizer (propylene carbonate) was added into prepolymer and salt mixtures together

with the photoinitiator. Thin films were prepared by casting and UV cured. It was observed that conductivity in PEUA– $LiCF_3SO_3$ based polymer electrolytes was influenced by the structure of PEUA in some degree and by a plasticizing solvent PC [135].

Recently polymer/ionic liquid composites were investigated as solvent-free electrolytes for lithium batteries [136]. Ternary electrolytes based upon poly(ethylene oxide), an ionic liquid and a conducting salt were UV crosslinked with benzophenone as the photoinitiator. Crosslinking leads to an increase in mechanical stability of the PEO composites. This straight-forward process provides a way to increase the content of ionic liquid and thus to raise ionic conductivity without loss of mechanical stability. Impedance measurements showed that the ionic conductivity of the composites is not affected by the UV curing process. Moreover, the UV curing process caused a decrease in the degree of crystallinity in the PEO composites which contributed to an increase in ionic conductivity.

Cross-linked membranes can be also prepared starting from monomers of appropriate functionalities and polymerising them. Photo-crosslinked membranes were proposed in a patent by 3M [137]: authors describe thiol-ene systems containing polyethylene oxide units (PEO), cured by UV light.

Recently highly ion-conductive gel polymer electrolyte with mechanical flexibility was developed by incorporating liquid electrolyte into polymer films fabricated by initiator-free photopolymerization of poly(ethylene glycol) dimethacrylate and pentaerythritol tetrakis (3-mercaptopropionate) (thiol monomer) blend. When UV is irradiated on the blend, the thiol monomers themselves produce radicals to initiate the polymerization. GPEs with 40–50 wt.% of thiol monomer content showed mechanically free standing characteristics with sufficient flexibility. The ionic conductivity of the GPE good values of conductivity at 25 ◦C. [138]

PEO acrylate membranes were synthesised [139] and, in following works, modified by addition of cianomethacrylate. [140, 141] A poly ethylene glycol dimethacrylate (PEGDMA) was crosslinked in presence of an alkyl monomer and a liquid electrolyte 1.3 M $LiPF_6$/EC. Flexibility and ionic conductivity of

the electrolyte was improved when the monomer content was varied. Song *et al.*[142] followed this research line investigating acrylic membranes. Other few membranes, based on acrylates containing poly-(ethylene oxide) chains are describes in the literature. [143- 147]

A recent work reported the results on siloxane containing photopolymers giving σ of $4 \cdot 10^{-3}$ S cm^{-1} (at room temperature) and high cyclability for the low and stable surface resistance, due to the good interfacial properties of the membrane. [148]

The polymer electrolyte above mentioned are gel membranes, obtained by swelling the UV-cured network prepared previously with the liquid lithium electrolyte. However, Gerbaldi *et al.*[149] already demonstrated that the Li-X salt can be introduced directly during polymerization, thus completely avoiding the time consuming activation of the membranes by swelling into a liquid electrolyte. By such a method, the complete electrolyte preparation takes less than 5 minutes. [150]

Attempts to prepare solid polymer electrolytes by UV polymerisation are reported. [151, 152] Conductivities are comparable to those of the solid membrane described in literature while the membrane preparation is faster and in principle can be done directly onto the battery electrodes.

UV curing has also been used in the field of lithium batteries for the improvement of the packaging of commercially available batteries[153]. In other works the UV curing technology has been exploited for enhancement of the interface between lithium electrode and polymer electrolytes, Choi et al[154] prepared a protected lithium electrode by forming a layer on the surface of lithium metal. The protection layer was prepared by ultraviolet radiation-curing of a mixture of crosslinking agent (1,6-hexanediol diacrylate), liquid electrolyte (ethylene carbonate (EC)/propylene carbonate (PC)/1M $LiClO_4$), and photoinitiator (methyl benzoylformate). The interfacial properties of a symmetric lithium cell containing the protected lithium electrode was better than those of the cell using a bare lithium electrode with storage. The performance of unit cells was enhanced by the introduction of the protection

layer on the surface of the lithium anode. The morphology of the solid electrolyte interphase (SEI) layer developed on the protected lithium anode after cycling was smoother at the surface and less porous.

Also Popall et al[155] described a new secondary battery in which a polymeric electrolyte is coated on the cathode material The systems EC (ethylene carbonate)/PC (propylene carbonate)/Li+-salt/ORMOCER® (composite commercial resin based on functionalised alkoxysilanes) were chosen as ternary systems (solvent/salt/polymer). Fort the preparation of this battery the components EC, PC, ORMOCER®-resin and Li+-salt mixed with the photoinitiator is applied on the electrodes (e.g. by back-filling machine), UV cured. Finally, after application as coating or bulk (or assembly of the electrodes towards a battery), the electrolyte is thermally cured at 100°C for one hour. Also in this case the performances of the cell resulted interesting. Recently Destro[156] et al developed an Electrode-Electrolyte composite by single-step UV-curing process for 3D Li-ion polymer cells consisting in an acrylic based matrix already containing the lithium salt which is coated and UV cured on a $LiFePO_4$ cathode.

I.5 Cellulose and Paper in Li batteries

The state of the art concerning the use of cellulose in the lithium batteries technology shows that this natural polymer and its derivatives are currently used in few existing batteries above all in the form of short fibers. Some example of its application are there reported.

Cellulose-based electrolytes

Cellulose and its derivatives are mainly used in traditional Li-batteries with liquid electrolytes. These were used to produce non-woven separators for lithium batteries as explained in many international patents. [157-164]. A non-woven separator is a fibrous mat made by bonding numerous fibers together through chemical, physical or mechanical methods, *Kuribayashi*[165] in 1996 describes a composite separator used in Li ion cells composed of fine

fibrilliform cellulosic fibres embedded in microporous cellulosic film and soaked in ethylene carbonate or other aprotic solvent. He shows that fibres can reduce the possibility of separator meltdown under exposure to heat, generated by overcharging or internal short circuiting. The resistances of these films are equal to or lower than the conventional polyolefin-based microporous separators. The long-term cycling performance is also very comparable, however in this kind of cell cellulose is used with a simple structural role in presence of liquid electrolyte.

Pasquier et al.[166] used paper-based separators in flat pouch-type lithium-ion batteries and compared the performance with cells made with Celgard® polyolefin-based separators. These paper separators have good wetting properties and good mechanical properties, but do not provide the shutdown effect essential for large Li-ion batteries. Their resistance is similar to polyolefin separators, and when all water traces are removed from paper, their cycling performance is similar to that of Celgard® separators. This kind of paper-based separators can be used in small flat pouch type cells where high strength and shutdown behaviour is not required.

Paper handsheets have also been used as a separator in other kinds of batteries such as the one claimed in Zhang's patent (Enfucel) that describes a carbon/zinc dry cell. [167] Thomas Danko has described the manufacturing process and properties of cellulose in details[168] for the use as separator in secondary alcalyne batteries.

Cellulose and cellulose derivatives are now proposed as a component of gel polymer electrolytes. A first strategy is the use of nano- and micro-cellulose as a reinforcement. Nanocomposite electrolytes using cellulose whisker as a filler have been studied by Azizi Samir et al[169, 171]. In one of the interesting works high molecular weight poly(oxyethylene) matrix containing LiTFSI are reinforced by cellulose nanocrystals extracted from tunicate. The performances are studied in presence or absence of a tetra(ethylene) glycol dimethyl ether (TEGDME) as plasticizer. It is shown that the filler causes a decrease of the crystallinity of the matrix and stabilizes the storage modulus above the melting point of the complexes POE\LiTFSI. That means that

cellulosic fillers can be used in order to solve crystallinity problem of PEO and to increase mechanical properties. However even if the ionic conductivity of those membranes is quite consistent with the specifications of lithium batteries it is always lower than in absence of the filler.

Also Alloin[172] et al recently presented PEO based polymer electrolytes reinforced by cellulose whiskers and microfibrils too.

A new lithium ion conductive material with good mechanical strength and high ionc conductivity based on bacterial cellulose was proposed by Shoichiro Yano et al [173] In this work a composite material based on a bacterial cellulose hydrogel is prepared and the water of the bacterial cellulose hydrogel is replaced by a nonaqueous solvent containing a lithium compound.

Chelmechky[174] et al prepared in 2007 a new materials consisting in oligo(ethylene oxide) side chains grafted via ether linkages to a cellulose backbone. Poly(ethylene oxide)-2-hydroxypropylcellulose (PEO-HPC) was blended with lithium bis(trifluoromethylsulfone) and the PEO-HPC/lithium salt blends have been thermally crosslinked with the application of urethane chemistry. The conductivity of these membranes reaches at best 2.5 x 10^{-4} S/cm.

While present works do not show the use of pure cellulose as an active component of the electrolyte, many cellulose derivatives have been used in polymer membranes for lithium batteries instead of polymers described in *I.3.2.3*, for example *Yue*[175-176] et al synthesized ion conducting cellulose esters with PEO side chains which are a relatively simple modification of the common cellulose derivative. The polymer studied in presence of $LiCF_3SO_3$ and a plasticizer showed high conductivity (10^{-3} Scm^{-1}at room temperature) resulting a good candidate for practical applications.

Cellulose triacetate has been investigated[177] as a new material for gel electrolytes being added to 1-methyl-1-propylpyrrolidinium bis(trifluoromethanesulfonyl)imide ionic liquid and LiTFSI. The test performed gave good electrochemical properties.

Z.Ren et al[178] realized a microporous gel electrolyte based on poly(vinylidene fluoride-co-hexafluoropropylene) and fully cyanoethylated cellulose derivative. In the presence of solvent the membrane showed an ionic conductivity of $=10^{-3}$ Scm^{-1} at 20°C and it was electrochemically stable up to about 4.8V vs. Li/Li resulting a good candidate for Li ion batteries.

Cellulose acetate, cellulose acetate butyrates, cellulose acetate propionates are proposed in a European Patent[179] as immobilizer for the liquid electrolytes in lithium secondary batteries.

Cellulose-based electrodes

Cellulose has been also used as a binder for the production of the electrodes; many patents claim the use of cellulose, and mainly of its derivatives, as binders for carbon based or lithium, metal oxides ($LiMO_2$) electrodes. [180-182] For instance carboxymethyl cellulose is one of the most used cellulose derivatives, it has been studied as a binder in negative[183] and positive[184] electrodes allowing the production of well performing components.

Recently natural cellulose has been also proposed, Jeong et al[185] prepared a composite $LiFePO_4$ cathode and a carbon based anode by solubilizing the cellulose in to an ionic liquid and incorporating then the active material before the phase separation for the extraction of ionic liquid. After the cell assembly and the testing of the cell prototypes these composite electrodes displays performance comparable to that of electrodes made using conventional binders.

Also microfibrillated cellulose particles[186] were used as binders for the aqueous processing of flexible electrodes for Li-ion batteries. In this case microfibrillated cellulose formed a nanostructured web-like network around graphite platelets conferring to the graphite anode a highly porous structure, excellent flexibility and good cycling performances. In this work self-standing and flexible electrodes are produce using a straightforward water evaporation process.

Claimed-paper based batteries

Some works have been found claiming the production of "paper batteries", interesting studies have been developed up to now.

Pushparaj in 2007[187] showed the realization of a ultrathin, flexible and safe energy storage devices based on nanoporous cellulose paper embedded with aligned carbon nanotube. The nanocomposite paper is used as cathode and a thin evaporated Li-metal layer as anode , with Al foil on both sides as current collectors. Aqueous 1 M $LiPF_6$ in ethylene carbonate and dimethyl carbonate (1:1 vol/vol) is used as the electrolyte. The battery uses the excess cellulose layer in the nanocomposite cathode as the spacer, without the use of any stand-alone spacer. The intimate configuration of CNT and cellulose helps in the efficient packaging, operation, and handling of these devices. The discharge capacity and performance observed here compare well with other flexible energy-storage devices. The robust integrated thin-film structure allows not only good electrochemical performance but also the ability to function over large ranges of mechanical deformation and record temperatures and with a wide variety of electrolytes. This kind of battery allows a great flexibility of shape and design.

In 2009 Nyström et al.[188] claimed the production of an "ultrafast all-polymer paper-based battery", this kind of engine is based on a novel nanostructured high-surface area electrode material composed of cellulose fibers of algal origin individually coated with a 50 nm thin layer of polypyrrole. In this case, concerninig the electrolyte, a cellulose separator soaked in a liquid electrolyte is simply sandwiched between the two electrodes.

In 2010 Hu [189] et al produced a tin and felxible secondary paper –lithium battery by integrating all of the components of a Li-ion battery into a single sheet of paper with a lamination process. Lightweight CNT thin films were used as current collectors for both the anode and cathode and were integrated with battery electrode materials through a coating and peeling process. The double layer films were laminated onto commercial paper, which functions as

both the mechanical support and Li-ion battery membrane. Due to the intrinsic porous structure of the paper, it functions effectively as a separator with lower impedance than commercial separators and has good cyclability in presence of a liquid electrolyte.

The present situation show big possibilities in the improvement of the use of cellulose, a green and common material, in the field of lithium batteries.

SECTION A

In this section a short description of the photopolymerisation process is given. A general discussion about the different processes of UV curing will be developed; UV polymer grafting procedures will also be presented.

I.A.1 Photopolymerisation process

Photochemical reactions in the most general sense are reactions induced by ultraviolet (~100- 400 nm), visible (~400- 760 nm) or infrared (~780- 20,000 nm) radiation. UV radiation is an electromagnetic radiation with wavelengths below those of visible blue light. While the energy of the radiation increases with decreasing wavelength, the depth of penetration into matter increases with the wavelength.

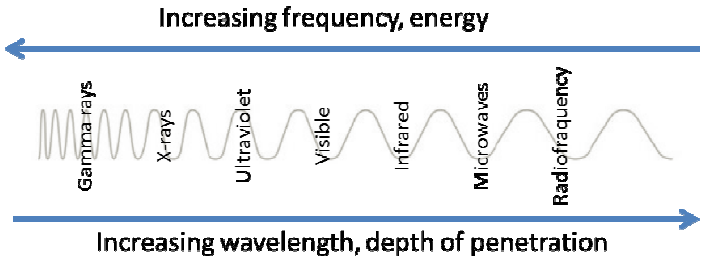

Figure. I.A.1. Electromagnetic spectrum, qualitatively[193]

UV radiation is normally best known for its deleterious effects on organic compounds, particularly upon prolonged sunlight exposure. By breaking chemical bonds, UV radiation causes severe changes in the mechanical and optical properties of polymer materials, thereby reducing their service life in outdoor applications. [190] Nevertheless, it was observed that UV radiation can also have a beneficial effect and be used to initiate desired chemical reactions, like polymerization. By exposing a monomer for a brief time to intense UV radiation, in the presence of a photoinitiator, large amounts of free species are generated at once. Under such high initiation rate conditions, it was expected the polymerization to proceed with short kinetic chains, because of

enhanced bimolecular termination, thus leading to low molecular weight waxy polymers. Actually, this prediction proved to be wrong for multifunctional monomers, such as di- or tri-acrylates which were found to polymerize extensively within a fraction of a second upon UV or laser irradiation to form strongly cross-linked polymer networks. [191,192]

UV radiation is contained in the spectrum of natural sunlight or can be generated by various types of light sources. [193]

Commonly used laboratory sources of UV radiation are mercury arc lamps or electrode-less microwave powered mercury lamps. In arc lamps, mercury vapour is ionized by a high voltage applied between the electrodes in the tube. As a current flows in the resulting plasma, an arc develops, which emits energy in the form of radiation at a characteristic wavelength. In microwave powered lamps, high frequency microwaves emitted from a magnetron generate mercury plasma, which provides the same spectral output as an arc lamp. However, the most widely used type is the medium pressure mercury arc lamp. Since the spectrum of the emitted radiation depends on the specific composition of the vapor in the lamp, metal halides are frequently added to the vapor in the lamps. The effect is a shift in the spectral output, which allows adaptation to the requirements imposed by the use and shifting towards longer wavelengths. Also incandescent lamps, light emitting diodes and excimer lasers the type can be used to generate an UV radiation; the source to be used depends on the requirements for radiation wavelength and intensity imposed by the chemistry of the photoinitiator. [194]

The intensity of UV radiation for continuous exposure is described by the irradiance (in units of W/m^2), which refers to the radiant energy flux (or power) incident on a surface, divided by the surface area. For time-integrated (or pulsed) exposure, the radiant exposure (in units of J/m^2) refers to the energy that reaches a surface because of an irradiance, which is maintained for a given time duration, divided by the surface area. [193]

Photopolimerisation by UV irradiation has become a well-accepted technology which has found a large variety of industrial applications because of its distinct advantages. [195] Usually UV induced polymerization is applied to

multifunctional monomers and is a powerful method to achieve, selectively in the illuminated areas, a quasi-instantaneous transformation of a liquid resin into a solid cross-linked polymer. It is usually referred as UV curing.

UV-curing technology has a steady development in the past 20 years; it has opened the way to an ever-increasing number of end-uses. The most important ones are to be found in the coating industry for the surface protection of all kinds of materials (metals, plastics, glass, paper, wood, etc.) by fast-drying varnishes, paints, or printing inks. In photolithography, light-induced insolubilization of photoresists is being used to produce the high definition images needed for the manufacture of printing plates, optical disks and microcircuits. Besides its great speed and spatial resolution, light-induced polymerization presents a number of other advantages, such as solvent-free formulation, low energy consumption, ambient temperature operations and tailor-made properties of the UV-cured polymers. During the last decade, a considerable amount of work has been devoted to UV-radiation curing, this technology is expanding rapidly on an industrial scale, principally by the increase on monomer and iniziators synthesis and production[196-200].

Photocurable formulations consist usually of multifunctional monomers and oligomers, with small amounts of a photoinitiator. One of the basic laws in photochemistry states that a photochemical reaction can only occur if light has been absorbed by the medium. As most monomers are essentially transparent to the radiations emitted by conventional UV sources, usually mercury lamps, they do not produce initiating species with sufficiently high yields. Therefore, it is necessary to introduce in the UV-curable formulation a photoinitiator which will effectively absorb the incident light and generate reactive free radicals or ions by cleavage of the electronically excited states. The overall process can be represented schematically as shown in Figure 2.

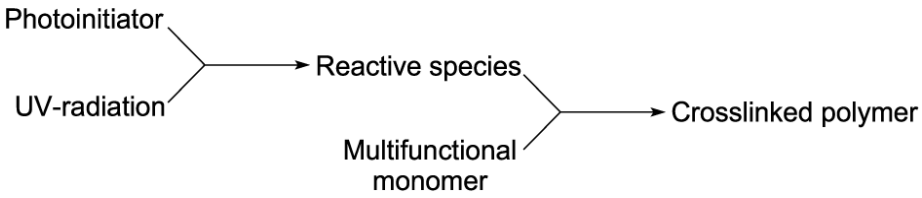

Figure I.A.2. Scheme of the photopolymerization reaction[201]

The photoinitiator plays a key role in that it governs both the rate of initiation and the depth of cure through its absorbance.

Once polymerization is started, by reaction of the initiating species with the monomer functional groups, the chain reaction proceeds very much as in a conventional thermal polymerization, except for the much larger rate of initiation that can be reached by intense illumination and for the lower temperature. With multifunctional monomers and telechelic oligomers, the polymerization will develop in three dimensions to yield strongly crosslinked polymer networks.

Polymerizations can be carried out under a wide range of conditions, including variations in monomer structures, the number and type of reactive functional groups, temperature, atmosphere, irradiation rate and photoinitiator type. [202-203]

There are two major classes of UV-curable resins which differ by their polymerization mechanism: photoinitiated radical polymerization of monomers like acrylates or unsaturated polyesters, and photoinitiated cationic polymerization of multifunctional epoxides and vinyl ethers. Initiating species are produced either by homolytic photocleavage of aromatic ketones or by photolysis of arylonium salts with formations of protonic acids. Polymer networks having different architectures and tailor-made properties have been obtained by UV irradiation of hybrid formulations containing more than one type of monomer. [197]

I.A.2 Photopolymerisation mechanism

I.A.2.1 Radical photopolymerization [200, 204]

Free radical polymerization involves the three steps:

- initiation
- propagation
- termination

In the first initiation step, a photo-initiator is decomposed to produce free radicals containing unpaired electrons, which can bond to other compounds at the site of the unpaired electrons. After this initiation, the radical bonds to a monomer molecule and, during propagation, other monomers are added. This involves the addition of free radicals to the double bond of a monomer, with regeneration of another radical. The active center is continuously relocated at the end of the growing polymer chain. Propagation continues until the growing chain radical is deactivated by chain termination. Termination is a reaction of a polymer chain radical with another radical.

Free radicals are readily produced upon UV irradiation of photo sensitive compounds. Radical species can be generated by two different kind of reaction designated Norrish type I and Norrish type II. In a type I reaction (Figure 3-A) a pothoinitiator molecule is decomposed in a radical pair by homolitic decomposition and directly forms radicals capable of iniziating the polymerization, in Norrish type II reaction (Figure 3-B) the photosensitive molecule preferably react with suitable hydrogen donating compounds, the resulting ion pair can be generated either by an homolytic cleavage of R-H bond or via an intermediate charge transfer complex.

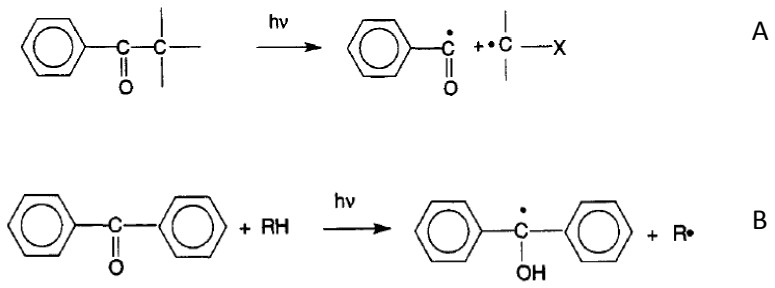

Figure I.A.3 Reaction steps involving during photolysis of a photo-initiator[197].

The photophysical and photochemical properties of the photoinitiators are therefore extremely important in controlling the reactivity.

The advantages of the free-radical polymerization are the availability of large sources of row materials, extremely fast cure rates, well-known chemical reaction and excellent physical properties. Free-radical polymerizations, however have several drawbacks: they are inhibited by oxygen[205] and exhibit a high percentage of shrinkage. This adverse effect can be overcome by using additives in the formulations and performing the curing process in vacuum or in an inert atmosphere. [206] The volume shrinkage of acrylates during polymerization is typically in the order of magnitude of 10% or even higher. [207] The high viscosity of the prepolymers often necessitates the addition of low molecular weight monomers, which will act as reactive diluents. Because of their high crosslink densities, such photo-cured polymers exhibit a great resistance to chemicals, heat and radiation, and show well designed physical properties depending on the length and chemical structure of the crosslink segments. Moreover the volatility, unpleasant odour and toxicity are commonly associated with the monomeric raw materials.

Different monomers can be polymerized by this kind of reaction, among them acrylates systems are widely diffused and particularly interesting for the development of this work.

Acrylates are known to be among the most reactive monomers polymerisable by free radical mechanism. This feature, together with the remarkable chemical, optical and mechanical properties of the polymers obtained, account for the great commercial success of acrylates based UV-curable resins. For a

diacrylate monomer irradiated in the presence of a photo cleavable aromatic ketone, the basic process can be represented in Figure 4.

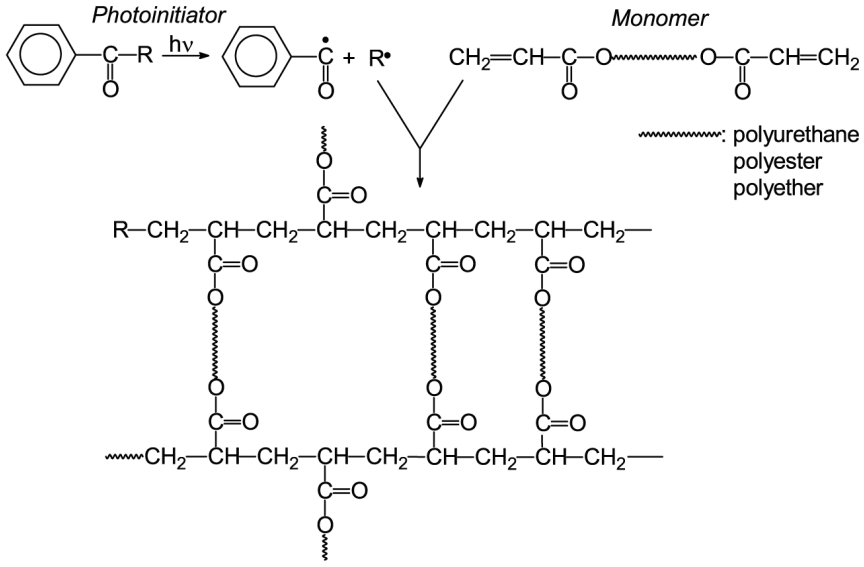

Figure I.A.4. Scheme of the reaction of an acrylate system[201]

Different types of structures (R) can be used for the telechelic polymer or oligomer backbone, such as polyurethanes, polyesters, polyethers, perfluorinated, alicyclic, aromatic and polysiloxanes according to the requirements of the application. The final properties of UV-cured acrylate polymers depend primarly on the chemical structure of the functionalized oligomer. Low-modulus elastomers are generally obtained with aliphatic compounds, whereas hard and glassy materials are formed when aromatic structures are introduced into the polymer chain. [201]

I.A.2.2 Cationic photopolymerization

Photoinitiated cationic polymerisation is being increasingly used to cure multifunctional monomers that are inactive towards radical species, in particular epoxides and vinyl ethers. [201]

Also the cationic reaction consists of different steps. The initiation reaction is a multistep process involving first, the photoexcitation of onium salts (such as diaryliodonium or triarylsulfonium salts) and then the decay of the resulting

excited singlet state with both heterolytic and homolytic cleavages. Onium salts (Figure 5) contain cationic moiety which is the light-absorbing component, the photolysis reaction, which produces both Brönsted acids and free radicals.

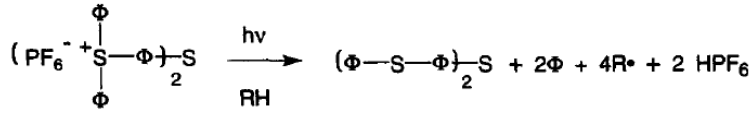

Figure I.A.5. Tryaril-sulphonium salt and its reaction upon excitation.

Cations and arylcations generated are very reactive with monomers to form a Bronsted acid, which is the actual initiator of cationic polymerization.[208]
Initiation of polymerization takes place by protonation of the epoxy monomer, followed by the addition of further monomer molecules, thus resulting in chain growth reaction. In addition to the usual mechanism, also the chain transfer mechanism can take place when the cationic polymerization of epoxides is carried out in the presence of alcohols.
During the polymerization, the growing ionic chain-end undergoes a nucleophilic attack by the alcohol to give a protonated ether. Deprotonation of this latter species by the epoxy monomers results in the termination of the growing chain and the proton transfer to the monomer can start a new chain.
An example of the ring opening reaction of an epoxyde group is represented in Figure 6.

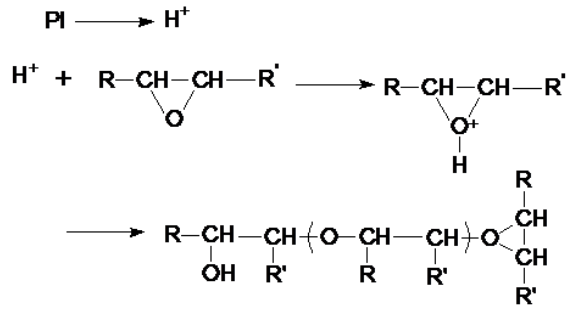

Figure I.A.6. Mechanism of cationic ring opening photopolymerization[201]

The two distinct features of photo-initiated cationic polymerisation are its lack of sensitivity toward atmospheric oxygen and its living character.
Cationic polymerization, in fact, once initiated may continue to proceed after the light source has been removed. This process, called the "dark reaction", is the result of the ability of relatively long-lived protonic acid or Lewis acid species to continue the polymerization. [201]

I.A.3 Grafting for polymer surface modification

Over many years, polymer surface modifications have been studied in various fields of industrial applications, using different innovative techniques including chemical and physical processes. Physical processes take advantage of surface segregation, radiation of electromagnetic waves, and oxidation with gases, while chemical modifications use wet-treatment, blending, coating, and metallization.

Grafting has advantages over other methods in several points, including easy and controllable introduction of graft chains with a high density and exact localization of graft chains to the surface with the bulk properties unchanged. Furthermore, covalent attachment of graft chains onto a polymer surface avoids their delamination, and assure the long-term chemical stability of introduced chains, in contrast to physically coated polymer chains.[209]

The use of UV irradiation appears to be an excellent method for surface grafting of polymers because of its simplicity and cleanliness. Additional reasons for the suitability of the photochemical method for surface grafting of polymers are as follows: 1) photochemically produced triplet states of carbonyl compounds can abstract hydrogen atoms from almost all polymers so that graft polymerization may be initiated; 2) high concentrations of active species can be produced locally at the interface between the substrate polymer and the monomer solution containing a sensitizer when UV-irradiation is applied through the substrate polymer film; 3) in addition to the simplicity of the

procedure, the cost of energy source is lower for UV radiation than for ionizing radiation.[210]

In a recent review three basically different grafting approaches are mentioned[211]. In the "grafting to" approach an end-functional pre-formed polymer with a reactive end-group is coupled with the functional group located on the polymer backbone. In the "grafting from" approach the growth of polymer chain occurs from initiating sites on the polymer backbone. In the "grafting through" approach a macro monomer, e.g. a vinyl derivative of cellulose, is copolymerized with a low molecular weight co-monomer.

In practice the "grafting from" approach is the most generally used procedure. The process requires formation of paramagnetic species (radicals, or charged intermediates) on the main chain polymer backbone. These species react with the monomer molecules and initiate polymerization reaction.

Many kinds of polymers with the aid of a photoinitiator or photosensitizer for many different applications have been modified by UV-grafting. There are several review papers on grafting and on practical applications of the grafted products.[212-214]

Only few works more interesting for our study will be here briefly mentioned.

Earlier reports were concerned with UV irradiation at the vapor phase of monomer and sensitizer such as benzophenone (BP) in the presence of inert gas [215–218].

Rånby[219] explained that in this single-step photografting technique, originally developed for flat surfaces, upon photoexcitation, the benzophenone molecules abstract hydrogen atoms from the polymer surface and the resulting surface radicals initiate surface graft polymerization. Although very convenient, this procedure also creates significant amounts of nongrafted polymer within the solution.

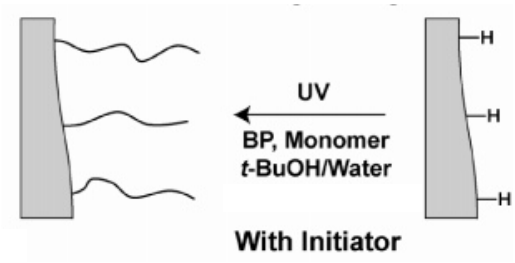

Figure I.A.7 UV grafting of monomers in the presence of benzophenone.[220]

The surface of polyethylene and polystyrene (PS) was modified by grafting with acrylic acid [219]. BP and AAc were UV-irradiated in the presence of a polymer substrate. It was observed that PS was easier to graft, presumably because it contains easily abstractable, tertiary hydrogens. Acetone was found to be suitable as a solvent because it also absorbs UV light below 320 nm, and when excited it can either undergo a Norrish type I cleavage and form methyl radicals or abstract a hydrogen.

PE film was also grafted with glycidyl acrylate and glycidyl methacrylate (GMA) by a similar photoinitiation method [221] GA and GMA were widely used for the surface modification of polymers[222-224].

A novel process was developed for continuous photoinitiated graft polymerization of acrylamide and acrylic acid onto the surface of high-density PE (HDPE) tape film, presoaked in a solution containing monomer and initiator under nitrogen atmosphere [225]. The technique was favorable and had many merits, e.g. easy and continuous operation, short irradiation times, no requirements of severe vacuum conditions, and low cost of equipment.

A photo-induced living graft polymerization method consisting of two steps was investigated[220, 226].

This method involves covalent attachment of photoinitiator to the polymer substrate. Specifically, the sequential photografting technique consists of the two steps shown in Figure 8. In the first one, initiator moieties are formed at the pore surface by UV irradiation of the substrate that is in contact with the benzophenone solution. This compound abstracts hydrogen from the polymer surface and creates a free radical. However, in the absence of monomers, the surface radical and the newly formed semipinacol radical combine to form

surface-bound initiator. The second step of graft polymerization is then carried out with a solution containing monomer and solvent. UV irradiation liberates the immobilized latent free radicals that initiate graft polymerization from the surface. Besides reducing the formation of nongrafted polymer in solution (in comparison to the single step techniques, where both initiator and monomer are present in solution), the sequential approach provides additional control over grafting because the overall process, including hydrogen abstraction and grafting polymerization, is decoupled into two separate steps. Thus, this two-step sequential photografting technique allows for a greater degree of control over the grafting process.[220]

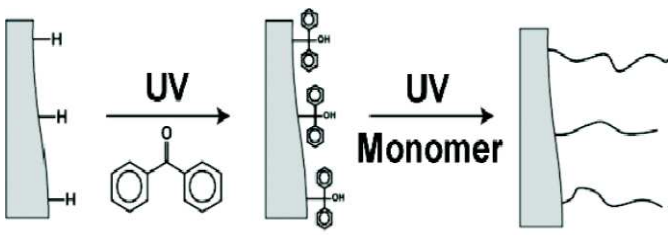

Figure I.A.8. "2 steps" grafting method.[220]

In addition, the method substantially eliminates formation of undesired homopolymer and crosslinked or branched polymer.

Many ways of photografting were developed; to fabricate a platelet-compatible polymer, phosphorylcholine was introduced onto the PAAc-grafted PE surface using UV energy through two different methods[227] PE film was first immersed in aqueous solution containing a photoinitiator (BP) and exposed to UV irradiation, followed by graft polymerization of AAc under UV irradiation. On the other hand, PE film was simultaneously UV irradiated in the presence of initiator and monomer.

SECTION B

In this section a short description of the cellulose and paper structure will be given. The discussion will start from the explanation of the wood structures and classification and it will descend to the chemical description of the cellulose molecule, being cellulose derived from wood the primary raw material for paper production. Some information about the cellulose fibers treatments for the preparation of commercial products will then be given.

Figure I.B.1. Schematic representation of the passage from wood to paper industrial products

I.B.1 Wood and fibers structures[228, 229]

Wood has always been the primary raw material for paper production; in 2010 it covered the 40% of the consumption in Europe, even if in the last decades the remarkable increase in recovering has putted the recovered paper even at a higher level. Other raw materials derive from non fibrous components and, in a very small quantity (1%), from pulp other than wood[230].

It has been stated that paper of some sort can be made from the fibers of any vascular plant found in nature. In a technical sense, it is true, but from an

economic standpoint the number of plant materials suitable for paper making is much more limited.

Trees are perennial, seed-bearing plants, which are classified into two broad categories known commercially as "softwoods" and "hardwoods". Softwoods are also referred to as coniferous woods since they have seeds that are produced in cones and not covered, while hardwood trees produce covered seeds within flowers. However, these general names cannot be used exclusively as a measure of "hardness" because considerable overlap occurs in the range of average specific gravities of softwoods and hardwoods; some softwoods are quite hard, and some hardwoods are relatively soft.

The observation of wood as it appears to the naked eye without any optical aids shows not only differences between softwoods and hardwoods as well as between various species, but also characteristic differences within one sample. All these differences are the result of the development and growth of wood tissue. In their fully mature state, the vast majority of softwood and hardwood cells are dead and hollow, and the resulting tissue is composed essentially of only cell walls and voids. In all the kinds of plants wood cells are chemically heterogeneous and built up of a polymeric matrix of structural components.

In general, depending on their principal functions, softwood and hardwood cells can be divided in different groups.

Softwoods cells are mainly constituted (90%-95%) by fibrous cells named tracheid. The arithmetic mean length of unbroken tracheids is important with regard to pulp properties, and it can vary considerably between different wood species as well as within various parts of the individual tree. However, fiber lengths of the vast majority of softwoods average between 2 and 6 mm. Tracheid cells assure the mechanical strength of wood and, at the same time, they act as channels for water. Further on softwood cells are constituted of parenchyma cells which allow the storage and transport of assimilates.

For the hardwood cells the macroscopic characteristics are reflected in the distribution and number of different cell types such as "fibers", "vessel

elements" and “parenchyma cells". The true fibers constitute the major component of hardwood pulps. The dimensions of the hardwood fibers, which form the basic tissue, are smaller than those of the softwood tracheids. They assure only the mechanical support to wood. Vessel elements are dead, hollow, and perforated at their ends in their fully mature state to facilitate the upward conduction of water and nutrients from the root system. Parenchyma cells are responsable of the stocking of nutrients. Their quantity in hardwoods, on the average, is higher than the one in softwoods. This higher amount of parenchyma cells in hardwoods is largely responsible for the generally higher fines content of hardwood pulps.

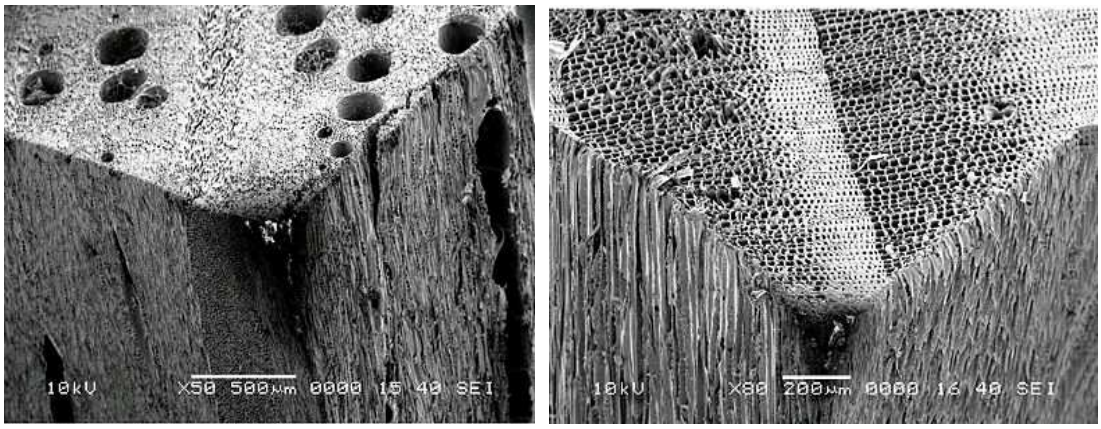

Figure I.B.2. Three sectional view of HW structure (left) and SW structure (right)

As a consequence, the morphological differences between fibers allows to identify their origin and give different properties to the material.

A summary of the most interesting properties of hardwood and softwood fibers is given in the following table:

HARDWOOD	SOFTWOOD
Short fibres	Long fibres
Less strong	Good mechanical property
Low porosity	High porosity
Compact Hand Sheets	No Uniformity
Low Mech. properties	

Table I.B. 1: Comparison between the characteristics of Hard Wood (HW) and Soft Wood (SW).

I.B.2 Cellulose [228, 229]

In natural fibers, cellulose is the substance that determines the character of the fibers and permits its use in paper making. Cellulose is the most abundant of the products of photosynthesis in the plant kingdom and it is produced annually in enormous amounts by natural plant growth. It is a carbohydrate, meaning that it is composed of carbon, oxygen and hydrogen with the latter two elements in the same proportion of water. It is represented by the formula $(C_6H_{10}O_5)_n$ where n is indefinite, varying with different sources of cellulose, and with the treatment that has received. The degree of polymerization (DP) of native wood cellulose is of the order of 10000 and lower than that of cotton cellulose (about 15000). These DP values correspond to molecular lengths of 5.2 and 7.7 mm, respectively. In technical processes, such as chemical pulping, the DP of cellulose can decrease to 500-2000. The polydispersity of cellulose is rather low (<2), indicating that the weight average molecular mass (Mw) and the number average molecular mass do not deviate much from each other.

The structure of cellulose is shown below, the recurring unit of the molecular chain is composed by two consecutive glucopyranose units forming a cellobiose unit.

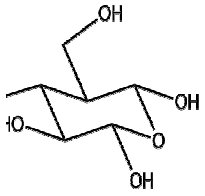

Figure I.B.3. Chemical structure of cellulose

Because of the strong tendency for intra- and intermolecular hydrogen bonding, bundles of cellulose molecules aggregate to microfibrils, which form either highly ordered (crystalline) or less ordered (amorphous) regions. These

microfibrils pass through several crystalline regions (about 60 nm in length) and, as a result of further aggregation of microfibrils, "fiber wall cellulose" with a high degree of crystallinity (60%-75%) is formed. This also means that cellulose is relatively inert during chemical treatments but also that it is soluble only in a few solvents. The most common cellulose solvents are cupriethylenediamine (CED) and cadmiumethylenediamine (Cadoxen), whereas less well known but powerful solvents are N-methylmorpholine N-oxide and lithium chloride/ dimethylformamide.

Most cellulose occurs in nature intimately associated with other substances composing the plant structure, from which it can be separated by long processes. The major chemical constituents of all wood species are so-called "structural substances" apart from cellulose they are hemicelluloses and lignin. Other polymeric constituents present in lower and often varying quantities are pectin, starch, and proteins. In addition to these macromolecular components, various "nonstructural" and mostly low-molecular-mass compounds (extractives, some water-soluble organics, and inorganics) can be found in small quantities in all kinds of wood.

Cellulose fibers can undergo different treatments and process according to the use they are designated to. They can be treated in order to obtain short fibers or pulpled to produce the slurry used for paper production.

I.B.3. Short fibers

I.B.3.1 Whiskers

In recent years, the use of natural fibers as reinforcements in polymers and composites has attracted much attention due to the environmental concerns. Cellulose nanowhiskers have generated a great deal of interest as a source of nanometer sized fillers because of their very good mechanical properties[231]. Extensive research has been reported by Dufresne et al. to extract single cellulose crystal from sea animals and plants, and use them as a reinforcing phase to form nanocomposites.[232, 233] Native cellulose present in macroscopic fibres, like for instance plant fibres, consists of a hierarchical structure. This

hierarchical structure, as said, is built up by smaller and mechanically stronger entities consisting of native cellulose fibrils. These fibrils interact strongly and aggregate to form the natural or native cellulose fibres. The lateral dimension of these fibrils depends on the source of the cellulose but it is typically of the order of a few nanometres. The fibrils contain crystalline cellulosic domains but also noncrystalline domains located at the surface and along their main axis. The noncrystalline domains form weak spots along the fibril. These fibrils display high stiffness and are therefore suitable for the reinforcement of nanocomposite materials.

There are numerous methods to prepare nanofibres from natural cellulose fibres. [234-244] A typical process involves steam explosion, homogenization, and acid hydrolysis. The submission of plant fibres to strong acid conditions combined with sonication leads to the hydrolysis of noncrystalline domains, and rod-like nanofibres called cellulose nanowhiskers result from this treatment. The dimensions of these resultant nanowhiskers depend on the source of the cellulose, but their length generally ranges between 100 and 300 nm.

In essence, the principle reason to utilise cellulose nanofibres in composite materials is because one can potentially exploit the high stiffness of the cellulose crystal for reinforcement. As the cellulose in the nanowhiskers is devoid of chain folding and contains only a small number of defects, its modulus and strength was calculated and measured to be around 130 and 7 GPa[231], respectively. On the other hand the process of extracting single crystal whiskers from plants is time consuming and very costly, despite the abundance and low price of the raw materials.

I.B.3.2 Microfibrils

By omitting the hydrolysis step and only submitting the fibres to high mechanical shearing forces, disintegration of the fibres occurs, leading to a material called microfibrillated cellulose (MFC). A combination of high mechanical shearing forces and mild enzymatic hydrolysis can also be used to

prepare MFC. [245] These microfibrils ideally consist of individual nanoparticles with a lateral dimension around 5 nm. Generally, MFC consists of nanofibril aggregates, whose lateral dimensions range between 10 and 30 nm, or more. The production and characterization of microfibrillar cellulose (MFC) from wood fibres has been described by Turbak et al.[246] and Herrick et al. . [247] MFC was obtained by disintegrating cellulose fibers at high shear. This procedure resulted in the production of a highly entangled network consisting of nanoscale size elements with a gellike behaviour for water dispersions at 1% or lower concentrations of MFC. [246-248] Because of the unique characteristics of MFC particles, such as; a very high specific surface area[249], and the formation of a highly porous network[250], an extensive amount of research has been done in the last 30 years.

Several recent publications demonstrate how MFC can be used for various purposes within material technology, such as; reinforcement in nanocomposites[251-254] dispersion stabilizers[255, 256], antimicrobial films[257], filtration media[258] and oxygen barrier material in food and pharmaceutical applications. [259]

I.B.4 Paper [228, 229]

Paper consist of a matted of felted sheet of fibers formed from water suspension and often modified by additional materials. The fibrous material or "pulp" is the most important raw material with which the paper industry is concerned.

The successful conversion of this pulp into a marketable product depends on a combination of original fiber properties (fiber morphology) and the response of the fibers to processing variables. Because of the great variety of wood types, the physical properties of a piece of paper from one species will often vary markedly from a similar piece from another species although processing conditions may have been identical. Investigations of relationships between the morphology of fibers and paper properties began in the early 1900's. [260] However, results have often been contradictory. One of the first fiber

properties related to paper strength properties was fiber length. Several investigators found that fiber length directly affects the tensile strength of paper. [261] This led to the conclusion that hardwood pulps are lower in paper strength properties because the fibers of hardwoods are shorter than those of softwoods. Several investigators have found contradicting evidence that suggests fiber length does not have a great influence on paper properties, especially on tensile strength. [262] Apart from the nature of the fibers also the treatments done on them can influence the properties of the paper.

A fast overview of the paper production steps will be given in the following pharagraps[263]:

Pulpling

Pulping refers to different processes by which wood or other fibrous feedstocks convert into a product mass with liberated fibers. These thermal conversions can be accomplished either chemically or mechanically or by combining these two types of treatments. Thus, with regard to the pulping processes, the term "pulp" is collectively used independently from the treatment it is subjected to. Although pulps are predominantly utilized for papermaking, some pulps are processed in various cellulose derivatives (cellulose esters and ethers) and regenerated celluloses. The different kinds of pulp available are then:

- Mechanical
- Semi-chemical
- Chemical

Mechanical pulps are produced by grinding wood into relatively short fibres. According to the treatment they undergo these can be classified as Stone groundwood which is only subjected to grinding and it is used mainly in newsprint and wood containing papers, like LWC (light-weight coated) and SC papers or Thermo-mechanical pulps (TMP) which are produced in a thermo-mechanical process where wood particles are softened by steam before entering a pressurised refiner. TMP has mainly the same end-uses as stone

groundwood. Variants of the above two processes produce pressurised stone groundwood pulp and refiner mechanical pulp.

Semi-chemical pulps undergo both a chemical and a mechanical treatment. Simple semi-chemical pulp is produced in a two-stage process which involves partial digestion with chemicals, followed by mechanical treatment in a disc refiner. This pulp is mainly used in the production of fluting medium for corrugated board. While Chemi-thermomechanical pulp (CTMP) is produced in a similar way to TMP, but the wood particles are chemically treated before entering the refiner. This pulp has properties suited to tissue manufacture. Some CTMP is used in printing and writing grades. CTMP is classified under semi-chemical pulps in the Harmonized System of the Customs Co-operation Council. In the FAO, as well as in other industry statistics, such chemi-thermomechanical pulps are grouped with mechanical pulp.

Chemical pulps are instead treated in presence of chemicals, they can be classified as Sulphite when they are produced by cooking wood chips in a pressure vessel in the presence of bisulphite liquor. End-uses range from newsprint, printing and writing papers, tissue and sanitary papers. Sulphite can be either bleached or unbleached. The second family of chemical pulps is composed by the Sulphate (Kraft) for whose production wood chips are cooked in pressure vessels in the presence of a sodium hydroxide (soda) liquor that break the bonds that link lignin to cellulose. Pulp produced by the Kraft process is stronger than that made by other pulping processes. Kraft pulping removes most of the lignin present originally in the wood. The pulp may be unbleached or bleached. End-uses are widespread, with bleached pulp particularly used for graphic papers, tissue and carton boards. Unbleached pulp is commonly used in liner for corrugated board, wrappings, sack and bag papers, envelopes and other unbleached specialty papers.

Bleaching

The absorbance of visible light by pulp is mainly associated with the chromophoric structures containing conjugated double bonds in its lignin constituent. Lignin in intact wood, as carbohydrates and extractives, is only

slightly colored but, especially after alkaline pulping and as a result of the pulping reactions, the residual lignin fragments of pulp are highly colored. In general, acid sulfite and bisulfite pulps are easier to bleach than kraft pulps are and, in the case of alkaline pulps, hardwood pulps can be decolorized more easily than softwood pulps. In contrast, mechanical pulps, by nature of their processing, contain all the structural components initially present in wood. However, in this case, lignin also mainly imparts the color to the pulp. However, many factors such as defibration conditions, wood species and age, storage time and conditions, and exposure to light and air influence pulp brightness.

Bleaching can basically be defined as a chemical process applied to chemical and mechanical pulps in order to increase their brightness. Thus, to reach an acceptable brightness level, bleaching should be performed either by removing the residual lignin of chemical pulps ("delignifying or lignin-removing bleaching") or by converting and stabilizing chromophoric groups of mechanical pulps without loss of substance ("lignin-preserving or retaining bleaching"). In both cases, however, the obvious prerequisite is that no significant losses in pulp strength occur.

After pulpling and bleaching fibers are dried in order to reduce the quantity of water during the transport of materials to the papers industries.

Once the commercial fibers arrive to the factory the paper production consist in the dispersion of these in water and the formation of thin layers that are then pressed and dried. Before the preparation of the sheets fibers can undergo a further process called refining.

Refining

Refining is an essential step in developing pulp fibers to their desired quality level in the papermaking process. During refining fibers are submitted to high frequency compression and shear stress. Fibers still flocculated are alternatively compressed, sheared and stretched. Deformations are firstly elastic and then plastics resulting in irreversible fibers deformations. During

the process phases of stress and relaxation are alternated, this alternance leads to the morphological modification of fibers.

Fibrillation causes then a variety of simultaneous structural changes, such as internal fibrillation, external fibrillation, fines formation, fiber shortening or cutting, and fiber curling or straightening. It has been reported that the shortening effect of refining would improve paper formation due to the decrease in the crowding number that leads to lower propensity to flocculate and also smaller flocs existence, but the other effects of refining worsen formation concluding that paper formation is made easier when the influence of fiber shortening outweighs the opposing influences of fibrillation and fiber straightening. The refining level achievable depends on the machine used; different refining strengths (liked to different existing equipments) or also different refining times leads to desired properties of the fibers.[231]

The modification of the fibers affects in different ways the paper properties, the most common parameters are listed in the following scheme:

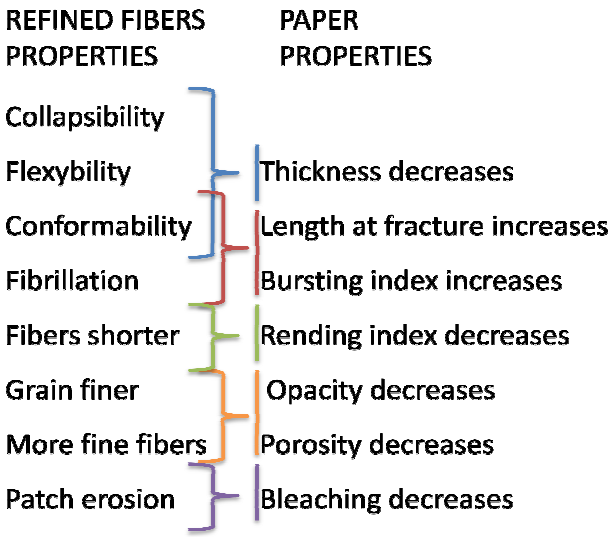

Figure I.B.4. Scheme of the influence of refining on paper properties.

The extent of refining is expressed as Schopper-Riegler degree (SR).

I.B.5 Cellulose modifications

The properties of cellulose can be modified by different treatments according to its final use requirements. In this paragraph, after a brief introduction of the chemical treatments commonly done of cellulose we will focus on the photochemical grafting and on the radiation chemistry of cellulose since the UV grafting technique has been adopted in the works developed in this thesis (*Chapter 1, Section A*).

The chemical treatments can be carried on to vary properties such as hydrophilicity or hydrophobicity, elasticity, water sorbency, adsorptive or ion exchange capability, resistance to microbiological attack and thermal resistance. [264]

The glucopyranose units which make up the cellulose chain contain one primary hydroxyl group and two secondary hydroxyl groups. Functional groups may be attached to these hydroxyl groups through a variety of chemistries.

The crystalline structure commonly found in native cellulose (Cellulose I) can be irreversible converted to its polymorphic form cellulose II by swelling cellulose in concentrated (~20%) NaOH solution (mercerization).[265]

Mercerization makes the hydroxyl groups of the cellulose macromolecules more accessible, decreases the cellulose crystalline content, and increases the tensile strength and modulus. [266, 267]

Two large categories of commonly used cellulose derivatives, cellulose esters and cellulose ethers should be mentioned. Cellulose succinate and carboxymethyl cellulose are two examples. Carboxymethyl cellulose (CMC) is a cellulose derivative with carboxymethyl groups (–CH_2–COOH) bound to some of the hydroxyl groups of the glucopyranose units of the cellulose backbone. [268] CMC can be prepared by treating cellulose with monochloroacetic acid and sodium hydroxide. Slight modification results in high improvement in accessibility.

Other treatment which can be done are for instance, halogenation and oxidation.

An important chemical modification of the cellulose is grafting. There is an intensive research with different grafted materials and the continuously increasing knowledge in the near future will allow careful selection of the grafted polymer for a given application. [269]

Graft copolymerisation is a process in which side chain grafts are covalently attached to a main chain of a polymer backbone to form branched copolymer. The extent of polymerisation graft is referred to as the degree of grafting (grafting yield) and is gravimetrically determined as the percentage of mass increase following copolymer preparation. Both the backbone and side chain grafts can be either homopolymer or copolymer. The active sites initiating polymerisation reactions may be free radical or ionic chemical groups. [270] Various methodologies including high energy radiation, photochemical and chemical initiation techniques have been used to activate or initiate the backbone cellulose polymer. [271] Initiation methods which generate free radicals have received the greatest amount of attention due to their practicality. Free radicals are formed on the cellulose molecules either by decomposition of a chemical initiator, ultraviolet (UV) light or high energy radiation.[272]

I.B.5.1 Radiation chemistry of cellulose

The radiation-induced reactions in the macromolecules of the cellulose are initiated through rapid localization of the absorbed energy within the molecules to produce highly reactive intermediates, long- and short-lived free radicals, ions, and excited states. [273, 274] Some of the radical species decay rather slowly: they are observable by EPR spectroscopy days after the irradiation. [275]

During irradiation of cellulose radicals are formed with localized unpaired electrons mainly in positions 1 and 4 of the pyranose ring. The most probable process is the dehydration of the radicals with double bond formation in the pyranose ring yielding allyl type radical (Figure 5). [276-278]

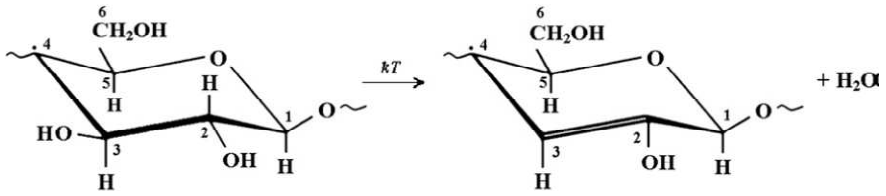

Figure I.B.5. Dehydration ofC4centredradicaltoallyltyperadical[279].

Free radicals are formed on the cellulose molecules either by decomposition of a chemical initiator, ultraviolet (UV) light or high energy radiation. Radiation-induced radical reactions in polymers may lead to chain scission (decreasing the molecular weight of polymer), and crosslinking (increasing the molecular weight of polymer)[280], cellulose belongs to the class of radiation degradable polymers. It has been observed that during irradiation, radicals produced in amorphous regions decay quickly, while others which are trapped in the crystalline and semi-crystalline regions (the interphase between the crystalline and amorphous regions) of the cellulose structure decay more slowly. The long lasting radicals may initiate polymerization during pre-irradiation grafting. When cellulose is irradiated in the presence of air, the radicals on the polymer backbone react with oxygen forming peroxy (and by their reaction alkoxy) radicals as it is shown by EPR measurements .[281] The signal of the radicals is well detectable even after a month's storage at room temperature, however, its intensity decreases, and its shape also shows some changes indicating altered radical structures. The decrease of intensity is due to formation of hydroperoxides and peroxides. We show the reactions on a simplified reaction scheme:

(1) Cellulose $\xrightarrow{\text{Radiation}}$ R•

(2) •R+O_2→••ROO

(3) •ROO+Cellulose→ROOH+••R

(4) •2 ROO→ROOR+O_2

The crystalline structure of cellulose is not affected by irradiation up to several hundred kGy absorbed doses; there is no change in the ratios of the crystalline and amorphous regions either. [282]

References

(1) M. Perrin, Y.M. Saint-Drenan, F. Mattera, P. Malbranche. J. Power Sources (2005) 144, p.402

(2) B.Scrosati. Journal of Power Sources (2010) 195, p.2419

(3) M.Winte,r R. Brodd. Chem. Rev. 104, (2004) p.4245

(4) K. Ozawa. Book "Lithium ion Rechargable Batteries" (2009), Wiley-vch ed.

(5) M.Armand, J-M. Tarascon. Nature (2008) 451, p.652

(6) B.Scrosati. J Solid State Electrochem (2011), 15, p.1623

(7) J-M. Tarascon, M.Armand. Nature, (2001) 414, p.359

(8) A Patil, V. Patil, D. Wook Shin, J.W.Choi, D.S. Paik, S. Yoon. Materials Research Bulletin (2008) 43, p.1913

(9) J.P. Phipps, T.G. Hayes, P.M. Skarstad, D. Untereker. Solid State Ionics (1986) 18–19, p.1073

(10) H. Ikeda, S. Narukawa, S. Nakaido. Proc. 29th Power Sources Con, Electrochemical Society: Pennington, NJ, USA (1980)

(11) Kang Xu. Chem. Rev (2004) 104, p.4303

(12) Di Heinz Albert Kiehne, Book "Battery technology handbook"(2003), Marce Dekker Inc. Ed.

(13) B. Scrosati. Book "Advances in Lithium-ion Batteries" (2002) KA/PP ed.

(14) T. Shodai, S. Okada, S. Tobishima. Journal of Power Sources (1997) 68-2, p.515

(15) Takeda Yasuo (2000) US Patent 6566011

(16) Q.F. Dong C.Z. Wu and M.G. Jin,Solid State Ionics (2004) 167- 1-2, p. 49

(17) R. Huggins. Journal of Power Sources (1999)81-82, p.13 18

(18) Y.Idota, T. Kubota, A. Matsufuji, Y. Maekawa, T. Miyasaka. Science (1997) 276, p.1395

(19) O. Mao, R. A. Dunlap, J. R. Dahn. Journal of The Electrochemical Society (1999) 146-2, p.405

(20) M. Winter ,J.O. Besenhard. Electrochimica Acta (1999) 45- 1-2, p.31

(21) M. M. Thackeray Vaughey, J. T. Kahaian A. J. Keple,r K. D. Benedek. Electrochemistry Communications (1999)1- 3,4, p.111

(22) Idota (1995) US Patent 5478671

(23) P.Poizot, S. Laruelle, S. Grugeon, L.Dupont, J.M. Tarascon. Nature (2000) 407, p. 496

(24) A. Ohzuko, N. Ueda, N. Yamamoto. J. Electrochem. Soc. (1995) 142, p.1431.

(25) P. Kubiak, J. Geserick, N. Hüsing, M. Wohlfahrt-Mehrens. J. Power Sources (2008) 175, p.510.

(26) Bo Peng, Jun Chen. Coordination Chemistry Reviews (2009) 253, p.2805

(27) M Whittingham. Chem Rev. (2004), 104, p. 4271

(28) K. Mizushima, P.C.Jones, P.J.Wiseman, J.B. Goodenough. Solid State Ionics (1981) 7, p.314

(29) H. Gabrisch R. Yazami, B. Fultz. Journal of The Electrochemical Society (2004) 151, p.891

(30) J.R Dahn von Sacken, U. Juzkow. J. Electrochem. Soc., (1991) 138- 8, p.207

(31) Yuan Gao, M. V. Yakovleva, W. B Ebner. Electrochem. Solid State Lett. (1998) 1, p.117

(32) R. Armstrong, P. G.Bruce. Nature(1996) 381, p.499

(33) E. M.Jin, B. Jeon Y.S., Park K.H., Gu H.B. Journal of Power Sources (2009)189, p.620

(34) G. Amatucci, A. Du Pasquier, A. Blyr, T. Zheng and J. -M. Tarascon. Electrochem. Acta (1999) 45, p.255

(35) A.K Padhi, K. S. Nanjundaswamy, J. B. Goodenough. J. Electrochem. Soc. (1997),144- 4, p.1188

(36) A.S Andersson, J.O. Thomas. J.Pow.Sources (2001) 97-98, p. 498

(37) S. Franger, F. Le Cras, C. Bourbon, H. Rouault. Journal of Power Sources (2003)119–121, p. 252

(38) P. Prosini, D.Zane, M.Pasquali. Electrochimica Acta (2001) 46, p. 3517

(39) M.E. Arroyo-de Dompablo, M. Armand, J.M. Tarascon, U. Amador. Electrochemistry Communications (2006) 8-8, p.1292

(40) W. Dong, J. S. Sakamoto, B. Dunn. Sci. Technol. Adv. Mater. (2003)4, p.3

(41) M. Armand. Solid State Ionics(1994) 69, p.309

(42) B. Scrosati. Electrochimica Acta (2000)45, p.2461

(43) D.Aurbach. Book "Nonaqueous electrochemistry" (1999) Marcel Dekker Ed.

(44) C.G. Zoski. Book "Handbook of electrochemistry" (2007) Elsevier

(45) P. B. Balbuena, Y. Wang. Book "Lithium-ion batteries: solid-electrolyte interphase" (2004) Imperial college press

(46) Di Gholam-Abbas Nazri, G. Pistoia Book "Lithium batteries: science and technolgy" (2004) Kluwer Academics Pub.

(47) S. Zhang. Journal of Power Sources (2007) 164, p. 351

(48) D. Adam. Nature (2000) 407, p.938.

(49) W. Lu., Science 297 (2002) 983.

(50) P. Wang, S.M. Zakeeruddin, I. Exnar, M. Gr€atzel. Chem. Commun. (2002) p.2972

(51) S. Panozzo, M. Armand, O. Stephan. Appl. Phys. Lett. (2002) 8, p. 679

(52) T.Welton, Chem. Rev. (1999) 99, p.2071.

(53) R.D. Rogers, K. Seddon. Book "Ionic Liquids: Industrial Applications to Green Chemistry" (2002) ACS Symposium Series

(54) J Barisci. Electrochemistry Communications (2004) 6, 1, p.22

(55) S. Zhang, N. Sung, X. He, X. Lu, X. Zhang. J. Phys. Chem. Ref. Data (2006) 35, p. 1475.

(56) M. Galinski, A.Lewandowski, I.Stepniak. Electrochimica Acta (2006) 51, p.5567

(57) Y.S. Fung, S.M. Chau. J. Appl. Electrochem. (1993) 23, p. 346.

(58) D.R. MacFarlane, J. Huang, M. Forsyth. Nature (1999) 402, p.792.

(59) J. Shin, W. A. Henderso, S.Passerini. Electrochemistry Communications (2003) 5, p.1016

(60) G.B.Appetecchi, F.Croce, B.Scrosati., J. of Power Sources (1997) 66, p.77

(61) A.M.Stephan: European Polymer Journal, (2006) 42, p.123

(62) J.Y. Song Y. Y. Wang, C. C. Wan. Journal of Power Sources (1999)77, p.183

(63) P.G. Bruce. Electrochim Acta (1995) 40, p.2077.

(64) J. R. MacCallum, C.A. Vincent. Book "Polymer Electrolytes Reviews-2" (1989)Elsevier Applied Science, London

(65) J.L. Acosta, E.Morales. Solid state ionics, (1996) 85- 1,4, p.85

(66) A.Carlsson, B. Mattsson, J. Swensson, L.M. Torell, M. Käll, L. Börjesson, R.L. Solid State Ionics(1998) 113–115, p.139

(67) A. Killis, J.F. LeNest, H. Cheradame, A. Gandini. Macromol. Chem. (1982) 183, p..2835.

(68) D.W. Kim, J.K. Park, M.S. Gong, H.Y. Song. Polym. Eng. Sci.(1994) 34 - 97, p.1305.

(69) F.M. Gray. Book " Solid Polymer Electrolytes" (1991) F.M. Gray Ed VCH, New York

(70) A. Bouridah, F. Dalard, D. Deroo, H. Cheradame, J.F. LeNest. Solid State Ionics(1985) 15, p.233.

(71) P.M. Blonsky, D.F. Shriver, P. Austin, H.R. Allock. J. Am. Chem. Soc. (1984) 106, p.6854

(72) B. Laik L. Legrand, A. Chausse and R. Messina. Electrochimica Acta (1998) 44-5 p. 773

(73) R. Uchiyama K. Kusagawa, K. Hanai, N. Imanishi, A. Hirano, Y. Takeda. Solid State Ionics (2009) 180, 2-3, p. 205

(74) R.Maccallum, M.Smith, C. Vincent. Solid state Ionics (1984) 11, p. 307

(75) L.M. Ding. Polymer (1997) 38, 16, p. 4267

(76) D.W. Xia, D. Soltz, J. Smid. Solid State Ionics (1984) 14

(77)S. Sanderson, T. Zawodzinski, R. Hermes, J. Davey, H. Dai. Proceedings "Lithium Polymer Batteries" J. Broadhead, B. Scrosati Eds. The Electrochemical Society, NJ, (1997) 96, 17 p. 136.

(78) Gadjourova, Y Andreev, D.P Tunstall, PG Bruce. Nature (2001) 412, p.148

(79) M. C. Alasdair, J. L. Scott, E. Staunton, Y. G. Andreev, P. G. Bruce. Nature (2005) 433, p.50

(80)J.E. Weston B.C.H. Steele. Solid State lonics (1982) 7, 1, p. 75

(81) F.Croce, G. B. Appetecchi, L. Persi, B. Scrosati. Nature (1998) 394, p. 456

(82) M. Stephan, K.S. Nahm. Polymer (2006) 47, p. 5952

(83) W. Wieczorek. Solid State Ionics (1992) 53-56 p. 1064

(84) W. Wieczorek, J.R. Stevens, Z. Florjanczyk. Solid State Ionics (1996) 85, p. 76

(85) F. Croce, R. Curini, A. Martinelli, L. Persi, F. Ronci, B. Scrosati, R. Caminiti. ,J. Phys. Chem. B (1999) 103, p. 10632

(86) F. Croce, L. Persi, B. Scrosati, F. Serraino-Fiory, E. Plichta, M. A. Hendrickson. Electrochimica Acta (2001) 46, p. 2457

(87) S. Panero, B. Scrosati, S.G. Greenbaum. Electrochim Acta (1992) 37, p. 1533

(88) B. Kumar, L.G. Scanlon. J Power Sources (1994) 52 p. 261

(89) M.C. Borghini, M. Mastragonstino, S. Passerini, B. Scrosati. J Electrochem Soc (1995)142, p.2118.

(90) W J Kim, KS Ji, JP Lee, JW Park. J Power Sources (2003) 119

(91) D Golodnitsky, G Ardel, E Peled. Solid State Ionics (2002)147, p.141

(92) JH Shin, S Passerini. J Electrochem Soc (2004) 151, p. 238.

(93) Y. Ito, K. Kanehori, K. Miyauchi and T. Kudo. J. Mater Sci (1987) 22, p. 1845.

(94) F.B. Dias Lambertus Plomp, B.J Jakobert Veldhuis. Journal of Power Sources (2000) 88, p.169

(95) B. Sander, T. Steurich, K. Wiesner, H. Bischoff. Polym Bull (1992)28, p. 355.

(96) G. Nagasubramanian, S. Di Stefano. J Electrochem Soc (1990) 137, p. 3830.

(97) S. Bhattarcharya, S.W. Smort, D.H. Whitmore. Solid State Ionics (1986) 18–19, p. 306.

(98) D. Fauteaux, J. Prud Nommi, P.E. Hardey. Solid State Ionics (1988) 28, 30, p. 923.

(99) J. T. Benedict, S. Banumathi, A. Veluchamy, A.Z. Ahmed, S. Rajendran. J Power Sources (1998) 75, p.171.

(100) F.J. Moulin, P. Damman, Dosier. Polymer (1999) 40, p.171

(101) L. Song, Y. Chen, J.W. Evans. J Electrochem Soc (1997) 144, p. 3797

(102) T. Shodai, B.B. Owens, H. Ohtsuke, J. Yamaki. J Electrochem Soc (1994) 141, p.2978.

(103) E.H. Cha, D.R. Macfarlane, M. Forsyth, C.W. Lee. Electrochim Acta (2004) 50, p. 335.

(104) W. Huang, R. Frech. Polymer (1994) 35, p. 235.

(105) G.B. Appetecchi, W. Henderson, P. Villaco, M. Berrettonie, S. Passerini. J Electrochem Soc (2001) 148, p.1171.

(106) F.M. Gray, J.R. MacCallum, C.A. Vincent. Solid State Ionics (1986) 18–19, p.295.

(107) M. Watanabe M. Kanba, K. Nagaoka, I. Shinohara. Journal of Polymer Science: Polymer Physics Edition(1983) 21, 6, p.939

(108) H. Hong, C. Liquan, H. Xuejie, X. Rongjian. Electrochim Acta (1992) 37, p.1671

(109) D. Peraninage, D.M. Pasquariello, K.M. Abraham. J Electrochem Soc (1995) 142, p.1789.

(110) H.S. Choe, B.G. Carroll, D.M. Pasquarillo, K.M. Abraham. Chem Mater (1997) 9, p. 369.

(111) F. Croce, F. Gerace, G. Dautzenberg, S. Passerini, G.B. Appetecchi, B. Scrosati. Electrochim Acta (1994) 39, p. 2187.

(112) G.B. Appetecchi, F. Croce, P. Ramagnoli, B. Scrosati, U. Heider, R. Osten. Electrochem Comm (1999) 1, p.83.

(113) Z. Wang, B. Huang, H. Huang, L. Chen, R. Xue, R.F. Wang. J Electrochem Soc (1996) 143, p. 1510.

(114) Z. Wang, B. Huang, H. Huang, L. Chen, R. Xue, R.F. Wang. Electrochim Acta (1996) 41, p.1443.

(115) O. Bohnke, G. Frand, M. Rezrazi, C. Rousselot, C. Truche. Solid State Ionics (1993) 66, p.97.

(116) S. Rajendran, T. Uma, T. Mahalingam. Ionics (1999) 5, 3-4, p. 232

(117) P.E. Stallworth, S.G. Greenbaum, F. Croce, S. Slane, M. Salomon. Electrochim Acta (1995) 40 p. 2137.

(118) F. Croce, S.D. Brown, S.G. Greenbaum, S.M. Slane, M. Salomon. Chem Mater (1993) 5, p. 1268.

(119) J. Vondrak, M. Sedlarikova, J. Velicka, B. Klapste, V. Novak Reiter. J.Electrochim Acta (2001) 46, p. 2047.

(120) G.B. Appetecchi, B.Scrosati. Electrochimica Acta (1995) 40, 8, p. 991

(121) N.S. Mohamed, A.K. Arof. Journal of Power Sources (2004)132, p. 229

(122) S.S. Sekhon, Harinder Pal Singh. Solid State Ionics (2002)152– 153, p. 169

(123) K.M. Abraham. Book " Applications of Electroactive Polymers" (1993) B. Scrosati (Ed.) Chapman & Hall, London.

(124) J.-M. Tarascon, A.S. Gozdz, C. Schmutz, F. Shokoohi, P.C. Warren, Solid State Ionics (1996) 86– 88, p. 49.

(125) K.H. Lee, K.H. Kim, H.S. Lim. J. Electrochem Soc (2001) 148, p. 1148.

(126) H.Y. Song, Y.Y. Wang, C.C.Wan J. Electrochem Soc (1998) 145 p.1207.

(127) M. Stephan A.J Power Sources (2003) 119–121, p.460.

(128) M. Stephan A. Electrochim Acta (2003) 48, p. 2143.

(129) Basile and Nunes ed. Book "Energy Advanced membranes for sustainable energy and environmental applications" (2011)Woodhead publishing series

(130) A. M. Elmer and P. Jannasch. J Polym Sci B: Polym Phys (2007) 45, p. 79

(131) Y. Liu, J. Y,Lee, L. Hong. J Power Sources, (2004) 129, p. 303.

(132) P. Jannasch, P. Gavelin Patent WO 2001/47047 (2001)

(133) C. Michot, A. Vallee, P. Harvey, M. Gauthier, M. Armand. Patent US 2002/018364. (2002),

(134) P. Santhosh, A. Gopalan, T. Vasudevan, K Lee. Materials Research Bulletin(2006) 41, p. 1023

(135) Cheon-Soo Kim, Bo-Hyun Kim, Keon Kim Journal of Power Sources (1999) 84, p.12

(136) B. Rupp, M. Schmuck, A. Balducci, M. Winter, W. Kern European Polymer Journal (2008) 44, p.2986

(137) K Chen, H Huang PCT Patent WO 96/35238 (1996).

(138) M.-H. Ryou, Y.Min Lee, K. Y.Cho, GB Han, J-N. Lee, DJin Le, J. Wook Choi, J-Ki Park. Electrochimica Acta (2012) 60 p. 23

(139) A. Reiche, J. Tubke, R. S. Sandner, A. Werther, B. Sandner, G. Fleischer. Electrochim Acta, (1998) 43, p.1429

(140) B. Sandner, A. Weinkauf, A. Reiche, K. Siury, J. Tübke, S. Wartewig, S. Shashkov. Electrochim Acta, (1998) 43, p1263.

(141) K. H. Lee, K. H. Kim, H. S. Lim. J Electrochem Soc (2001) 148, p. 1148.

(142) M. Song, J. Cho, B. W. Cho, H. Rhee, J. Power Sources, (2002) 110, p. 209.

(143) J. J. Hwang and H. J. Liu. Macromolecules, (2002) 35, p. 7314.

(144) H. Jiang and S. B. Fang. J. Power Sources, (2006) 159, p. 673.

(145) J. Nair R., C. Gerbaldi, G. Meligrana, R. Bongiovanni, S. Bodoardo, N. Penazzi, P. Reale, V. Gentili. J. Power Sources, (2008), 178, p. 751.

(146) C. Gerbaldi, J. Nair, C. Bonatto Minella, G. Meligrana, G. Mulas, S. Bodoardo, R. Bongiovanni, N. Penazzi. J Appl Electrochem, (2008), 38, p.985.

(147) N. Penazzi, S. Bodoardo, R. Bongiovanni, C. Gerbaldi, G. Meligrana, G. Mulas, J. Nair. Fuel Cells, (2009), 9, p. 273.

(148) C. Gerbaldi, J. R.Nair, G.Meligrana, R. Bongiovanni, S. Bodoardo, N. Penazzi. Electrochim Acta (2010) 55, p.1460.

(149) C. Gerbaldi, J. R. Nair, S. Ahmad, G. Meligrana, R. Bongiovanni, S. Bodoardo, N. Penazzi. J Power Sources (2010) 195, p. 1706.

(150) C. Gerbaldi, J. Nair, G. Meligrana, S. Bodoardo, R. Bongiovanni, N. Penazzi. J Appl Electrochem (2009) 39, p. 2199.

(151) C. Gerbaldi. Ionics (2010) 16, p. 777.

(152) J. R. Nair, C. Gerbaldi, M. Destro, R. Bongiovanni, N. Penazzi. React Funct Polym, (2011),71-4 p. 409.

(153) G. Bates W. Dudney S. Weatherspoon. Patent number: 5561004- 1994

(154) N.S. Choi, Y. M. Lee, J. Hwa Park, J.-Ki Park. Journal of Power Sources (2003) 119–121, p. 610.

(155) M. Popall, R. Buestrich, G. Semrau, G. Eichinger, M. Andrei, W.O. Parker, S. Skaarup, K. West. Electrochimica Acta (2001) 46, 10–11, 15 p. 1499

(156) M. Destro, J. R. Nair, C. Gerbaldi, G. B. Appetecchi, M. Montanino, S. Bodoardo, R. Bongiovanni, N. Penazzi Congress book of abstract LiBD-5 2011 – Electrode materials - Arcachon, France 12-17 Juin 2011

(157) W.F. Schortmann, U.S. Patent 5,204,165 (1993).

(158) S.J. Law, H. Street, G.J. Askew, U.S. Patent 6,358,461 (2002).

(159) J.F. Audebert, H.J. Feistner, G. Frey, R. Farer, G.L. Thrasher. Patent PCT/US2002/035924 (WO 2003/043103) (2003).

(160) S. Tasaki, M. Nagai, N. Ando. Japanese Pantent JP 2006/324767 (WO 2007/072713) (2007) Fuji Jukogo Kabushiki kisha

(161) A. Gozdz. Patent PCT/US2002/028784 (WO/2003/029524) (2003) Telcordia Technologies Inc.

(162) W. Huang. Patent PCT/US2001/030509 (WO/2002/027820) (2002) Eveready Battery Company Inc.

(163) T. Tsukuda, H.Funae. Patent PCT/JP1998/000113 (WO/1998/032184) (1998) Mitsubishi Paper Mills

(164) G.MacGlashan, C. Marshall, S.Read. Patent PCT/EP2002/004470 (WO/2002/091500) (2002)

(165) I.Kuribayashi J. of Power sources, (1996), 63, 1, p. 87

(166) A.D. Pasquier, A. Gozdz, I. Plitz, J. Shelburne. 201st meeting of The Electrochemical Society, Philadelphia, May 12-17 (2002).

(167) Zhang, Xia-Chang, Patent WO 2008/096033 (2008) Enfucell

(168) T. Danko, Properties of cellulose separators for alkaline secondary batteries. Proceedings of the 10th Annual Battery Conference on Applications & Advances, IEEE: New York, (1995).

(169) M.A.S. Azizi Samir, Fannie Alloin, Jean-Yves Sanchez, and Alain Dufresne. Polymer (2004) 45, p. 4149

(170) M.A.S. Azizi Samir, A. Montero Mateosa, F. Alloin, J.Y. Sanchez, Alain Dufresne. Electrochimica Acta (2004) 49, p. 4667

(171) M.A.S. Azizi Samir, L .Chazeau, F.Alloin, J.Y. Cavaillé, A. Dufresne and J.Y. Sanchez. Electrochimica Acta (2005)50, p. 3897

(172) F.Alloin, A.D'Aprea, N.Kissi, A.Dufresne, F.Bossard, Electrochimica Acta (2010) 55, p. 5186

(173) S. Yano, T. Sawaguchi, T. Hagiwara, H. Hyogo, M. Nakajima, K. Sasaki. Patent US 2008 0220333 (2008)

(174) M. Chemelcki, W.H. Meyer, G.Wegner. Journal of applied polymer science (2007) 105,1, p. 25

(175) Z Yue, J.M.G Cowie. Polymer (2002) 43, 16, p. 4453

(176) Z. Yue, I.J. McEwen, J.M.G. Cowie. Solid State Ionics (2003) 156, p. 155

(177) D.Q. Nquyen Ji-hee Oh, Hyunjoo Lee, Hoon Sik Kim and Sang Deuk Lee. AIChE Spring National Meeting -New Orleans, LA 4/6-10/2008.

(178) Z.Ren, Y. Liu, K. Sun, X. Zhou and N. Zhang. Electrochimica Acta (2009) 54, p. 1888–1892

(179) A.Wendsjo, S.Yde-Andersen Patent PCT/EP1997/007275 (WO/1998/028812) (1998) Danionics A/S

(180) Kim Suwon Patent US 2005 0238958 (2005)

(181) N Stefan Hochgatterer S. Koller M. Rene M. Winter A C. Wurm APerner Thomas Wohrle Patent US 2010 0239915 (2010)

(182) Jan Dee Kim Seok Kim Su Suk Choi Ji Seong Han Patent US 2004 0234851 (2004)

(183) B. Lestriez, S. Bahri, I. Sandu, L. Roué and D. Guyomard Electrochemistry Communications(2007) 9, p.2801

(184) J. Li, R. Klöpsch, S. Nowak, M. Kunze, M. Winter, S. Passerini. Journal of Power Sources (2011) 196, p. 7687

(185) S.S. Jeong, N. Böckenfeld, A. Balducci, M. Winter, S. Passerini. Journal of Power Sources (2012) 199, p.331

(186) L. Jabbour, C. Gerbaldi, D.Chaussy, E.Zeno, S. Bodoardo, D. Beneventi J. Mater. Chem. (2010) 20, p. 7344

(187) V. L. Pushparaj, M. M. Shaijumon, A. Kumar, S.Murugesan, L. Ci, R.Vajtai, R. J. Linhardt, O. Nalamasu, P. M. Ajayan. PNAS (2007) 104, 34, p.13574

(188) G. Nyström, A. Razaq, M. Strømme, L. Nyholm,A. Mihranyan. Nano Lett. (2009) 9-10, p. 3635.

(189) L. Hu, H. Wu, F. La Mantia, Y.Yang, Y. Cui. ACS Nano (2000) 4-10, p. 5843

(190) Faucitano, A., Buttafava, A., Camino, G. & Greci, L., T rends Polym. Sci. (1996) 4, p.92.

(191) G. L. Collins, J. R. Costanza. J. Coat. T echn. (1979) 51, 648, p. 57.

(192) C. Decker. J. Polym. Sci., Polym. Chem. (1983) 21, p. 2451.

(193) A. Endruweit, M.S. Johnson, A.C. Long, Polymer composites (2006) 27, p. 119

(194) S. Black. Compos. Technol (2004) 10, p. 34

(195) Oldring, P. K. T. (ed.), Book "Chemistry and Technology of UV and EB Formulation for Coatings, Inks and Paints" (1991) SITA Techn., London Vols 1-5.

(196) Decker, C Polymer International (1998) 45, p. 133

(197) J. P. Fouassier, J.F. Rabek, (eds), Book " Radiation Curing in Polymer Science and Technology" (1992) Chapman and Hall, London, Vols 1-5.

(198) J. P. Fouassier. Book " Photoinitiator, Photopolymerisation and Photocuring" (1995) Hanser Publishers, Munich–Vienna–New York

(199) J. V. Crivello. Adv. Polym. Sci. (1984) 62, p.2.

(200) C. Decker. Progr. Polym. Sci., (1996) 21, p.593.

(201) C. Decker. Pigment Resin Technol. (2001) 30, p.278

(202). V.V. Krongauz, R.M. Yohannan. Polymer (1990) 31, p.1130.

(203). C. Decker, L. Keller, K. Zahouily, S. Benfarhi. Polymer (2005) 46, p. 6640.

(204) Norman S. Allen. J. Photochemistry and Photobiology A: Chem. (1996) 100

(205) S. Adanur and Y.Arumugham, J. Ind. Text. (2002) 32, p. 93

(206) J.V. Crivello. J. Polym. Sci. Part A: Polym. Chem., (1999) 37, p.4241

(207) E. J. K. Verstegen, J. H. P. Faasen, H. R. Stapert, P. C. Duineveld, and J. G. Kloosterboer: J. Appl. Polym. Sci. (2003) 90, p. 2364.

(208) Kevin D. Belfield, James V. Crivello. Book "photoinitiated polymerization" (2003) American Chemical Society

(209) Fouassier JP, Burr D, Crivello JV. J Macromol Sci (1994) 31, p.677

(210) S. Penczek, P. Kubisa, K. Matjaszewski. Advances In Polymer Science (1985) 68/69

(211) D. Roy, M. Semsarilar, J.T. Guthrie, S. Perrier. Chem. Soc. Rev. (2009) 38, p. 2046

(212) K. Kato, E. Uchid, En-Tang Kangc, Yoshikimi Uyamaa, Yoshito Ikadad. Prog. Polym. Sci. (2003) 28, p.209

(213) Y. Uyama, K. Kato, Y. Ikada Advances in Polymer Science (1998) 137-3

(214) L. Wojnarovits, Cs.M.Foldvary, E.Takacs. Radiation Physics and Chemistry (2010) 79, p. 848

(215) A.N. Wright. Nature (1967) 215, p 953

(216) Y .Ogiwara, M .Kanda, M. Takumi, H. Kubota. J Polym Sci, Polym Lett Ed (1981) 19, p.457.

(217) S Tazuke, Kimura H. Makromol Chem (1978) 179, p.2603.

(218). Allmer K, Hult A, Ranby B.J Polym Sci, Polym Chem (1988) 26, p. 2099.

(219) Ranby B. in: Allen N.S.; Edge M.; Bellobono J.R.; Selli E. (Eds.); Current Trends in Polymer Photochemistry, Ch. 2, Ellis Horwood, New York, 1995, p. 23.

(220) H. Ma, RH Davis, CN Bowman. Macromolecules (2000) 33, 2 p.331.

(221) K. Allmer, A. Hult, B. Ranby. J Polym Sci, Polym Chem (1989) 27, p.1641.

(222) K. Kato, E. Uchida, E. Kang, Y. Uyamaa, Y. Ikada. Prog. Polym. Sci. (2003) 28, p. 209.

(223) H. Kubota, S. Ujita; Journal of Applied Polymer Science,(1995) 56 ,1, p. 25.

(224) K. Allmer, J. Hilborn, P.H. Larsson, A. Hult, B. Ranby; J Polym Sci, Polym Chem (1990) 28, p. 173.

(225) P.Y. Zhang, B. Ranby. J Appl Polym Sci (1990) 40, p.1647.

(226) T.B. Stachowiak, F. Svec, J.M.J. Frechet, Chem. Mater. (2006) 18, p.5950.

(227) J.H. Liu, H.L. Jen, Y.C. Chung. J Appl Polym Sci (1999) 74, p.2947.

(228) K.W.Britt. Book: "Handbook of pulp and paper technology" New York : Reinhold ; London : Chapman and Hall, copyr. 1964

(229) J. Gullichsen, H. Paulapuro. Book: "Papermaking and science technology - Book 3: Forest Products Chemistry" (2000) Per Stenius ed.

(230) Confederation of European Paper Industries-CEPI- European Pulp and Paper Industry. Key statistic 2010

(231)R.J. Kerekes, C.J. Schell, J. Pulp Pap. Sci. (1992) 18 p.32.

(232) M. Samir, F. Alloin, A. Dufresne. Biomacromolecules (2005) 6, p. 612.

(233) M.N. Angles, A. Dufresne. Macromolecules (2000) 33 p. 8344.

(234) A. Dufresne, J.Y. Cavaille, W. Helbert. Macromolecules (1996) 29 p.7624.

(235) A. Dufresne, D. Dupeyre, M.R. Vignon. J Appl Polym Sci (2000) 76, p. 2080.

(236) Jue Lu, Tao Wang, L. T. Drzal Compsites Part A (2008) 39 p.738.

(237) I .Kvien, B.S. Tanem, K. Oksman. Biomacromolecules (2005) 6, p.3160

(238) M.N. Angles, A. Dufresne (2001) Macromolecules 34 p.2921.

(239) K. Fleming, D. Gray, S. Prasannan, S. Matthews. J Am Chem Soc (2000) 122, p.5224.

(240) Y. Habibi, A.L. Goffin, N. Schiltz, E. Duquesne, P. Dubois, A. Dufresne J Mater Chem 1(2008) 8, p.5002.

(241) G. Siqueira, J. Bras, A. Dufresne. Biomacromolecules(2009) 10, p.425.

(242) W. Helbert, J.Y. Cavaille, A. Dufresne. Polym Compos (1996) 17 p. 604.

(243) M. Grunert, W.T. Winter. J Polym Environ (2002) 10 p.27.

(244) M. Samir, F. Alloin, M. Paillet, A. Dufresne. Macromolecules (2004) 37 p. 4313.

(245) M. Henriksson, G. Henriksson, L.A. Berglund, T. Lindstrom. Eur Polym J (2007) 43, p. 3434.

(246) A.F. Turbak, F.W. Snyder, K.R. Sandberg. J Appl Polym Sci: Appl Polym Symp(1983) 37, p. 815.

(247) F.W. Herrick, R.L. Casebier, J.K. Hamilton, K.R. Sandberg .J Appl Polym Sci: Appl Polym Symp (1983) 37, p.797

(248) A.N. Nakagaito, H. Yano Appl Phys A: Mater Sci Process (2004) 78, 4 p. 547

(249) Z-M Huang, Y-Z Zhang, M Kotaki, S Ramakrishna Compos Sci Technol (2003) 63 p.2223

(250) S. Ramakrishna, K. Fujihara, W.-E. Teo, T. Yong, Z. Ma, R. Ramaseshan. Mater Today(2006) 9 p. 40

(251) D.M. Bruce, R.N. Hobson, J.W. Farrent, D.G. Hepworth. Compos Part A (2005) 26 p.1486

(252) A. Lopez-Rubio, J.M. Lagaron, M. Ankerfors, T. Lindstrom, D. Nordqvist, A. Mattozzi, M.S. Hedenqvist Carbohydr Polym (2007), 68, 4 p. 718

(253) K.P. Oza, S.G.J.J Frank. Dispersion Sci Technol (1986) 7, p. 543

(254) H .Ougiya, K. Watanabe, Y. Morinaga, F .Yoshinaga. Biosci Biotechnol Biochem (1997) 61, p.1541

(255) AJ Khopade, NK Jain. Drug Dev Ind Pharm (1990) 24, 3, p. 289

(256) M Andresen, L-S Johansson, BS Tanem, P Stenius. Cellulose (2006) 13, p.665

(257) M Andresen, P Stenstad, T Møretrø, S Langsrud, K Syverud, L-S Johansson, P Stenius Biomacromolecules(2007) 8, 7, p. 2149

(258) C Burger, BS Hsiao, B Chu. Annu Rev Mater Res. (2006), 36, p.333

(259) Syverud K, Stenius P Cellulose (2009) 16 p.75

(260) R.A. Horn USDA Forest service research paper FPL 242 (1995)

(261) H.E.Dadswell, A.B. Wardrop. Appita (1954), 12,1 p. 129

(262) G. Annergren, S. Rydholm, S. Vardheim. Svensk Papperstidn. (1963), 66, 6 p. 196.

(263) Confederation of European Paper Industries-CEPI website-Definitions. http://www.cepi.org

(264) D.J. McDowall, B.S. Gupta, V.T. Stannett Progress in Polymer Science, (1984), 10, 1 p. 1

(265) O.A. El Seoud, L.C. Fidale, N. Ruiz, M.L.O. D'Almeida, E. FrolliniC ellulose(2008), 15, p. 371

(266) J. Gassan, A.K. Bledzki Compos. Sci. Technol. (1999) , 59, p. 1303

(267) Cs.M. Földváry, E. Takács, L. Wojnárovits Radiat. Phys. Chem. (2003) , 67, p. 505

(268) I. Rácz, A. Deák, J. Borsa Text. Res. J. (1995), 65, p. 348

(269) L. Wojnárovits, Cs.M. Földváry, E. Takács Radiation Physics and Chemistry (2010) 79, 8, p.848

(270) M.M. Nasef, A.H. El-Sayed Progress in Polymer Science (2004) , 29, pp. 499–561

(271) A. Bhattacharya, B.N. Misra Progress in Polymer Science(2004), 29, 8, p. 767

(272) D.W. O'Connel, C. Birkinshaw, T. F. O'Dwyer. Bioresource Technology (2008) 99, 15,p. 6709

(273) A.G. Chmielewski, M. Haji-Saeid, S. Ahmed Nucl. Instrum. Methods Phys. Res. B.(2005), 236, p. 44

(274) C.P. Yang, Z.Q. Shen, G.C. Yu, J.L. Wang Biores. Technol. (2008) , 99, p. 6240

(275) L. Andreozzi, V. Castelvetro, G. Ciardelli, L. Corsi, M. Faetti, E. Fatarella, F. Zulli J. Colloid Interf. Sci. (2005), 289, p. 455

(276) B.G. Ershov, A.S. Klimentov Russ. Chem. Rev. (1984), 53, p. 1195

(277) B.G. Ershov, O.V. Isakova Russ. Chem. Bull. (1984), 33, p. 1171

(278) B.G. Ershov Russ. Chem. Rev. (1998), 67, p. 315

(279) S.I. Kuzina, A.I. Mikhailov Russ. J. Phys. Chem. (2006) ,80, p. 1666

(280) N. Pekel, F. Yoshii, T. Kume, O. Güven Carbohyd. Polym. (2004), 55, p. 139

(281) E. Takács, L. Wojnárovits, J. Borsa, J. Papp, P. Hargittai, L. Korecz Nucl. Instrum. Methods Phys. Res. B, (2005), 236 p. 259

(282) J.C. Arthur Jr. N.M. Bikales, L. Segal (Eds.), Book: "Cellulose and Cellulose Derivatives" Part V, Wiley Interscience, New York (1971)

CHAPTER II

COMPOSITE POLYMER ELECTROLYTES USING CELLULOSE MICROFIBRILS AS A REINFORCEMENT

Research efforts are nowadays focused on the development of polymer systems showing high ionic conductivity together with superior mechanical properties and stable performances since they can find practical applications as electrolytes in high energy density, thin and lightweight secondary Li-ion batteries[1–3]. In this respect, the need of a low cost, green, safe and up-scalable production process becomes fundamental for the sustainable mass production of the next generation energy storage systems.

As a possible answer to this request methacrylic-based thermo-set gel-polymer membranes obtained by a very easy, fast and reliable free radical photo-polymerisation process and reinforced with microfibrillated cellulose are here proposed.

Cellulose microfibrils (MFC) are easily available, biodegradable, they have high strength and stiffness, low weight and their preparation process is easy, low cost and does not involve chemical reactions[4-6], for all those reasons nano and micro-scale cellulose fibres serve as promising candidates for bio-composite production.

Two different membranes reinforced by MFC will be presented in this Chapter: in *Section A* the preparation and characterisation of an high

performing composite gel polymer electrolyte will be discussed, while in *Section B* a completely solid composite polymer electrolyte for high temperatures applications will be described.

In both cases, the composites prepared present excellent mechanical properties; at the same time good overall electrochemical performances are maintained, enlightening that such specific approach would make these hybrid organic, cellulose-based composite polymer electrolyte systems a strong contender in the field of thin and flexible Li-based power sources.

SECTION A

MFC reinforced gel polymer electrolytes

II.A.1. Materials and methods

1.1. Materials

Bisphenol A ethoxylate (15 EO/phenol) dimethacrylate (BEMA, average M_n: 1700), and poly(ethylene glycol) methyl ether methacrylate (PEGMA, average M_n: 475) were obtained from Sigma–Aldrich. 2-Hydroxy-2-methyl-1-phenyl-1-propanon (Darocure 1173) from Ciba Specialty Chemicals was used as the free radical photo-initiator. The 1.0 M LiPF6 in EC/DEC (1:1, w/w) solution (battery grade) was obtained from Ferro Corp., USA. The LiFePO4/C cathode material was synthesized in the form of nanostructured powder through a mild hydrothermal procedure developed at Politecnico di Torino[7,8]. Lithium metal foils with a thickness of 200 μm were obtained from Chemetall. Before their use, BEMA and PEGMA were kept open in the inert atmosphere of a dry glove box (Braun Labstar, O_2 and H_2O con-tent < 0.1 ppm) filled with extra pure Ar 6.0 for several days and, also, treated with molecular sieves (Molecular sieves, beads 4Å, 8–12 mesh, Aldrich) to ensure the complete removal of traces of water/moisture from the liquid monomers.

1.2. Microfibrils preparation

MFC particles were prepared by treating bleached cellulose fibres at high pressure in a microfluidizer processor (Microfluidics, model M-110 EH-30) with a 400 and 200 μm diameter chamber. Cycles were varied in order to optimize the fibrillation process[9]. A MFC aqueous suspension (1 % wt) was prepared.

1.3. Synthesis of the membrane

The reactive formulation for the preparation of gel-polymer membranes was based on BEMA, PEGMA in 50:50 ratio. 2-hydroxy-2-methyl-1-phenyl-1-propanon (Darocure 1173, Ciba Specialty Chemicals) was the free radical photo-initiator (2 % wt). The MFC suspension was added to the reactive formulation in different ratios in order to obtain composites containing 1, 3, 5% wt of microfibrils, respectively. The liquid mixture was left 12 hours in oven at 60 °C to obtain the water evaporation and subsequently UV irradiated for 3 min. under N_2 flux by using a medium vapour pressure Hg lamp (Helios Italquartz, Italy), with a radiation intensity of 30 mW cm^{-2}. Later, free, self standing films were peeled off from the glass plates and treated in vacuum at 70 °C overnight.

The MFC-polymer membranes were then swelled into a 1.0 M $LiPF_6$ in EC/DEC (1:1 w/w) solution (swelling time =2 hours; under inert atmosphere of an Ar-filled dry glove box (MBraun Labstar, O_2 and H_2O content\0.1 ppm).

1.4 Characterisation methods

Thickness measurement

The thickness of the reinforced membranes was measured with a Mitutoyo series 547 thickness gauge equipped with an ABSOLUTE Digimatic Indicator model ID-C112XBS, with a resolution of ± 1 µm and a max measuring force of 1.5 N.

Determination of the cross-linked fraction (gel-content)

The insoluble fraction (gel content) of the cured products was determined as described in the following, according to the standard test method ASTM D2765-84. The samples were held in a metal net, accurately weighed, and subsequently extracted with $CHCl_3$ to dissolve the non cross-linked polymer chains. Extraction included 24 h of residence time for the solvents to appeal the membranes at room temperature. The cross-linked fraction was then calculated by dividing the mass of the dry sample left after the extraction by the calculated mass of the original sample (relative error = ±1%).

Swelling percentage

The electrolyte uptake, indicating the quantity of liquid electrolyte present in the final Gel Polymer Electrolyte will be called Swelling percentage (SP%), it was calculated by the formula:

$$(Wf - Wi)/ Wf \times 100$$

where Wf is the weight of the membrane after swelling and Wi is the weight before swelling).

Dimentional stability

The dimentional stability of the polymer membranes to the swelling in the liquid electrolyte was calculated by measuring the variation of the volume of a sample after the swelling procedure; the samples used had a surface area of 4 cm^2. The values reported are calculated by the formula

$$(Vf - Vi/ Vi) * 100$$

Where Vf is the volume of the sample after swelling and Vi is the volume before swelling.

SEM analysis

Morphological characterization of the films was performed employing a FEI Quanta Inspect 200LV scanning electron microscope (SEM, max magnification of 1.5×10^5). Prior to analysis, all the samples were coated a thin Cr layer (thickness around 10 nm). Top analysis was performed in order to evaluate qualitatively the MFC dispersion. Test membranes were also broken under cryogenic conditions and a cross-sectional analysis was performed to estimate the uniformity of MFC filling across the membrane thickness.

Thermal analysis

The glass transition temperature (T_g) of the materials was evaluated by differential scanning calorimetry (DSC) with a METTLER DSC-30 (Greifensee, Switzerland) instrument, equipped with a low temperature probe. Samples were put in aluminium pans, prepared in a dry glove box. In a typical measurement, the electrolyte samples were cooled from ambient temperature down to –120 °C and then heated at 10°C min^{-1} up to 120°C. For

each sample, the same heating module was applied and the final heat flow value was recorded during the second heating cycle. The T_g was defined as the midpoint of the heat capacity change observed in the DSC trace during the transition from glassy to rubbery state. The thermal stability was tested by thermo-gravimetric analysis using a TGA/SDTA-851 instrument from METTLER (Switzerland) over a temperature range of 25 – 800 °C under N_2 flux (60 ml/min) at a heating rate of 10 °C min^{-1}.

Mechanical properties

Mechanical measurements on the polymer before swelling were carried out through tensile experiments according to ASTM Standard D638, using a Sintech 10/D instrument equipped with an electromechanical extensometer (clip gauge). At least five specimens for each sample were tested; the standard deviation in Young modulus (E) was 5 %. Mechanical properties after swelling were evaluated by a bending test for which the membranes have been rolled up around cylindrical hoses with radii ranging between 3 and 32 mm.

UV- VIS spectroscopy

Transmittance measurement were carried out by using a double beam UNIVAM UV2 spectrophotometer (ATI Unicam, Cambridge, UK) with variable slit width in a spectral range from 400 to 800nm, interfaced to a computer via "Vision 32"software for data elaboration.

Ionic conductivity measurement

The conductivity tests were carried out on a heating stepped ramp from 20 °C to 80 °C. The cells were housed in a Memmert GmbH oven model UFE-400 with a temperature control of ±1 °C. The resistance of the electrolyte was given by the high frequency intercept determined by analysing the impedance response using a fitting program provided with the Electrochemistry Power Suite software (version 2.58, Princeton Applied Research). Each sample was equilibrated at the experimental temperature for about 1 h before measurement, to allow thermal equilibration of the cells. All measurements

were carried out on at least three different fresh samples in order to verify the reproducibility of the obtained results.

Electrochemical stability measurement

The electrochemical stability window (ESW) was evaluated at ambient temperature by linear sweep voltammetry (Li metal as the reference electrode) using an Arbin Instrument Testing System model BT-2000. Separate tests were carried out on each polymer electrolyte sample to determine the cathodic and anodic stability limits. The measurements were performed by scanning the cell voltage from the open circuit voltage (OCV) towards 0.0 V vs. Li (cathodic scan) or 5.5 V vs. Li (anodic scan). In both cases, the potential was scanned at a rate of 0.100 mV s^{-1}. The current onset of the cell was associated with the decomposition voltage of the electrolyte. Cell configuration adopted for anodic scan: acetylene black (Shawinigan Black AB-50, Chevron Corp., USA.) over Al current collector and Li metal as electrodes and the given membrane as electrolyte (active area equal to 2.54 cm^2); cathodic scan: Cu foil and Li metal as electrodes and the given membrane as electrolyte (active area equal to 2.54 cm^2).

Lithium polymer cell assembly and electrochemical tests

The lithium polymer cell was assembled by contacting in sequence a lithium metal disk anode, a layer of the nanocomposite gel-polymer electrolyte and a $LiFePO_4$/C disk composite cathode (electrode area: 2.54 cm^2). The latter was prepared by a quick and low cost mild hydrothermal synthesis[7]. The electrodes/electrolyte assembly was housed in an Electrochemical Test Cell purchased from EL-Cell GmbH. Both electrode fabrication and cell assembly were performed in the environmentally controlled Ar-filled dry glove box. The lithium cell was tested for its electrochemical performance at room temperature in terms of charge/discharge galvanostatic cycling using an Arbin Instrument Testing System model BT-2000. The voltage cut-offs were fixed at 4.0 V vs. Li/Li^+ (charge step) and 2.5 V vs. Li/Li^+ (discharge step), respectively.

II.A.2. Results

2.1 Chemical and structural characterization of the polymer membranes

Liquid electrolyte-free polymer membranes were prepared by photo-copolymerising the di-functional methacrylic oligomer BEMA and the mono-functional PEGMA with the in situ addition of microfibrillated cellulose. Table II.A.1 shows the composition of the various salt-free solid polymer membranes prepared. A MFC-free sample, namely MFC-0, was made of only BEMA and PEGMA in 50:50 ratio. BEMA was chosen because it is well known that can be readily polymerised by UV-curing and form a cross-linked homopolymeric network, already employed as an electrolytic membrane. PEGMA, usually referred as reactive diluent, is meant to be useful to increase the mobility of Li^+ ions inside the polymer matrix along with an enhancement in the ionic conductivity through their pendant ethoxy groups. Membranes based on BEMA and PEGMA are described in previous works by Nair et al.[10,11]

	BEMA: PEGMA Ratio	MFC content (wt. %)	Gel-content (%)	Transmittance 400-800nm(%)	T_g (°C)	$T_{5\%}$ (°C)	$T_{10\%}$ (°C)	$T_{50\%}$ (°C)
MFC-0	50:50	0	93	87	– 56.2	225	285	377
MFC-1	50:50	1	92	42	– 53.2	249	286	377
MFC-3	50:50	3	82	10	– 54.0	265	300	379
MFC-5	50:50	5	80	7	– 53.4	275	312	386

Table II.A.1. Brief summary of the most relevant features of the synthesized polymer composite membranes

The polymer membranes obtained copolymerising the monomers with the in situ addition of cellulose microfibrils have a final thickness ranging between 150 and 500 μm, they are freestanding, extremely flexible and non-sticky, as shown in Figure II.A.1.

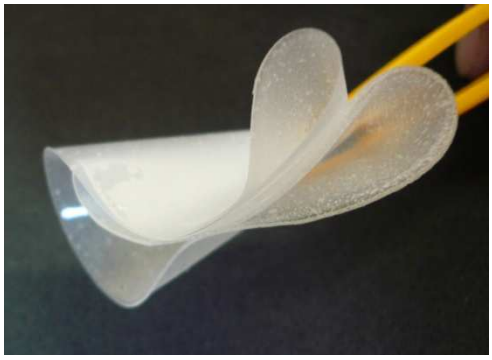

Figure II.A.1 . Appearance of the MFC3% polymer membrane obtained by copolymerising the monomers BEMA and PEGMA via UV irradiation with the in situ addition of the 3% of MFC in acqueous suspension.

In the absence of the filler the polymer is transparent while it becomes opaque increasing the quantity of microfibrils. Measurements performed by an UV-visible spectrophotometer in the range of the visible light (400-800nm) give for the neat membrane a value of transmittance of 87% indicating the effective transparency of the sample; when the 1%wt of microfibrils is added the value is halved to 42% and in presence of the 5%wt of additive it reaches the 7% indicating an opaque membrane (Table II.A.1).

The curing of the polymers have been evaluated by the measurement of the gel content and showed a decrease of the cross-linking in the presence of higher quantities of MFC. The obtained values are reported in Table II.A.1.

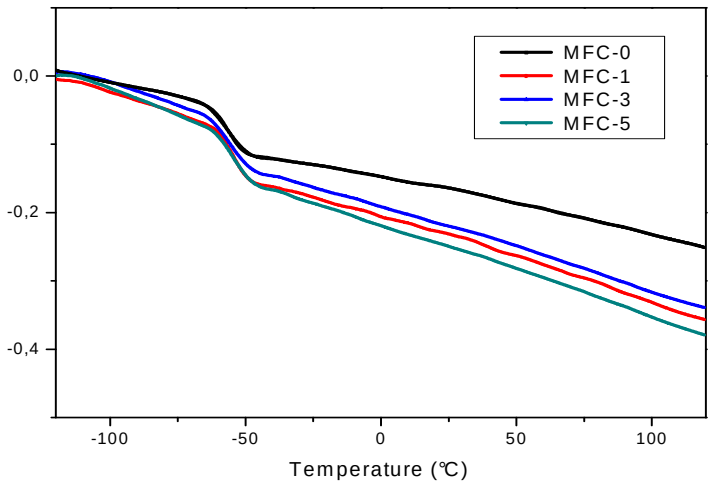

Figure II.A.2. DSC mesurements plot on the polymer composites membranes: the presence of MFC slightly increase the Tg values

Figure II.A.2 shows the curves obtained from the differential scanning calorimetry analysis performed in the range of temperatures between -120°C and 120°C. The plot evidences a Tg value of about -56°C for the copolymer indicating that at room temperature the membrane is in a rubbery state, the different percentage of filler in the polymer matrix does not modify in a significant way the DSC curve, however the Tg value in presence of the filler is increased even if only of a few degrees (Tab1). As clearly depicted in Fig. 1, though the Tg is very low, the membranes are self standing, extremely flexible and easy to handle.

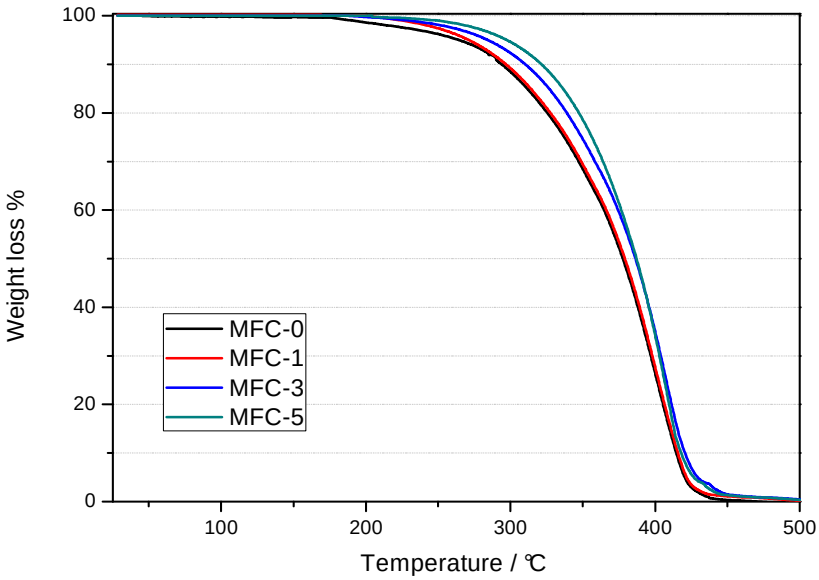

Figure II.A.3. TGA mesurements on the polymer composites membranes: the presence of MFC improves thermal stability

Figure II.A.3 shows the thermal stability of the membranes that has been assessed by Thermogravimetrical-analysis. The main degradation temperatures ($T_{5\%}$, $T_{10\ \%\ and}$ $T_{50\ \%}$) are collected in Table II.A.1. The neat membrane starts degradating at 225°C (where the weight loss is 5%) . The reinforced membranes can be used up to higher temperatures depending on the MFC content, in particular 5% of MFC assure stability up to 275°C.

The morphology of the MFC composite polymers was characterised by SEM analysis. SEM micrographs were obtained, for both surfaces and cross-

sections, on all the samples in order to observe the dispersion of MFCs into the polymer matrix. Some examples are shown in Fig. 4, illustrating that MFCs were uniformly dispersed, whatever the spot probed in the sample. The composite appear highly homogeneous, showing a complete interpenetration between the fibres network and the polymer: cellulose microfibrils are completely covered by the polymer matrix. In Fig. 5 the cross-sectional images, at different magnification, of the sample with 3% of MFC is shown. A good affinity between the matrix and the filler was obtained even without functionalization of MFCs. This could be attributed to the good compatibility resulting from the chemical similarities between the polymer characterized by ethoxy groups and MFCs and, consequently, the hydrogen bonding interactions existing at the interface. For all the composite samples, it was observed a homogeneous dispersion of white dots that were associated with the presence of microfibrils. These white dots do not correspond to isolated particles since the particle dimensions were too small to be observed at this scale. As already reported by Dufresne and co-workers[12,13], the white dots result from charge concentration effects due to the emerging of cellulose microfibrils from the observed surface, which increase the apparent cross-section of MFCs present over the surface. It is worth noting that white dots are homogeneously dispersed within the polymer matrix with no apparent formation of large aggregates, suggesting good compatibility between fillers and matrix. Such uniform distribution of the fillers in the matrix could play an important role in improving the mechanical performance of the resulting composite films.

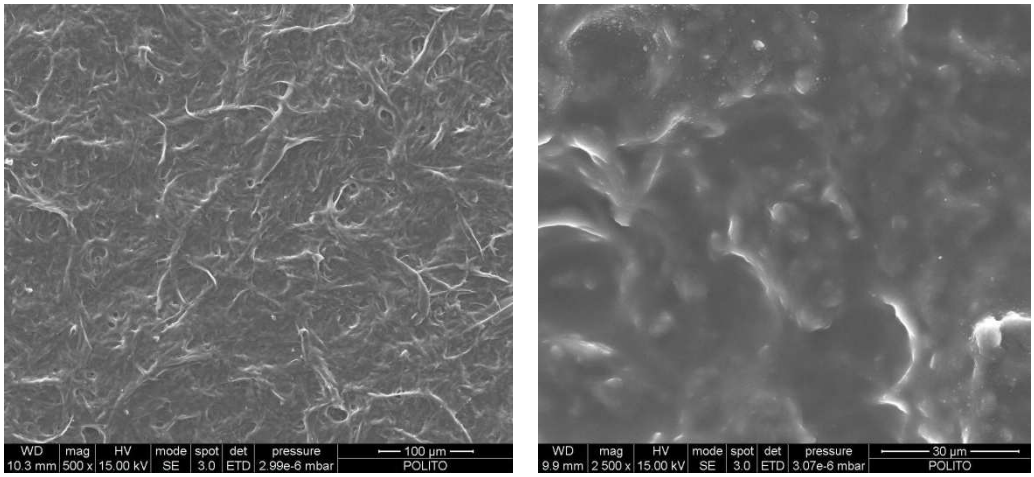

Figure II.A.4. SEM images of the polymer composite membrane MFC3 at different magnitudes (2500x left -a- and 5000x right -b-). It´s possible to observe that the cellulose microfibrils are completely surrounded by the polymer matrix.

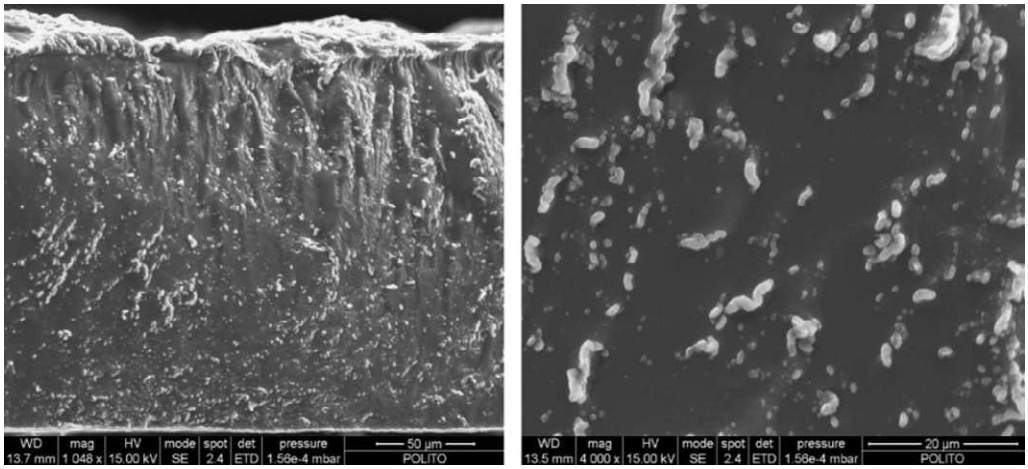

Figure II.A.5. Cross-sectional SEM images of the composite polymer membrane MFC-3 at different magnitudes: ~1000× left and 4000× right.

Compared to the acrylic based membranes described in literature[10,11] which already had good thermal and electrochemical properties, this composite polymer shows an important improvement in mechanical properties obtained by means of tensile test studies. As shown in Table II.A.2 the addition of microfibrils can widely increase the Young's modulus and the tensile resistance, leading to values that are satisfactory for the possible application in tin flexible batteries. The curves stress / strain obtained from the tensile test show an elastic behaviour of the samples (Figure II.A.6).

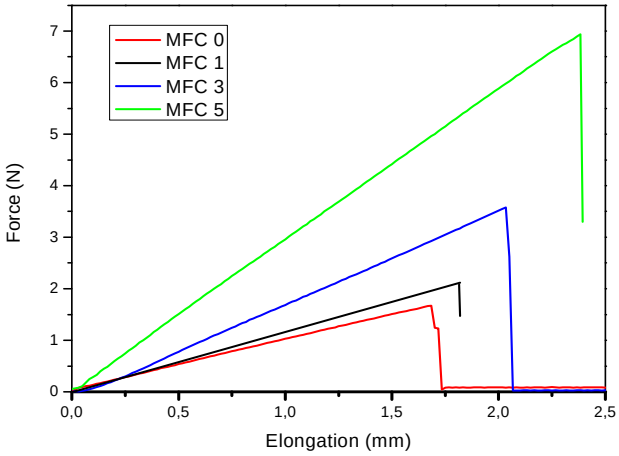

Figure II.A.6. Curve Force vs Elongation obtained from the tensile tests of the polymer membranes.

Sample	*Young's Modulus (MPa)*	*σ max (MPa)*
MFC 0	12 ± 2	0,5 ± 0,35
MFC 1	20 ± 3	0,9 ± 0,4
MFC 3	42 ± 4	2,1 ± 0,6
MFC5	79 ± 6	3,5 ± 0,3

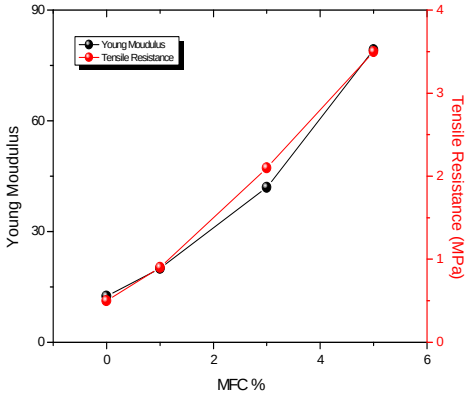

Table II.A.2 Young's modulus and resistance to traction of the polymer composite membranes. The figure on the right shows how improves Young´s modulus increasing the quantity of filler

Such an excellent mechanical behaviour may also improve the safety features of the Gel Polymer Electrolyte (GPE) membranes, in fact the cellulose fibres, being highly crystalline and very strong, can block the growth of lithium dendrites.

2.2 Gel polymer electrolyte characterisation

The composite membranes were swelled in the electrolyte solution made of 1.0 M LiPF6 in EC/DEC (1:1,w/w). The quantity of electrolyte uptaken will be

called Swelling percentage (SP%). The SP% measured for the neat membrane and the reinforced ones are reported in Table II.A.3.

Sample	*Active Swelling %*	*Dimensional Changes %*
MFC 0	51	35
MFC 1	55	30
MFC 3	59.5	20
MFC5	57	18

Table II.A.3. Swelling Percentage of the samples

It was observed that the dimensional stability of the membranes is remarkably increased by the presence of the filler; after swelling the MFC-0 membrane has an increase in volume of the 35% while in the presence of only 3% of MFC the dimensional variation is already reduced to the 20%.

The mechanical properties of the swelled membranes have been tested in terms of bending test since it was not possible to perform correctly the tensile test on wet membranes. Also after swelling the membranes containing MFC showed better mechanical behaviour. The bending test performed on the membranes MFC 0 and MFC 3 after swelling for 2 hours in a EC:DEC (1:1) mixture demonstrate that the MFC-3 membrane can still be easily rolled up on the cylinders used for the test withstanding all the bending radius till 3 mm. While the membrane without microfibrils is hard to handle and it breaks if bended on a cylinder with a 10mm radius. Figure II.A. 7 shows the aspect of the membranes after swelling.

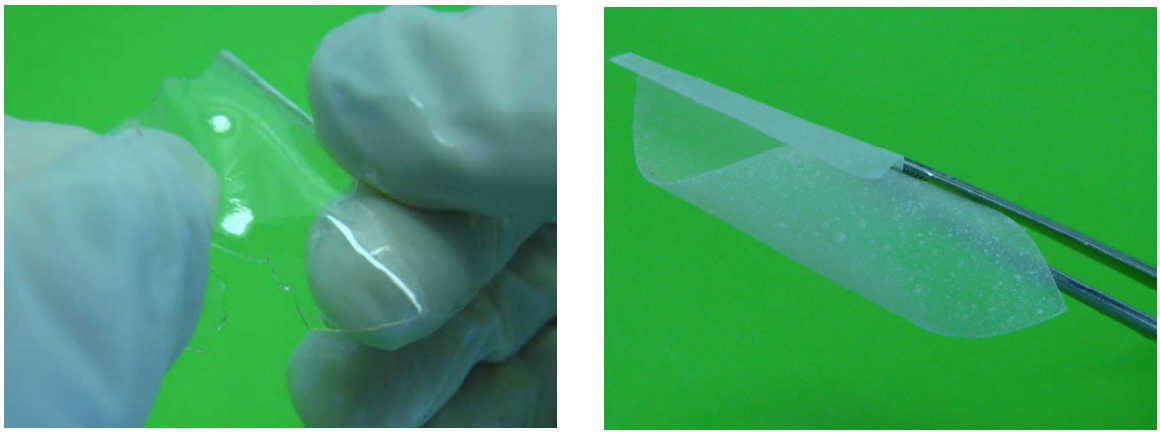

Figure II.A.7. Appearance of the MFC 0 (a) and MFC 3 (b)gel- polymer composite membrane. After a 2hrs swelling the MFC 0 membrane can not be handled while the MFC3 it´s easily bendable.

The thermal stability of the membrane MFC-3 after swelling has been evaluated by TGA analysis, the resulting curve is shown in Fig.8 where it is compared to the curve obtained before swelling. In the thermogram of the GPE there is a continuos weight loss up to 250°C, then the weight remain stable for about 10°C, finally there is a further degradation to a constant weight (3,4% at 450°C). It is possible to observe that the complete evaporation of the organic solvent, that is considered at 250 °C confirms the active swelling percentage: 55 %. After 250° C it is possible to observe the decomposition of the polymer composite. While for the membrane before swelling the residue at high temperature is around 0,6 % and is completely attributable to the presence of cellulose ashes, for the membrane after swelling the residue has higher values (3,4 %) that are explainable considering the presence of the Lithium salt.

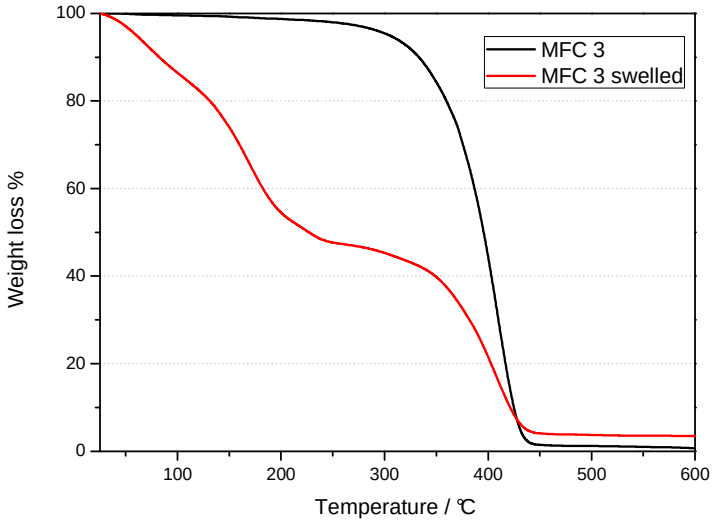

Figure II.A.8. TGA measurements on MFC-3membrane before and after swelling

2.3Electrochemical characterisation

In view of their application in lithium batteries, we first screened the samples by determining their ionic conductivity. The ionic conductivity of all the samples is evaluated by impedance spectroscopy. Figure II.A. 9 shows the impedance response, in the form of Nyquist plots, of four independent cells formed by sandwiching the given electrolyte membrane sample between two blocking stainless-steel electrodes, recorded after one week of storage at room temperature.

The intercepts with the real axis allow calculation of the conductivity values of the membranes. Notably, in the whole investigated frequency range, no signs of charge transfer or passivating layer formation are detectable. A linear response, as typically expected for blocking electrodes, indicates that our membranes do not undergo unexpected collateral reactions or undesired phenomena when placed in contact with the stainless steel electrodes.

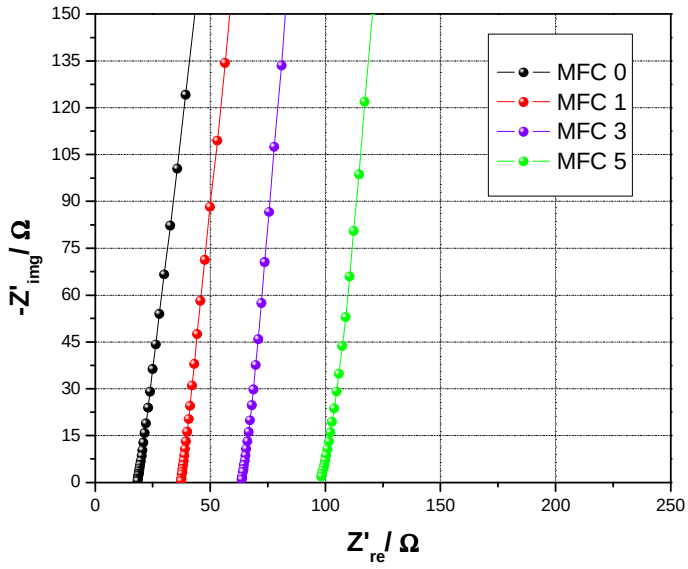

Figure II.A.9. Typical impedance response of the four gel-polymer electrolyte mem-branes developed in this study. Stainless-steel blocking electrodes. Fre-quency = 1 Hz–100 kHz.

Fig. 10 shows the temperature dependence of the ionic conductivity of the membranes in the form of Arrhenius plots. The MFC-0 sample displayed the highest conductivity in the whole range of temperatures investigated in this study, attaining values of the order of 10^{-3} S cm^{-1} at room temperature. The membranes containing the filler showed a slightly lower conductivity, in particular MFC-1(6,4 10^{-4} at room temperature), while MFC-3 and MFC-5 behave almost in the same way. The ionic conductivities of the MFC membranes are about 6×10^{-4} S cm^{-1} at room temperature and they increase with the increase of the temperature, reaching a high value of about 3×10^{-3} S cm^{-1} at 80 ◦C. The regular increase in conductivity upon heating is observed for all the membranes and confirms that neither physical transitions nor segregation phenomena occurred during the test. Moreover, all impedance spectra obtained in the selected temperature range do not show any sign of high-frequency semicircles which could indicate lack of gel homogeneity due to phase separation.

It is also possible to see from the Arrhenius plots that the conductivity behaviour of the samples MFC-3 and 5 is the most similar to the MFC-0 one, while the worst performance is given for the sample MFC-1. Such a result

could be due to the lower polymerisation level of the samples MFC-3 and 5 as indicated by the values of the gel content (Table II.A.1). A lower conversion of the oligomers leads to a more mobile network and, moreover, the unreacted monomers can be easily replaced by the swelled electrolyte.

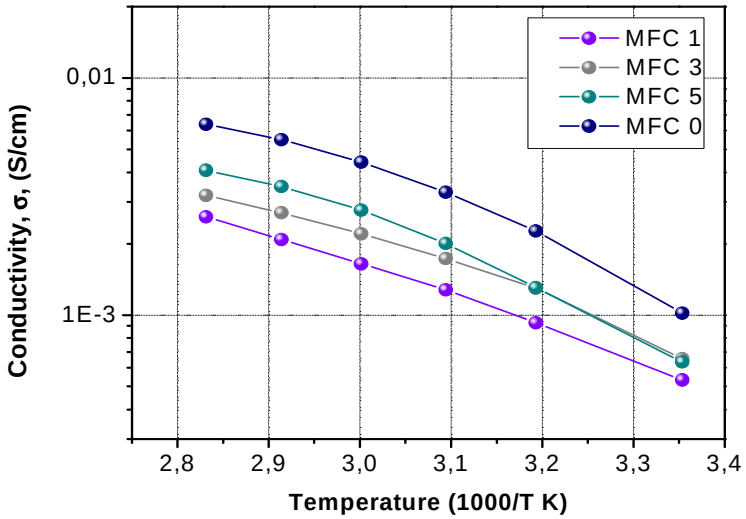

Figure II.A.10. Ionic conductivity Arrhenius plots of the four composite polymer elec-trolytes developed in this work. Data obtained from impedance spectroscopy.

The electrochemical stability window (ESW) is a fundamental parameter regarding cycling reversibility. In general, for a lithium battery, the anodic reaction occurs in the vicinity of 0 V vs. Li/Li^+, while the cathode potentials can approach values as high as 4.5 V vs. Li/Li^+. The ESW of the MFC-3 composite polymer electrolyte measured at ambient temperature is depicted in Fig. 11A and B.

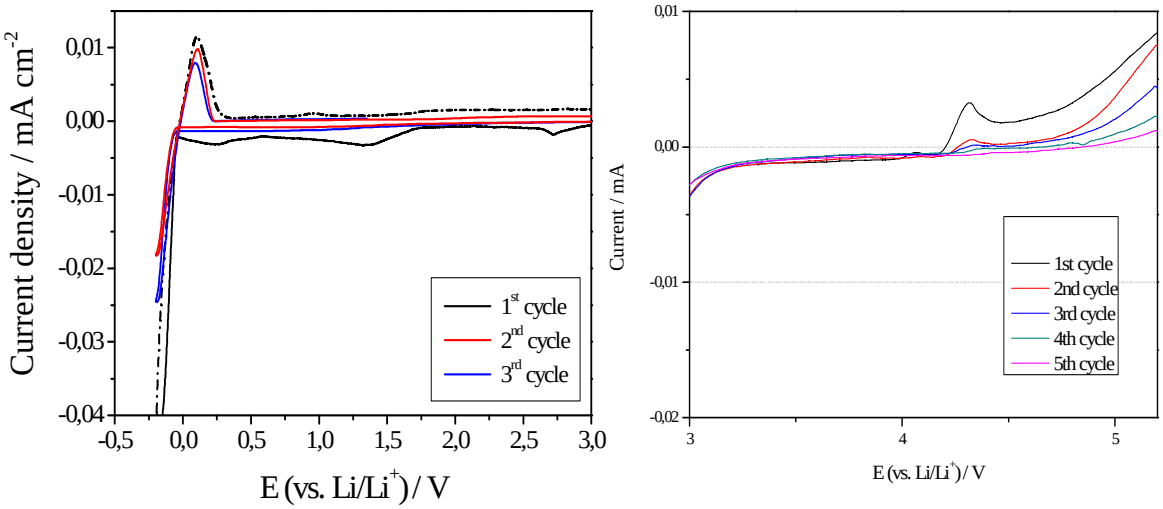

Figure II.A.11. Electrochemical stability window (ESW) of MFC-3 at 25 ◦C; potential scan rate of 0.100 mV s−1. (A) Electrochemical stability window in the cathodic voltage range and (B) electrochemical stability window in the anodic voltage range

MFC 3 is representative for all the samples prepared, in fact, independently of the amount of MFC added, all samples exhibited a wide ESW ranging from the lithium plating to around 5.0 V vs. Li/Li+. Considering the cathodic stability the current–voltage traces (Fig. 9A) showed in the first sweeping cycle a current flow at about 2.7 V vs. Li/Li+, followed by a large current flow starting at around 1.5 V. The first event is most probably due to some decomposition of the cellulosic material, while the latter is associated with a multistep decomposition process, very likely due to the reduction of the carbonate solution component, with the consequent formation of a passivating film on the testing electrode. This interpretation is supported by a series of findings, such as: (a) the irreversibility of the peaks, and (b) the trend of the second sweep cycle where no marked trace of events is detected. The current flow in the 0.25 V voltage range can be ascribed to another sort of "passivation" phenomenon, as the peak is clearly visible during the first cycle which immediately disappears with subsequent cycling. As a whole, the Figure II.A.11.A illustrates a cathodic scan starting from the open-circuit voltage and extending down to the lithium deposition range, i.e., to −0.2 V vs. Li/Li+. The lithium deposition–lithium stripping peaks on and from the copper substrate are clearly visible [14]. The increase of the current during the

first anodic scan, which is related the decomposition of the electrolyte, was taken in correspondence to the onset of a low current peak at approx. 4.3 V vs. Li/Li+. However, even if the current rises at a lower voltage, after few cycles its trend consistently deviates from that observed in the first cycle, showing a sort of "passivation" phenomenon which extends the anodic stability up to higher voltage, i.e., above 5 V vs. Li/Li+.

Three important features can be derived by the ESW results, namely: (a) the anodic onset of the current is detected at around 5 V vs. Li/Li+, which is assumed as the membrane decomposition voltage, i.e., a value high enough to allow a safe use of the membrane in connection with Li-ion electrode couples which typically cycle above 3.5 V; (b) the occurrence of a reversible cathodic peak around 0 V related to the lithium deposition-stripping process on the copper electrode, which demonstrates the applicability of these membranes for lithium rechargeable batteries; and (c) the very flat current–potential curves between the two limits, which is a clear evidence of the purity and the integrity of the membranes and of the efficient preparation method adopted.

High ionic conductivity and wide electrochemical stability window are highly welcomed properties in battery applications; hence, we selected the MFC-3 membrane and concentrated our attention on this membrane for further characterization. A laboratory scale lithium cell was assembled by combining a lithium metal anode with a LiFePO4/C cathode and using the MFC-3 as the electrolyte. It was tested in order to evaluate the capability of the electrolyte to perform in a real battery configuration. Its electro-chemical behavior was investigated by means of galvanostatic charge/discharge cycling performed at room temperature. The electrochemical process of this battery is the reversible removal-uptake of lithium from and to lithium iron phosphate:

$$LiFePO_4 \leftrightarrow xLi + Li_{(1-x)}FePO_4$$

which is expected to develop a theoretical specific capacity of 170 mAh g^{-1} along a 3.5 V vs. Li/Li^+ flat plateau[7].

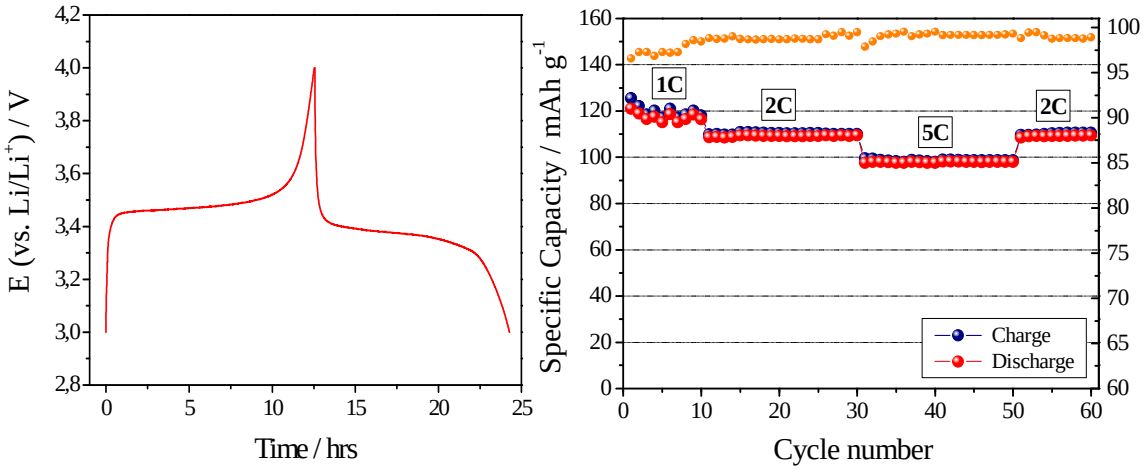

Figure II.A.12. (A) Typical charge and discharge cycle run at ambient temperature. (B) Specific capacity vs. cycle number of the lithium cell assembled by contacting in sequence the $LiFePO_4$ composite cathode, the MFC-3 membrane and a Li metal anode, at ambient temperature and at different current rates from 1 C to 5 C.

Fig. 12A illustrates a typical charge (lithium removal from $LiFePO_4$ to form $FePO_4$) and discharge (lithium acceptance by $FePO_4$ to reconvert into $LiFePO_4$) cycle run at ambient temperature. Fig.12 B shows the specific capacity vs. cycle number at ambient temperature and at different current rates from 1C to 5 C (1 C = 0.7 mA with respect to a $LiFePO_4$ active mass of about 4 mg). Reproducible voltage profiles were obtained where the initial specific capacity approaches the value of 120 mAh g^{-1} at 1C The capacity retention is satisfactory: at high 5 C current rate the cell still delivers specific capacity values around 100 mAh g^{-1}, with a drop in capacity of less than 18% with respect to the initial value at 1C. The battery operates with the expected voltage profiles delivering a good fraction of the theoretical capacity even at rates as high as 5C. The cycle response is also encouraging since no decay in capacity is shown during this initial test and the charge–discharge efficiency following the first cycles, where rearrangements in the structure of the electrode take place, is maintained to be always higher than 98%. Finally, it is important to note that the system behaves correctly, with no abnormal drift even at high regimes; in fact, reducing the C-rate completely restores the specific capacity (see, in Fig. 10B, the specific capacity values from 5C to 2C after the 50th cycle). The results here discussed, although preliminary,

demonstrate the feasibility of the MFC reinforced membranes as a new electrolyte for advanced lithium polymer batteries.

II.A.3.Conclusion

Microfibrillated cellulose at a concentration of 1–5% by weight was used to reinforce methacrylic-based composite polymer electrolyte membranes prepared by UV-curing process. It has been shown that Young's modulus, tensile strength and thermal stability of the composite films increase with increasing the MFC contents. Mechanical properties and dimensional stability of the membranes after swelling in the electrolyte solution are also improved with the addition of microfibrils. The impedance spectroscopy performed on the composite GPEs showed high ionic conductivity values approaching 10^{-3} S cm^{-1} even at ambient temperature and the analysis of the electrochemical behavior evidenced a wide stability window and interesting performance in real battery con-figuration. These excellent results added to the easy preparation method and the low processing costs make MFCs a perfect candidate for the production of composite membranes that can be used as gel-polymer electrolytes for application in lithium-based thin flexible batteries and open further studies about the role of cellulose in ion conduction. It is here also confirmed that, compared to other techniques, UV curing is versatile due to its easiness and rapidity in processing.

SECTION B

MFC reinforced solid polymer electrolytes

II.B.1. Materials and methods

1.1 Materials

Bisphenol A ethoxylate (15 EO/phenol) dimethacrylate (BEMA, average M_n: 1700), and poly(ethylene glycol) methyl ether methacrylate (PEGMA, average M_n: 1100) purchased from Sigma-Aldrich were used as oligomers to produce the polymer matrix. The di-functional oligomer constitutes the backbone of the polymer network while the mono-functional one is attached to the network and with its high number of –EO units helps lithium ions mobility. 2-hydroxy-2-methyl-1-phenyl-1-propanon (Darocure 1173) from Ciba Specialty Chemicals was used as the free radical photo-initiator. LiTFSI (lithium bistrifluoromethane-sulfonimide,$CF_3SO_2NLiSO_2CF_3$, Aldrich) salt was added to the reactive formulation as the source of lithium ions..
The $LiFePO_4$/C cathode material was synthesized in the form of nanostructured powder through a mild hydrothermal procedure[7]. Lithium metal foils with a thickness of 200 µm were obtained from Chemetall.

1.2. Microfibrillated cellulose nanoparticles (MFC) preparation

The same batch of MFC used for the previous work were used, prepared by treating bleached cellulose fibres at high pressure in a microfluidizer processor (Microfluidics, model M-110 EH-30) with a 400 and 200 µm diameter chamber. A MFC aqueous suspension (1 wt. %) was prepared.

1.3. Composite polymer electrolytes preparation

BEMA and PEGMA1100 were mixed together, the lithium salt was dissolved in the mixture and the photoiniziator was then added;. The components of the

formulation were used with the following weight ratios: BEMA: PEGMA: LiTFSI: Darocure 25:60:12:3. Subsequently the water suspension of microfibrils was added in different ratios in order to obtain composites containing 1 and 3% of MFC. As MFC aqueous suspensions are inherently stable no sonication step was necessary. The liquid mixtures were then placed in a petri dish and left 24 hours in a oven at 70 °C to obtain the water evaporation and subsequently UV cured for 3 min. under N_2 flux by using a medium vapour pressure Hg lamp (Helios Italquartz, Italy), with a radiation intensity on the surface of 30 mW cm^{-2}. Later, self standing films were peeled off from the glass plates and treated in high vacuum at 100 °C overnight. The samples were then stored in the dry glove box.
Samples will be here labelled as SP-MFC0, SP-MFC1, SP-MFC3.

1.4 Characterisation methods

The same characterisation methods described in Chapter IV *Section A* (*IV.A.1* - 1.4) were used. The all-solid polymer electrolyte was characterised by SEM analysis, Gel Content measurement, Thermal Analysis (DSC, TGA) and Tensile test.
Only SEM elements mapping analysis was added to the characterisation. The distribution of lithium salt in the polymer matrix was evaluated by a mapping process using a SEM-EDX instrument at different focal areas. The elements mapped were O, F, C and N, the components of anion part of lithium salt.
Also the electrochemical testing was developed as described in Chapter IV *Section A* (*IV.A.1* - 1.4). Galvanostatic Cycling Test in this case was performed at high temperature (70°C).

II.B.2 Results

2.1 Chemical and structural characterization of the polymer membranes

The new formulation composed of BEMA: PEGMA 1100: LiTFSI: Darocure (25:60:12:3) was chosen on the basis of previous studies developed in our laboratories[10,11] it was in fact previously demonstrated that a high quantity of a high molecular weight monofunctional oligomer can help the ion mobility. In this case LiTFSI had to be used instead of Li PF_6 because of its stability to the UV light and in contact with water.

The polymer membranes containing LiTFSI salt and reinforced with cellulose microfibrils are freestanding, extremely flexible and non-sticky, as shown in Fig. 1 they have a final thickness of about 200-500 µm. In absence of the filler the polymer is transparent while it becomes opaque by adding microfibrils to its formulation.

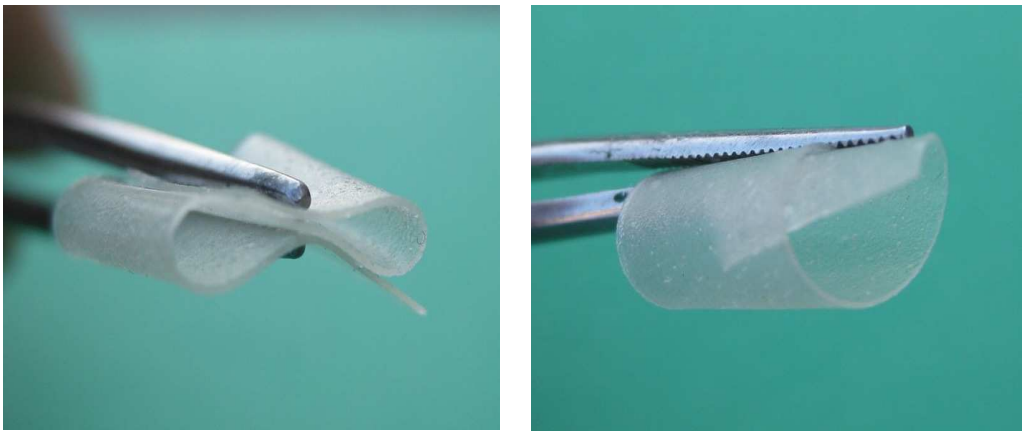

Figure II.B.1 . Appearance of the SP- MFC3 polymer membrane thickness 500µm

The curing of the polymers containing Li-salt and MFC was evaluated by the measurement of the gel content. The results are reported in Table II.B.1.

	Gel content (%)	*Tg (°C)*	*$T_{5\%}$ (°C)*	*$T_{10\%}$ (°C)*	*$T_{50\%}$ (°C)*	*Residue (%)*
SP-MFC0	86	-56	295	338	385	5
SP-MFC1	63	-56	320	360	395	5
SP-MFC3	64	-54	350	369	405	5

Table II.B.1. Brief summary of the most relevant features of the synthesized polymer composite membranes

The thermal properties of the polymer composites have been evaluated by DSC, the thermograms are reported in Figure II.B.2 and the results obtained are summarized in Table II.B.1. DSC analysis performed under nitrogen flux in the range of temperature between -120 and 120 °C showed that the membranes have a low Tg (about -55°C) which is not influenced by the presence of the filler. The T_g values found in literature as well as the previous reports for similar systems composed by BEMA 1700 and PEGDA 1100[11] were lower (~60°C), but in the present case the T_g is slightly higher due to the presence of lithium salt during the preparation. The ionic interactions produced by the incorporation of lithium salt into the polymer matrix can restrict the chain mobility as well as reduce the free volume of the final membrane, thus leading to an increase in the glass transition temperature[11, 15].

The curves obtained (Fig.2) showed a peack of cristallisation and then one of melting respectively at -30 and 20°C for the membranes with and without filler. Those are due to the use of PEGMA1100 whose long chains can arrange in cristallites. This directs the use of this kind of membranes towards high temperatures applications as, however, is usually suggested for the all-solid structures.

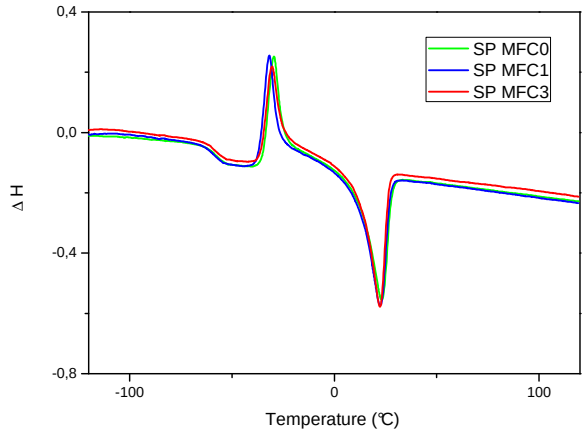

Figure II.B. 2. DSC traces of the series of composite polymer membranes prepared.

The thermal stability of the prepared membranes was assessed by thermo-gravimetric analysis under flowing nitrogen in the temperature range between 25 °C and 600 °C. The results are shown in Figure II.B.3 and summarized in Table II.B.1 where $T_{5\%}$ $T_{10\%}$ and $T_{50\%}$ and the residues are reported. The not reinforced membrane starts degrading earlier) than the others, it loose the 5% of its weight at 295°C while the reinforced membranes show the same weight loss at 320°C (SP-MFC1) and 350°C (SP-MFC3). The residues observed at 500°C can be attributed to the presence of the salt.

The results of the TGA anlysis indicate that the polymer membrane can be safely used in Li-based polymer batteries for high-temperature application.

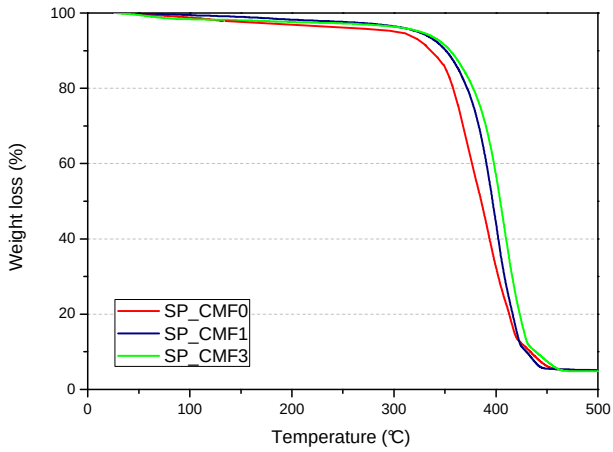

Figure II.B.3. TGA measurements on the composite polymer membranes: the presence of MCFs improves thermal stability.

The good interpenetration between the microfibrils network and the polymer was confirmed by the SEM analysis, and the corresponding topographical view at different magnification have been shown in Figure II.B.4. the images obtained for these samples were very similar to those shown for the membranes described in section A allowing then the same interpetation, two top view are reported in Fig. 4. It is possible to observe that the cellulose micro fibrils are completely surrounded by the polymer matrix. A good affinity between the matrix and the filler was obtained even without functionalization of MFCs. This could be attributed to the good compatibility resulting from the chemical similarities between polymer and MFCs and, consequently, the hydrogen bonding interactions existing at the interface.

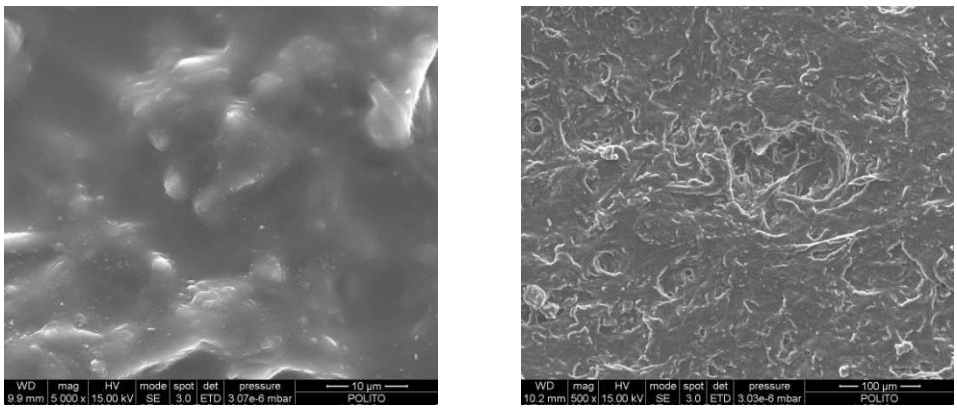

Figure II.B.4. SEM images of the polymer composite membrane SP MFC3 at different magnitudes (5000x left and 500x right). It´s possible to observe that the cellulose microfibrils are completely surrounded by the polymer matrix.

In addition to the SEM images EDS mapping has also been performed to analyze the distribution of lithium salt in the polymer matrix. For this purpose the elemental mapping was carried out and the elements, fluorine and sulfur only present in the anion (of Lithium salt LiTFSI) were detected and mapped. The resulting images, that give morphological and compositional information, showed ah homogeneous distribution of those elements for all the samples. The mapped images are given in Figure II.B.5, and it is clear from the images that the anion is well distributed in the polymer matrix thus Li^+ ion too.

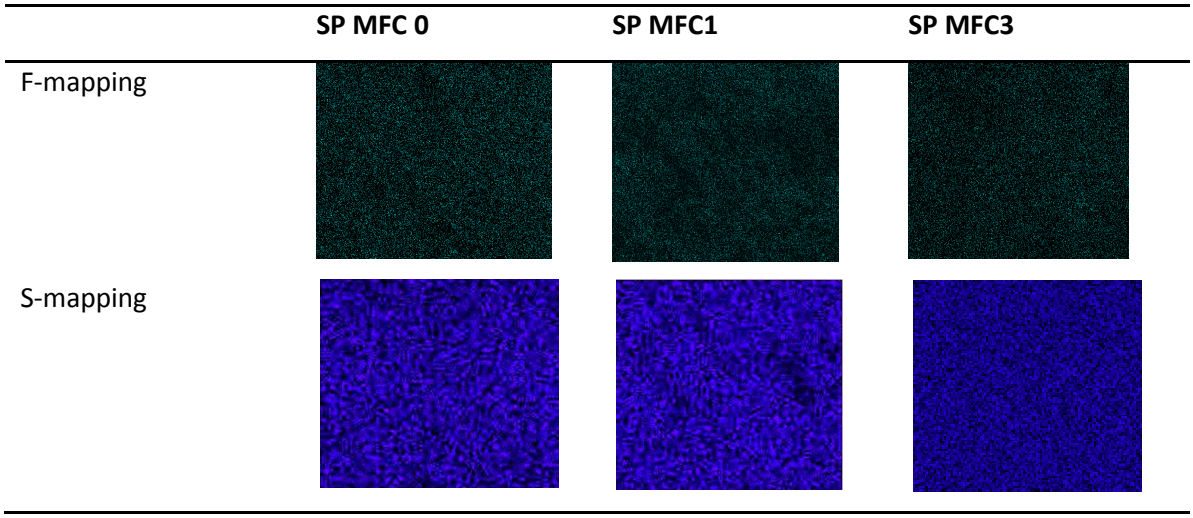

Figure II.B. 5. SEM-EDS mapping of Fluorine and Sulfur

The mechanical behaviour of the ready-to-use MFC composite electrolyte was investigated by means of tensile test to observe the effect of the addition of cellulosic filler on the mechanical properties of the membrane. A typical curve is reported in Figure II.B.6 and the results are summarized in Table II.B.2.

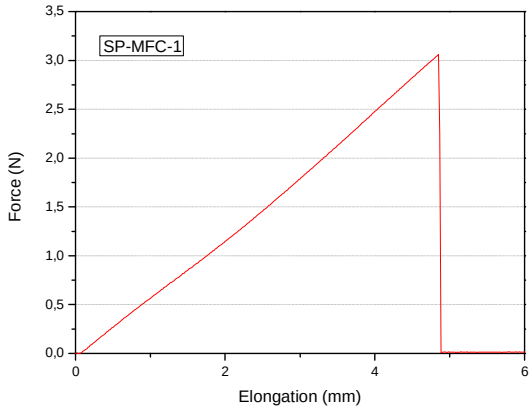

Figure II.B.6. Curve Force vs Elongation obtained from the tensile tests of the membrane SP MFC 1

	Young's modulus (MPa)	*σmax (MPa)*
SP-MFC0	-	-
SP-MFC1	9 ± 2	0,38 ± 0,05
SP-MFC3	32 ± 4	2,3 ± 0,4

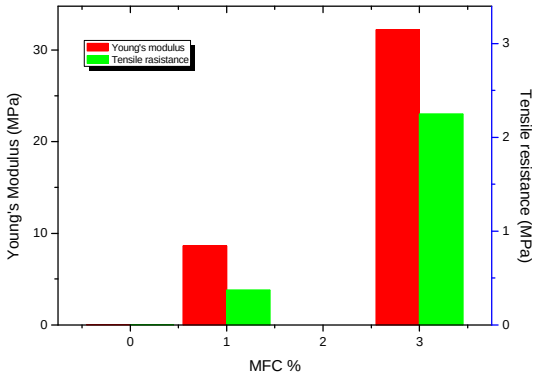

Table II.B.2 Increase of Young's modulus and tensile resistance with the increase of MFC content with a graphical representation of the left

Sample SP-MFC0 couldn't be tested because it couldn't stand the pressure of the clamps of the instrument. The composite polymer membranes, which had a high flexibility, also showed an important improvement in mechanical properties in terms of Young's modulus and tensile resistance. Microfibrils can create a strong network which is interpenetrated with the polymer matrix leading to a strong increase in the handability and resistance of the membrane. Considering that these membranes are ready-to-use and do not need any activation by swelling in the liquid electrolyte the values of Young's modulus and tensile resistance obtained are more than satisfactory for the possible application in tin flexible batteries. Figure II.B.6 shows that, under tensile strength, the membranes have an elastic behaviour.

2.2 Electrochemical characterisation

The ionic conductivity of the samples was measured by impedance spectroscopy in the temperature range between 25°C and 90°C by constructing a symmetric cell with the analyzed membrane between two stainless steel electrodes. The Arrhenius plots obtained for the 3 samples are reported in Figure II.B.7. The plot exhibited the typical Vogel-Tamman-Fulcher curvature associated with amorphous materials[16-18], the melting temperature of the crystalline areas detected by DSC was in fact at about 20 °C. The polymer membranes showed very similar conductivity values as expected from the DSC measurements for this range of temperature where

the polymer membranes exhibited similar Tg. Conductivity values are low compared to the GPEs described in Section A. The values are perfectly in line with those found in literature for solid polymer electrolytes, going from $1,8*10^{-5}$ at room temperature to $3,3*10^{-40}$ at 90°C[11,19,20].

The slight increase observed in presence of the filler could be explained by considering the measure of the insoluble fraction (%gel) previously discussed; a lower insoluble fraction indicates the presence of unreacted monomer that could act as a diluent in our membrane helping the ion mobility.

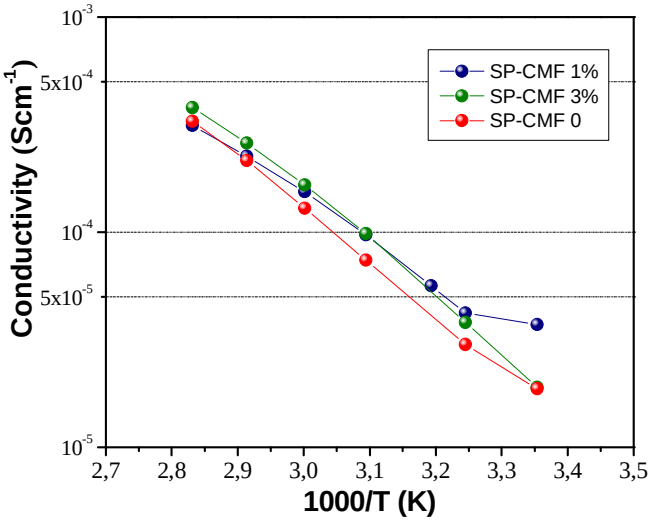

Figure II.B.7. Arrhenius plot of the ionic conductivity for samples SP-MFC0, SP-MFC1, SP-MFC3

In view of their possible application as electrolytes in Li based polymer batteries, the samples were further tested in terms of other general electrochemical properties; in particular, their electrochemical stability window was evaluated by linear sweep voltammetry performed at 70 °C. For the evaluation of the anodic stability the potential range between O.C.V and 5,2 V was scanned by using a Li metal/ SP-CMF3/ acetylene black cell configuration; for the cathodic part the range between O.C.V and -0,2 V was scanned, the cell configuration was: Li metal/ SP-CMF3/ copper. Then, combining both the cathodic and anodic stability windows the whole electrochemical stability window was obtained, which is shown in Figure II.B.8. Considering the higher potential range it is possible to observe that

the system is stable up to above 4,5 V vs. Li/Li^+ where the current starts to rapidly increase. No decomposition phenomena are evident while approaching 0.0 V vs. Li/Li^+. At lower potential it is possible to observe, around 0.0 V, the characteristic peaks of deposition and stripping of lithium ions on and from the copper electrode (Figure II.B.8 Capture). Again, as already explained for the reinforced membranes presented in Section A, the presence of the lithium deposition-stripping peak confirms the correct working of the solid polymer electrolyte in a lithium-based cell. The anodic breakdown occurring at potentials higher than 4,5 V vs. Li/Li+ allows a safe use of the membrane at the standard working conditions and the very flat plateau in the stability region indicates the purity of the entire system. Moreover, as the membrane preparation process was water-based, the absence of any characteristic peak around 4.0 V vs. Li/Li^+ region confirms that the membrane is moisture-free hence suitable for the application in lithium based batteries where even a small quantity of water could ruin the cell performance.

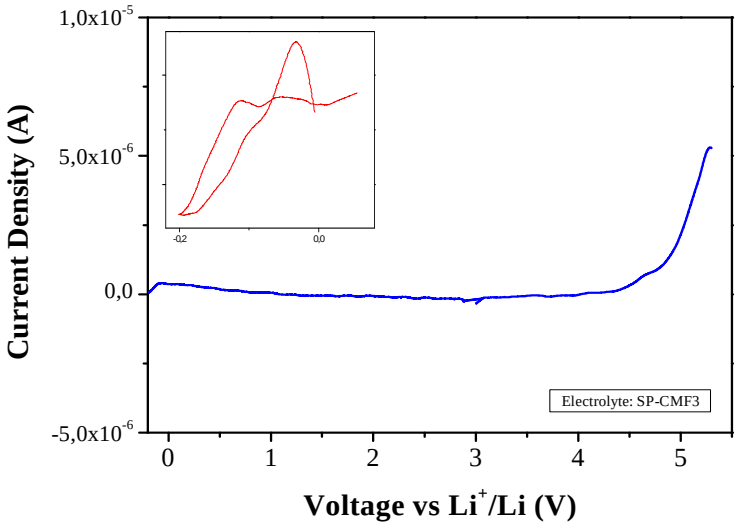

FigureII.B. 8 Electrochemical stability window of the membrane SP-MFC3, the red curve in the Capture frame represents the lithium deposition-stripping process observed in the cathodic scan.

The polymer membrane SP-MFC3 was then tested for galvanostatic charge/discharge cyclability tests as electrolyte in a lithium cell with $LiFePO_4$ as cathode and Li metal as anode. The test was carried out in a temperature

controlled oven at 70 °C. The results appeared highly promising, showing good reversibility and cyclability at different current rates.

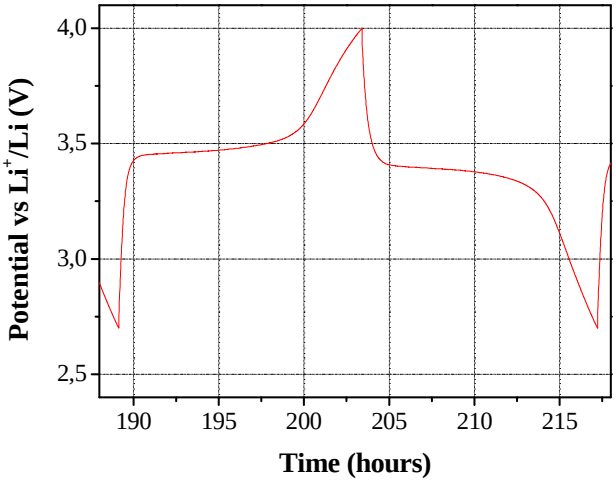

FigureII.B. 9. Typical charge and discharge cycle run at 70°C after 200 hours working

Figure II.B.9 shows a charge/discharge cycle of the $LiFePO_4$/SP-MF3/Li polymer cell at low current rate of C/20 after 200 hours of work. The cycle evolves around 3.45 V vs. Li/Li+ as indeed expected on the basis of the $LiFePO_4$ electrochemical reaction, with an almost stable plateau over the entire cycle[7].

Figure II.B.10 shows the specific capacity vs. cycle number of the cell at different currents rate, compared with a $LiFePO_4$/Li cell, assembled with the same $LiFePO_4$ cathode material but with liquid electrolyte. By comparing the two plots, it's clearly evident that the specific capacity obtained for the all-solid $LiFePO_4$/SP-MF3/Li polymer cell even if only at low current rate can be considered more than satisfactory. The cycle response is also encouraging since the cell is able to work even at high C/2 current rate. Furthermore, the Coulombic efficiency, which is quite low (about 80 %) during the initial cycles, after ten cycles is clearly approaching 99 % and it is then maintained very stable for all the tested current rates. This is a convincing indication of a good interfacial contact between the electrode and the polymeric electrolyte.

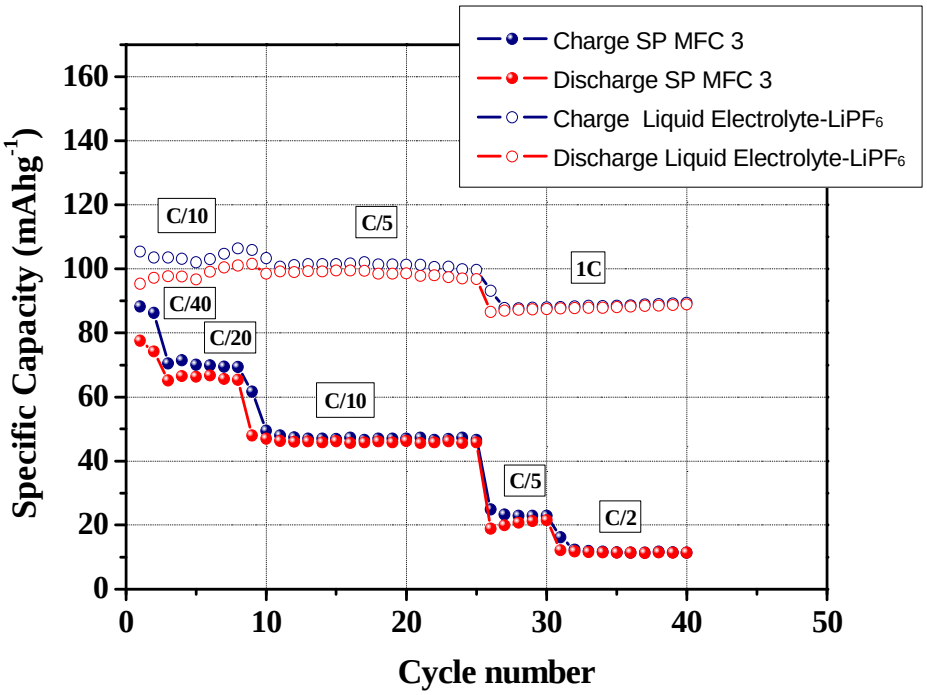

Figure II.B.10 Specific capacity vs cycle number of the lithium cell assembled by contacting in sequence the $LiFePO_4$ cathode, the SP-MFC3 and a Li metal anode at 70°C at different current rate from C/40 to C/2(Full symbols) compared to the specific capacity vs cycle number of the lithium cell assembled by using $LiFePO_4$ cathode and a Li metal anode in presence of a liquid electrolyte (1M LiTFSI in EC:DEC)(empty symbols).

II.B.3.Conclusion

Microfibrillated cellulose at a concentration of 1 and 3 % by weight was used to reinforce methacrylic-based all-solid composite polymer electrolyte membranes prepared by UV-curing process. It has been shown that flexibility, Young's modulus, tensile strength and thermal stability of the composite films increase in presence of the cellulosic filler. The impedance spectroscopy performed on the composite solid electrolytes showed good ionic conductivity values being higher than 10^{-5} S cm^{-1} even at ambient temperature and the analysis of the electrochemical behavior evidenced a wide stability window and interesting performance in real battery configuration. Always considering the important safety advantages that a solid polymer can have when compared to a liquid one, the excellent results obtained added to the easy preparation method and the low processing costs

of MFC make such membranes the perfect candidate for the use as solid-polymer electrolytes for safe lithium-based thin and flexible batteries.

References

(1) *B. Scrosati, Chem. Rec. 5 (2005) 286.*

(2) B. Scrosati, J. Garche, J. Power Sources 195 (2010) 2419.

(3) *A.S.Aricò, P.Bruce, B.Scrosati, J.M.Tarascon, W.VanSchalkwijk, Nat.Mater.4(2005)366.*

(4) Herrick FW, Casebier RL, Hamilton JK, Sandberg KR (1983) J Appl Polym Sci: Appl Polym Symp 37:797

(5) Turbak A, Snyder F, Sandberg K. (1983)U.S. Patent 4,378.

(6) J.Lu, Tao Wang, Lawrence T. Drzal (2008) Composites: Part A 39 738

(7) G.Meligrana, C.Gerbaldi, A,Tuel, S.Bodoardo, N.Penazzi, J.Power Sources16(2006)516.

(8) S.Bodoardo, C. Gerbaldi, G. Meligrana, A. Tuel, S. Enzo, N. Penazzi, Ionics 15 (2009) 19.

(9) G. Siqueira, J. Bras, A. Dufresne, Biomacromolecules 10 (2009) 425.

(10) J. R. Nair, C Gerbaldi, G. Meligrana, R. Bongiovanni, S. Bodoardo, N. Penazzi, P. Reale, V. Gentili (2008), J Power Sources, 178, 751.

(11) Jijeesh R. Nair, C. Gerbaldi, M. Destro, R. Bongiovanni, N. Penazzi, (2011) Reactive & Functional Polymers 71 409

(12) M.A.S. Azizi Samir, F. Alloin, J.-Y. Sanchez, A. Dufresne, Polymer 45 (2004) 4149.

(13) M.N. Anglés, A. Dufresne, Macromolecules 33 (2000) 8344.

(14) P. Reale, A. Fernicola, B. Scrosati, J. Power Sources 194 (2009) 182.

(15)W. Wieczorek, J.R. Stevens, Z. Florjanczyk, Solid State Ion. 85 (1996) 76.

(16) H Vogel (1921) Phys Z 22:645

(17) GS Fulcher (1925) J Am Chem Soc 8:339

(18) G Tamman, W Hesse (1926) Z Anorg Allg Chem 156:245

(19) F. L. Tanzella, W. Bailey, D. Frydrych, G. C. Farrington Solid State lonics 5 (1981) 681-684 North-Holland Publishing Company

(20) R. Uchiyama, K. Kusagawa, K. Hanai, N. Imanishi, A. Hirano, Y. Takeda. Solid State Ionics 180 (2009) 205

CHAPTER III

TOWARDS FEASIBLE GEL-POLYMER ELECTROLYTES

Methacrylic-based thermo-set membranes obtained by free radical photo-polymerisation have been proposed in last years [1,2] as polymer electrolytes for Li-based battery application. A fast and easy preparation process called "One Shot" has been developed[3]; in such procedure Li-X salt is introduced directly in to the reactive formulation before polymerization, thus, after reticulation, it can be completely avoided the activation of the membranes by swelling into a liquid electrolyte. By such a method, the complete electrolyte preparation takes less than 5 minutes. Though these membranes are flexible, self standing and easy to handle, there is room for improving mechanical strength, in particular if application in flexible batteries is taken into consideration.

The use of MFC or fibres in aqueous suspension as a reinforcement (as described in *Chapter IV*) is hardly adaptable to this kind of process because the use of water requires long times for its evaporation. Thus, this part of the work, focused onto the use of fibre networks (paper) in order to reinforce the membranes, prepared with the fast and efficient "one shot" method. The advantage of paper is that it can be easily impregnated, by the current methods used in papermaking, with the components of the membrane formulation and then irradiated for obtaining at the same time the membrane synthesis and likely some anchoring points between the fibres and

the polymeric substrate. Actually, previous studies showed that UV light is able to activate the cellulose substrate for the polymerization initiation. (3-5)
In such a way, one could imagine to couple the continuous papermaking process with the membrane synthesis, leading to large are, mass production of reinforced membranes
On the other hand the production at the industrial scale of One Shot membranes could result expensive since the presence of the Lithium salt requires inert production rooms. The possibility to introduce the lithium salt in a second moment could also be taken in consideration.
A methacrylic photopolymerisable system was chosen as a reference among the different polymers developed in past studies [1-3, 6, 7]. Different types of handsheets were produced, in order to vary the main morphological and physico-chemical characteristics. Actually, the handsheet properties can be varied by varying the nature or the structure of the fibers or by adding different additives. The papers studied have been specifically designed for the analysis of the influence of the different characteristics on the behaviour of the hybrid membranes. Various fiber compositions, grammages, refining degrees and additives have been evaluated.
Finally the gel polymer electrolytes reinforced by different kinds of handsheet have been tested in terms of conductivity and mechanical properties. In this chapter the results of the tests performed on the reinforced membranes will be presented and relationships between electrochemical performances and paper characteristics will be proposed. This chapter reports the impact of the use of paper and of its characteristics on the final mechanical and electrochemical properties of the reinforced membranes.

III.1 Materials and methods

1.1 Fibers and additives for handsheets preparation

Cellulose fibers deriving from Hardwood(Eucaliptus) and Softwood (Pine from Tarascon, Fr) plants were used to produce paper sheets.

Papers containing additives were also prepared, the materials used were:

- Cationic Starch (Roquette), DS 0.040 (Nitrogen active 0.37%)

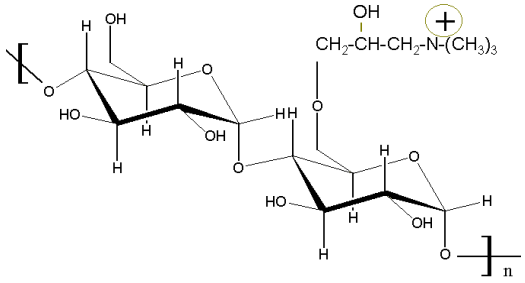

- Alkylketene dimers (AKD) (Hercules). Stable emulsion of alkylketene dimer, stabilized by cationic CPAM

.

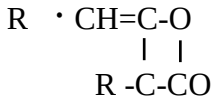

- Cationic polyacrylamide (CPAM) (Kemira), Copolymer of acrylamide and an acrylate based quaternary amine, Mw: $7 \cdot 10^6$:

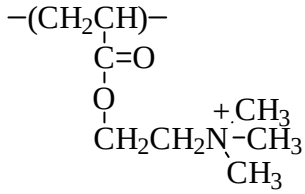

- Calcium carbonate($CaCo_3$) (Omnya), Slurry with CaCO3>98%, MgCO3 <0.52% and Fe2O3<0.02

- Calcium phosphate $Ca_3(PO_4)_2$ (Aldrich)

- Alumina(Al_2O_3) (Aldrich).

1.2 Fibers treatments

Bleached cellulose fibers stored in laboratory in the form of thick sheets are re-pulped and blended using a high speed blender, the desired amounts of Softwood and Hardwoodfibers are mixed in order to obtain the samples for the paper characterization. The fibers suspension is then submitted to the refining treatment. Refining can be defined as the mechanical treatment of the fibers in water to increase surface area, flexibility and promote bonding when dried. One of the unintended effects of beating is fiber length reduction. This mechanical modification is done by a laboratory equipment for pulp refining called Valley beater, according to ISO 5264-1 in order to beat pulp in a uniform, standard and reproducible way.

Figure III. 1Valley beater

For the preparation of some of the handsheets the shortest fibers produced during refining were removed by washing the pulp with an high pressure water jet on a mesh with light of 100µm.

1.3 Handsheet preparation

The fibers suspensions composed by the desired SW/HW fibers ratio and with the desired Shopper Riegler degree are later diluted to the various concentrations (2, 1.5, 1, 0.7, 0.5 g/l); a liter of these suspensions is than is introduced into a sheet-former that automatically steers the solution. The filtrate laying on copper wires is then dried at 90 °C for 7 minutes under high vacuum to give a handsheet of the desired weight (2, 1.5, 1, 0.7, 0.5 g). By

varying the weight of the handsheet its grammage (g/m^2) is modified and, as a consequence, its thickness and porosity.

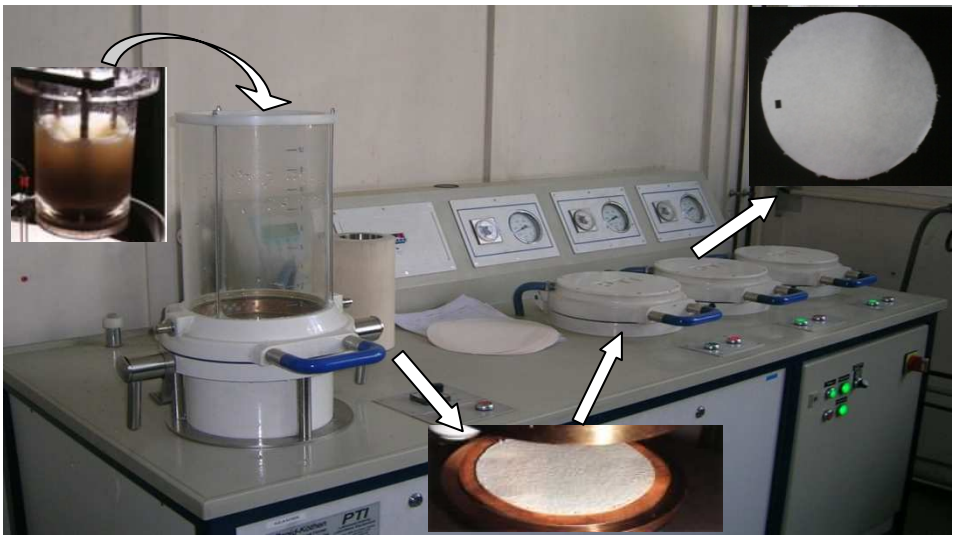

Figure III. 2 Scheme of the preparation of the handsheet

The papers containing additives were prepared by diluting the fillers in water and adding the obtained suspension to the pulp slurry before the introduction in the sheet former.

Handsheets with different properties have been prepared in order to understand their influence on the behavior of a reinforced membrane.
The properties of the handsheet that have been considered were:

- Composition. Cellulose fibers can have different nature, depending on the raw material: they can be hardwood (HW) or softwood (SW). They are often used in mixtures, to control the paper mechanical properties and the fibre flocculation that influences the final paper characteristics (appearance, porosity etc.). Handsheets containing different percentages of HW-SW fibers have been prepared: SW-HW 100:0, 80:20, 60:40, 40:60, 20:80, 0:100.
- Grammage (g/m^2). A variation in the grammage allows to controlling its thickness and can lead to thinner substrates, likely more suitable for the battery application. The target grammages were 13, 16, 22, 32, 51, 57g/m^2.

- Refining degree (measured in Riegler-Shopper degrees-°SR). Refining is a mechanical treatment that allows to dramatically change the fiber and consequently the paper properties: it is generally performed to increase the fiber surface area and flexibility and to promote bonding between fibers when dried. It also results in internal and external fibrillation, fiber shortening and fines formation. This treatment directly impacts the paper formation and its final properties. Handsheet containing 3 different mixture of fibers (SW100-SW40 and HW100) have been prepared with various refining degrees (0, 20, 35, 50 °SR). The same samples have also been prepared washing away the short fiber elements from the suspension before the handsheet formation.

The handsheets that will be here analyzed are summarized in the following table:

Sample (Label)	Fibers Mixture (HW%:SW%)	Grammage (g/m^2)	Refining degree (°SR)	Washing of short fibers
1 (HW100)	100:0	70,7	35	-
2 (SW20)	80:20	72,6	35	-
3 (SW40)	60:40	76,4	35	-
4 (SW60)	40:60	71,6	35	-
5 (SW80)	20:80	67,5	35	-
6 (SW100)	0:100	69,0	35	-
7 (SW40-16)	60:40	16,2	35	-
8 (SW40-23)	60:40	23,0	35	-
9 (SW40-32)	60:40	32,2	35	-
10 (SW40-47)	60:40	47,5	35	-
11 (SW100 SR 0)	0:100	22,2	0	-
12 (SW100 SR 20)	0:100	22,0	20	-
13 (SW100 SR 35)	0:100	23,0	35	-
14 (SW100 SR 50)	0:100	23,7	50	-
15 (SW100 SR 0 NF)	0:100	23,7	0	yes
16 (SW100 SR 20 NF)	0:100	23,2	20	yes
17 (SW100 SR 35 NF)	0:100	21,9	35	yes
18 (SW100 SR 50 NF)	0:100	23,5	50	yes

Table III.1. Summary of the characteristics of the handsheets prepared

The presence of additives added to the paper pulp was also investigated. Handsheet SW40, grammage 55 g/m^2, refining degree 35 °SR were added of additives. The papers prepared are reported in the following table:

Sample SW 40-55g/m^2-35°SR	Additive	Quantity (Wt%)
19	Cationic Starch	5
20	Cationic Starch	10
21	Cationic Starch	15
22	AKD	5
23	AKD	10
24	AKD	15
25	CPAM	5
26	CPAM	10
27	CPAM	15
28	$CaCO_3$	5
29	$CaCO_3$	10
30	$CaCO_3$	15
31	$Ca_3(PO_4)_2$	5
32	$Ca_3(PO_4)_2$	10
33	$Ca_3(PO_4)_2$	15
34	Al_2O_3	5
35	Al_2O_3	10
36	Al_2O_3	15

Table III.2. Summary of the handsheets containing additives prepared

1.4 Membrane formulation

The UV cured polymer membrane was composed by:

- Bisphenol A ethoxylate (15 EO/phenol) dimethacrylate BEMA, Mn = 1700 Aldrich product, chemical formula:

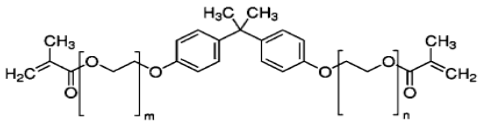

- Poly(ethylene glycol) methyl ether methacrylate PEGMA, average Mn= 475 (Aldrich). Chemical formula:

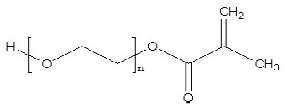

1:1 w/w ethylene carbonate – diethyl carbonate (EC-DEC, Fluka) solution. It has been used as a solvent.

LiTFSI (lithium bistrifluoromethanesulfonimide,$CF_3SO_2NLiSO_2CF_3$ purchased from Aldrich has been chosen as lithium salt.

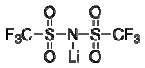

2-hydroxy-2-methyl-1-phenyl-1-propanon Darocur 1173, Ciba Specialty Chemicals has been used as photo-initiator.

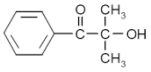

Before their use, BEMA and PEGMA were kept open in the inert atmosphere of a dry glove box (MBraun Labstar, O_2 and H_2O content < 0.1 ppm) filled with extra pure Ar 6.0 for several days and also treated with molecular sieves (Molecular sieves, beads 4 Å, 8–12 mesh, Aldrich) to ensure the complete removal of traces of water/moisture from the liquid monomers, as they may affect long–term properties when the membranes are considered used for rechargeable Li-based batteries.

1.5 Preparation of the gel polymer electrolyte membrane

The chemical formulation chosen is:
BEMA: PEGMA: EC-DEC: LiTFSI 35: 15: 30: 20 + 2%wt Darocure 1173

The formulation of this membrane had already been used in previous works[3].

Membranes were prepared by a fast "one shot" process. This consists in few and easy steps showed in Figure III. 3:

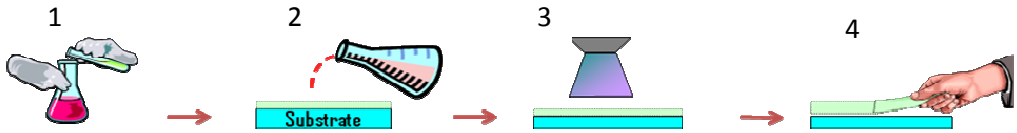

Figure III. 3. Scheme of the preparation of the membrane

1- Preparation in dry box (Argon atmosphere) of the active formulation containing BEMA : PEGMA : EC-DEC: LiTFSI and the photoinitiator.
2- Draw down of the formulation on the cellulosic substrate (4cm^2) laying on a polyethylene (PE) substrate by using a coating bar of 200 µm in dry box, (the formulation spread on the substrate was always in excess) and waiting for 30 seconds.
3- UV curing of the membrane for 3 minutes by using a medium vapour pressure Hg lamp (Helios Italquartz, Italy), with a radiation intensity of 30 mW cm^{-2}. The membrane is placed in a quartz tube sealed in dry box and irradiated.
4- The Gel Polymer Electrolyte is removed from the PE substrate.

Samples for tensile tests do not contain lithium salt and are prepared as before outside the dry box and irradiated under N_2 flux.The preparation described is manual, even by following and performing carefully all the steps the membranes obtained have a variable thickness that ranges between 70µm and 400µm that is mostly due to a variable quantity of polymer matrix in the membrane. The membranes prepared with this technique will be labeled with "OS" before the indication of the kind of handsheet used.

An alternative procedure named "dry" has also been developed. It consists in dipping for 10 minutes a paper sample with a surface area of 4 cm^2 in the reactive mixture and then eliminating the reactive mixture in excess by

adsorbing it with blotting paper before polymerisation; these steps are carried on in dry box. The impregnated paper is then placed on a PE substrate, sealed in a quartz tube and subjected to photopolymerisation for 3 minutes. The membranes prepared with this technique will be labeled with "DRY" before the indication of the kind of handsheet used.

A third preparation method, the swelling procedure, has been tested. The membranes were prepared and UV irradiated as previously described but the Lithium salt was not added to the reactive formulation of oligomers, organic solvent and photoiniziator. The reinforced membranes were then swelled into a 1.0 M LiTFSI in EC/DEC (1:1 w/w) solution (swelling time =15 minutes; under inert atmosphere of an Ar-filled dry glove box (MBraun Labstar, O_2 and H_2O content\0.1 ppm).

1.6 Characteristion methods

1.6.1 Pulp & Paper characterization

Fibers refining degree evaluation

The refining degree of the fibers suspension was evaluated by the equipment for pulp sample drainability measurement and determination, as well as refining behavioral assessments, according to ISO 5627-1. The procedure consists in measuring the quantity of water that is filtered from an homogeneous suspension of 2g of fibrous material dispersed in 1l of water placed on a container whose base consist in a copper wire. The filtered water is collected in a graduated cylinder, since highest is the quantity of water collected lower is the refining degree, the cylinder is calibrated in a way that 1l of water corresponds to 0 Shopper Riegler (SR) degrees and lower amounts of water will correspond to higher SR degrees.

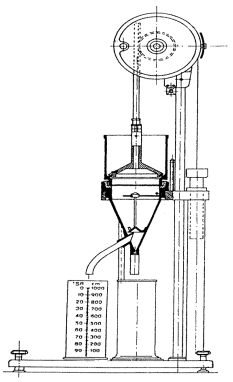

Figure III. 4 Equipment for pulp sample drainability measurement

Thickness measurements

Thickness was measured by an Adamel Lhomargy-M120 instrument. Five readings were taken for each hand-sheet and the average thickness was taken as final value.

Grammage measurements

Grammage of cellulose papers was calculated by cutting a 10×10 cm piece from the hand-sheet and, then, weighing it on a balance. Every time, three readings were taken and subsequently averaged to obtain a final value. The final reading was expressed as g m^{-2}.

Flocculation index

Flocculation index (FI) test was performed using a 2D online Lab formation sensor developed by CTP and Techpap. This test gives the fiber floc size claissification, by image analysis and a calculation part based on original algorithms which use a two-dimensional Fast Fourier Transform. It is a measure of the degree of flocculation of fibres in the final hand-sheet. A lower value indicates a lower flocculation, which indicates a more uniform hand-sheet. In this test as well, three to five samples were tested and the final value was taken as an average.

SEM analysis

Some morphological characterizations of the handsheets were performed employing a FEI Quanta Inspect 200LV scanning electron microscope (SEM, max magnification of 1.5×10^5) equipped with an energy-dispersive X-ray analyzer EDAX Genesis system with SUTW detector. Prior to analysis, all the samples were coated a thin Cr layer (thickness around 10 nm) to minimize the effect of the electron beam irradiation which may possibly lead to charging and "burning" of the polymer network. Top analysis was performed in order to observe the handsheet structure. Moreover, test membranes were broken under cryogenic conditions (after dipping in liquid nitrogen in order to avoid any change in the morphology) and a cross-sectional analysis was also performed.

Porosity measurements

The theoretical value of the porosity has been calculated by using the simple formula

$$V_{tot} = V_{cell} + V_{por}$$

where V tot is the volume of the sample, V por the volume of the pores and V cell the volume occupied by the cellulose assumed as completely crystalline with a density of 1,582 g/cm^3.

Experimental Hg porosity measurements were carried out at the PTS institute in Heidenau. The tests were conducted by using a Poremaster GT60 instrument (Quantachrome Instruments). The samples were conditioned before the test by 23°C and 50 % relative humidity, for each sample 2 or 3 single measurements were done.

Mechanical measurements

Mechanical measurements were carried out through tensile experiments according to ASTM Standard D638, using a Sintech 10/D instrument equipped with an electromechanical extensometer (clip gauge). At least five specimens for each sample were tested; the Tensile resistance and Young modulus (standard deviation 5%.) were evaluated by the instrument. The tensile index is an indication of the mechanical properties characteristic of the paper industry; it is calculated as:

(Tensile Resistance / Grammage) (KN*m/g)

1.6.2 Membrane characterisation

Density measurement

The density of the polymer solution has been measured by a glass picnometer with a volume of 5cm^3.

Active Swelling

The quantity of polymer electrolyte present in the entire membrane, called Active Swelling percentage (AS%), was calculated by the formula:

$$(W_{GPE}\text{-}Wpap) / W_{GPE} * 100$$

where W_{GPE} is the weight of the final reinforced membrane and Wpap is the weight of the reinforcing substrate.

Differential scanning calorimetry (DSC)

The glass transition temperature (T_g) of the materials was evaluated by differential scanning calorimetry (DSC) with a METTLER DSC-30 instrument, equipped with a low temperature probe. Samples were put in aluminium pans, prepared in a dry glove box. In a typical measurement, the electrolyte samples were cooled from ambient temperature down to –120 °C and then heated at 10°C min^{-1} up to 120°C. For each sample, the same heating module was applied and the final heat flow value was recorded during the second heating cycle. The T_g was defined as the midpoint of the heat capacity change observed in the DSC trace during the transition from glassy to rubbery state.

SEM analysis and Mechanical measurements

As described in the previous pharagraph for hansheets.

Thickness measurement

The thickness of the reinforced membranes was measured with a Mitutoyo series 547 thickness gauge equipped with an ABSOLUTE Digimatic Indicator model ID-C112XBS, with a resolution of ± 1 µm and a max measuring force of 1.5 N.

Ionic conductivity

The ionic conductivity of the gel-polymer membrane at various temperatures was determined by electrochemical impedance spectroscopy (EIS) analysis of cells formed by sandwiching discs of 0.785 cm^2 of the given GPE between two stainless-steel 316 blocking electrodes. The cells were housed in an oven to control the temperature. A PARSTAT2273 instrument was employed for measurements over a1 Hz to 100 KHz frequency range. The resistance of the electrolyte was given by the high frequency intercept determined by analyzing the impedance response using a fitting program provided with the

Electrochemistry Power Suite software (version 2.58, Princeton Applied Research)

III.2. Results

Most relevant results obtained in the development of a Gel Polymer Cellulose Electrolyte (GPCE) membrane are presented in this section.

It should be noticed that the Gel Polymer Electrolyte membrane used in this study as a reference, was previously developed in the Politecnico laboratories[3], by mean of a fast, easy and reliable method. Such a membrane was fully characterized and results displayed a good repetability.

The polymer, composed by BEMA: PEGMA475: EC/DEC: LiTFSI (35: 15: 30: 20), is in the rubbery state at room temperature (Tg under -60°C) and it presents a conductivity in line with the results generally obtained for amorphous GPEs, reaching a value of about $3*10^{-4}$ s/cm at room temperature that increases up to $2*10^{-3}$ s/cm at 80°C. The Arrhenius plot obtained from the impedance spectroscopy measurement is reported in Figure III. **5**.

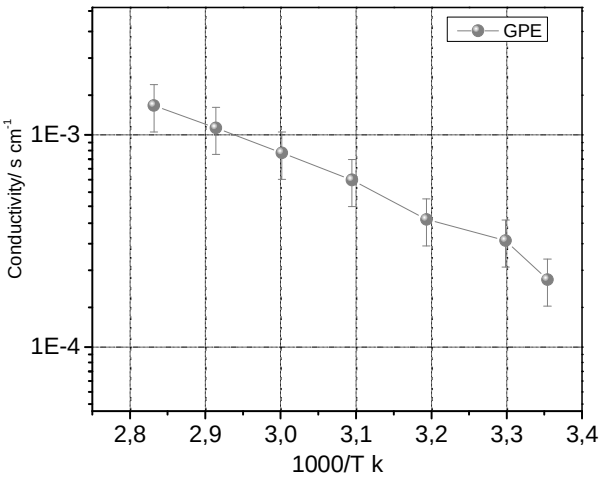

Figure III. 5. Arrhenius plot obtained from the impedance spectroscopy perfomed on BMPFSI membrane not reinforced. The average error is 25%.

The tensile resistance of this membrane could not be measured because of its too low mechanical properties. With the intention of overcome this drawback, paper has been proposed and evaluated as a reinforcement.

The procedure followed was adapted from the reference method, taking into account an eventual industrial process in which a monomer formulation is deposited (by size press treatment or by coating) on the paper substrate, directly during papermaking.

An example of such a process is given in the figure below:

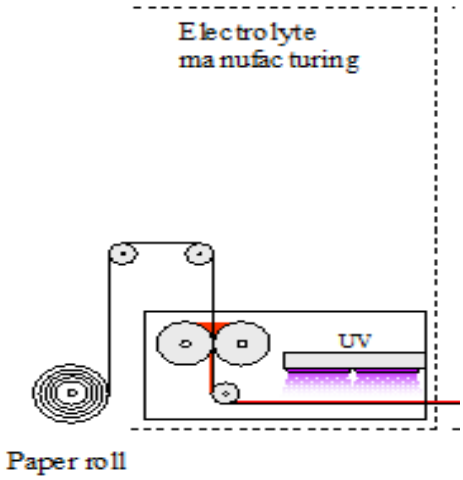

Figure III. 6.Industrial process for the preparation of reinforced GPEs

2.1 GPCE synthesis and structure

Considering that the oligomeric formulation should impregnate the paper, first the behavior of the formulation when it is put into contact with the paper was studied. Then, the structure and the characteristics of the developed membranes were characterized, with a special focus on the impact of the paper substrate.

Finally, considering the results obtained, alternative routes to increase the electrochemical properties were investigated: the use of additives and the increase in the Litium content.

In the next paragraphs, the results obtained are presented and discussed.

2.1.1 Wettability and liquid penetration in the hansheets

Before the use of the paper as reinforcement for the GPE membranes the wettability of the hansheet by the liquid membrane formulation, as well as its penetration in the paper pores, have been checked.

However, it was very difficult to measure the initial contact angle of the oligomer mixture on the handsheet, because of the very rapid spreading, so wettability was assumed to be complete.

Concerning the penetration in the pores, some calculations were done, based on the Washburn equation (reported below), that correlates the rate at which a liquid penetrates a porous solid to its surface tension, viscosity and to the pores radius (or fibers distance).

$$\text{Washburn equation: } dh/dt = (\gamma R \cos\theta) / 4\eta h$$

Where γ is the surface tension of the liquid, η its viscosity, R is the pore radius and can be evaluated by mercury intrusion, θ is the contact angle observed, and h is the thickness of the sample considered.

By the integration of the Washburn equation it is possible to write:

$$h^2 = ((\gamma R \cos\theta) / 2\eta) t$$

$$\text{that is } t = h^2 / ((\gamma R \cos\theta) / 2\eta)$$

By developing this calculation the impregnation time needed to completely fill the pores can be determined. R, γ and h have been experimentally measured: they could vary according to the handsheet and to the oligomeric formulation, for the three parameters the worse scenario has always been taken in consideration.

The values considered for the calculation are reported in Table 4.

Parameter	Value
h	142 µm grammage=70g/m^2 (worse situation)
γ	37,25 dyne/cm
R	1 µm (worse situation)
θ	60° (assumed)
η	9* 10^{-4}< η< 10 Pa*s (assumed)

Table III.4 Values of the parameters of the Washburn equation

R has been taken as 1 µm : according to the experimental results, most of the pores have a diameter approximately of 20 µm; however, the pore diameter distribution indicates the presence of a low quantity of pores with lower sizes (1 µm).

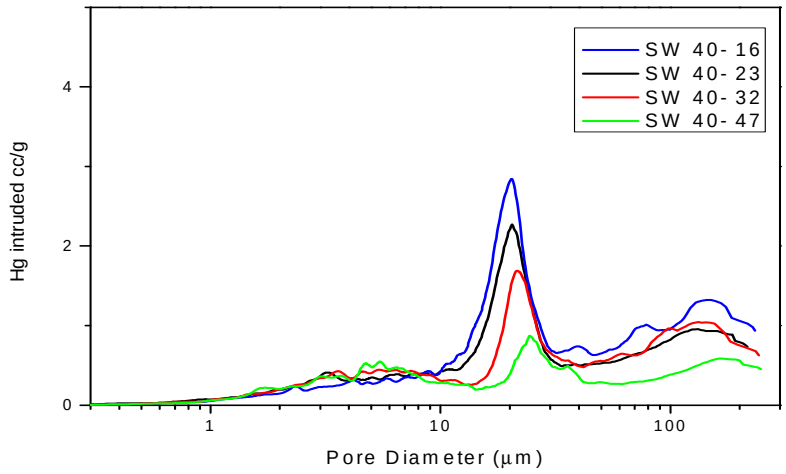

Figure III. 7 Pore diameters distribution for the samples SW40 16, 23, 32 and 47

The contact angle and the viscosity were set according to some general considerations : the high wettability, close to that of the water, and the worst case for viscosity.

Actually, the formulation is liquid and its viscosity could be compared to that of the water (8,94*10^{-4} Pa*s), however, considering the worst condition of a very viscous liquid, as for example honey, η = 10 Pa*s, a range of values has been considered in order to estimate the impregnation time.

After calculation, with the values discussed above, the impregnation time needed resulted ranging from 0,1ms for low viscosities to about 22 s for a viscosity of 10 Pa*s which is surely higher than the real one. The preparation procedure itself requires times longer than 22 s between the drawing down of the formulation and the irradiation (sealing of the quartz tube, transport to the UV lamp), nevertheless it has been chosen to introduce a constant impregnation time of 30 s right after the spreading of the formulation on the paper substrate.

2.1.2 Use of paper

One shot method, previously developed for not reinforced membranes and described in paragraph 1.4 and Figure III. **3**.

The first excellent result was that the reinforced electrolytes ready to be used, maintain the paper flexibility and are easy to handle as shown in Figure III. 8.

Figure III. 8 Appearence of a GPE membrane reinfoced with a cellulose handsheet

Considering that the final membrane properties may depend on the polymer nature and also onto its distribution/interpenetration in the cellulose network, it was decided to deeper study the impregnation / oligomer up-take of the paper porous substrate, as a function of paper characteristics.

In particular, it was decided to better investigate the effect of porosity on the Active Swelling (A.S.), as defined in the paragraph 1.6.2 and correlated with the quantity of polymer present in the composite membrane that should influence its final properties.

So, porosity was varied by varying i) the paper grammage/thickness, ii) the fibre composition (HW/SW ratio), iii) the refining level. Theoretical values were calculated for all the samples, according to the equation in the paragraph 1.6.1.

The evolutions are illustrated in the following graphs:

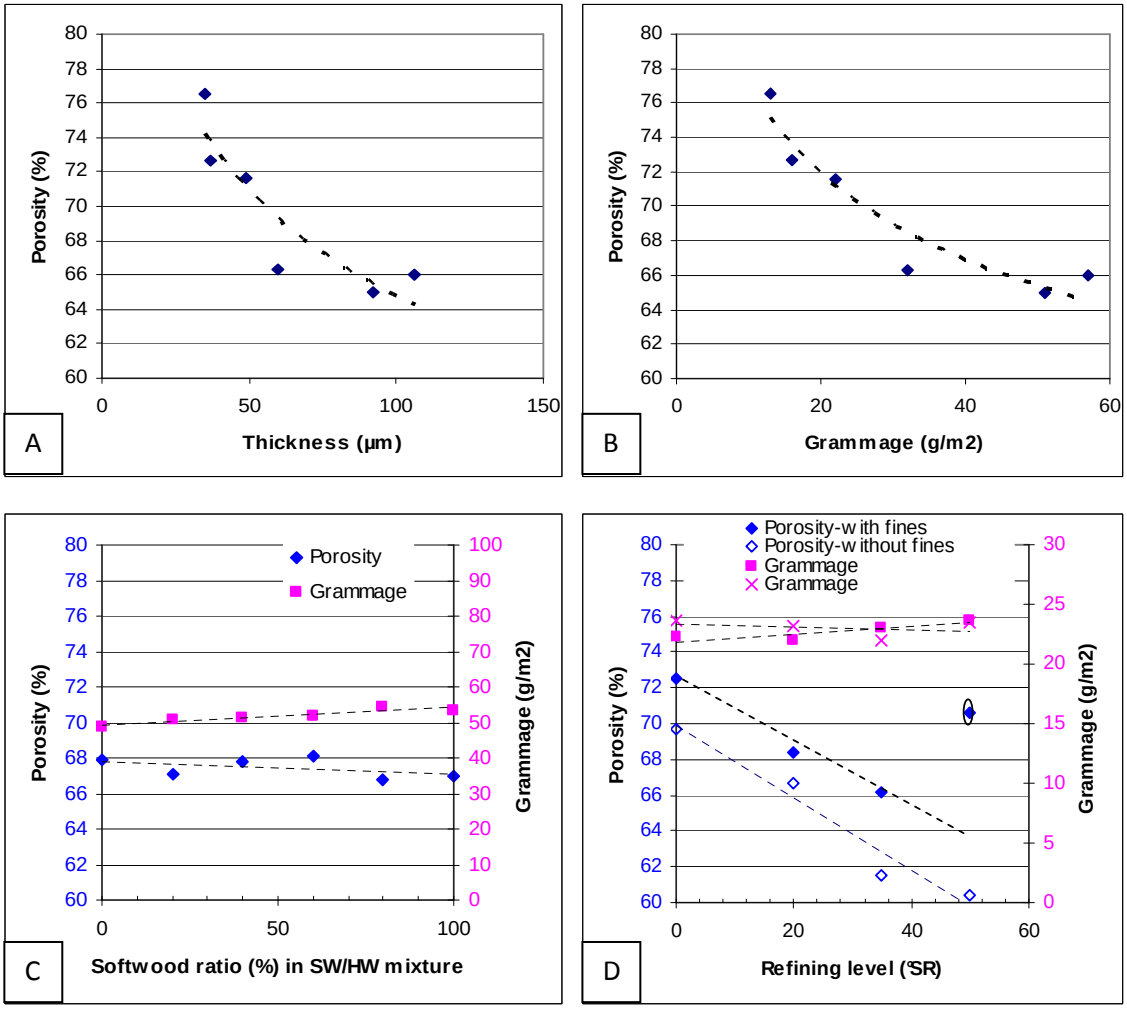

Figure III. 9 Porosity of the handsheets as a function of their thickness (A), Grammage (B), Fibers mixture (C) and Refining level (D)

As it can be seen, the largest variations in the porosity can be obtained by grammage variation or by refining level variation, because both induce a change in the sample mass/thickness, and consequently in the cellulose occupied volume or in the total occupied volume.

When varying the fiber composition, no changes of the theoretical value are expected at the same grammage/thickness. However, as a change in the

HW/SW ratio should induce a change in the flocculation level and consequently in the final grammage/thickness, this set of samples was also evaluated. Actually, small variations were observed, but they did not translate in significant changes of the theoretical porosity.

For some of the samples, it was also possible to perform mercury intrusion porosity measurements. The results obtained, compared to theoretical values, are reported in Figure III. 10

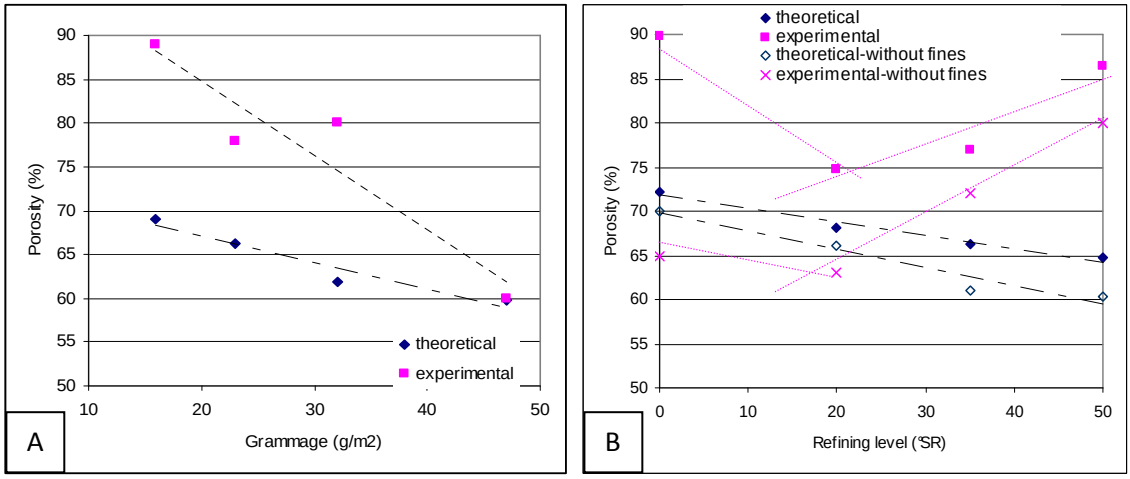

Figure III. 10 Measured porosity versus grammage (A) and refining degree (B).

It can be noticed that the percentage of porosity measured experimentally does not always match with the values predicted by the calculation, this can be due to the wrong assumption done for the calculation when considering cellulose as completely crystalline and also to the imprecision of the experimental measurement due to the high heterogeneity of the paper and to the sensibility of the instrument.

The evolution of porosity versus grammage is in line with the theoretical prediction (porosity decreases as grammage increases), mainly for the highest grammage (that presents the lowest porosity).

Conversely, the experimental values for the porosity as a function of the refining level did not follow the expected trend, confirmed by the theoretical calculations. Actually, porosity seems to decrease when refining at low level (from 0 to 20 °SR), while then it increases when increasing the °SR. This is not in agreement with the impact of refining on the final paper density

(Figure III. 11), that increased because of the increase in the fiber flexibility and the subsequent better fiber "packaging"

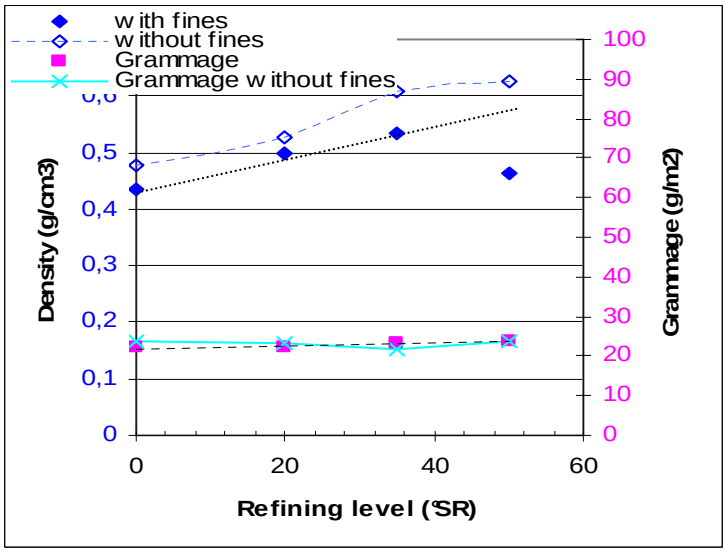

Figure III. 11 Variation of the paper density as a function of the refining degree

This unexpected result for higher refining levels could be explained by a problem in the sheet formation (high flocculation with heterogeneous floc distribution) or by a too high fibrillation of fibres, creating additional porosity (and not filled by fines, when present, likely because they adsorb onto the surface). However, further work would be necessary to find and validate any explanation.

After having assessed the porosity variations of the substrate, it was investigated if this parameter influences the active swelling.

As expected, the active swelling increased with the porosity increase, due to the grammage variation, as shown in the Figure 10, A, where theoretical values are taken for porosity (as they followed the same trend as experimental values, see Figure III. 12).

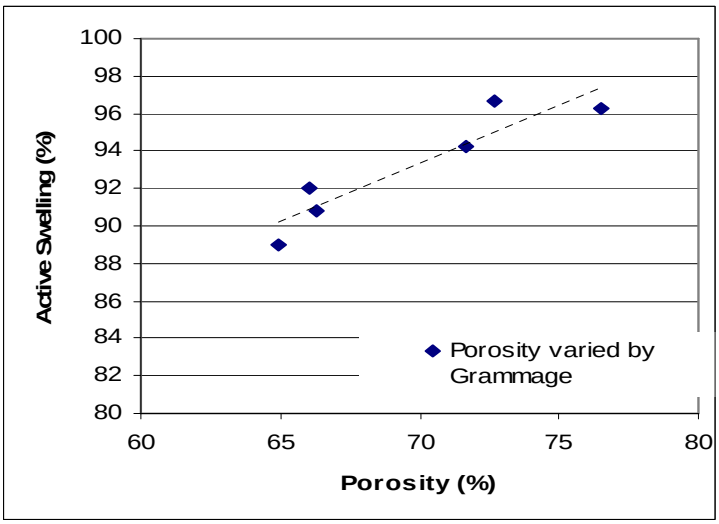

Figure III. 12 Active swelling values as a function of the porosity in the grammage series

No discussion is possible on the impact of fibre composition because of the lack of experimental values for porosity. It can only be noticed that in that case, very few variations of theoretical porosity corresponded to some variations in the A.S. This could be due to the influence of the fiber composition (hw/sw ratio) on the pulp flocculation level and consequently of the sheet formation. In this sense, the mixture expected to give the most uniform structure (thanks to the compromise between the amount of long and short fibres) gave also the highest A.S. (SW40, A.S. 95%)

Finally, for the variation of the refining level, it can be observed that in this case, no clear trend is visible, especially for the hyperwashed pulp (without fines), whereas for the entire pulp, A.S. seems even to decrease when increasing porosity. This could partially be explained by considering that with refining some structural modifications of the fibre take place, leading to potential modification not only of the inter-fibre porosity but also of the intra-fiber porosity.

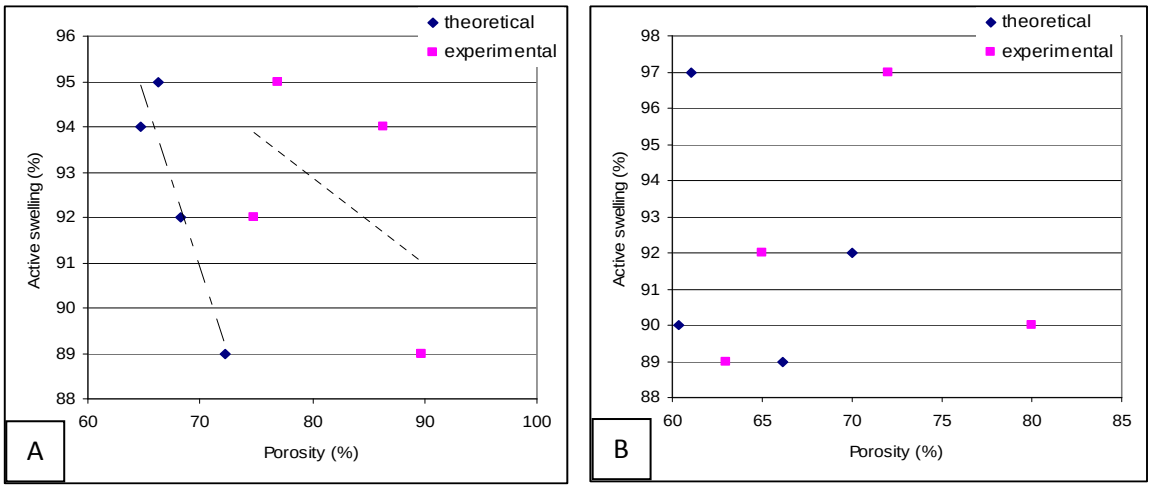

Figure III. 13 Variation of the Active Swelling as a function of the porosity for the refining series with (A) and without (B) short elements

Additionally, it should be taken into account that the variation range for both parameters (porosity and especially AS, which is very high-80 to 90%) is quite narrow, so it is much more difficult to point out clear trends, not influenced by the experimental errors.

Taking into account previous discussion, it seems that the oligomeric formulation can fill all the paper porosity, even if the results obtained with the pulps refined at different level, suggest that in some cases (high macrofibrillation) the pore accessibility might be more difficult.

Additionally, as very high active swellings were measured, the theoretical active swelling was calculated to check if the porosity was completely filled. Theoretical active swelling is calculated considering the weight of the polymer that should be measured when the porosity of the polymer is completely filled by the formulation. For such a calculation, the density of the formulation was measured by a glass picnometer and resulted to be about 1,3 gcm^{-3}, the density of the gel-polymer after polymerization was considered the same.

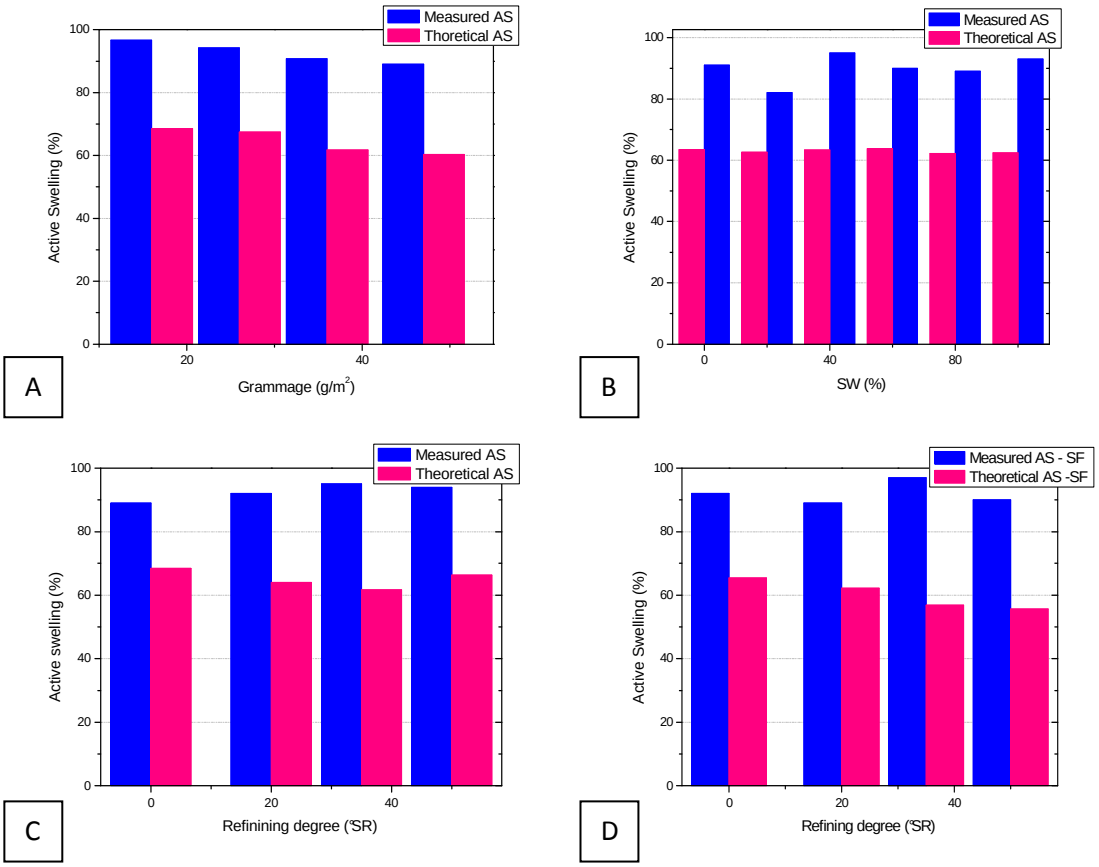

Figure III. 14 Comparison between the effective active swelling and the theoretical active swelling for the grammage series (A), the fibers mixture series (B), and the refining degree with (C) and without (D) short elements

As it can be observed, in all of the cases, porosity was totally filled and an extra-amount of formulation was present. In order to explain this behaviour, microscopic analysis were performed and it was observed that the One Shot preparation procedure leads to the formation of a layered structure. As an example, the membrane formed with paper Softwood100 SR0 23 g/m^2 is shown in Figure III. 15

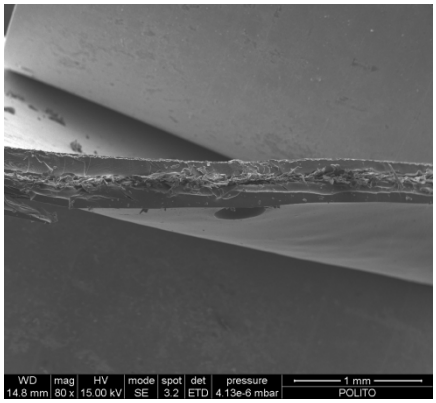

Figure III. 15 SEM cross section image of a reinforced membrane, it is possible to observe the layered structure formed during the One Shot preparation

In Figure III. 16 a schematic representation of this structure is reported, the membrane (C) is constituted by the impregnated paper layer (A) and two polymer layers (B).

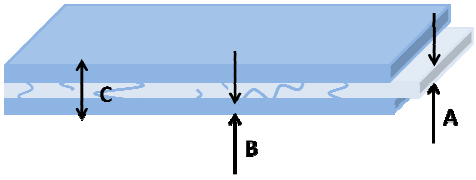

Figure III. 16 Schematic representation of the layered structure is reported, the membrane (C) is constituted by the impregnated paper layer (A) and two polymer layers (B) The volume of the pores will be labeled “D”.

This structure can be explained considering that an excess of oligomeric formulation was always used for the membrane synthesis. Actually, the quantity of formulation used was approximatively 0,1g/cm^2 Because of the manual preparation, during the draw down step, a fraction of the formulation was always lost. When considering the whole pore volume, as previously calculated, it appears that the quantity of mixture used is always much higher than the one needed to fill the pores. Additionally, it was even higher of that required for the formation of the layered structure.

To conclude, with this membrane synthesis, in most cases the paper is completely impregnated by the formulation used; moreover, a small fraction of the mixture fills the paper pores, the most of the excess forms the double

polymer layer and another fraction is lost during the bar passage or on the PE substrate used for the polymerization.

An alternative "drying" preparation procedure for the reinforced membrane has been developed in order to avoid the formation of polymer layers on the impregnated cellulose and to understand the influence of these layers on the membrane properties. The membrane obtained with such a procedure was used for comparison with standard one, so only few conditions were tested: SW100-SR 23 g/m²-SR0, 20, 35, 50. The membranes defined "dry" presented active swelling values ranging from 38 and 45 %.

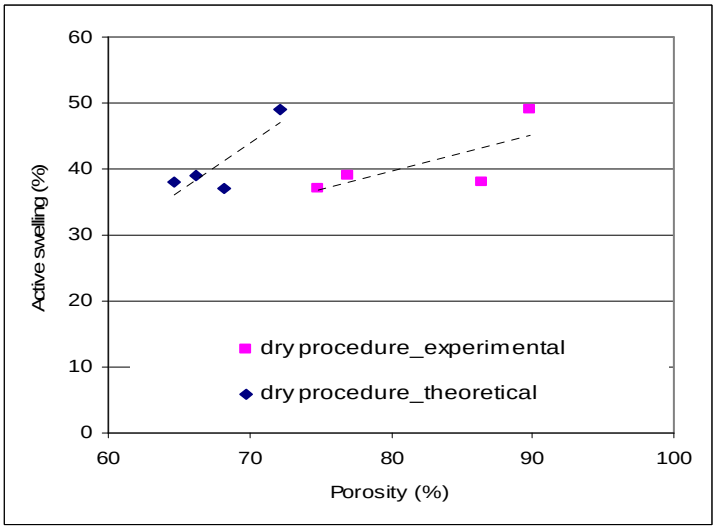

Figure III. 17 Active swelling values obtained from the Drying preparation of reinforced GPEs

Once again, the A.S. variations fall in a narrow range, so it is difficult to draw any conclusion; however, a general trend towards the increase in the A.S. when increasing the porosity was observed.

Moreover, in this case the A.S. values seem to be lower than that expected to fill all the pores. Thus, probably this procedure will not allow to have membranes with sufficient conduction.

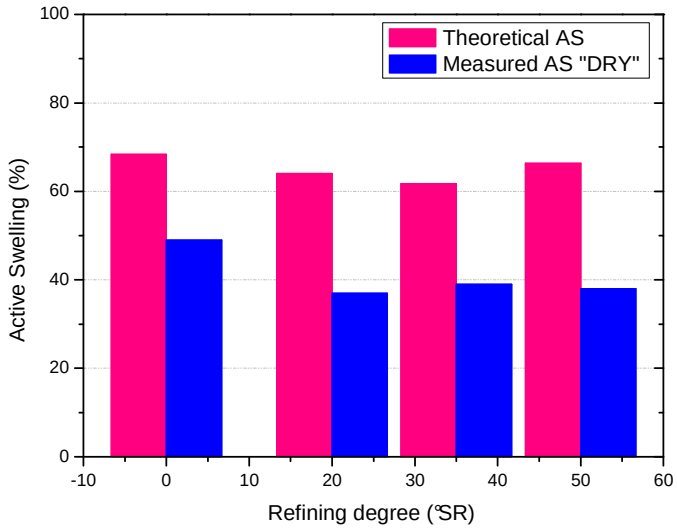

Figure III. 18 Comparison between the effective active swelling measured for the drying procedure and the theoretical active swelling for the refining series

As an example of the membranes obtained with the modified procedure, Figure III. 19 shows the system prepared from handsheet SR0 (SW100, 23g/m^2).

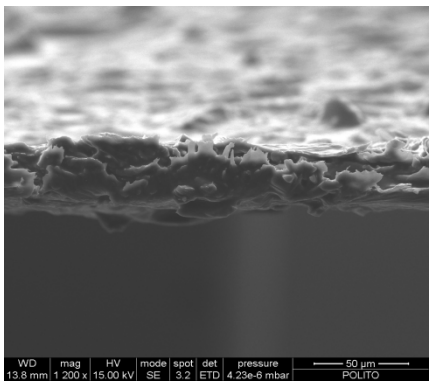

Figure III. 19 SEM cross section image of a "dry membrane", in this case the layered structure has been avoided

Finally, concerning the membrane synthesis, a third route has been developed: considering the possibility of introducing the lithium salt in the last step of the GPE preparation, the swelling procedure has also been tested. A reinforced membrane composed of BEMA, PEGMA and EC/DEC (without Li-salt) has been prepared and then swelled in a liquid electrolyte (1M solution of LiTFSI in EC/DEC), after only 15 minutes the polymer starts to

detach from the cellulose substrate, as visually observed. The UV irradiation of the reactive mixture does not lead to the creation of a sufficient quantity of chemical bonds between the polymer and the cellulose reinforcement, as supposed by considering the activation of cellulose by UV-ligth (ref). The composite membrane produced in such way can not resist the swelling procedure. Figure III. 20 shows a reinforced membrane after 15 minutes of swelling.

Figure III. 20. Reinforced membrane after 15 minutes of swelling in a liquid electrolyte.

2.2 GPCE electrochemical properties

The results concerning the ionic conductivity of the membranes reinforced by papers prepared by varying the fibers mixture, the grammage and the refining degree are presented and discussed in this paragraph.

It is possible to observe for all the handsheets series that, when the One shot procedure is followed, the presence of a layer of cellulosic fibers in the membrane causes a decrease of conductivity of about one order of magnitude. It was also observed that the percentage error on a series of measurements is higher in presence of the reinforcing substrate if compared to the neat membrane rising from 25% for this last to 43% for the reinforced GPE, this behaviour is likely due to the heterogeneity of the paper.

2.3.1 Impact of fibre composition

Arrhenius plots obtained for the samples reinforced with papers containing different fibers mixture are shown in Figure III. 21.

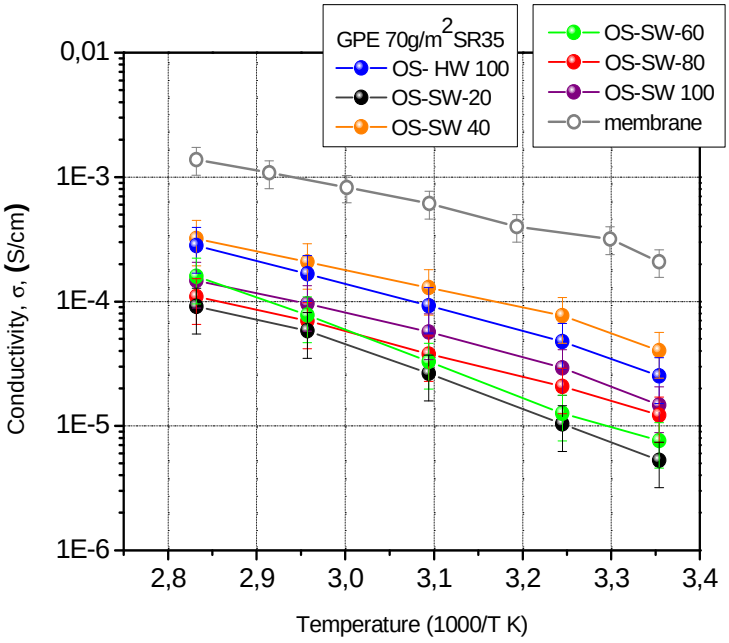

Figure III. 21 Arrhenius plots of the conductivity of One shot GPEs reinforced with handsheets containing different quantities of HW-SW fibers

As anticipated, the use of paper led to a decrease in the ionic conductivity, whatever the temperature tested. Concerning, the impact of the fibre composition (and consequently of the paper formation), it can be seen that the differences between the samples are often in the range of error, so that no clear trend can be detected. Nevertheless, it seemed that the sample SW40 was better performing with respect to the other mixtures of fibers. In reference to active swelling (A.S.) previously shown in Figure III. **14**. B it is possible to notice that the highest conductivity found for SW40 corresponds to the highest A.S. and, on the other hand, the lowest values for the sample SW20, correspond to the lowest A.S.

This is in agreement with the hypothesis that higher the quantity of the polymer matrix, higher the conductivity.

Moreover, a better uniformity in the substrate (as given by a correct flocculation level, as in SW40) could also lead to a better interpenetrated polymer-fibers network, with consequent higher A.S. and conductivity values.
The relationship between A.S. and conductivity is less clear for the other samples, but it should be said that the differences between values are quite small and the conductivity ranges of error are overlapping.
It can be concluded that the use of paper induces a decrease in the ionic conduction, slightly or nor impacted by the morphological characteristics of the fibre furnish. This is likely maybe due to the inert role of cellulose from the ion conduction point of view.

2.2.2 Impact of grammage

For that reason, it was decided to try to reduce the quantity of cellulose used, by varying the paper grammage (g/m^2) and consequently the thickness of the Handsheets. This was the easiest way to obtain a thinner and with a more variable porosity.
According to the results previously shown, handsheets composed of a mixture of fibers HW-SW (60-40) SR 35 were prepared, in order to have different final grammages / thicknesses for the membrane elaboration.

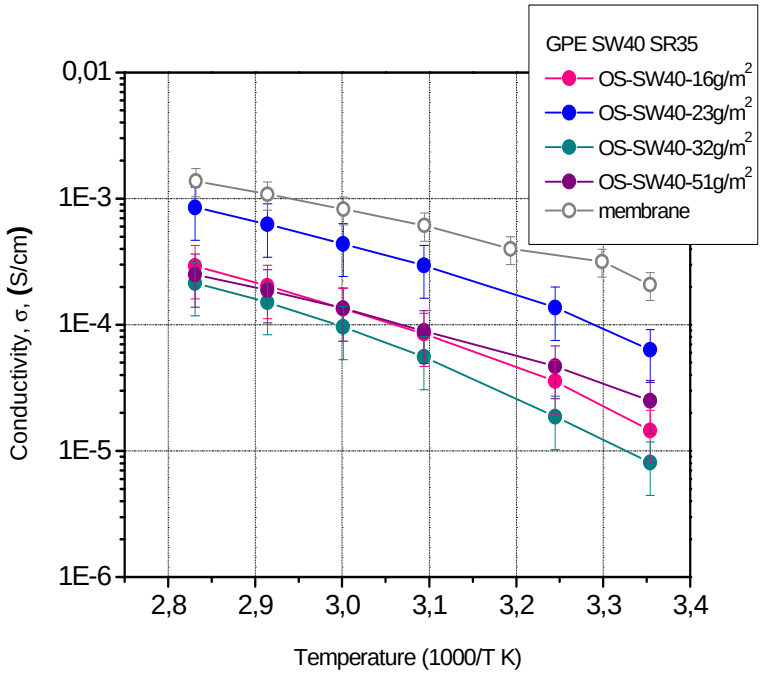

Figure III. 22 Arrhenius plots of the conductivity of One shot GPEs reinforced with handsheets with different grammages.

Figure III. 22 shows the Arrhenius plots obtained; the best behaviour is shown for OS-SW40-22 membrane that was also characterized by one of the highest active swelling (Figure III. **14**.A)

Sample OS-SW40-16 is the thinnest sample and it had the highest A.S., but relatively low conductivity: this can be partially explained by some practical difficulties to handle the sample: it had tendency to roll up and it was hardly stretchable for its use, the solicitations it was subjected to during the preparation of the cell could have damaged its performance.

However, with the exception of sample OS-SW40-16, also in this series, as for the series obtained when varying the fiber composition, the best performing sample resulted to be the one showing the highest A.S. When the Arrhenius plot here presented is compared to the one in Figure III. 21 it is possible to see that the GPE SW40-22 has a conductivity only slightly higher with respect to the SW40 (the best performing in that series) which had a grammage of about 70g/m^2, both samples have an A.S. of 95%. The higher grammage of sample SW40 would imply a higher density of the handsheet and thus a worse interpenetrated structure between polymer and cellulose fibers, the small difference between the conductivity values of samples OS-

SW40 (70g/m²) and OS-SW40-22 demonstrates again that the presence of an excess of polymer matrix reduces the effect of the paper structure.

To conclude, a reduction in the ratio cellulose/polymer can induce a slight increase in the ionic conduction. Nevertheless, the variation observed are quite modest and likely as long as the bilayered structure is present, and the ratio cellulose/gel polymer is quite similar (0.12<x<0,03), the influence of the paper is drastically reduced.

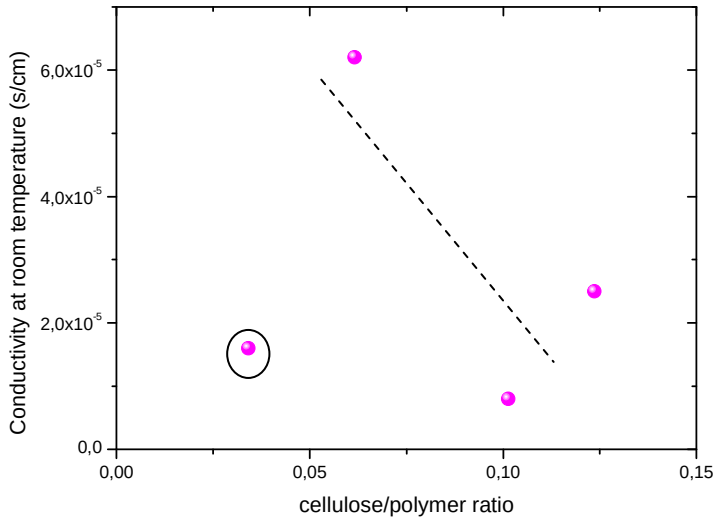

Figure III. 23 Variation of the ionic conductivity at room temperature as a function of the cellulose/polymer ratio.

2.2.2 Impact of refining level

The third way to modify the paper structure, in order to study the impact on ionic conduction, was the fibre refining. It modifies the fiber morphology, flexibility, and consequently the resulting paper porosity, density and fiber arrangement. During the refining, short fines are also produced, by shortening of longer fibers, due to the strong mechanical action in the refiners. These fines can fill some of the paper porosity, so handsheets were done with the entire pulp or with the hyperwashed pulp (washed on a 100µm screen, by pressurized water, in order to remove the fines). For the screening of the influence of paper characteristics on the behavior of reinforced GPEs,

samples composed by different mixtures of fibers (SW100, SW40 and HW100) with different grammages (16, 22, 32, 50 g/m^2) and different refining degrees (0, 20, 35, 50 °SR) were prepared. GPEs reinforced by handsheet with a grammage of 22 gm^{-2} (that gave the highest conductivity, when studying the impact of grammage), with and without short elements were tested by impedance spectroscopy.

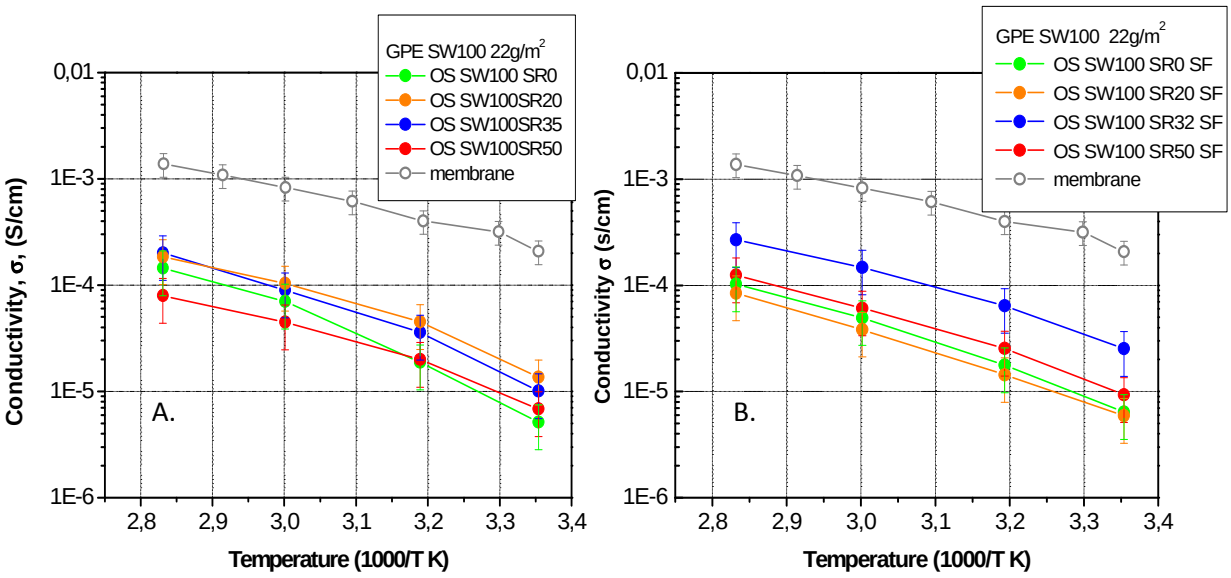

Figure III. 24. Arrhenius plots of the conductivity of One shot GPEs reinforced with handsheets with different refininig degrees with (A) and without (B) short elements

Once again, the differences induced by the variation in the paper structure are very modest, and negligible in most of the cases. Thus, it is hard to detect any trend or to conclude on a specific effect of the paper characteristics on the final conductivity, in spite of the quite important variations induced on the porosity.

When the dying procedure was adopted the conductivity values see a further decrease, as shown by the Arrhenius plot obtained for the Dry membranes (Figure III. 25).

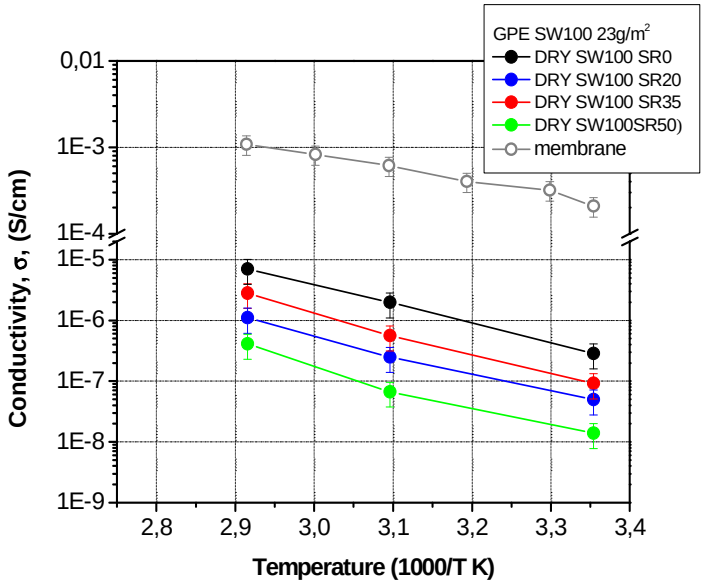

Figure III. 25 Arrhenius plots of the conductivity of DRY GPEs reinforced with handsheets with different refining degrees

The drying procedure causes a decrease of the conductivity of the membranes of about 4 orders of magnitude if compared to the neat membrane and of 2 orders of magnitude with respect to the one shot ones (from 10^{-5} to 10^{-7} at RT). This can be explained considering that the active swelling and thus the quantity of active material (Li salt) is reduced to the half (from about 90% of A.S. to 49%), consequently the ratio cellulose / gel polymer increases in favor of cellulose, it ranges from 1 to 1,8, i.e. one order of magnitude more than the value with the standard procedure).

However, in this case, the influence of the cellulose substrate is much more pronounced, and the relationship between the conductivity and the ratio cellulose / gel-polymer is more evident (Figure III. 26).

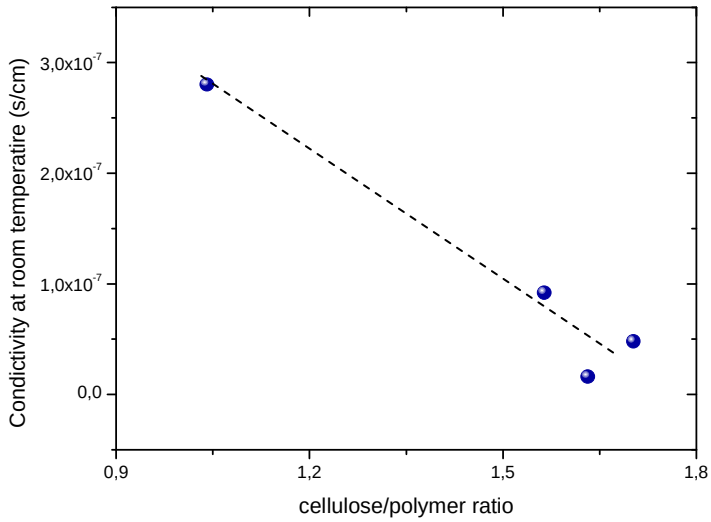

Figure III. 26 Variation of the ionic conductivity at room temperature as a function of the cellulose/polymer ratio for the "dry" membranes.

The best results (i.e. the highest conductivity in the whole range of temperatures investigated, from 20 °C to 70°C) was obtained for samples SW100 SR0, confirming that a higher quantity of polymer, and thus of lithium salt, is necessary.

It can be concluded that the use of cellulose, from the electrochemical point of view, impairs the ionic conduction and thus the performances of the membrane. For this reason, its ratio towards the gel-polymer should be limited and polymer should be added in excess in respect to the amount needed to fill paper porosity. But when this is done, it translates in the formation of a bilayer structure. This conclusion opens new research routes for increasing the compatibility among layers.

2.4 Mechanical properties

The mechanical properties of the reinforced membranes will be now discussed and related to the paper properties. It is necessary to remember that the neat membrane is self standing but its flexibility and resistance are limited; the tensile test can not be performed because the sample can not outstand the pressure of the clamps.

The membrane was firstly reinforced by handsheets with a grammage of about 70 g/m^2 and refining degree of 35°SR, papers containing different ratios of Hardwoodand Softwood fibers were tested.

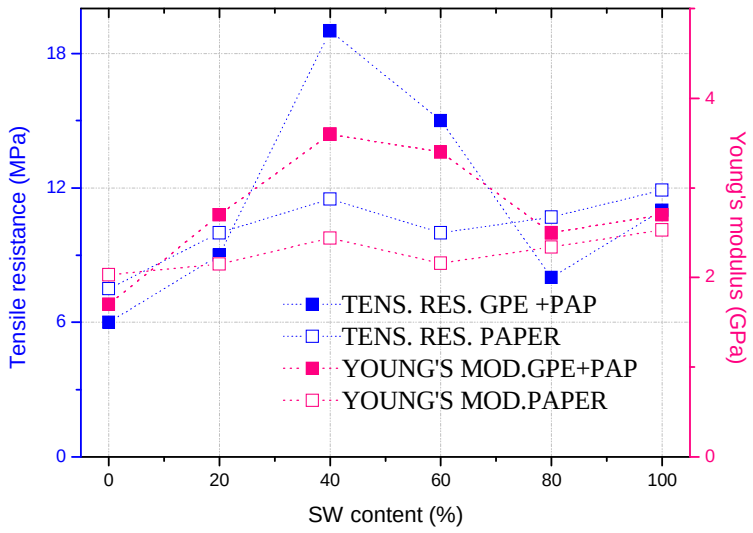

Figure III. 27 Mechanical properties of the reinforced GPEs (filled symbols) compared with the mechanical properties of cellulose hansheets (empty symbols).

The results of the tensile tests performed on the reinforced membranes are plotted in Figure III. 27. The mechanical performances are largely increased by the presence of the cellulose substrate, so that it was possible to perform the measurements on all the samples. High values of Young's modulus and tensile resistance were measured; also in this case sample SW40 gives better results. An explanation of this behaviour can be found by analyzing the structure of the handsheets and their properties in absence of the polymer matrix.

The analysis performed on the set of handsheets confirmed that the variation of the SW/HW ratio led to different properties, as expected. SW fibers are generally longer and have an higher L/T ratio (Length/cell wall Thickness), their use leads to the preparation of handsheets with high mechanical properties due to the high number fiber-fiber interactions but low homogeneity, HW fibers on the contrary are shorter, they allow the production of homogeneous and not flocculated paper with lower mechanical properties.[9-11] So, often mixture of the two fibre type are used to find a

compromise between strength/flocculation. The values of the formation index measured are summarized in the following table, and clearly show the impact of HW on the flocculation:

Sample	F.I
SW-100	149,1
SW-80	142,2
SW-60	143,6
SW-40	124,8
SW-20	114,9
SW-0	106,7

Table III.5 Flocculation index of the handsheets containing different fibers mixtures (SR35, 70 g/m^2)

When decreasing the amount of SW, the F.I. decreased, too, indicating a better formation, i.e. a more homogeneous material.

Whereas for the mechanical properties, the trend is reversed, with a tensile resistance of 12 MPa for SW 100 (only SW fibres), which was reduced to 8 MPa in the case of sample SW-0 (where only HW fibres are present).

However, for mechanical properties a relative maximum for sample SW40 in the tensile index and in the Young's modulus is observed. This result might be explained by the existence of an optimal compromise between the properties induced by the intrinsic fibre properties (higher for SW) and those induced by the network characteristics, namely its uniformity (better formation when adding HW).

The mechanical behaviour of the GPE reinforced membranes reflects the trends shown by the handsheets, with values close to those of the handsheets, except for the samples SW40 and SW60, where the membrane is much more performing than paper itself. This unexpected result could be correlated to the more uniform fibrous structure that allows a more homogeneous formation of the final composite membrane.

According to the results here described, handsheets formed by a mixture of softwood and hardwood fibres in the ratio 40-60 can be suggested for further works. It can be noticed that such mixtures are often used in papermaking for printing/writing grades, so this indirectly confirms their optimal properties, at least for the paper application. The work performed so far suggest that they represent also the best combination for gel-polymer-cellulose electrolytes.

The properties obtained with handsheets at different grammages (fibre compositon SW-HW (40-60) SR 35) are reported in the following figure and compared to the paper properties.

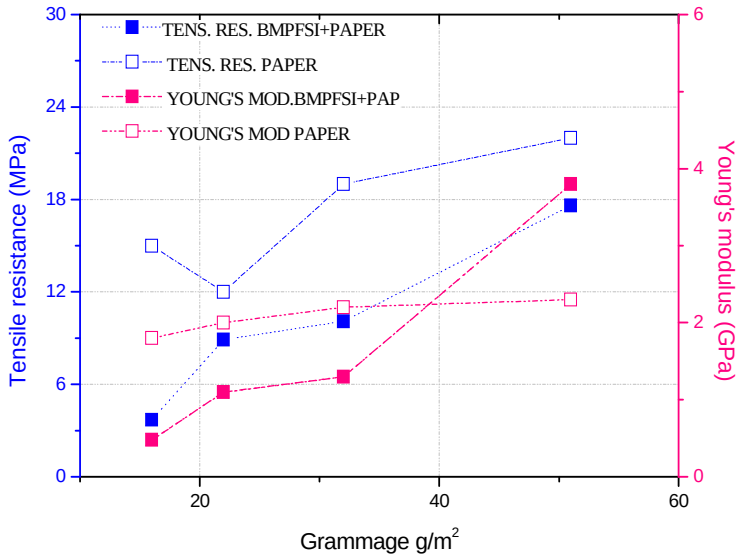

Figure III. 28. Mechanical properties of the reinforced GPEs (filled symbols) compared with the mechanical properties of cellulose hansheets (empty symbols).

Once again, high values of Young's modulus and Tensile resistance were measured, and they are likely more than sufficient for the envisaged application. As expected, the mechanical performances improve by increasing the grammage and decreasing the porosity of the paper (see Figure III. 28) for the simple hansheet and for the reinforced membrane. From Figure III. 28 it is visible that the presence of the polymer matrix for samples reinforced by handsheets causes a decrease of the mechanical properties if compared to those of the substrate alone. The tensile resistance in the handheet is given

by the resistance of the single fibers but also by the fiber-fiber interactions, in a non-compact structure the impregnation of an organic formulation can reduce those interactions causing the decrease of the properties. However, for the highest grammage, the trend seems to be reversed, with higher mechanical properties for the membrane than for the paper, as already previously observed (Figure III. 27), for a even higher grammage (70 gm^{-2} vs 50 gm^{-2}). To try to explain this result, SEM measurements were performed.

SEM images taken on hansheets with grammage of 16 and 50 gm^{-1} showed a more dense structure for samples with higher grammage, Figure III. 29 compares the images of the top views and cross sections of the two samples. While sample SW40-16 is constituted of few layers of fibers sample SW40-51 is more compact and it is composed of an higher number of fibers layers. This corresponds to an expected increase in the handsheet density, as shown in Figure III. 30.

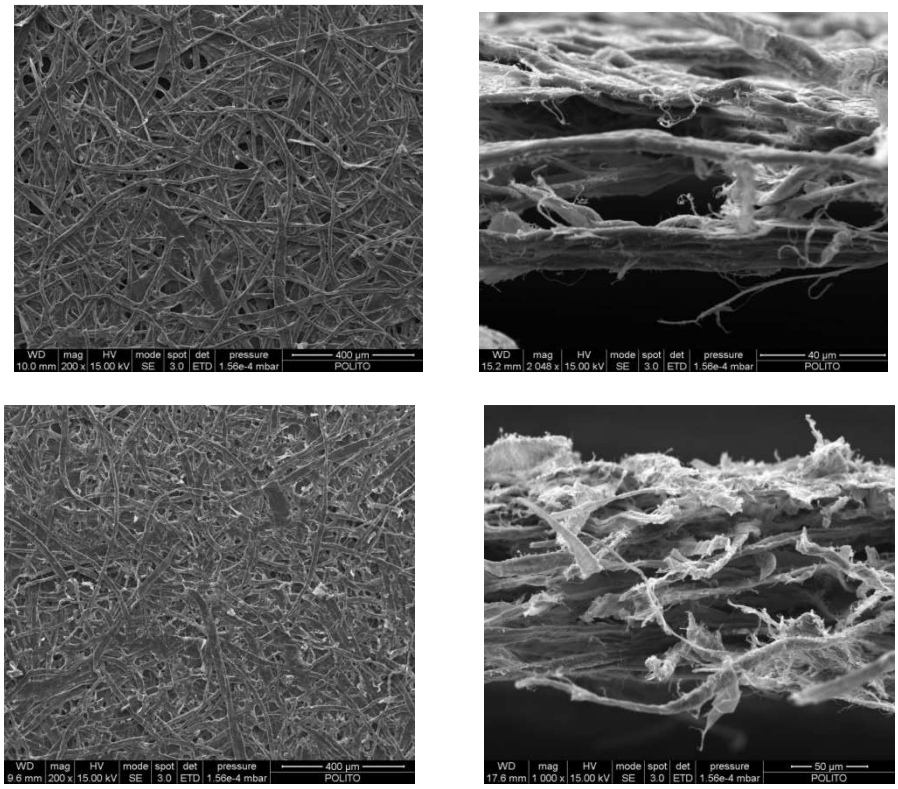

Figure III. 29. SEM images of sample SW40-16 (upper line) top view (left) and cross section (right) and of sample SW40-51 (second line) top view (left) and cross section (right)

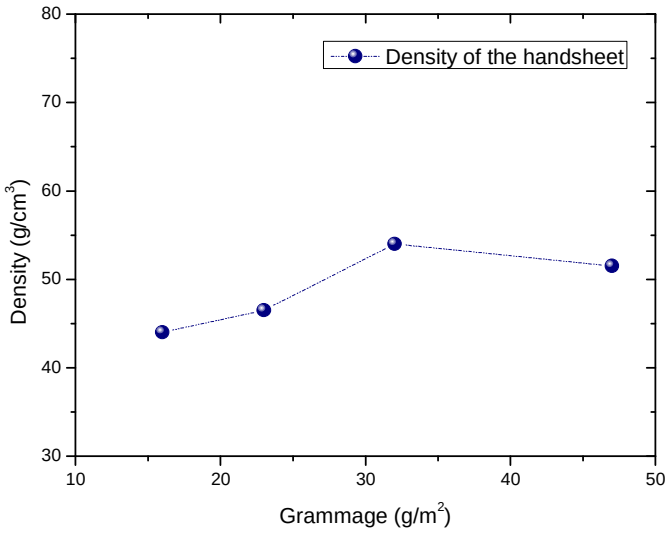

Figure III. 30 Density of the hansheets with different grammages.

So, for more dense structures, the matrix impregnation in all the pores (as shown when comparing theoretical and measured active swelling), allows to even increase the initial mechanical properties. This could be due to a better interpenetration of the fibrous and polymeric networks, creating a sort of quite continuous material (with likely some anchoring point if grafting onto fibres takes place by UV-ligth activation), and resulting in better properties than the paper itself. On the contrary, for more porous structures, the formation of a heterogeneous two-phase material with few bonding points led to a decrease of the mechanical properties of the paper.

It can be interesting to notice that when considering the tensile index (i.e. the index calculated to avoid the impact of the grammage) of the handsheets plotted in Figure III. 31.A it has an average value of 0,02 KN*m/g whatever the grammage considered. When the tensile index is calculated for the reinforced membranes by considering the new grammage including the polymer weight it is possible to see that the data trend follows the one observed for the tensile resistance values being the differences in the grammages of the handsheets made irrelevant in the measure of the final grammage of the membrane. (Figure III. 31.B)

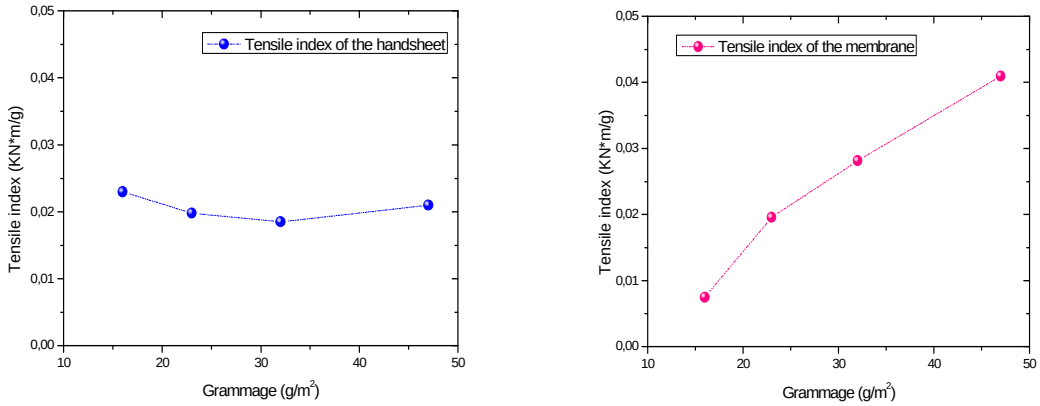

Figure III. 31 Variation of the tensile index (tensile resistance/ grammage) of grammage series of handsheets (A) and of the grammage series of GPEs membranes (B)

Considering the results above discussed, and those obtained from the conductivity measurements, the handsheet SW40 with the grammage of 22 g/m^2 can be chosen as the best compromise in order to obtain a better conductivity and good mechanical strength.

Finally, mechanical properties of the merbanes obtained with handsheets at different refining level were assesed.

As already discussed, the refining treatment can modify the morphology of fibers, and particularly, their length, thickness, surface area and flexibility. This results in different final paper properties, as shown in Figure III. 32.

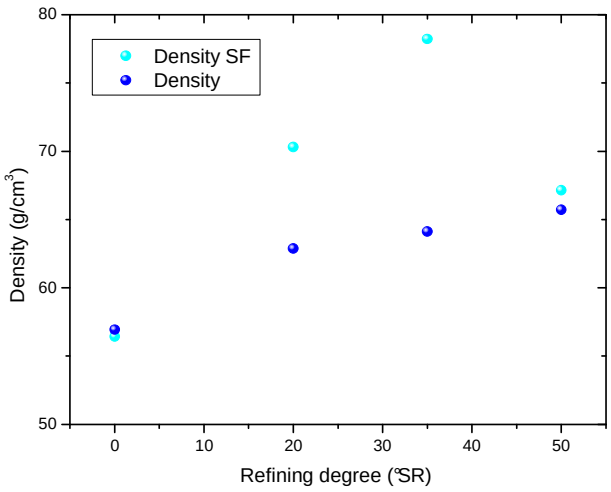

Figure III. 32 Density of the hansheets with different refining degrees with (blue) and without (light blue) short elements

The main treatment drawback is that some fibres can be damaged because of too high mechanical shears and longer fibres can be shortened, thus fine elements are created. Handsheets were prepared with the entire pulp (containing the fine elements) or with hyperwashed pulp (in which fines were removed).

Considering previous results and considering that the same trends were detected whatever the grammage, it was decided to report hereafter the results for the SW100 grammage 22 gm^{-2}.

Results concerning SW40 and HW100 series will be reported in appendix A, SW100 handsheets have been chosen because SW fibers, being longer and larger than HW ones, are more sensitive to the beating operation. Moreover, the trends with such a pulp are clearer than with the mixture 60/40, in which the combined effects of refining on the HW and SW should be considered (and they can be opposite).

Once again, mechanical properties of the GPCE follow the same trend as for paper: as expected, they improve when the refining degree is increased (Figure III. 33). Paper done with unrefined pulp have poor mechanical properties, while when fibers are refined tensile resistance and Young's modulus increases, even if they seem to reach a plateau at 20°SR.

In agreement with previous results for the same grammage (22 gm^{-2}), the composite membrane properties are lower than those of the paper used to produce the membrane, except for the sample SR0 whose very low tensile resistance is improved by the polymer.

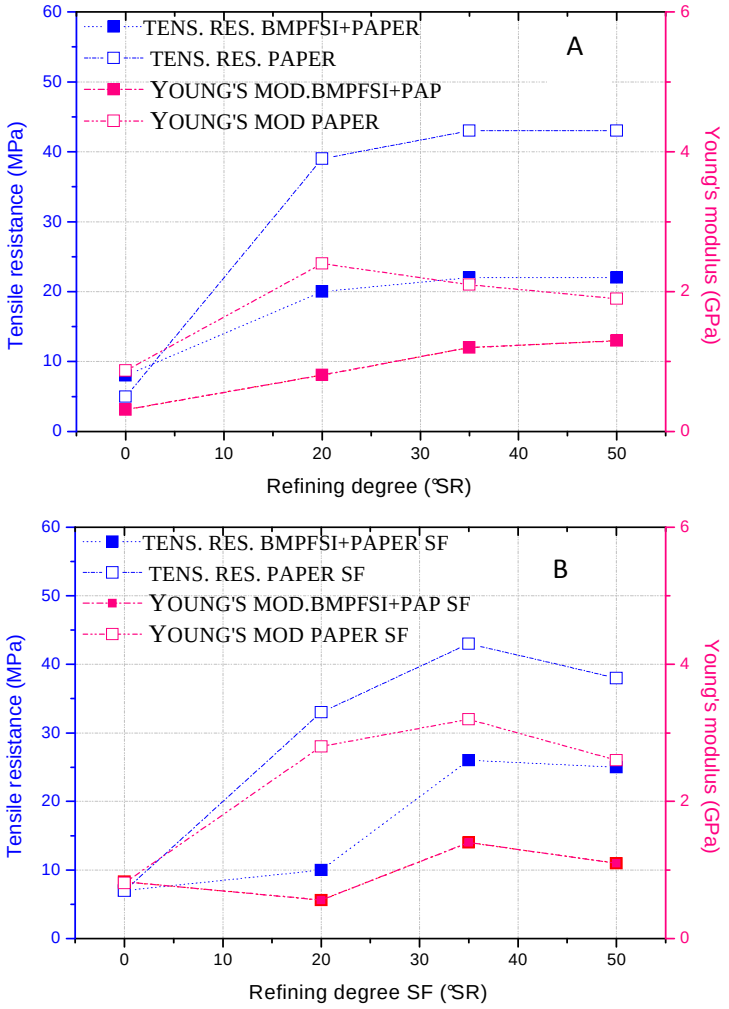

Figure III. 33 Mechanical properties of the reinforced GPEs (filled symbols) compared with the mechanical properties of cellulose hansheets (empty symbols) with (B) and without (D) short elements

Tensile test has also been performed on the membrane polymerized after drying the excess of reactive mixture. The results in terms of Tensile resistance are compared to those obtained for the simple handsheet and for the reinforced membrane not dried in the following figures.

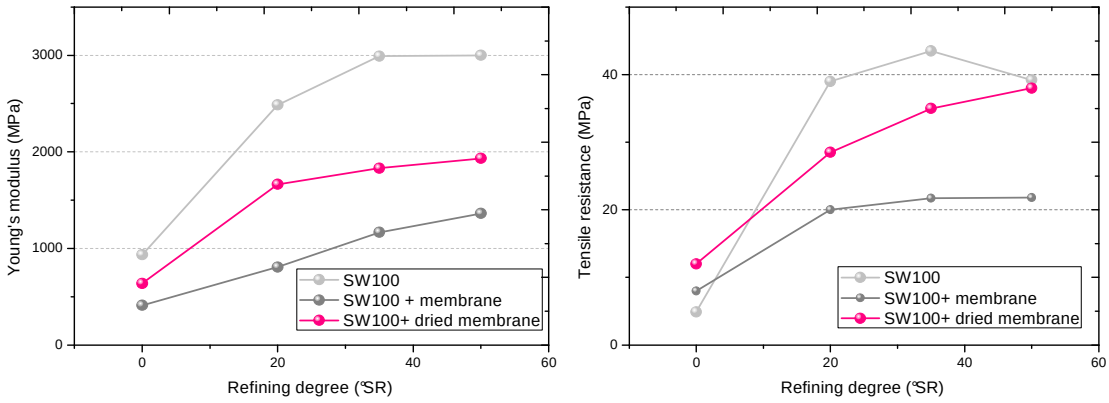

Figure III. 34 Young's modulus (left) and tensile resistance (right) of samples SW100-22g/m^2 SR 0, 20, 35, 50 handsheet (light grey), SW100-22g/m^2 SR 0, 20, 35, 50 dryed membrane (red), SW100-22g/m2 SR 0, 20, 35, 50 One shot membrane (dark grey)

Comparing the sample prepared following the One Shot procedure and the dried ones is it possible to observe that a lower amount of polymer gives better properties, thus confirming the relative negative effect of the polymer presence in the fiber network. However, even if this procedure allows to obtain better mechanical performances, it resulted in lower electrochemical properties, as already discuss, so this is not a valuable alternative.

Thus, it can be concluded that the use of paper really confers excellent mechanical properties to the composite membrane.

The latter have tensile strength only slightly lower than that of the paper itself, unless the paper used has high grammage. In this last case, the membrane mechanical properties were higher than that of the paper itself, but, considering the negative impact of high grammage on the ionic conductivity, the use of such paper should be avoided. An optimal mixture of hardwood and softwood fibres, as well as pulp refining can allow to further increase mechanical properties. However, it should be underlined that all the values measured, even the lowest, are much higher than the values found in literature for this kind of electrolytes . Thus, considering also the conductivity results, it is possible to conclude that, from the application point of view, even an handsheet prepared with unrefined fibers and only long fibres (SW100-22-SR0) can give acceptable performances[12].

Nevertheless, with the perspective of the industrial up-scaling and the use of roll-to-roll techniques, process motivations could lead to select a mixture of hardwoodand softwood, refined at an intermediate level (approximately 20-30°SR).

Unfortunately, if the use of paper allows to obtain membranes with outstanding mechanical properties, on the other hand, it negatively impacts the electrochemical performances. To limit this impact, the ratio cellulose/gel polymer should be reduced, as shown by experimental results, by the use of paper with low basis weights. Moreover, the use of fiber mixtures (hardwoodand softwood) leading to more uniform cellulose substrate seems to result in lower ionic conductivity losses. Nevertheless, likely because of membrane structure (bi-layer), paper properties seem to have little or quite no influence on the final membrane electrochemical properties.
Thus, tailoring of the paper properties, to restore the electrochemical properties of the original GPE membrane, is not a viable route. Alternative strategies to increase the GPCE properties were investigated and are presented in the next paragraph.

2.5 Strategies for increasing the ionic conductivity

2. 5.1 Use of additives

Commercial papers are produced by adding to fibers a large variety of additives, to modify the bulk or the surface properties of the paper or to facilitate the process. Generally, they are categorized either as process additives or as functional additives. Process additives are materials that improve the operation of the paper machine, such as retention and drainage aids (ionic or non-ionic polymers), biocides, dispersants and defoamers (surfactants). Functional additives are materials that enhance or change specific properties of the paper product, such as fillers (inorganic), sizing

agents (hydrophobic molecules), dyes, optical brighteners, and wet- and dry-strength additives (polymers)[13].

As it can be seen, they can be very different in chemical nature and properties, and, in this large spectrum of products, some might influence the electrochemical conduction in the membrane: so, in order to understand their eventual influence on a gel polymer electrolyte behavior, they have been added to our handsheets, by selecting the most common or those supposed to potentially affect the final GPCE electrochemical properties.

According to previous results, the reference pulp slurry was 40% of softwood fibers and 60% of hardwood fibres, refined at 35°SR, handsheets with a grammage of about 55 gm^{-2} were prepared and used to reinforce the GPE One Shot membrane. In spite of the better performances of 22gm^{-2}, such a high grammage was necessary in order to assure a good dispersion of the additives in the paper. The electrolytes have than been tested in terms of mechanical properties and ionic conductivity; results were compared with a standard membrane without additives. (SR35-50 gm^{-2}). In the following paragraphs the results obtained will be briefly summarized, the labels refer to the One Shot procedure (OS) and to the number of paper sample indicated in Table 2.

-Cationic starch

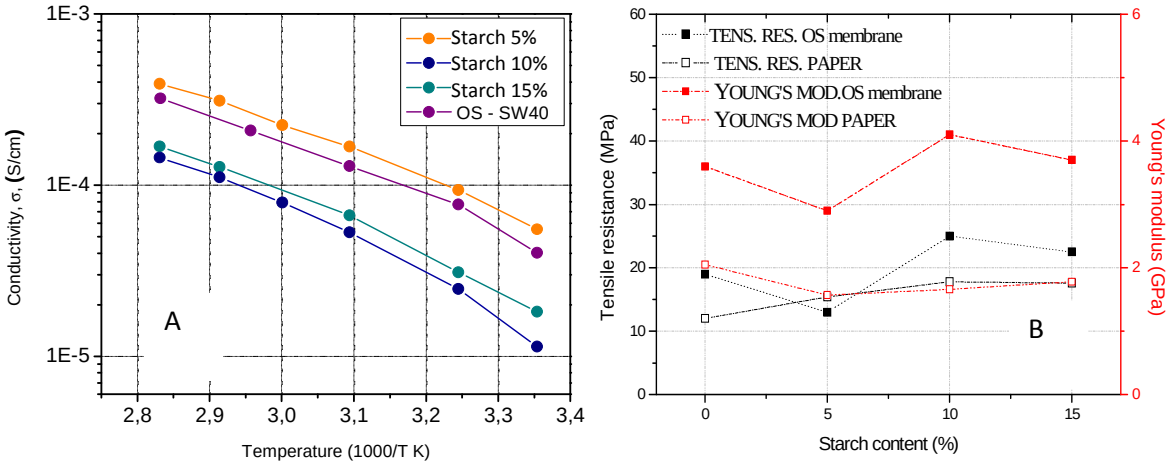

Figure III. 35 A. Arrhenius plot for membranes reinforced by handsheets containing starch. B. Mechanical properties of membrane GPE+SW40 50g/m^2 containing cationic starch (full symbols) compared to mechanical properties of the handsheets without polymer matrix (empty symbols).

Cationic starch is often used in papermaking, as retention aid and as strengthener[13]. Actually, opacifying filler particles usually used in paper production are ca 0.3–5µm in diameter and are much smaller than most pulp fibers, therefore, they are not effectively retained by filtration through the pulp mat as it forms on the machine. Furthermore, in an aqueous suspension, most fillers like most paper-pulp fibers and fines, develop a negative surface charge which prevents coflocculation of fillers with fines. Retention aids encourage coflocculation by two mechanisms: they neutralize the negative charges on fillers, fibers, or fines so that van der Waals forces can hold them together, and they form molecular bridges between two particles to which they are adsorbed.

The addition of this additive slightly improved the tensile resistance of the paper; do not significantly enhance the mechanical properties of the membrane. Furthermore, it does not help to reach higher values of conductivity, the decrease observed for high concentrations of starch can be due to its cationic nature.

AKD

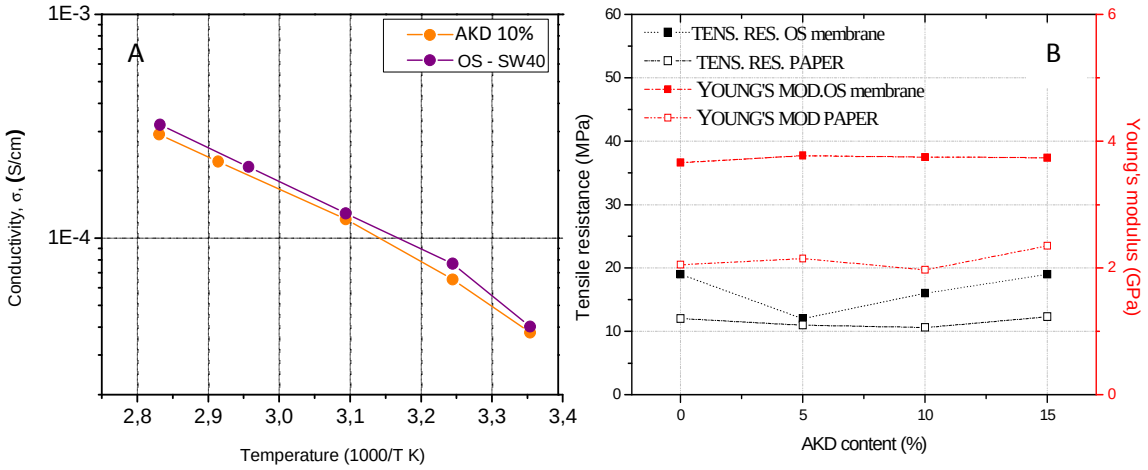

Figure III. 36 A. Arrhenius plot for membranes reinforced by handsheets containing AKD. B. Mechanical properties of membrane GPE+SW40 50g/m^2 containing AKD (full symbols) compared to mechanical properties of the handsheets without polymer matrix (empty symbols).

Alkylketene dimers (AKD) is normally used as sizing agent, paper sizing provides paper and paperboard with resistance to wetting by liquids. The usual purpose of sizing is to produce water repellency, the presence of AKD in the paper should modify superficial energy being highly hydrophobic[13].

The presence of AKD did not vary mechanical properties in both cases of paper and membrane; the electrochemical measurement did not show any influence of this additive on ionic conductivity.

-CPAM

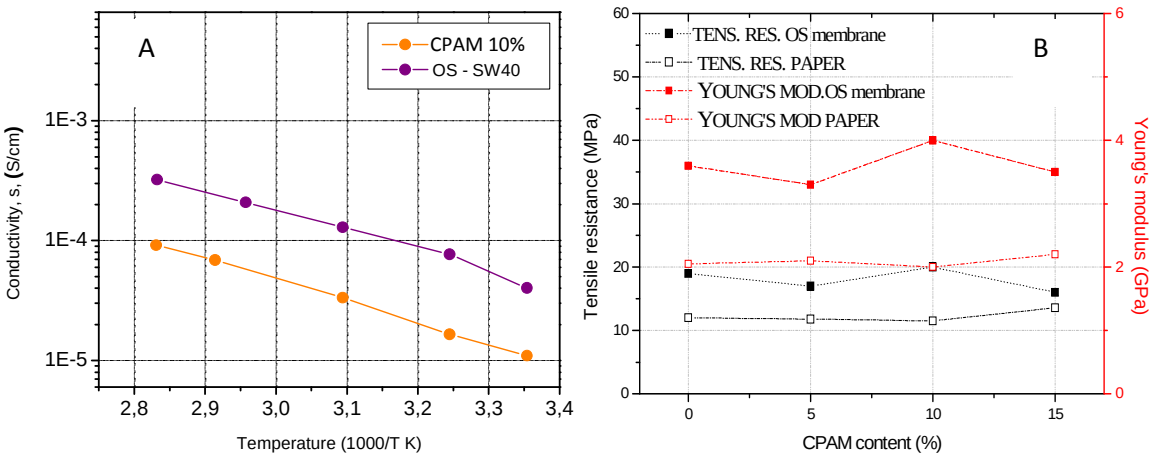

Figure III. 37. A. Arrhenius plot for membranes reinforced by handsheets containing CPAM. B. Mechanical properties of membrane GPEI+SW40 50g/m^2 containing CPAM (full symbols) compared to mechanical properties of the handsheets without polymer matrix (empty symbols).

Cationic polyacrylamide is usually used as a retention aid. CPAM is one of the mostly used additives in paper industry, its presence leads to higher flocculation, and consequently it varies the porosity of the sheet [13].

Tensile test showed that the presence of this additive did not affect in a consistent way mechanical properties; ionic conductivity was largely decreased by the use of this additive. The bad influence of CPAM on ionic conductivity can be due to the different paper structure formed in presence of the additive or to the possible interactions of the molecule with lithium ions. A deeper study would be required, in order to validate the negative impact of such a polymer In this case, not only, this additive is not able to improve the electrochemical properties, but, in addition, it would be necessary to recommend to avoid its use in paper production for GPC electrolyte applications.

-Calcium carbonate

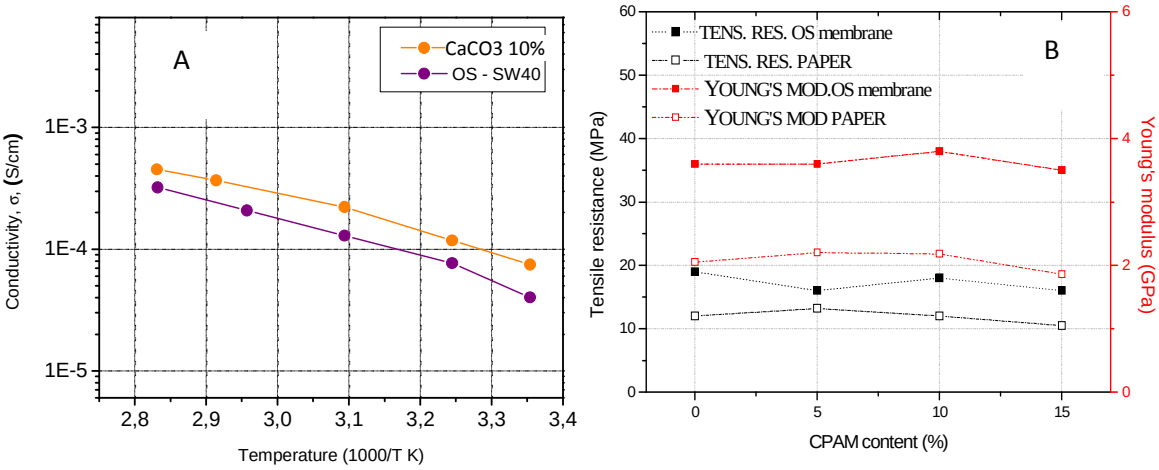

Figure III. 38 A. Arrhenius plot for membranes reinforced by handsheets containing calcium carbonate. B. Mechanical properties of membrane GPE+SW40 50g/m^2 containing calcium carbonate (full symbols) compared to mechanical properties of the handsheets without polymer matrix (empty symbols).

Calcium carbonate is the most widely used mineral in the paper industries both as a filler and, due to its special white color, as a coating pigment. In the paper industry it is valued worldwide for its high brightness and light scattering characteristics, and is used as an inexpensive filler to make bright and smooth opaque paper[13]. In the range of amount added, the use of calcium carbonate do not vary the behavior of the gel polymer electrolyte nor in terms of mechanical properties neither in terms of ionic conductivity.

It can be concluded that for GPCE purposes, any of the additives mostly used in papermaking is not able to increase the ionic conduction. Furthermore, the retention aids tested seem even to be detrimental: if this preliminary observation is verified, and if the GPCE developed in the present study are of industrial interest, it will be necessary to find out a retention system not impacting the ionic conduction of the membranes.

Many studies reported in literature reveal that composite polymer electrolytes alone can offer lithium polymer batteries with improved electrolyte/electrode compatibilities and safety hazards[14-17]. One of the most promising ways to improve the morphological and electrochemical properties

of polymer electrolytes is addition of ceramic fillers. It has been well established that the addition of these additives improves the conductivity of polymer hosts and their interfacial properties in contact with the lithium electrode. This is the reason why some ceramic filler, unusual for the paper industry, have been also added to the pulp slurry.

Calcium phosphate

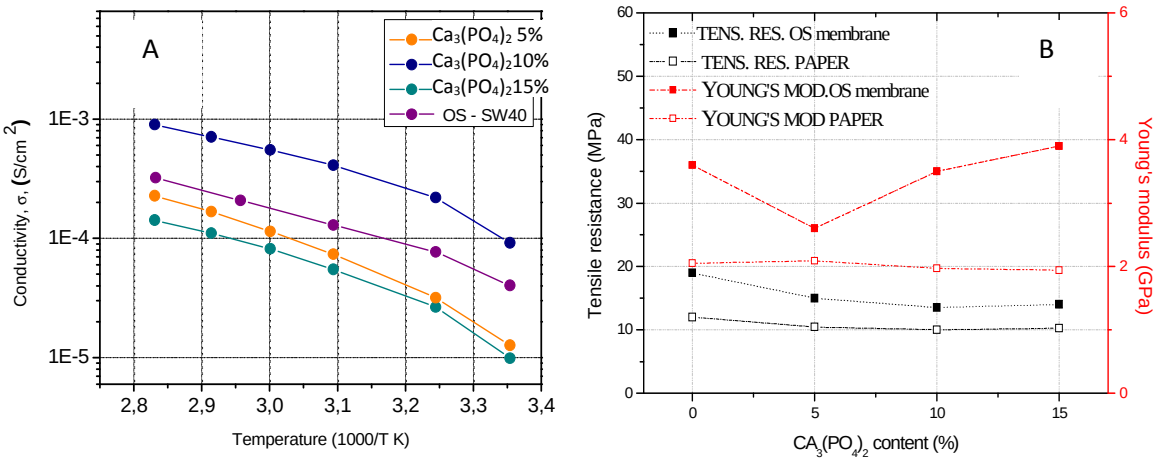

Figure III. 39 A. Arrhenius plot for membranes reinforced by handsheets containing $Ca3(PO_4)_2$. B. Mechanical properties of membrane GPE+SW40 50g/m^2 containing $Ca3(PO_4)_2$ (full symbols) compared to mechanical properties of the handsheets without polymer matrix (empty symbols).

Calcium phosphate has been tested as innovative filler for GPEs membranes, few works are present in literature presenting the use of this additive [18] and showing that it can increase conductivity and reduce interfacial resistance. In our case the use of calcium phosphates leads to the production of reinforced membranes with good mechanical properties and, in presence of the correct amount of filler, with improved ionic conductivity. In fact in presence of the 10% wt of $Ca_3(PO_4)_2$ conductivity reaches values as high as 10^{-4} at room temperature. No linear trend is observed for conductivity when the quantity of calcium phosphate in the handsheet is increased; the presence of the phosphate group, also present in currently used cathode materials, could play a role in lithium mobility.

-Alumina

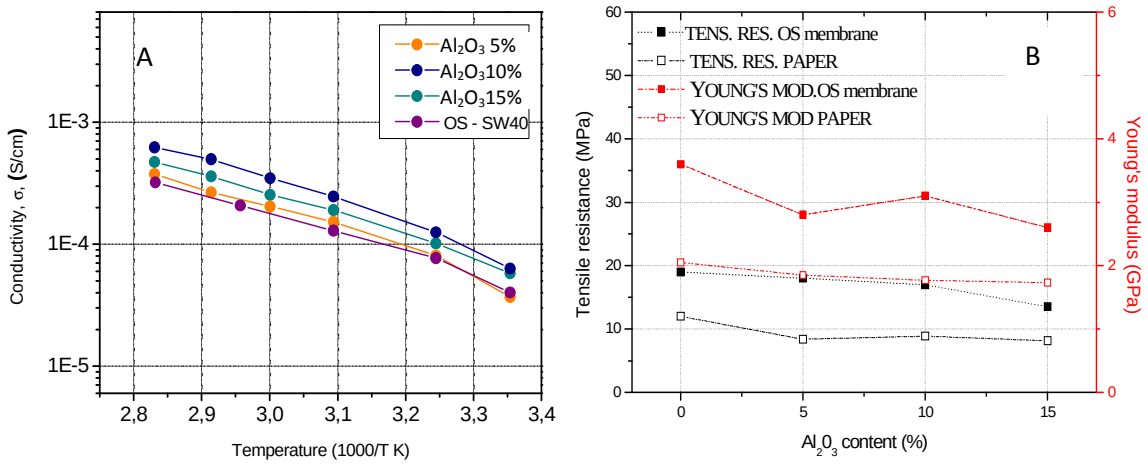

Figure III. 40. A. Arrhenius plot for membranes reinforced by handsheets containing Alumina. B. Mechanical properties of membrane GPE+SW40 50g/m^2 containing Alumina (full symbols) compared to mechanical properties of the handsheets without polymer matrix (empty symbols).

Alumina is one of the most promising additives; it is the most used additive for the preparation of composite polymer electrolytes, it is known[14-17] that the use of this filler enhances conductivity and interfacial stability with the electrodes.

Tensile test showed that the presence of alumina slightly decreases mechanical properties of the membrane if compared to the one reinforced with a simple SW40 handsheet; however the values obtained are more than enough for the envisaged application. The ionic conductivity is increased by the presence of the additive, in this case the trend observed is the same already described in literature[2]. The lithium ions conductivity is not significantly improved in presence of low quantities of alumina (5%wt), it has the highest increase in presence of 10%wt of additive while for higher quantities the beneficial effect is no longer detectable, for 15 wt.% Al_2O_3 the ionic conductivity decreases, because the inorganic fillers tend to impede ionic movement by acting as an insulator or an agglomerator.

To conclude, considering the values here presented for the common pulp and paper industry additives, it is possible to see that the most of the additives do not improve the paper and membrane behavior, however, in most of the cases,

their effect is not significant and thus those additives could be used, when needed, without influence on the GPEs performances.

Instead, considering the remarkable increase in conductivity, handsheets containing the 10%wt of $Ca_3(PO_2)_4$ and Al_2O_3 can be suggested for the production of more performing GPCEs. The use of such additives can help to regain the loss in conductivity given by the presence of the reinforcing handsheet leading to values close to those obtained from a not reinforced GPE.

2.5.2 Evaluation of the influence of the formulation-Li quantity

After the evaluation of the influence of the variation of paper properties and of the use of additives, a last study has been developed in order to try to restore GPE conductivity, when using paper as a reinforcement.

As it was shown that the 'drying' procedure causes a decrease of conductivity (Paragraph 2.2.2) likely due to the presence of porosity in the membrane, but maybe also due to a minor Li-ion content, a new formulation has been prepared in order to obtain, by the drying procedure, a membrane containing the same quantity of lithium salt than the 'One shot' membranes prepared with the formulation used here as a reference(GPE).

For the testing of this new membrane composition only handsheets SW100 SR0 and SW100 SR0SF have been used.

The ratio BEMA:PEGMA was kept the same, while an higher quantity of organic solvent was needed obtain an homogeneus solution of the lithium salt during preparation. The new formulation resulted as: BEMA:PEGMA:EC-DEC:LiTFSI 14: 6: 40: 40 +2% photoinitiator. It is labeled Li40-dry. Conductivity measurements are reported in the form of an Arrhenius plot (**Figure III. 41 Arrhenius plot of the ionic conductivity obtained for samples SW100 22g/m2 SR 0, and SR0SF with the Li40 dried membrane compared with the GPE One Shot and dry membranes reinforced by SW100 22g/m2 SR 0SFhandsheet.**Figure III. 41).

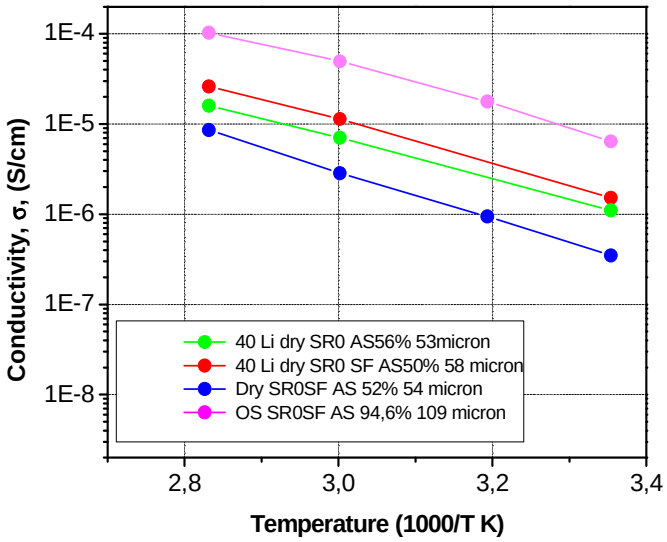

Figure III. 41 Arrhenius plot of the ionic conductivity obtained for samples SW100 22g/m2 SR 0, and SR0SF with the Li40 dried membrane compared with the GPE One Shot and dry membranes reinforced by SW100 22g/m2 SR 0SFhandsheet.

As one can see, conductivity increases, however the values obtained remain lower than the values for the 'One shot' membranes; this indicates that the GPCE structure plays a key role and that filling all the paper porosity is essential.

However, for sure, both the quantity of lithium salt and the quantity of polymer are crucial, since the latter, together with the organic solvents, influences the dissociation and the mobility of ion species.

To further verify if conductivity could simply be increased by an additional amount of Li salt,the formulation Li40-dry has been used to prepare a 'one shot' membrane; in this case conductivity was greatly increased, as shown ahead in Figure III. 42.

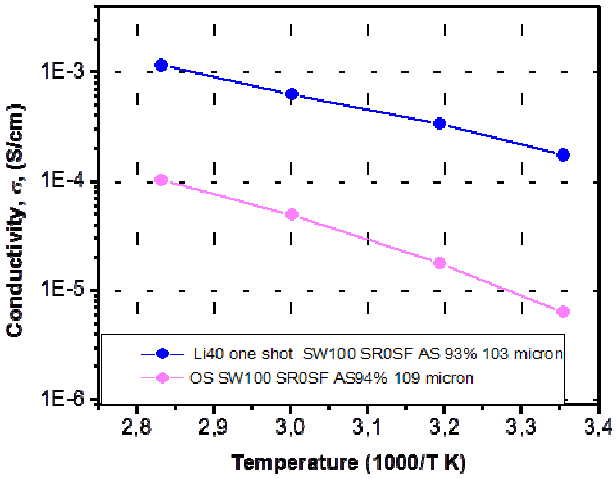

Figure III. 42Arrhenius plot of the ionic conductivity obtained for samples SW100 22g/m2 SR0SF with the Li40 dryed and one shot reference GPE membrane compared

The mechanical properties of this membrane were quite poor, the membranes were not easy to handle. The membrane prepared with the handsheet SW100 SR0 was not integer at the end of the conductivity measurement.

In general, the addition of higher amounts of lithium salt (and consequently of solvent) led to a decrease in the mechanical properties of the membranes, whatever the procedure followed, moreover by using a not refined handsheet for the study of the improvement of the conductivity the contribution of this to the mechanical properties last is limited.

It can be said that ionic conductivity can be improved by varying the polymer formulation, at the same time a refined handsheet should be preferred when high amount of organic solvent are used.

The new formulation presented also a lower surface tension leading to an easier impregnation of the paper.

Surface tension values change from γ=37,25 dyne/cm for the reference GPE formulation to γ= 35,04 dyne/cm for Li 40. These observations indicate that playing with the formulation of the membrane the properties of the electrolyte can be easily modeled.

III.3. Conclusions

Novel UV-cured and cellulose-based membrane for gel-polymer electrolytes have been developed for the use in Li-ion batteries.

Their production calls for a fast, easy One Shot method , that could be implemented at industrial scale, by using conventional technologies, known in papermaking. Actually, the use of paper allowed to produce self-sanding and easy to handle electrolytes, with excellent mechanical properties, close to that of paper.

The major drawback of this approach is the reduction of the electrochemical properties of the final membrane, when it is paper-based.

The investigations carried out suggested that this negative effect can be limited i) by reducing the paper basis-weight, ii) by selecting an optimal fibre composition to have a cellulose substrate as homogeneous as possible, iii) by adding specific products, such as alumina, iv) by increasing the amount of Lithium salt. This latest strategy negatively impacts the final mechanical properties of the membrane, however, as shown, they can be varied by playing on the cellulose substrate, for example by increasing its tensile strength through the pulp refining to a certain extent.

From the practical point of view, results obtained suggest to use as paper reference for performing GPCE, a fiber mixture composed by hardwoodfibers (60%) and softwood (40%), a thin and porous paper with a grammage of approximately 22 g/m^2. The pulp refining degree will be a compromise between the porosity requirements (in this sense, unrefined pulp could be a good choice) and papermaking requirements (a pulp refined at 20-30°SR gave also good results). The use of fillers such as alumina and calcium phosphate is also strongly suggested in order to obtain an improvement in conductivity, The existence of an optimal dosage has been observed, so that it is necessary to optimize it as a function of the pulp slurry characteristics.

The works performed allow to show the feasibility of gel-polymer cellulose based membranes, and to assess the impact of paper. Some strategies to counteract its negative effect (from the electrochemical point of view) were studied, and some solutions were provided. Nevertheless, it was also shown that the most influencing component results to be the polymer, the choice of a better performing formulation could surely give interesting performances as demonstrated in the last tests shown in the chapter.

In addition, the specific structure of such membranes (bi-layer) suggests to further investigate the adhesion between the polymer matrix and the cellulose fibres, and namely the grafting of the polymer on the cellulose fibres. This study would also to open the way to an alternative process, in which Li-salt is introduced in the last steps of the production (swelling), for limiting the cost and the difficulties of the present process. Actually, the presence of lithium during the whole preparation steps means the need to maintain an inert ambient all along the process, with related high costs.

Preliminary tests performed with the swelling procedure showed, after the swelling of the reinforced samples, a detachment of the polymer membrane from the cellulosic substrate, confirming the poor adhesion.

Thus, the need for a stronger adhesion, through the grafting of the polymer on fibers, motivated the work presented in the following chapter.

References

(1) J. Nair, C. Gerbaldi, G. Meligrana, R. Bongiovanni, S. Bodoardo, N. Penazzi, P. Reale, V. Gentili, J. Power Sources 178 (2008).751-757.

(2) International patent WO0147047 28/06/2001.

(3) C. Gerbaldi, J. Nair, G. Meligrana, R. Bongiovanni, S. Bodoardo, N. Penazzi, J. Appl. Electrochem. 39 (2009) 2199-2207

(4) A.G. Chmielewski, M. Haji-Saeid, S. Ahmed Nucl. Instrum. Methods Phys. Res. B.(2005), 236, p. 44

(5) C.P. Yang, Z.Q. Shen, G.C. Yu, J.L. Wang Biores. Technol. (2008) , 99, p. 6240

(6) L. Andreozzi, V. Castelvetro, G. Ciardelli, L. Corsi, M. Faetti, E. Fatarella, F. Zulli J. Colloid Interf. Sci. (2005), 289, p. 455

(7) C. Gerbaldi, J.R. Nair, Shahazada Ahmad, G. Meligrana, R. Bongiovanni, S. Bodoardo, N. Penazzi, J. Power Sources 195 (2010) 1706-1716.

(8) C. Gerbaldi, J.R. Nair, G. Meligrana, R. Bongiovanni, S. Bodoardo, N. Penazzi, Electrochim. Acta 55 (2010) 1460-1472

(9) R. A. Horn USDA FOREST SERVICE RESEARCH PAPER FPL 242 (1974)

(10) R.A. Horn USDA FOREST SERVICE RESEARCH PAPER FPL 312 (1978)

(11) Koskenhely K., Ämmälä A., Jokinen H., Paulapuro H. Nordic Pulp and Paper Research Journal 20 (2005) 169-175.

(12) P.M. Blonsky, US Patent No. 5,648,011, (1997).

(13) Kirk-Othmer Encyclopedia of Chemical Technology. John Wiley & Sons(1999)

(14) A. Manuel Stephan, K.S. Nahm / Polymer 47 (2006) 5952-5964

(15) F Croce, GB Appetecchi, L Perci, B Scrosati. Nature 394 (1998) 456-458.

(16) GB Appetecchi, F Croce, L Persi, F Ronci, B Scrosati. J Electrochem Soc 147 (2000) 4448-4459.

(17) LM Bronstein, RL Karlinsey, K Ritter, CG Joo, B Stein, JW Zw. J Mater Chem 14 (2004) 1812-1824

(18) M. Stephan T. Prem Kumar, S. Thomas, P. Selvin Thomas, R. Bongiovanni, J.R. Nair, N. Angulakshmi Journal of Applied Polymer Science (2011) DOI 10.1002/app

CHAPTER IV

IMPROVED GEL POLYMER-CELLULOSE ELECTROLYTES

New process of fabrication including polymer-cellulose bonding by UV-grafting methods

The preliminary studies developed for the production of reinforced salt-in Gel Polymer Electrolytes by the fast one shot method gave interesting results showing that by using a cellulose handsheet embedded in a photopolymer matrix it is possible to produce self standing, mechanical resistant and extremely flexible membranes.

The electrochemical performances of the GPEs can be optimized by choosing the proper type of handsheet adjusting the composition of the active formulation forming the photopolymer matrix. The preparation method used was based on the direct photopolymerisation of the reactive mixtures containing the lithium salt in the presence of the handsheet. This method permits a fast fabrication of a membrane, being made of two step, i.e. the deposition of the reactive mixture on the handsheet by a common coating technique and its irradiation. Due to the presence of the lithium salt, it requires to be done in inert atmosphere, in the complete absence of water; therefore any manipulation was done in a glove box. From an industrial point of view this would result too expensive, thus the activity was addressed to modify the process of fabrication in order to introduce the lithium salt in the membrane in a separate production step and minimize the cost of

inertisation. Introduction of the salt means the swelling of the reinforced polymer membranes by a liquid electrolyte. Swelling processes usually affect the adhesion between the polymer matrix and the reinforcement, in our case the cellulose handsheet. To avoid delamination between the handsheet and the photopolymer matrix, methods to promote polymer-cellulose adhesion were studied, mainly based on grafting induced by UV radiation. In this chapter new improved reinforced gel polymer electrolytes will be proposed showing successful grafting of the polymer at the cellulose surface the alternative fabrication process made by swelling the polymer-handsheet composites with the electrolyte solution of the lithium salt will also be presented.

Three different UV-grafting processes for preventing delamination will be discussed. In the first part of the chapter (*Section A*) an "in situ" grafting in the presence of Benzophenone (BP) is presented. When BP is added to the formulation both graft polymerization onto cellulose and homopolymerization of the oligomers could occur under UV light leading to a more stable structure.

In the second part of the chapter (*Section B*), a two step UV-grafting procedure is proposed. This two-step sequential photografting technique enables a greater degree of control over the grafting process and allows the use of BP only as an "anchor" for the polymer grafting avoiding its participation in the polymer curing.

The third grafting proposed (*Section C*) involves the use of Glycidyl Acrylate (GA) as a grafting agent combining radical grafting and chain transfer reaction to the cellulose.

SECTION A

POLYMER-CELLULOSE BONDING:

In situ grafting by Benzophenone

The first grafting procedure tested in order to overcome the problem of adhesion between the polymer matrix and the cellulose substrate was ades on the addition of benzophenone to the reactive formulation. The use of this photoinitiator permits the modification of polymer surfaces caused by irradiation. Upon excitation, the benzophenone molecules abstract hydrogen atoms both from the oligomers and from the polymer surface, in our case cellulose. The oligomeric radicals start the polymerization propagation, while the surface radicals initiate surface graft polymerization from the surface, i.e. an in situ grafting.

A new reactive mixture was designed in order to improve the ionic conductivity and benzophenone was introduces. Reinforced gel polymer electrolytes were first prepared by the one shot method and characterized. Then the alternative process of fabrication of the gel polymer electrolyte based on the swelling of the membranes by the Li-solution was tested.

IV.A.1. Materials and methods

1.1 Fibers and additives for handsheets preparation

Cellulose fibers deriving from Hardwood (Eucaliptus) and Softwood (Pine from Tarascon, Fr) plants were used to produce paper sheets.

Papers containing Calcium phosphate $Ca_3(PO_4)_2$ and Alumina(Al_2O_3) (Aldrich products) were also prepared.

1.2 Fibers treatments

Untreated cellulose fibers stored in laboratory in the form of thick sheets were re-pulped and blended using a high speed blender, Softwood and Hardwood fibers (40 and 60% respectively) were mixed in order to obtain the handseets. The fibers suspension was then submitted to the refining treatment to reach a refining degree of 35°SR. This mechanical modification was done by an equipment for pulp refining called Valley beater, according to ISO 5264-1 in order to beat pulp in a uniform, standard and reproducible way.

1.3 Handsheet preparation

The fibers suspensions composed by the 40% of softwood fibers and the 60 of hardwood, (°SR 35) were diluted to a concentration of 1.5 g/L; a liter of this suspension was than is introduced into a sheet-former that automatically steers the solution. The filtrate laying on copper wires was then dried at 90 °C for 7 minutes under high vacuum to give a handsheet of the weight of 1,5g corresponding to a grammage of about 51 g/m^2.
The papers containing additives were prepared by diluting the fillers in water and adding the obtained suspension to the pulp slurry before the introduction in the sheet former.

1.4 Membrane formulation

The UV cured polymer membrane was composed by:
Bisphenol A ethoxylate (15 EO/phenol) dimethacrylate BEMA, Mn = 1700
Aldrich product, chemical formula:

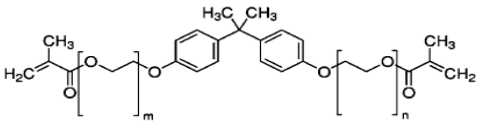

Poly(ethylene glycol) methyl ether methacrylate PEGMA, average Mn= 475 (Aldrich). Chemical formula:

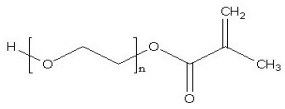

1:1 w/w ethylene carbonate – diethyl carbonate (EC-DEC, Fluka) solution. It has been used as a solvent.

LiTFSI (lithium bistrifluoromethanesulfonimide, $CF_3SO_2NLiSO_2CF_3$ purchased from Aldrich has been chosen as lithium salt.

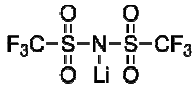

2-hydroxy-2-methyl-1-phenyl-1-propanon Darocur 1173, Ciba Specialty Chemicals has been used as photo-initiator.

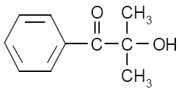

Benzophenone (Aldrich) was also been added to the formulation as photoinitiator.

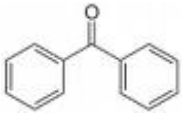

Before their use, BEMA and PEGMA were kept open in the inert atmosphere of a dry glove box (MBraun Labstar, O_2 and H_2O content < 0.1 ppm) filled with extra pure Ar 6.0 for several days and also treated with molecular sieves (Molecular sieves, beads 4 Å, 8–12 mesh, Aldrich) to ensure the complete removal of traces of water/moisture from the liquid monomers, as they may affect long–term properties when the membranes are considered used for rechargeable Li-based batteries

1.5 Preparation of the gel polymer electrolyte membrane

Membranes were prepared both by the“One Shot” process and the new Swelling Method.

One Shot

The One Shot procedure consists in few and easy steps already shown and here recalled:

5- Preparation in dry box (Argon atmosphere) of the active formulation containing BEMA : PEGMA : EC-DEC: LiTFSI and the photoinitiator.
6- Draw down of the formulation on the cellulosic substrate (4cm^2) laying on a polyethylene (PE) substrate by using a coating bar of 100 μm in dry box, (the formulation spread on the substrate was always in excess) and waiting for 30 seconds.
7- UV curing of the membrane for 3 minutes by using a medium vapour pressure Hg lamp (Helios Italquartz, Italy), with a radiation intensity of 30 mW cm^{-2}. The membrane was placed in a quartz tube sealed in dry box and irradiated.
8- Removing of the Gel Polymer Electrolyte from the PE substrate.

Swelling

The swelling procedure was also tested. The reactive formulations were prepared by mixing the oligomers, the organic solvent and the photoinitiators, in this case the Lithium salt was not added. The mixtures were coated on the handsheet substrate and UV irradiated as previously described for the One Shot process. The reinforced composite membranes were then immersed into 10 ml of a 1.0 M LiTFSI in EC/DEC (1:1 w/w) solution (swelling time =15 minutes; under inert atmosphere of an Ar-filled dry glove box (MBraun Labstar, O_2 and H_2O content\0.1 ppm). After 15 minutes the membranes were taken out of the solution and leant on blotting paper.

1.6 Characterisation methods

Handsheet thickness measurements

Thickness was measured by an Adamel Lhomargy-M120 instrument. Five readings were taken for each hand-sheet and the average thickness was taken as final value.

Handsheet grammage measurements

Grammage of cellulose papers was calculated by cutting a 10×10 cm piece from the hand-sheet and, then, weighing it on a balance. Every time, three readings were taken and subsequently averaged to obtain a final value. The final reading was expressed as g m^{-2}.

Active Swelling

The quantity of polymer electrolyte present in the reinforced membrane with respect to the paper weight, called Active Swelling percentage (AS%), was calculated by the formula:

$$(W_{GPE}\text{-Wpap}) / W_{GPE} * 100$$

where W_{GPE} is the weight of the final reinforced membrane and Wpap is the weight of the reinforcing substrate.

Thickness measurement

The thickness of the reinforced membranes was measured with a Mitutoyo series 547 thickness gauge equipped with an ABSOLUTE Digimatic Indicator model ID-C112XBS, with a resolution of ± 1 µm and a max measuring force of 1.5 N.

SEM analysis

Morphological characterization of the handsheets and of the reinforced membranes was performed employing a FEI Quanta Inspect 200LV scanning electron microscope (SEM, max magnification of 1.5×10^5) equipped with an energy-dispersive X-ray analyzer EDAX Genesis system with SUTW detector. Prior to analysis, all the samples were coated a thin Cr layer (thickness around 10 nm) to minimize the effect of the electron beam irradiation which may possibly lead to charging and "burning" of the polymer network. Test membranes were broken under cryogenic conditions (after dipping in liquid nitrogen in order to avoid any change in the morphology) and a cross-sectional analysis was performed.

Thermal analysis

The glass transition temperature (T_g) of the materials was evaluated by differential scanning calorimetry (DSC) with a METTLER DSC-30 (Greifensee, Switzerland) instrument, equipped with a low temperature probe. Samples were put in aluminium pans, prepared in a dry glove box. In a typical measurement, the electrolyte samples were cooled from ambient temperature down to –80 °C and then heated at 10°C min^{-1} up to 120°C. For each sample, the same heating module was applied and the final heat flow value was recorded during the second heating cycle. The T_g was defined as the midpoint of the heat capacity change observed in the DSC trace during the transition from glassy to rubbery state. The thermal stability was tested by thermo-gravimetric analysis using a TGA/SDTA-851 instrument from METTLER (Switzerland) over a temperature range of 25 – 800 °C under N_2 flux (60 ml/min) at a heating rate of 10 °C min^{-1}.

Mechanical properties

Mechanical measurements on the polymer before swelling were carried out through tensile experiments according to ASTM Standard D638, using a Sintech 10/D instrument equipped with an electromechanical extensometer (clip gauge). At least five specimens for each sample were tested; the standard deviation in Young modulus (E) was 5 %. Mechanical properties after swelling were evaluated by a bending test for which the membranes have been rolled up around cylindrical hoses with radii ranging between 3 and 32 mm.

Ionic conductivity measurement

The conductivity tests were carried out on a heating stepped ramp from 20 °C to 80 °C. The cells were housed in a Memmert GmbH oven model UFE-400 with a temperature control of ±1 °C. The resistance of the electrolyte was given by the high frequency intercept determined by analysing the impedance response using a fitting program provided with the Electrochemistry Power Suite software (version 2.58, Princeton Applied Research). Each sample was equilibrated at the experimental temperature for about 1 h before measurement, to allow thermal equilibration of the cells. All measurements

were carried out on at least three different fresh samples in order to verify the reproducibility of the obtained results.

Electrochemical stability measurement

The electrochemical stability window (ESW) was evaluated at ambient temperature by linear sweep voltammetry (Li metal as the reference electrode) using an Arbin Instrument Testing System model BT-2000. Separate tests were carried out on each polymer electrolyte sample to determine the cathodic and anodic stability limits. The measurements were performed by scanning the cell voltage from the open circuit voltage (OCV) towards 0.0 V vs. Li (cathodic scan) or 5.5 V vs. Li (anodic scan). In both cases, the potential was scanned at a rate of 0.100 mV s^{-1}. The current onset of the cell was associated with the decomposition voltage of the electrolyte. Cell configuration adopted for anodic scan: acetylene black (Shawinigan Black AB-50, Chevron Corp., USA.) over Al current collector and Li metal as electrodes and the given membrane as electrolyte (active area equal to 2.54 cm^2); cathodic scan: Cu foil and Li metal as electrodes and the given membrane as electrolyte (active area equal to 2.54 cm^2).

Lithium polymer cell assembly and electrochemical tests

The lithium polymer cell was assembled by contacting in sequence a lithium metal disk anode, a layer of the nanocomposite gel-polymer electrolyte and a $LiFePO_4$/C disk composite cathode (electrode area: 2.54 cm^2). The latter was prepared by a quick and low cost mild hydrothermal synthesis(1). The electrodes/electrolyte assembly was housed in an Electrochemical Test Cell purchased from EL-Cell GmbH. Both electrode fabrication and cell assembly were performed in the environmentally controlled Ar-filled dry glove box. The lithium cell was tested for its electrochemical performance at room temperature in terms of charge/discharge galvanostatic cycling using an Arbin Instrument Testing System model BT-2000. The voltage cut-offs were fixed at 4.0 V vs. Li/Li^+ (charge step) and 2.5 V vs. Li/Li^+ (discharge step), respectively.

IV.A.2 Results

2.1 Synthesis of the membranes

At first several gel membranes were prepared by the one shot method using the SW40 handsheets (the characteristics of the handsheets are summarized in Table IV.A.1).

Sample	Fibers mixture (%) HW:SW	Refining degree (°SR)	Grammage (g/m^2)	Thickness (µm)
SW40	60:40	35	51	132

Table IV.A. 1 Characteristics of the handsheet used

In order to find an optimum formulation different GPE compositions were tested by changing the ratios of BEMA, PEGMA, EC/DEC and LiTFSI (Table IV.A.2).As already shown in previous works, [2, 3] the di-functional monomer BEMA that can be readily polymerised by UV-curing, gives a highly cross-linked thermo-set membrane, which is rather flexible and, at the same time, resistant up to 300°C. The mono-functional monomer PEGMA is added in order to control the cross-linking density of the cured polymer and to reduce the Tg of the membranes; moreover, it increases the mobility of lithium ions inside the polymer matrix and enhances the ionic conductivity by the presence of pendant ethoxy groups. The EC-DEC solution was added to the monomers mixture in which was also dissolved the Lithium salt LiTFSI. The interaction between polymer, salt and solvent depends on their nature and their relative concentrations.

Sample SW40-SR35 51g/m^2	BEMA	PEGMA	EC:DEC	LiTFSI	Darocure 1173	Active (%wt)	Swelling
PCS1	15	35	35	15	+3	77	
PCS2	11	24	50	15	+3	64	
PCS3	10	10	65	15	+3	60	
PCS4	10	10	60	20	+3	64	

Table IV.A. 2 Compositions of the membranes tested for the optimization of the formulation. All the membranes were reinforced by hansheets SW40 (SR35, 51g/m^2).

The first membrane prepared, PCS1, contained the 50 % wt of oligomers, the ratio BEMA: PEGMA was settled to 30: 70 in order to obtain a crosslinked polymer with low Tg and high chain mobility according to the role of PEGMA mentioned above. The quantities of EC:DEC and Li-salt were taken of 35 and 15%wt respectively. Membranes PCS2 and PCS3 were prepared keeping constant the quantity of LITFSI with respect to the membrane PCS1 (15%wt) and increasing the amount of organic solvent reducing the quantity of monomers.

PCS3 contains only the 20% of oligomers able to give a solid network: therefore this composition can not give a self standing membrane unless a reinforcing handsheet is present.

PCS4 has a composition similar to PCS3, the amount of lithium salt is increased and the organic solvent is reduced. All the compositions were added of the photoinitiator (3% of the total weight). The membranes were cured: the irradiation time and the light intensity selected (see experimental details IV.A.1.5) guarantee the complete crosslinking of the BEMA-PEGMA. All the membranes obtained were self-standing thanks to the presence of the handsheet. Tg values of all the systems were of about -70 °C (obtained by DSC analysis), no difference between the samples was appreciated.

The first electrochemical characterization of the systems prepared was the evaluation of the ionic conductivities.

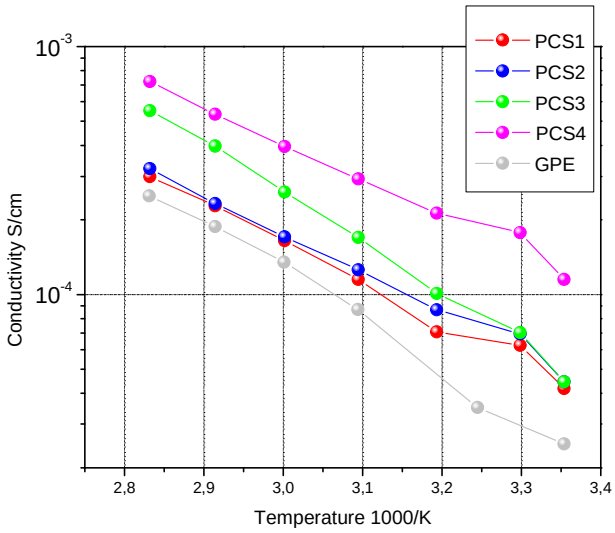

Figure IV.A. 1 Arrhenius plot of samples PCS1, PCS2, PCS3, PCS4 and GPE (Chapter III)

Figure IV.A. 1 reports the Arrhenius plots obtained for the samples summarized in Table IV.A. 2. The gray plot represents the conductivity of the GPE membrane used in Chapter III and reported as a reference (BEMA: PEGMA: EC/DEC LiTFSI 35: 15: 30: 20). It is possible to see that when a high quantity of monofunctional monomer is used the conductivity can be increased. Interesting comparisons can be done between the performances of samples PCS1, PCS2 and PCS3 investigating the influence of the quantities of polymer, organic solvent and lithium salt.

It is known from literature [4-7] that the use of an organic solvent reduces the Tg and enhances the Li transport leading to an increase of the conductivity. Nevertheless it was observed that the degrees of ion dissociation of the salt in the gel electrolytes are larger than in the liquid electrolytes leading to the assumption that the solvation is favored by the polymer which correlates the ions, but, at the same time, the ionic conductivities of the gels are lower than that of the liquids due to the slower diffusion of the lithium ion. From diffusion behaviours observed at various salt concentrations in the gels, it was found that the lithium ions are trapped in the polymer matrix.

The influence of the concentration of the Li-salt and its relation with the electrolyte performances has been largely discussed; generally it has been observed that conductivity, as a function of the salt concentration, increases

up to a maximum in correspondence of a determined polymer/salt (O/Li) ratio. Reiche[6] observed a decrease of the transference number of the lithium ion in correspondence of the O/Li ratio giving the maximum in conductivity caused by increased ion aggregation.

From Figure IV.A. 1 Arrhenius plot of samples PCS1, PCS2, PCS3, PCS4it is visible that PCS 3 and PCS2 membranes have similar conductivities to PCS1 at room temperature (around 4,4 10^{-5} scm^{-1}); the variations made do not allow to appreciate an important difference in conductivity. Interestingly PCS3 has a much higher conductivity when the temperature is increased reaching values of 5,5 10^{-4} s/cm at 80°C and thus giving the best results for this series of samples. Evidently all the compositions assure a similar solvation of the lithium salt whose concentration is relatively low, while the increase of the quantity of organic solvent can increase the mobility of the ions at least at high temperature. Assuming that in the presence of the 20%wt of oligomers and 15% wt of lithium salt this last can be completely solvated (PCS3), the increase of the amount of lithium salt in presence of the same amount of oligomer has been tested (sample PCS4). Conductivity at room temperature increases from 4.4 10^{-5} to 1,1 10^{-4} for sample PCS4 indicating that a higher quantity of salt (20%wt) can still be dissolved by the gel-polymer and, thanks to the higher amount of Li ions in solution, conductivity is increased. Comparing all the data PCS4 was chosen as the reference for setting a new method of fabrication of the membranes (Swelling Method).

2.2 Improving the GPE membrane by grafting

As explained in *Chapter V* the One Shot procedure is fast and easy but, thinking to the industrialization of the production of reinforced GPEs, the presence of the Li-salt could mean high costs for the maintenance of inert rooms. The possibility of introducing the salt in the last production steps implies the necessity of swelling the membrane in a liquid electrolyte. In *Chapter V* was demonstrated that swelling of the membranes induces delamination, therefore the need of grafting the polymer matrix to the cellulose substrate to make possible the swelling procedure.

Additionally, it was shown that the membrane produced presented a bi-layer structure, with consequent issues of layer adhesion. Therefore, there is a need of grafting the polymer matrix to the cellulose substrate, to increase the adhesion and to make possible the swelling procedure.

To promote the polymer-cellulose grafting Benzophenone (BP) can be used.

When benzophenone absorbs a UV photon, it is excited to the short-lived singlet state and then relaxes to a more stable triplet state, which then abstracts a hydrogen atom from the polymer backbone generating a polymer macro-radical. This then becomes the active site for the surface grafting[8,9]. In our systems BP can abstract a hydrogen from the cellulose surface leaving an active site able to react with the monomers creating a chemical bonds between the membrane and its reinforcement. The reaction is represented in the following schemes.

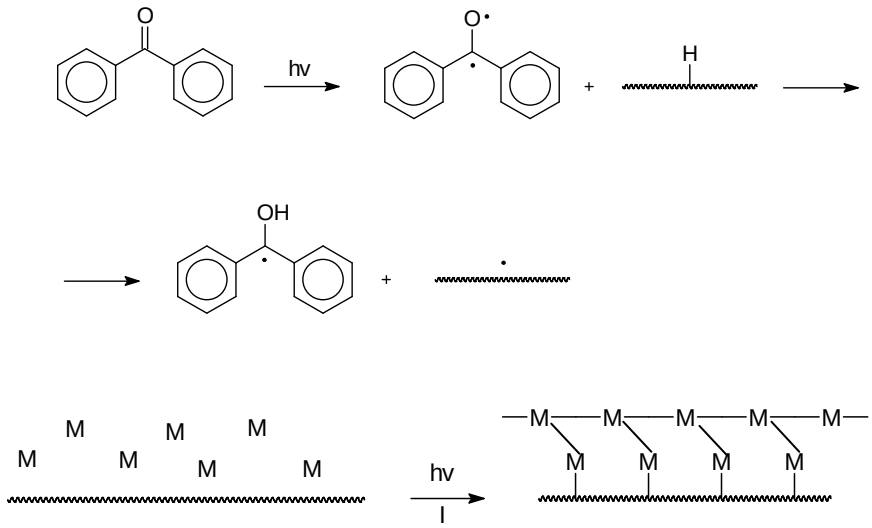

Figure IV.A. 2Scheme of the photodissociation of the photoinitiator and hydrogen abstraction from the cellulose and subsequent photografting of the monomer M onto cellulose and its photopolymerisation.

For the development of this idea, the membrane PCS5 (BEMA: PEGMA: EC/DEC: LiTFSI 10: 10: 60: 20) was chosen. It was added of two photoinitiator: Darocure (3%) to generate crosslinking and of Benzophenone (1%) to obtain grafting. The membrane containing BP was named PCS5.

PCS5 membrane is flexible with a Tg ~ -60°C (Table IV.A. 3). This value is higher than the Tg of PCS4 (~ -70°C), this increase indicates that BP effectively promotes grafting of the polymer to the cellulose and reduces the chain mobility.

Sample	Tg (°C)	T_5 (°C)	T_{10} (°C)	T_{50} (°C)
PCS5 SW40	-65	110	143	349

Table IV.A. 3 Thermal properties of sample PCS5 reinforced with handsheet SW40 (SR35, 51g/m^2).

Table IV.A. 3 also reports the main degradation temperatures of the membrane (T_5, T_{10} and T_{50}), the onset of the weight loss is 110°C corresponding to the loss of the EC:DEC solvent; degradation of the network starts at 143°C and a weight loss of 50% is at 349°C as expected for this kind of crosslinked polymer. Clearly the membrane can be safely used up to 110 °C and this limit is only due to the solvent used. Choice of new solvents (like ionic liquids) could allow application till 140°C.

The mechanical behavior of PCS5 was evaluated by means of tensile test. Table IV.A. 4 Young's modulus and tensile resistance of samples PCS 4 and PCS5.r**Error! Reference source not found.**eports the tensile curve obtained. The Young's modulus and the tensile resistance of the membrane PCS5 can be calculated (Table IV.A.4). The values obtained with a young modulus of about 2000 MPa and tensile resistance of 6,5 MPa are largely satisfactory, above all when considering that such formulation without the cellulose reinforcement does not allow the production of a self standing membrane. By comparing the values obtained for sample PCS5 to those of sample PCS 4 (no BP) it is possible to observe and increase of the Young's modulus and a decrease of the tensile resistance when the BP is added to the reactive formulation of the membrane. This is consistent with polymer grafting on cellulose; as a matter of fact when a grafted system is formed, the polymer chains are anchored in some points to the cellulose surface and their mobility is limited, resulting in

an increase of the stiffness of the material with a relative decrease of the tensile resistance.

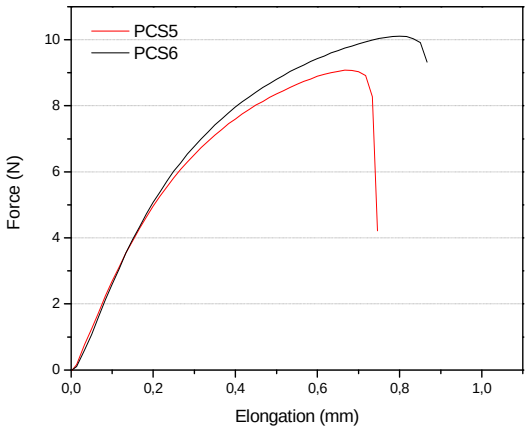

Sample	Young's modulus (MPa)	Tensile resistance (MPa)
PCS4	1500	6,9
PCS5	2170	6,5

Figure IV.A. 3 Figure 2 Elongation vs Force plots for sample PCS4 and PCS5.

Table IV.A. 4 Young's modulus and tensile resistance of samples PCS 4 and PCS5.

The composite membrane PCS5 was characterized by SEM analysis in order to observe the polymer- cellulose interpenetrated and interconnected network which should have been formed as the Tg and E increase and the tensile resistance decrease were observed. Some of the captured cross-sectional images, at different magnification are reported in Figure IV.A. 4. In Figure IV.A. 4.A the sample shows to be continuous and compact, examining the interface fibres- polymer (Figure IV.A. 4. B) disruptions or voids appears that could be due to the cryo-fracturing process. However, interestingly there are connections of the polymer to the fibres surface in the form of threads.

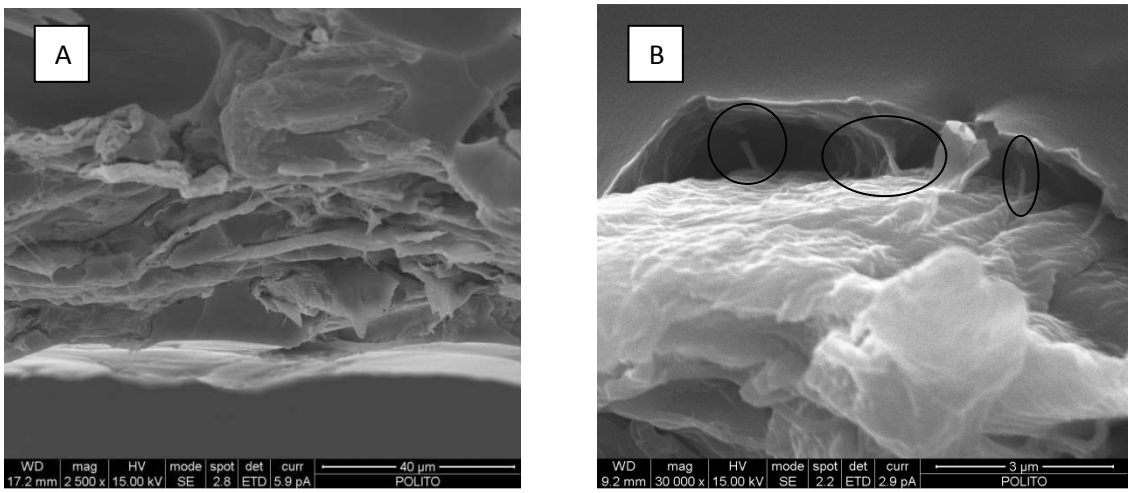

Figure IV.A. 4Figure 3 SEM images of membranes PCS5 at different magnification.

Conductivity of the sample PCS5 was measured and compared to sample PCS4, Figure IV.A. 5 reports the Arrhenius plot obtained compared to the one of sample PCS5. In presence of BP the conductivity values are slightly lower but still interesting (around $6*10^{-5}$ at RT). The decrease is in agreement with the hypothesis of the formation of a network between cellulose and polymer, i.e. an interconnected network hindering the ion mobility. The loss observed with the addition of BP is however acceptable as the presence of cellulose-polymer bonds improves the mechanical modulus and as discussed below the stability of the membrane.

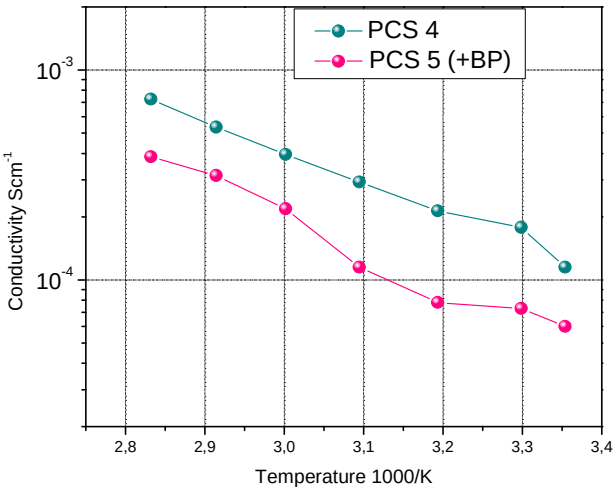

Figure IV.A. 5 Arrhenius plot of samples PCS4 and PCS5. Samples are reinforced with handsheets SW40 (SR35 51g/m^2).

The electrochemical stability window of the reinforced GPE was evaluated by running cyclic voltammetries at room temperature. The resulting cathodic (from −0,2 to 3.0 V vs. Li) and anodic (from O.C.V. to 5,2 V vs. Li) scan are reported, linked together in Figure IV.A. 6. For the cathodic configuration, PCS5 was sandwiched between a copper electrode and a Li-metal counter electrode. A current flow is visible starting from about 2 V vs. Li, this flow decreases in the subsequent cycles but does not disappear, thus indicating the possible presence of secondary reactions at this voltage. Furthermore, on scanning the system towards lower potential direction, a cathodic peak was observed at about −0.2 V vs. Li, which corresponds to the deposition of lithium metal onto the electrode. On the reverse scan, stripping of lithium ions was observed at about 0.1 V vs. Li (see the inset in Figure IV.A. 6), the presence of this peaks indicates that the lithium ions can effectively move in/out the polymer membrane.

The anodic configuration, composed of PCS5 between Li-metal and acetylene black electrodes, was scanned up to a potential of 5,2 V vs. Li. The oxidation peak related to the decomposition of the polymer electrolyte could be easily detected at about 4,4 V vs. Li, implying that the polymer electrolyte is electrochemically stable up to this voltage. Consequently, the reinforced gel polymer electrolyte PCS6 was found to be electrochemically stable between the potential range of 2 to 4.4. V vs. Li, sufficient enough to be safely used in rechargeable lithium-based batteries.

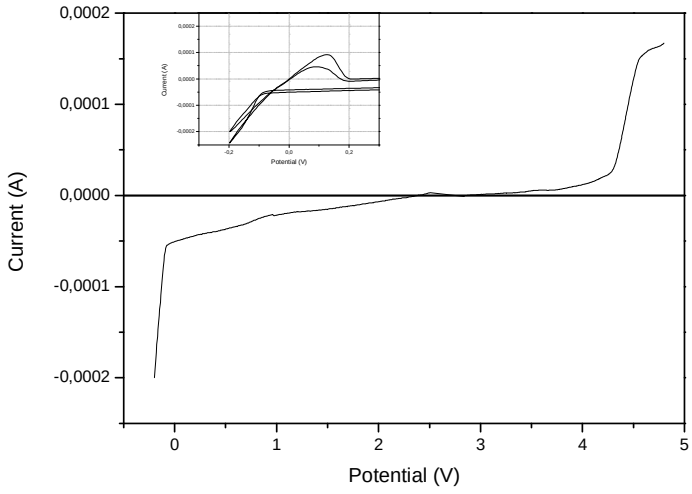

Figure IV.A. 6 Cyclic voltammetric profiles (current/potential vs. Li/Li^+) of the PCS5 reinforced GPE membrane. Cathodic stability window cell configuration Li-metal/PCS5/copper, anodic stability window, cell configuration Li-metal/PCS6/acetylene black. The plot in the inset represents the lithium plating-stripping process.

The electrochemical behaviour as electrolyte in lithium cell of the PCS5 reinforced membrane was analysed by assembling a cell with the configuration $LiFePO_4$/C-PCS5-Li metal and testing it by means of galvanostatic charge-discharge cycling at room temperature and at different current rates (Figure IV.A. 7 A, B). In Figure IV.A. 7 A the potential vs. time plot of cell is illustrated. It shows the regular charge-discharge profile of the first cycles at C/10 during which the lithium is removed from $LiFePO_4$ to form $FePO_4$ (charge) and then lithium is re-inserted into $FePO_4$ to reconvert to $LiFePO_4$ (discharge). The galvanostatic charge-discharge profiles show very flat voltage plateaus at 3.47-3.65 V vs. Li on charge and at 3.38-3.20 V vs. Li on discharge, reflecting the good performance of the GPE membrane and the properties of the $LiFePO_4$/C cathode, namely high specific capacity and steepness of the plateau with minimum overpotential.

The particular $LiFePO_4$/C cathode used for this test and produced in the electrochemistry laboratories at POLITO, when tested in a lithium test cell with a liquid electrolyte shows a specific capacity of about 90 mAh g^{-1} at a current rate of 1C. Observing the plot in Figure IV.A. 7 B it is then possible to appreciate the very good specific capacity allowed by the use of the reinforced GPE, that reaches values as high as 100 mAh g^{-1} at low current rates and about 80 mAh g^{-1} at 1C. The cell presents also a high stability upon cycling even after prolonged number of cycles, actually no loss in capacity is observed even at the 70^{th} cycle. With the exception of the first cycle, in which some secondary reactions occur at the electrodes (this phenomenon is typical of the particular $LiFePO_4$/C used[1]), the Coulombic efficiency was found to be always very high, showing values of about 98 % at low current rates and approaching even 100 % at 1C. Furthermore, it is also important to notice that no degradation occurs inside the cell both in the electrode and the electrolyte: in fact, when the current rate is changed from 1C to C/5 no

abnormal drift is observable, actually restoring the 1C current rate the specific capacity is even slightly increased (83 mAh g^{-1}).

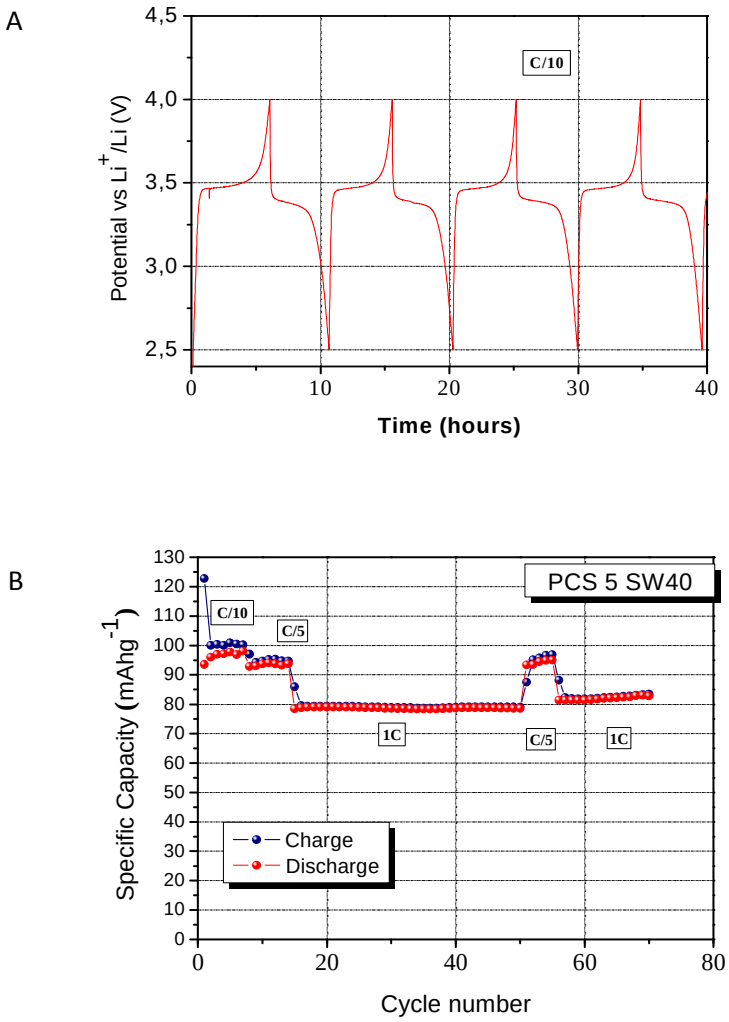

Figure IV.A. 7 (A) Typical charge and discharge cycle runs at ambient temperature (B) Specific capacity vs. cycle number of the lithium cell assembled by contacting in sequence the $LiFePO_4$ composite cathode, the PCS5 reinforced membrane and a Li metal anode, at ambient temperature and at different current rates from C/10 to 1C.

2.3 Improvement of the electrochemical behaviour using additives

The PCS5 membrane reinforced with the handsheet SW40 (SR35 51 g m^{-2}) presents outstanding mechanical properties and good electrochemical performances, therefore it could be then proposed for the production of thin and flexible lithium-based batteries. Considering its excellent behaviour, the

same formulation was also reinforced and tested with handsheets containing additives due to the positive effect of ceramic fillers on the electrochemical performances already demonstrated in *Chapter III*.

The formulation of the membrane PCS5 composed of BEMA: PEGMA475: EC/DEC: LiTFSI (10: 10: 60: 20) + 3 % Darocure + 1 % BP was used to produce GPEs reinforced with handsheets containing Alumina and Calcium Phosphate in different quantities. The various samples prepared are summarized in Table IV.A. 5.

Sample	Additive	Quantity of additive (%Wt)
Formulation BEMA: PEGMA: EC/DEC: LiTFSI 10: 10: 60:20 Darocure 3% BP1%		
Handsheet SW40, °SR35, 51 g m^{-2}		
PCS7	$Ca_3(PO_4)_2$	5
PCS8	$Ca_3(PO_4)_2$	10
PCS9	$Ca_3(PO_4)_2$	15
PCS10	Al_2O_3	5
PCS11	Al_2O_3	10
PCS12	Al_2O_3	15

Table IV.A. 5 Summary of the samples prepared by using handsheets containing ceramic fillers.

As already described in *Chapter III* the use of handsheets containing additives did not significantly affect the mechanical properties. Also the thermal properties of the membranes are not varied by the presence of additives in the handsheets (Table IV.A.6)

Sample	Tg (°C)	T_5 (°C)	T_{10} (°C)	T_{50} (°C)
PCS8 $Ca_3(PO_4)_2$10%	-64	115	140	345
PCS11 Al_2O_3 10%	-67	108	146	338

Table IV.A 6 Thermal properties of the gel polymer membranes reinforced by the handsheets containing the 10% of $Ca_3(PO_4)_2$ (PCS8) and 10% of Al_2O_3(PCS11)

The Tg is not varied with respect to sample PCS5 (-65°C) and the same degradation steps are observed from the TGA analysis; for both samples the

evaporation of the solvent causes the first weight loss, while the degradation of the network starts at higher temperatures (~ 145°C) and a weight loss of 50% is at about 340°C.

The electrochemical performances of the new samples were firstly evaluated by measuring their ionic conductivity. The corresponding Arrhenius plots are reported in Figure IV.A.8.

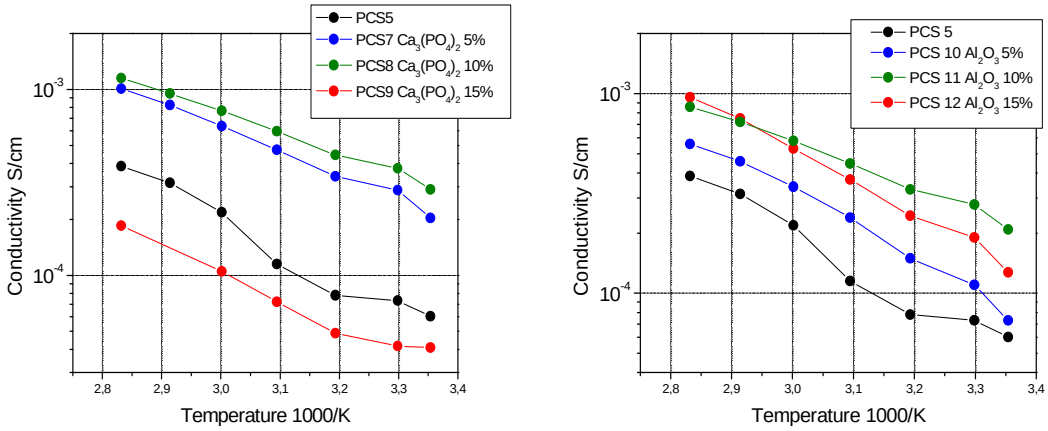

Figure IV.A. 8 Arrhenius plots of the obtained GPE membranes reinforced with handsheets containing different percentages of calcium phosphate (A) and different percentages of alumina (B).

As clearly evident, the use of additives remarkably increased the ionic conductivity. From Figure IV.A. 8. A it is possible to see that with the 5 and 10 wt. % of $Ca_3(PO_4)_2$ a big enhancement in conductivity is obtainable while a further increase in the quantity of the additive till the 15 wt. % it causes a huge decay to values even lower than those given by the pristine SW40 handsheet. This behaviour was observed also in other composite electrolytes described in literature using alumina or ceramic fillers different from the calcium phosphate [10] , the case here described is however quite different being the additives incorporated in the handsheet structure and not directly in the polymer. Most probably, in the latter case, the high quantity of the ceramic filler added can create agglomerates that hinder the ion mobility. In fact, the role of calcium phosphate has still to be fully understood; however, the presence of the phosphate group (also present in some cathodes commonly

used in lithium batteries [1]) could influence the ionic mobility inside the membranes.

Handsheets containing alumina were also tested. Again the ionic conductivity was evidently enhanced by the presence of the additive (see Figure IV.A. 8.B). It is possible to observe that the best conductivity was reached when a 10 wt. % of filler was added, while for higher quantities the same drop already evidenced with calcium phosphate occurred.

Alumina particles can probably interact with the -EO groups present in the polymer and with the Li-salt anion, thus weakening the polymer-cation complexation, resulting in an increased ionic conductivity[11]. It should also be considered that the use of alumina, as for the previously presented filler, could modify the handsheet morphology, thus leading to an improved ionic mobility.

The membranes showing the highest ionic conductivity (i.e., PCS8 and PCS11) were then tested in terms of their electrochemical stability window. The plots reported in Figure IV.A. 9 show the stability windows obtained by joining together the first cycle of the cathodic and the anodic scans. In the capture frame, the peaks relative to the lithium deposition-stripping processes in the first and third cycle are reported.

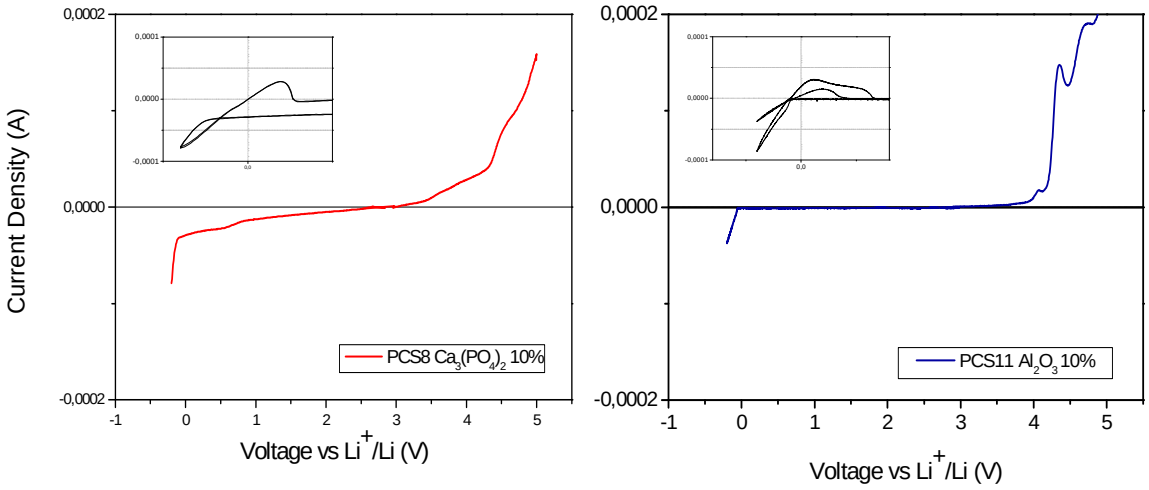

Figure IV.A. 9 Cyclic voltammetric profiles of the anodic and cathodic scans (current/potential vs. Li/Li^+) performed on samples PCS8 (A) and PCS11(B). The plots in the frames represent the lithium plating-stripping peaks. Cathodic stability window cell configuration (Li-metal/PCS--/copper), B-Anodic stability window, cell configuration Li-metal/PCS--/acetylene black.

Figure IV.A. 9 .A shows that by using calcium phosphate the stability was not improved with respect to the one observed for sample PCS4 (see Figure IV.A. 6), actually slightly reduced. In fact, in the anodic part it was possible to observe the drastic anodic breakdown at about 4,4 V vs. Li (as it was observed without additives); but, most important, starting from 3,4 V vs. Li it was already visible a slight increase of the current density that indicates the presence of secondary reactions that compromise the stability of the resulting GPE membrane and need further investigations.

On the contrary, the use of alumina (Figure IV.A. 9. B) resulted in a very flat plateau which ranges from about 0 V to 4 V vs. Li indicating the high purity of the system. The small peak visible at about 4 V vs. Li could be ascribed to presence small amount of residual humidity, the main increase in the current density being in fact observable again at about 4,4 V vs. Li. More interestingly, no current flow is visible in the cathodic scan before the peak corresponding to the lithium plating, which indicates that the use of alumina as additive extends the electrochemical stability window of the resulting GPE membranes towards lower potential values. In fact, sample PCS11 demonstrated a wide electrochemical stability window of about 4.4 V, a very interesting value for a practical application. The presence of the peaks relative to the processes of lithium plating and stripping (see the capture frames in Figure IV.A. 9) in both the systems tested is a highly relevant feature which demostrates the proper working of the membrane as a Li+ ions conductor. As a matter of fact, the conductivity measured by impedance spectroscopy is not only due to the single lithium ions movements but also to the movements of ion pairs which do not effectively participate to the cell functioning. The different dissociation of the Li-salt due to presence of the filler can lead to different transport processes, and the detecting of the peaks assures the effective passage of the charge carriers trough the membrane[12].

The membranes PCS8 and PCS11 were also tested in a laboratory cell prototype by using $LiFePO_4$ as cathode and a lithium metal foil as anode. The cycling performances were investigated by running a galvanostatic cycling

test at room temperature, at different current rates ranging from C/10 to 1C in the voltage range between 2,5 V and 4 V vs. Li (Figure IV.A. 10).

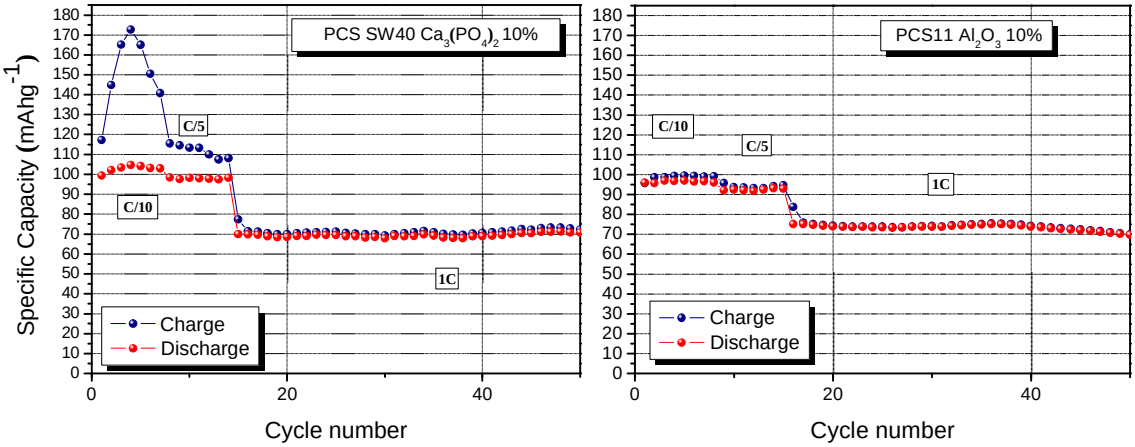

Figure IV.A. 10 Specific capacity vs. cycle number of the lithium cell assembled by contacting in sequence the $LiFePO_4$ composite cathode, the reinforced membrane and a Li metal anode, at ambient temperature and at different current rates from C/10 to 1C. Membrane PCS8 (A) and PCS11 (B).

Even in this case, the particular cathode used, when tested with a liquid electrolyte, demonstrates a specific capacity of about 90 mAh g^{-1} at a current rate of 1C.

From the analysis of the plot reported in Figure IV.A. 10.A (sample PCS8) it was possible to observe an irregular behaviour in terms of Coulombic efficiency for the sample containing calcium phosphate during the initial cycles at low C/10 current regime. This can be easily ascribed to some secondary reaction occurring at low current rates during charge and can be expected on the basis of the electrochemical stability window of the sample (see Figure IV.A. 10.A). At higher current rate of 1C, the specific capacity decreases to about 70 mAh g^{-1}, but the Coulombic efficiency evidently increases approaching 100 %, implying that the influence of the secondary reactions is current-dependent and becomes negligible while cycling the cell at high current regimes The cycling stability after 50 cycles was found to be remarkable, which demonstrates the overall good electrochemical behaviour of the prepared electrolyte.

In Figure IV.A. 10.B, the specific capacity measured for sample PCS11 is represented. In this case, the specific capacity at low current rate (C/10) was found to be about 98 mAh g^{-1} and at high 1C current rate it resulted slightly better than the one observed for the previous sample standing on the average value of 75 mAh g^{-1}. For this second sample the Coulombic efficiency was found to be always very high (near to 100 %), as well as its stability while cycling, thus resulting more reliable than sample PCS8.

Summarising, both the samples reinforced by handsheets containing inert fillers did not demonstrate an evident improvement in the cycling performances when compared to sample PCS5.

Nevertheless, the remarkable ionic conductivity and high electrochemical stability of the sample containing alumina make this electrolyte extremely interesting for future works.

2.4 Swelling procedure

After the characterization of the One Shot membrane the swelling procedure was tested; formulations not containing the lithium salt (BEMA: PEGMA: EC/DEC 12,5: 12,5: 75 + Darocure 3 % + Benzophenone 1 %) were prepared, coated on the handsheet and UV irradiated. In order to activate them, samples were swelled into a liquid electrolyte (1.0 M solution of LiTFSI in EC/DEC). After 15 minutes, the membranes were taken out of the solution, but, at the visual inspection, these did not result completely integer: even in this case, in fact, the polymer was partially detached from the cellulose. The characterization of the swelled membrane was then not possible, the grafting promoted by the presence of the BP did not allow to obtain a sufficient adhesion between the polymer and the cellulose fibres to outstand the swelling by an organic solution.

VI.A.3 Conclusion

The aim of the study reported in this chapter was to develop new polymer membranes reinforced by handsheets having good electrochemical

performances, good mechanical properties and suitable to be prepared by a process where the introduction of the electrolyte could be made by swelling.

An interesting membrane (PCS4) showing conductivity as high as 1,2 10^{-4} scm^{-1} was prepared. To promote the adhesion between the polymer matrix and the cellulose grafting was attempted by using benzophenone as an additional photoinitiator. The increase of Tg, E, the reduction of the tensile resistance and of the conductivity indicate that a network with some bonding between cellulose and polymer was obtained. The use of handsheets containing additives could improve the electrochemical performances of the electrolyte. However the membrane could not stand the swelling procedure and gave partial delamination showing that the grafting was probably limited and does not prevent the debonding of the cellulose/polymer structure.

SECTION B

POLYMER-CELLULOSE BONDING:

Two steps grafting by Benzophenone

As observed in the previous section the use of benzophenone as second photoinitiator improves the adhesion between the polymer and the cellulose by bonding the chains but the grafting obtained is not sufficient to enable the preparation by swelling. The direct use of BP in the polymer formulation caused the creation of a more interconnected network with the consequent decrease in conductivity. Aiming to further improve the adhesion without affecting conductivity a second grafting procedure was tested in the part of the work presented in the following section. Specifically, the procedure consists of two steps and involves covalent attachment of Benzophenone to the polymer substrate[13] with the subsequent attachment of the monomer to the active sites. Besides reducing the formation of non-grafted polymer in solution, the sequential approach provides additional control over grafting because the overall process, including hydrogen abstraction and grafting polymerization, is decoupled into two separate steps. Thus, this two-step sequential photografting technique allows for a greater degree of control over the grafting process.[13, 14] Reinforced One Shot GPEs were first prepared and characterized giving positive results. Then the swelling procedure for the preparation of the membranes was tested.

IV.B.1. Materials and methods

1.1 Materials

The handsheet used for this study has been the SW40 with a grammage of 51 gm^{-2}. For the handsheet preparation and the materials used for the membrane see *Chapter IV Section A.*

1.2 Modification of the handsheet by UV grafting

The scheme of the process is shown in Figure IV.B. 1. The cellulose hand-sheets were swelled into a solution of benzophenone in ethanol (5:95) for 15 minutes.[13]

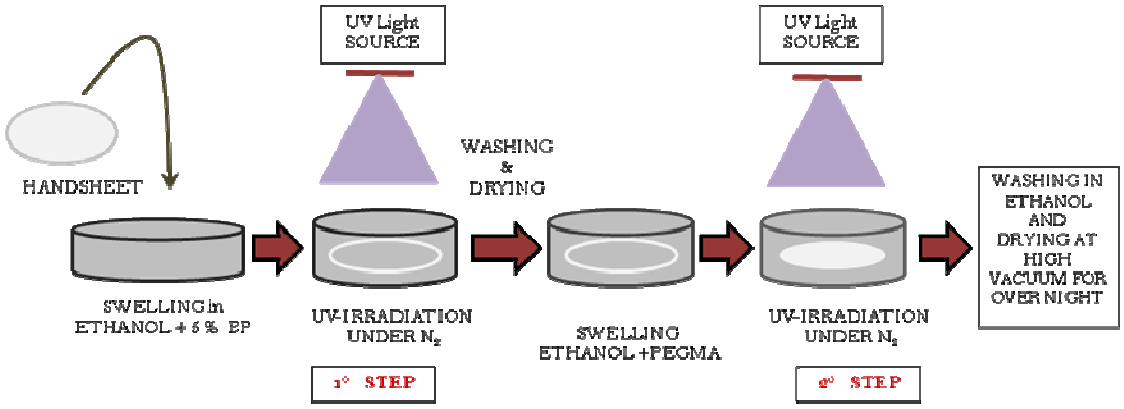

Figure IV.B. 1 Complete process involved in the grafting of cellulose SW-40 hand-sheets by PEGMA-475 using a benzophenone-based two step procedure.

The swelled cellulose hand-sheets were UV irradiated for approx. 1 min under N_2 flux then washed in ethanol and dried at 60 °C till constant weight. These pre-treated hand-sheets were successively swelled into a mixed PEGMA/ethanol solution (50:50) and, soon after, UV irradiated under flowing nitrogen. After washing in ethanol, the obtained modified cellulose was then dried under vacuum conditions at 120 °C to assure the complete removal of water and ethanol.

1.3 Preparation of the electrolyte

The electrolyte was prepared by the fast and easy ONE-SHOT process. (see *Chapter IV*). Also the swelling process was tested (see *Chapter IV*). Various formulations were tested.

1.4 Characterisation methods

For the handsheet thickness and grammage measurements, the membrane thickness measurement, thermal analysis, active swelling, ionic conductivity, electrochemical stability, cycling performances, see *Chapter IV – Section A.*

Weight gain

The weight gain test was carried out after the first and the second step of the modification of SW-40 hand-sheet and calculated by using the equations given below:

$$\text{Percent of BP grafted: } [(W_1-W_0) / W_0] *100$$

$$\text{Percent of PEGMA grafted: } [(W_2-W_1) / W_0] *100$$

where W_0 is the initial weight of the sample after, W_1 is the weight of the BP-grafted hand-sheet after vigorous washing in ethanol/water mixture and drying and W_2 is the weight of the sample grafted with PEGMA measured after the same washing and drying steps, all the samples were also treated under vacuum condition before weighing.

FT-IR ATR

To investigate the presence of grafted polymer on the surface of cellulose hand sheet the FT-IR NICOLET-5700 spectrophotometer was used in ATR mode. Analyses were performed on hand-sheets before and after the grafting treatment. The appearance of the ester peak at 1735 cm^{-1} indicated the presence of the monomer used for the grafting on the surface of the hand-sheet. Measurements were carried on by a using a diamond prism. Each spectrum was collected by cumulating of 64 scans at a 1 cm^{-1} resolution. Spectra were collected in 5 differenbt points of the sample.

VI.B.2. Results

2.1 Handsheets modification

The grafting performed is a sequential two step process; the reactions taking place are sketched in Figure IV.B.2. In the first step, initiator moieties are formed at the cellulose surface by UV irradiation of the substrate that is in contact with the benzophenone solution. This compound abstracts hydrogen from the polymer surface and creates a free radical. However, in the absence of monomers, the surface radical and the newly formed semipinacol radical combine to form surface-bound initiator. The unreacted BP is then removed by washing.

The second step of graft polymerization is then carried out with a solution containing monomer and solvent. UV irradiation liberates the immobilized latent free radicals that initiate graft polymerization from the surface[13,14].

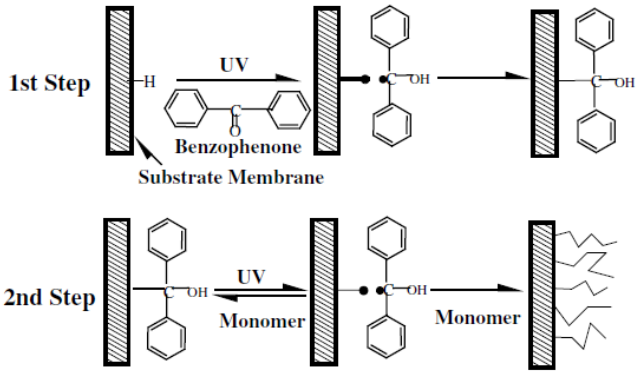

Figure IV.B. 2 Two step photografting reaction[13]

The procedure adopted was optimized starting from the indications of Stachowiak et al[13]. The concentration of BP was fixed at 5% in ethanol while the concentration of PEGMA for the second step was fixed at 50% in ethanol. Different times of immersion in the iniziator and monomer solutions were investigated as well as the UV irradiation time. Measurements of weight were done to control the effect of each parameter on each step of the process i.e. grafting of benzofenone and graftiong of PEGMA. Measurements were done after a careful washing of the samples. Figure IV.B. 3. A shows the weight increase of the handsheet varying the swelling time in the solutions, while the irradiation time was kept constant (1minute)

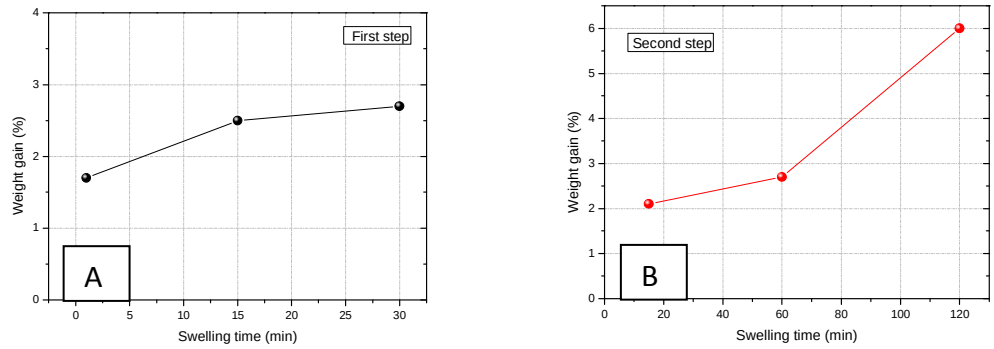

.

Figure IV.B. 3 A Graphic results of the weight gain as a function of the swelling time after the first step (benzophenone). B-after the second step (PEGMA grafting)

A swelling time of 15 minutes resulted then sufficient for the achievement of an acceptable surface bonding of the initiator. In Figure IV.B. 3. B is reported the weight increase of samples swelled 15 minutes in the BP solution, treated with the PEGMA solution for different time and UV irradiated for 3 minutes. The PEGMA curve showed a big increase in the weight only after 2 hr, longer times were not tested in order not to obtain a too long procedure.

In the same way the irradiation times were evaluated keeping constant the swelling time

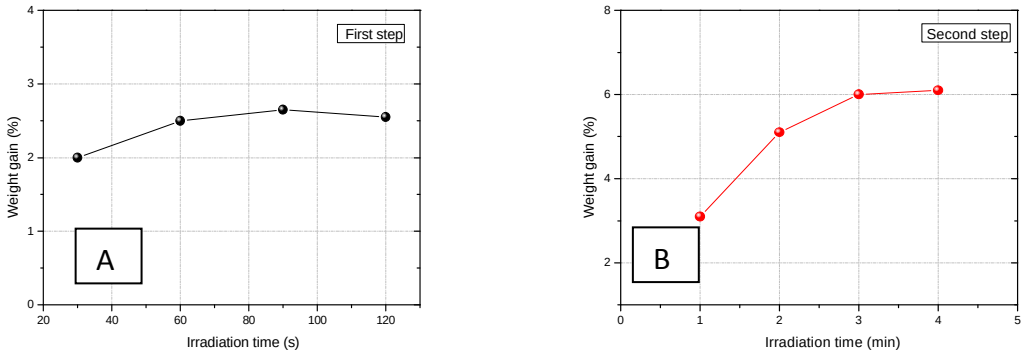

Figure IV.B. 4 A Graphic results of the weight gain as a function of the irradiation time after the first step (benzophenone). B-after the second step (PEGMA grafting)

Figure IV.B. 3. A shows the weight increase of the handsheet varying the UV irradiation time, while the swelling time was kept constant (15 min). As evident after 1 min the weight increase reaches a plateau, 1 min was then settled as the irradiation time for the first step. In Figure IV.B. 3. B the study of the weight gain as a function of the irradiation time of the second

step is presented. Also in this case a plateau is reached after 3 min indicating that this time can be adopted for the optimized procedure.
The parameters chosen are summarized in Table IV.B.1 together with the weight gain obtained for the optimized procedure.

Parameter	Value	Weight gain (%)
BP-Ethanol concentration (% Wt)	5:95	
Swelling in BP-EtOH (min)	15	1st step
UV irradiation time (min)	1	2,5
PEGMA-Ethanol concentration (% Wt)	50:50	
Swelling in PEGMA-EtOH (min)	120	2 nd step
UV irradiation time (min)	3	6

Table IV.B. 1 Parameters chosen for the two step grafting procedure

Applying these conditions the weight increase was of the 2,5% after the first step and 6% after the second one.
Considering the weight gain measured and the molecular weight of the chemicals used it is possible to develop a calculation of the suface grafting yield in mmol*m^{-2} for the two steps.

GRAFTING OF BP:

Weight of BP /1g of paper = 0,025 g (weight gain 2,5%)

Moles of BP / 1g of paper = 0,136 mmol (BP Mw = 183 $gmol^{-1}$)

GRAFTING OF PEGMA:

Weight of PEGMA / 1g of paper = 0,06 g (weight gain 6%)

Moles of PEGMA / 1g of paper = 0,126 mmol (PEGMA Mw = 475$gmol^{-1}$)

(0,126 mmol*g^{-1} /0,136 mmol*g^{-1})*100= 92%

The calculation indicates that theoretically the 92% of the radical pinacols formed during the first step are consumed in the second one

FTIR-ATR investigation was performed on handsheets before and after the two step grafting process. A typical spectrum is reported in Figure IV.B. 5 The appearance of the characteristic absorption peak of the carbonyl groups of PEGMA (ν C=O = 1735 cm^{-1}) after the grafting treatment indicates the presence of the PEGMA monomer, other bands of PEGMA (ν CO= 1110 cm^{-1}, ν CH =2930 and2875 cm^{-1}, CH=CH =1650cm^{-1}) could not be observed since they overlap with the cellulose signal. (Figure IV.B.5).

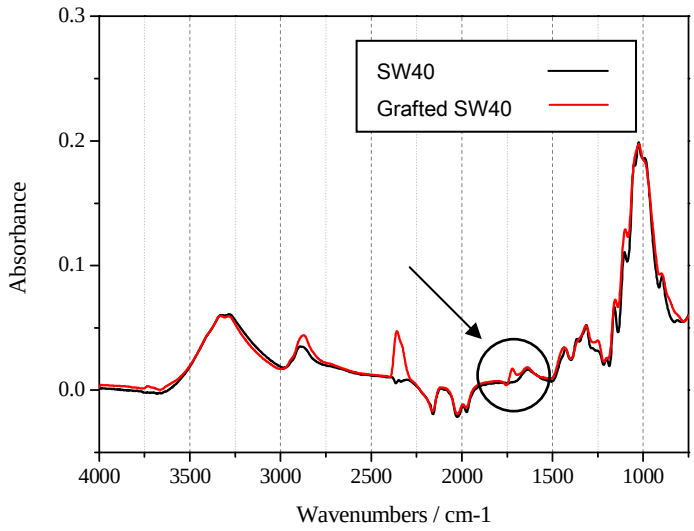

Figure IV.B. 5 FT-ATR spectra of SW40 (SR35, 51gm^{-2}) and SW40 grafted-PEGMA

The SEM analysis of the grafted handsheet surface confirms that the cellulose fibers surface was successfully modified by PEGMA grafting. Figure 5 compares the surface of cellulose before grafting and after grafting. It is very clear from the image that the fibers surface is smoothened by grafting.

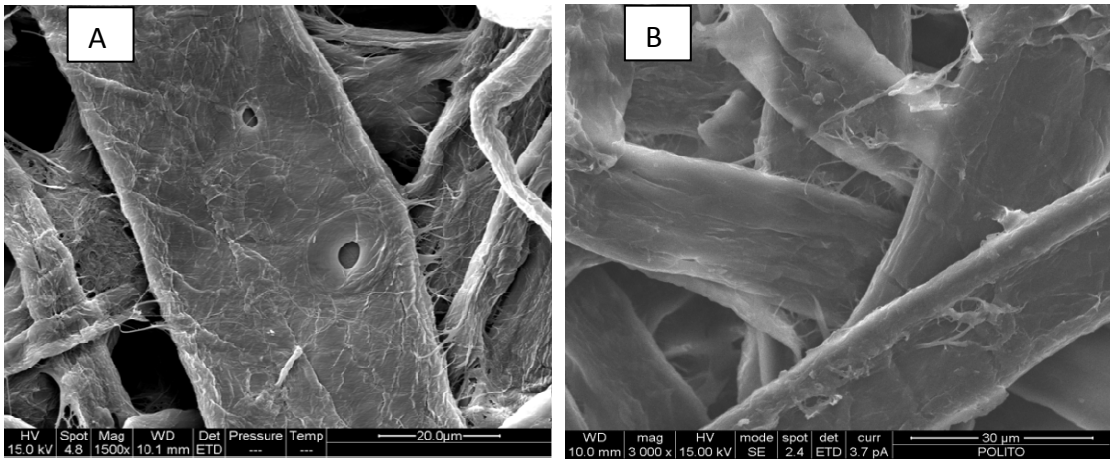

Figure IV.B. 6 SEM micrographs of A) pure cellulose SW-40 (SR35, 51gm^{-2}) and B) grafted cellulose SW-40.

TGA analyses performed in nitrogen atmosphere on pure cellulose and on the grafted one are shown in Figure IV.B. 7. The thermogram of cellulose shows a first decrease of weight before 100°C which can be correlated to the loss of water, the weight is then stable up to 280°C, temperature at which the main degradation starts with a decrease of weight from the 90 to the 19% at 370°C. Above this temperature the weight still has a slight decrease resulting in a residue at 600°C of the 12 % of the initial weight.

The curve of the grafted sample shows a smaller decrease before 100°C followed by a slight but constant decrease till 270 °C where the main degradation step starts with a variation from the 90 to the 9% at 400°C. The residue at 600°C is in this case of the 5%.

The comparison of the two samples suggests that:

- The amount of free water contained in the samples is different and the content of water considered at 90°C is lower (1,1%) in the treated handsheet.
- The water absorbed (chemisorbed) on cellulose is different: 0,8% for the neat cellulose and 1,6 for the treated sample (variation of weight from 90°C to 270°C).
- Above 370°C one observes a higher weight loss of the modified sample due to the presence of PEGMA.
- The difference between the residues is ~7% and can be correlated to the weight of PEGMA grafted to the cellulose.

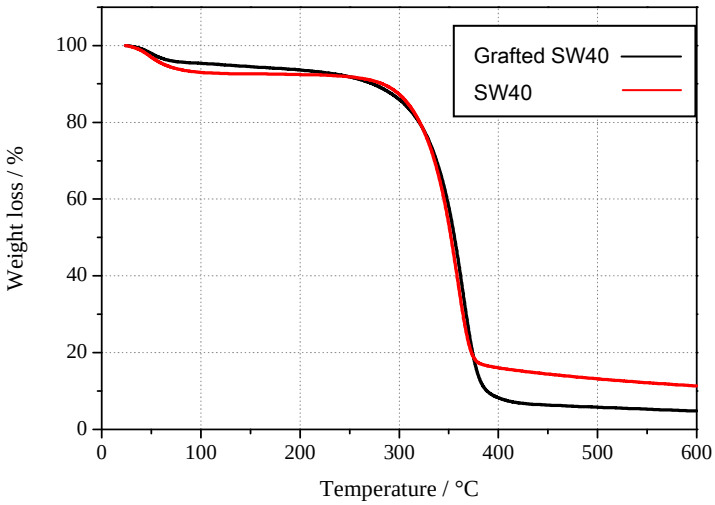

Figure IV.B. 7TGA analysis of SW40 (SR35, 51gm^{-2}) and SW40 grafted-PEGMA

Overall the results from the TGA analysis confirm the grafting of PEGMA. The tensile studies performed on the SW40 handsheet as well as the PEGMA grafted handsheet are reported in Figure IV.B. 8. From the initial slope of the curve the Young's modulus can be calculated while the tensile resistance corresponds to the maximum of the curve. The values are reported in Table IV.B. 2. As visible there is almost no change in E and in the resistance, this fact indicates that the surface treatment does not affect the bulk properties of the handsheet.

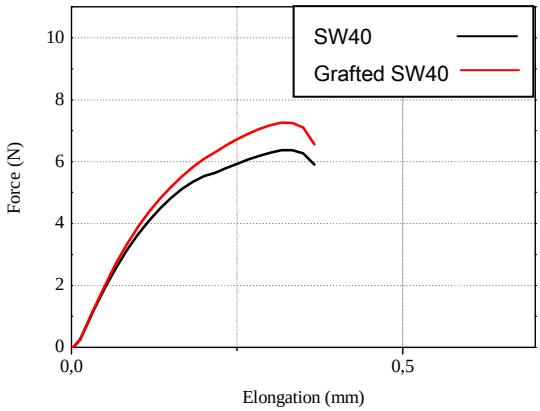

	Young's modulus (MPa)	Tensile resistance (MPa)
SW-40	3820	7,04
G-SW-40	3860	7,46

Figure IV.B. 8 Elongation vs force curve of teh grafted cellulose compared with the untreated handsheet.

Table IV.B. 2 Comparison between tensile strength and Young's modulus of SW-40 (SR 35, 51 gm^{-2}) and its grafted version

2.2 Preparation of the membranes

The treated handsheets were used to prepare various GPE membranes. The One Shot and the swelling procedures were tested. Starting from the reference formulation (see *Chapter III*) the quantities of the components were varied in order to find the optimal composition.

The different samples prepared are summarized in Table IV.B.3.

The reactive mixtures composed of BEMA, PEGMA EC/DEC and LiTFSI salt, were prepared in glove box and spread on the handsheet by using a coating bar (200 µm), the impregnated hansheets were then sealed in a quartz tube and UV irradiated for 3 minutes in order to obtain membranes ready to be used.

Sample	**Handsheet**	**BEMA (%)**	**PEGMA (%)**	**EC:DEC (%)**	**LiTFSI (%)**	**Photoiniz (%)**	**Active swell. (%)**
P50 (GPE)	SW40	35	15	30	20	+3	93
P50 - G	SW40graf	35	15	30	20	+3	95
P40	SW40	20	20	30	30	+3	92
P40-2G	SW40graf	20	20	30	30	+3	89
P30	SW40	20	10	40	30	+3	88
P30-3G	SW40graf	20	10	40	30	+3	91

Table IV.B. 3 Composition of the samples prepared. The membrane label indicates the total quantity of oligomer used in the formulation The handsheet used were always SW40 (SR 35°, 51 gm^{-2})

The quantity of polymer- electrolyte present in the membrane, represented by the Active Swelling value (Table IV.B.3) was very high for all the samples (about 90 % wt).

All the One Shot GPEs were self-standing, extremely flexible and easy to handle, Figure IV.B.9, A represents the appearance of one of P30-G while in Figure IV.B.9 B it is possible to observe a SEM micrograph which shows the good interpenetration between polymer and cellulose.

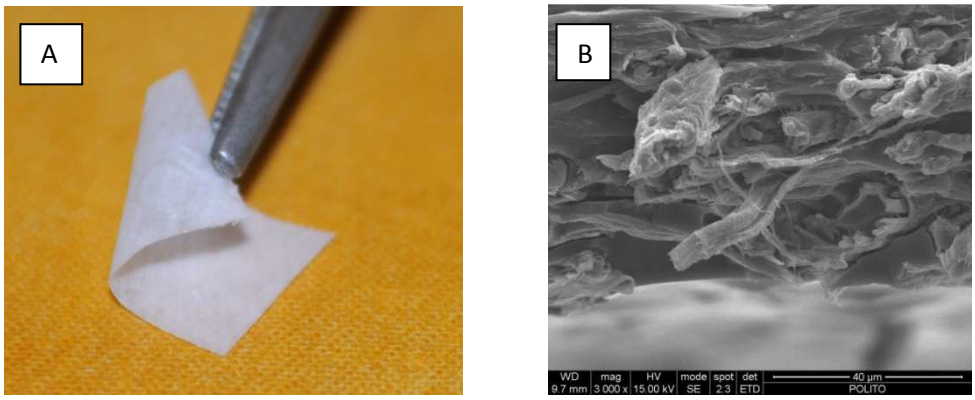

Figure IV.B. 9 A-Appearance of sample 6 reinforced GPE. B-SEM micrograph of sample 6

2.3 Characterization of the GPEs

The ionic conductivity of the membranes was evaluated aiming to find the best performing one. Firstly the conductivities of sample P50 (corresponding to the reference GPE used in *Chapter III*) and P50-G (using the grafted

handsheet) were measured and compared. Arrhenius plots of samples P50, and P50-G are reported in Figure IV.B. 10. Similar results are obtained, it is evident that the two step grafting procedure, which improves the adhesion between polymer and cellulose, does not cause a decrease in conductivity, the polymer chains of the photocured formulation in this case are not directly anchored to the cellulose surface. This was not the conclusion obtained when BP was using during the photopolymerisation of the same system. As discussed in Section A the direct grafting of the polymer caused an interconnected network between cellulose and crosslinked polymer hindering the mobility and causing a decrease in conductivity. For an easier comparison the Arrhenius plot of a sample prepared by adding BP to the formulation is reported. The reactive mixture used for sample P50 was added of the 1% of BP and polymerized, a untreated handsheet was used as a reinforcement, the sample is labeled P50-BP.

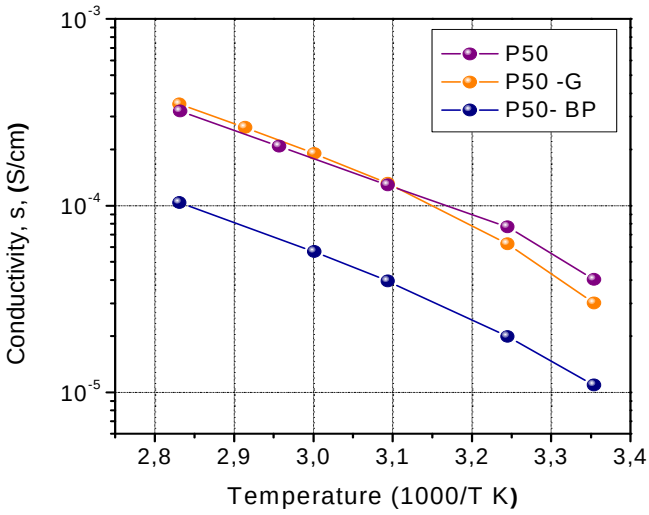

Figure IV.B. 10 Arrhenius plot of the ionic conductivity of P50 (reference membrane reinforced by SW40 handsheet) and P50-G (same handsheet modified by the two step procedure). The blue curve (P50-BP) represents the conductivity of the same membrane membrane reinforced SW40 handsheet with the addition of BP to the formulation.

As it was observed that conductivity is not affected by the two step grafting only the Arrhenius plot of samples P40-G and P30-G will now be reported (Figure IV.B.11) and compared to sample P50-G. Starting from this last the first trial has been the reduction of the quantity of polymer in favor of a

bigger quantity of lithium salt (P40-G). The conductivity measurement did not reveal any significant improvement. For this reason it has been chosen to further reduce the quantity of the monomers in order to increase the organic solvent that plays a major role in lithium ion mobility. P30-G showed a good increase in ionic conductivity reaching values of $2*10^{-4}$ at room temperature. The quantity of polymer present is evidently enough to dissociate the salt while the organic solvent enhances the ion mobility.

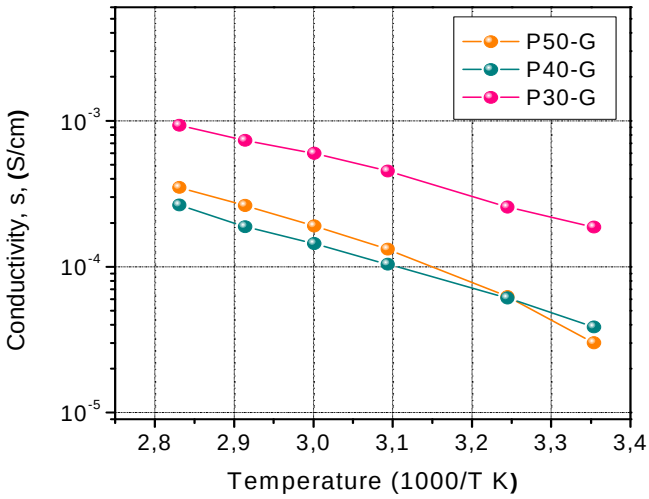

Figure IV.B. 11 Arrhenius plot of the ionic conductivity of P50-G compared with samples P40-G and P30-G.

The formulation used for the preparation of sample 6 has then been chosen for the development of the work. It could have been expected to find even higher conductivity by a further increasing the quantity of organic solvent (as observed in the previous section) but, considering safety issues, a compromise must be accepted.

Sample P30-G has then been subjected to a deeper characterization.

The thermal stability of the composite polymer film was assessed by thermo-gravimetric analysis under nitrogen. A distinct weight loss was found at approx. 130°C, as the solvents begin to evaporate: this means that the GPE can be safely used in thin flexible Li-based polymer batteries up to 100 °C. Figure IV.B. 12 shows the plot obtained from the TGA analysis while in Table IV.B.4 the representative degradation temperatures are reported together with the Tg of the system.

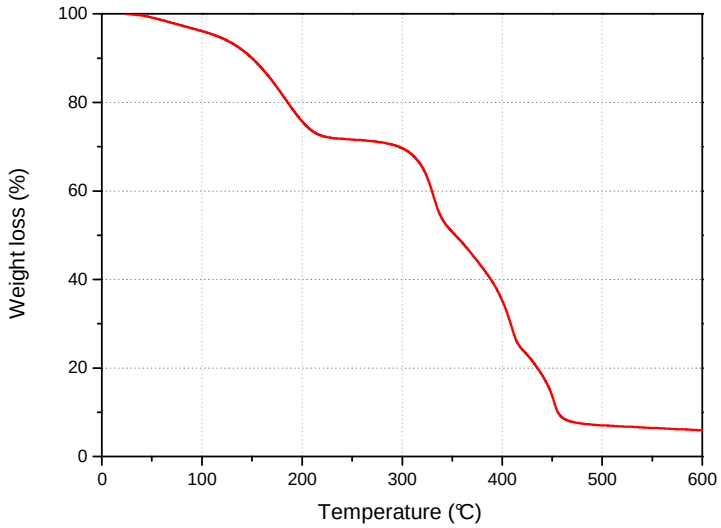

Figure IV.B. 12 TGA plot for sample P30-G

Sample	Tg (°C)	T_5 (°C)	T_{10} (°C)	T_{50} (°C)
P30-G	-62	108	150	353

Table IV.B 4 Thermal properties of sample P30-G

The mechanical properties of the membrane were evaluated by the tensile test. The results obtained are reported in Table IV.B. 5 and compared to the sample prepared with an untreated handsheet. It is evident that the modification of cellulose causes a decrease of the mechanical properties. Even when the worse are considered, the mechanical properties of all the membranes are largely improved with respect to a not reinforced membrane and are sufficient for the possible application in flexible devices. The presence of the grafted monomer could improve the penetration of the polymer chains into the cellulose network, breaking the hydrogen bonds among the fibers and reducing the strength of this last.

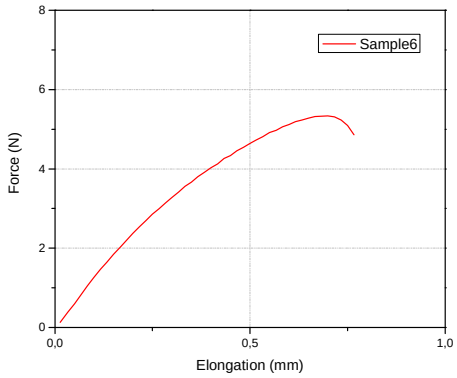

Figure IV.B. 13 Force vs Elongation plot for sample P30-G

Sample	**Young's modulus (MPa)**	**Tensile Resistance (MPa)**
P30-G	400	2,7
P30	2089	7,9

Table IV.B 5 Mechanical properties of the samples prepared

A deeper electrochemical characterization was then carried on for sample P30-G. The electrochemical stability and the behavior during the galvanostatic cycling were evaluated.

Commonly, in a lithium battery, the anodic reaction occurs in the vicinity of 0 V vs. Li/Li^+, whilst the cathode potentials can approach as high as 4.5 V vs. Li/Li^+, implying that the E.S.W. is a fundamental parameter to assess its stability during cycling. In addition to high ionic conductivity, this prepared GPE showed an appreciably wide electrochemical stability window, which makes it particularly valuable in view of a practical application in real battery configuration. This is shown in Figure IV.B. 14 (A,B) which illustrates the current-voltage response of GPE, obtained in the voltage range between 0 and 5.5 V vs. Li/Li^+ at room temperature by means of linear sweep voltammetry. Measurements were performed by scanning the cell voltage from the O.C.V. towards 0.0 V vs. Li/Li^+ (cathodic scan) or 5.5 V vs. Li/Li^+ (anodic scan). In both cases, the potential was scanned at a rate of 0.100 mV s^{-1}. An appreciably wide ESW was obtained: no electrochemical reactions occurred at positive potentials ranging from the lithium plating to above 4.3 V

vs. Li/Li^+ at 25 °C. Moreover, the current–potential curves showed very low residual current prior to breakdown voltages, confirming the purity of the synthesized membrane and the synthesis method adopted, because the system as in whole is sensitive to oxygen, water and other impurities. The increase of the current during anodic scan, which is related the decomposition of the electrolyte, was taken in correspondence to the onset of a low current peak at approx. 4.3 V vs. Li/Li^+. Nevertheless, even if the current rises at a lower voltage, after few cycles its trend consistently deviates from that observed in the first cycle, showing a sort of "passivation" phenomenon which apparently extends the anodic stability up to higher voltage, i.e. approx. 5 V vs. Li/Li^+. The reason for this particular behaviour is still unclear; however, such a high decomposition voltage is certainly welcome and, so, worth investigation further. A similar "passivation" phenomenon seems to occur during cathodic scan, in which during the first cycle a peak is clearly visible, which disappears after subsequent cycling.

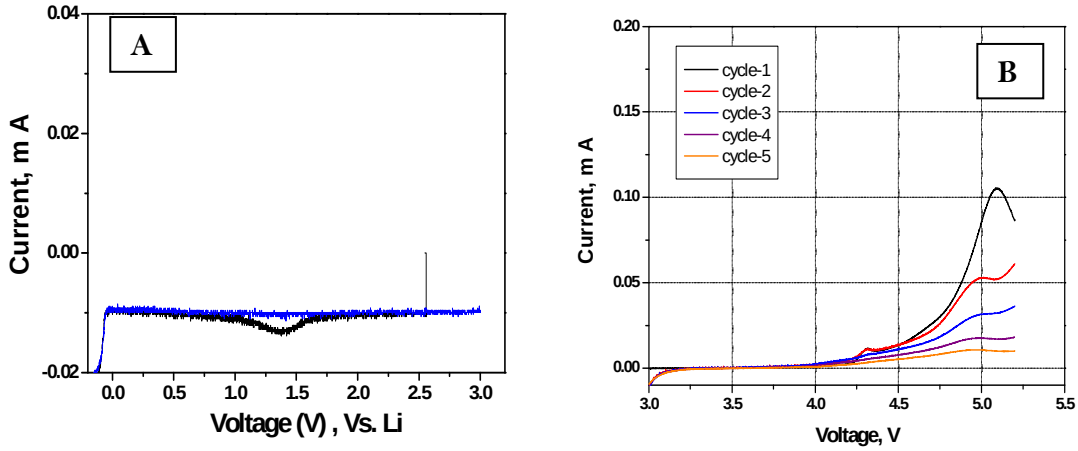

Figure IV.B. 14 Electrochemical stability window (ESW) of GPE at 25 °C; potential scan rate of 0.100 mV s^{-1}.

In view of the possible practical application of the prepared GPE, to get a more thorough insight on its performances, it was assembled in a laboratory-scale lithium polymer cell, and its electrochemical behaviour was investigated by means of galvanostatic charge/discharge cycling. The response of the prototype, assembled by combining a lithium metal anode with a $LiFePO_4/C$

cathode and using the sample P30-G GPE membrane as the separator, is reported in Figure IV.B. 15 and 16.

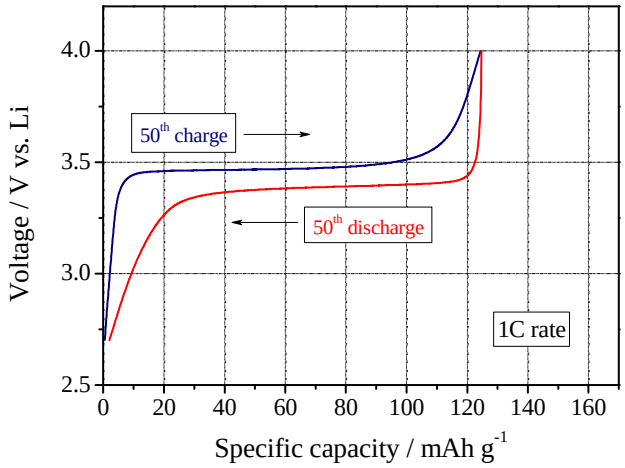

Figure IV.B. 15. Room temperature galvanostatic charge-discharge profiles of the Li polymer cell, assembled by sandwiching sample P30-G between a $LiFePO_4$/C cathode and a Li metal anode, at 1C current rate.

The results of the galvanostatic cycling are very interesting as depicted in Figure IV.B. 15, which shows the 50th galvanostatic charge and discharge profiles at 1C current regime. The galvanostatic charge-discharge profiles allow to appreciate the specific capacity and steepness of the plateau with minimum over-potential linked to the cathode performances. A very flat plateau indicates the occurring of the biphasic Li+ extraction/insertion mechanism typical of $LiFePO_4$ cathode.

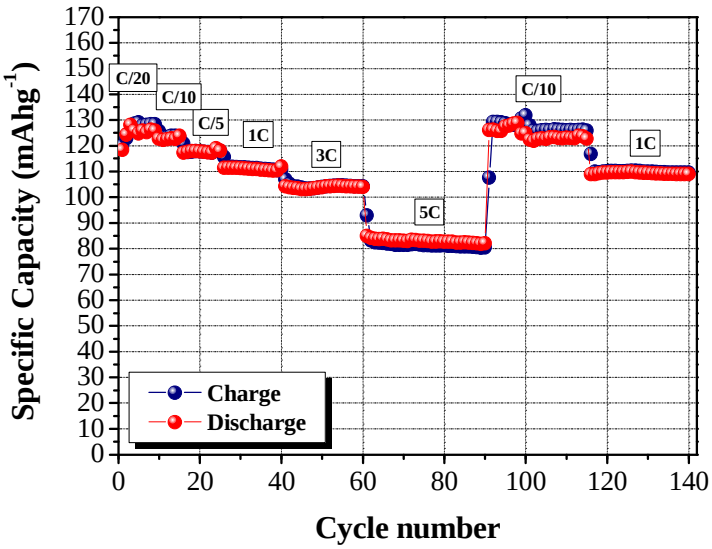

Figure IV.B. 16. Room temperature galvanostatic charge-discharge cycling test of the lithium polymer cell, assembled by sandwiching sample P30-G between a $LiFePO_4$/C cathode and a Li metal anode, at different C-rates (from C/20 to 5C) The results obtained reflect the electrolyte performance they are already rescaled in function of the capacity of the cathode

Figure IV.B. 16 shows the cycling performance of the cell as a function of cycle number, at room temperature and at different C-rates ranging from C/20 to 3C. This figure shows good capacity retention with the repeated cycling. This is a convincing indication of a good interfacial contact between electrodes and separator. The coulombic efficiency, after the first cycles, it is found to be 95% and it is maintained to be higher than 99% after the 40th cycle, at C-rates higher than C/10. The rate capability of the lithium metal polymer cell was also good, with a slight decrease in both average discharge voltage and discharge capacity. Good performance at high current rate may be ascribed to the efficient ionic conduction in the polymer-coated separator and the favourable interfacial charge transport between electrodes and electrolyte in the cell. The extraction and insertion of lithium ions into the structure of $LiFePO_4$ is not only reversible on repeated cycling; the capacity actually increases slightly with the initial cycling. Moreover, reducing the C-rate completely restores the specific capacity (see, in Figure IV.B. 16, the restoring of the specific capacity values from 5C to C/10 after the 120th cycle). implying that no degradation occurred, the system being highly stable to the electrochemical redox reaction.

2.4 Swelling method

After the characterization of the One Shot membrane the swelling procedure was tested; formulations not containing the lithium salt (BEMA: PEGMA: EC/DEC 35: 15: 50 + Darocure 3 %) were prepared, coated on the pre-treated handsheet and UV irradiated. In order to activate them, samples were swelled into a liquid electrolyte (1.0 M solution of LiTFSI in EC/DEC). After 15 minutes, the membranes were taken out of the solution, but, at the visual inspection, these did not result completely integer: even in this case, in fact, a partial delamination of the polymer from the cellulose was observable. The characterization of the swelled membrane was then not possible, UV curing of the membranes embedding cellulose handsheets grafted with PEGMA did not allow to obtain a sufficient interpenetration between the polymer and the cellulose fibres to outstand the swelling by an organic solution.

IV. B. 3. Conclusion

The aim of the study reported in this chapter was to develop new polymer membranes reinforced by handsheets having good electrochemical performances, good mechanical properties and suitable to be prepared by a process where the introduction of the electrolyte could be made by swelling.
In order to improve the adhesion between polymer and cellulose a pre-garfting of the monofunctional PEGMA on the handsheet was performed. An increase of the weight of the treated handsheet after washing, ATR, TGA and SEM analysis confirmed the presence of the monomer at the cellulose surface. An interesting membrane using the pre-treated handsheet was then developed (P30-G) showing conductivity as high as $2*10^{-4}$ scm^{-1} and appreciable electrochemical performances.. No loss in conductivity was observed when this kind of grafting was used. However the membrane could not stand the swelling procedure and gave partial delamination.

SECTION C

POLYMER-CELLULOSE BONDING:

In situ grafting of Glycidyl Acrylate

The last procedure of fabrication of membranes involves a grafting using Glycidyl Acrylate as bonding agent between the polymer matrix and the cellulose substrate. Glycidyl Acrylate (GA) and methacrylate (GMA) have been largely used to modify polymer surfaces[15-18]. In this work it was chosen to use GA. This monomer presenting an acrylic group is more reactive than mathacrylates and can be grafted onto cellulose and/or copolymerize with the photocurable formulation. It also has a reactive epoxy group, which is highly reactive and on opening can give chain transfer reaction to the hydroxyl groups of cellulose[19]. GA has been added to the curable formulation for the preparation of multilayered handsheets-polymer electrolytes. The membranes obtained were swelled in a solution of lithium salt in organic solvent. The production of swelled Gel Polymer Electrolytes was possible. The GPEs prepared by this method were competitive for the application in Li-based batteries.

VI.C.1. Materials and methods

1.1 Handsheet materials and preparation

The handsheet used for this study was the SW40 with a grammage of 51 gm^{-2}. See description in *Chapter VI - Section A*.

1.2 Membrane formulation

The UV cured polymer membrane was composed by :

Bisphenol A ethoxylate (15 EO/phenol) dimethacrylate BEMA, avg M_n = 1700 (Aldrich product)

Poly(ethylene glycol) methyl ether methacrylate PEGMA, average 1100 (Aldrich product, see *Chapter I - Section B*)

Glycidyl acrylate (GA) (Aldrich product). It is a monomer which has an epoxy group and an acrylic group as sketched in the Figure below.

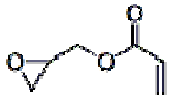

2-hydroxy-2-methyl-1-phenyl-1-propanone (Darocure 1173) from Ciba Specialty Chemicals used as the free radical photo-initiator.

Triarylsulphonium exafluoro phosphate was used as cationic photoinitiator.

LiTFSI (lithium bistrifluoromethane-sulfonimide,$CF_3SO_2NLiSO_2CF_3$, Aldrich) salt was dissolved in a 1:1 w/w ethylene carbonate – diethyl carbonate (EC-DEC, Fluka) solution in order to obtain a 1 M solution of liquid electrolyte.

1.3 Preparation of the membrane

Various reactive formulations were prepared in dry box, the ratio BEMA: PEGMA was varied while EC/DEC was kept constant (50% of the formulation), GA was the 5% unless in the reference membrane. These were then drawn down on the handsheets by a 100 µm bar. The paper impregnated was placed in a quartz tube sealed in dry box and irradiated. The irradiation was done for 3 minutes by using a medium vapour pressure Hg lamp (Helios Italquartz, Italy), with a radiation intensity of 30 mW cm^{-2}.

Then the membrane was immersed for 15 minutes in a 10 ml of a 1M solution of LiTFSI in EC/DEC, after swelling the excess of liquid electrolyte was absorbed by blotting paper and finally the GPE was then ready to be used.

1.4 Characterisation methods

For the handsheet thickness and grammage measurements, the membrane thickness measurement, thermal analysis, ionic conductivity, electrochemical stability and cycling performances see *Chapter VI – Section A. For* FT-IR-ATR and weight gain see *Section B*

FT-IR spectroscopy

The kinetics of the photo-polymerisation process was investigated by using a NICOLET-5700 Real Time FT-IR instrument, which collects the spectra in real time while the sample is irradiated by UV light, following the decrease of the band attributable to the methacrylate and epoxy groups. The tests were carried out at ambient temperature on an UV transparent SiC wafer by irradiating the mixtures of monomers for 3 min. The UV lampused was Lightning curve LC-8 with an intensity of 15–16mWcm^{-2}. The intensity of the UV lampwas measured using an ORIEL photometer.

Swelling percentage

The electrolyte uptake, indicating the quantity of liquid electrolyte present in the final Gel Polymer Electrolyte will be called Swelling percentage (SP %), it was calculated by the formula:

$$(Wf - Wi)/ Wf \times 100$$

where Wf is the weight of the membrane after swelling and Wi is the weight before swelling).

Bending test

The mechanical properties of the gel polymer electrolytes after swelling were evaluated by a bending test for which the membranes were rolled up around cylindrical hoses with radii ranging between 3 and 32 mm.

XPS

The XPS (X-ray Photoelectron Spectroscopy) analyses were performed by a scanning ESCA microprobe PHI 5000 Versaprobe, with a monochromatic Al ka line (1486.6 eV). The calibration was performed on the Au 4f7/2, Cu 2p3/2 and Ag 3d5/2 peaks, following the "Elemental binding energies for X-ray photoelectron spectroscopy." Materials were analyzed with a combined

electron and argon ion gun neutralizer system in order to reduce the charging effect during the measurements. The survey scans were acquired with a pass energy of 187.85 eV and the high resolution scan with 23.50 eV.
The x-ray beam size was settled at 100 µm for high sensitivity.

VI.C.2. Results

2.1 Membrane preparation

2.1.1 Study of the polymerisation

The preparation of the GPE membrane was made of two steps:
- preparation of the multilayered handsheet-polymer membrane according to the one shot method, using formulations not containing the lithium salt.
-swelling of the multilayered membrane in a lithium salt solution.
The preliminary investigation was devoted to study the polymerization of a reference formulation made of BEMA, PEGMA1100 and a radical photoinitiator and to compare it with the homologue containing GA. As GA contains an epoxy ring, whose reactivity is trough a cationic mechanism, it was chosen to monitor the influence of the addition of a cationic photoinitiator.
The compositions of the samples prepared are reported in Table 1. The kinetics plot of the systems are in Figure 1.

Sample	BEMA (%)	PEGMA1100(%)	GA(%)	Radical PI (%) Darocure1173	Cationic PI (%)
A	50	50	-	+3	-
B	47,5	47,5	5	+3	-
C	47,5	47,5	5	+3	+3

Table IV.C. 1 Composition of the samples prepared for the preliminary swelling test

The percentage of conversion of the double bond of the acrylic groups and the opening of the epoxy rings of the monomers, during the UV exposure was evaluated by kinetic studies using real-time FT-IR technique. The overall reactions were monitored during irradiation through the change in the

intensity of the absorption band of the methacrylic groups at around 1634 cm^{-1} and the epoxy ring at 910 cm^{-1} (only for samples B and C) the C=O bond at 1730 was used as an internal standard. The conversion of the reactive functions is calculated as follows:

$$\eta\% = 1 - \frac{(A_{\text{reactive f, t}} / A_{\text{ref,t}})}{(A_{\text{reactive f, 0}} / A_{\text{ref,0}})} * 100$$

Where $A_{\text{reactive f.t}}$ represent the peak areas under the reactive functionality bands at the at time t, $A_{\text{reactive f.0}}$ is the area at the beginning of the reaction and A_{ref} represents the area under the band of the internal reference at a time = t and at the beginning of the reaction (this area should be unvaried).

The conversion curves are shown in Figure IV.C. 1.

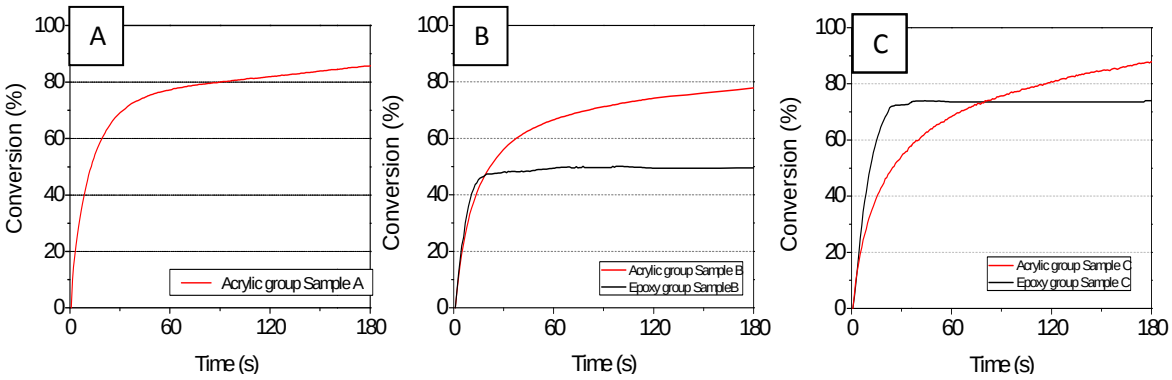

Figure IV.C. 1 Kinetic plot of the conversion of the acrylic and epoxy(when present) groups in samples A (left), B (middle) and C (right).

As visible in Figure IV.C. 1.A the double bond reaction is very fast in the presence of the radical PI and reaches the 70% in about 30 seconds and, after 3 minutes it is higher than 80%. The conversion is not quantitative even after 3 minutes as PEGMA 1100 has a high viscosity and tends to crystallise. In fact, it is a waxy solid material at room temperature and was solubilised in BEMA by heating. However, after polymerisation, the longer pendant –EO- chains tend to recrystallise [2, 3].

When GA is added to the BEMA-PEGMA mixture in the presence of the radical PI (Figure IV.C. 1.B) the conversion of the double bond of the acrylic group becomes slower and reaches the 80% after 3 min. At the same time, even if no cationic initiator is present in the mixture also the epoxy ring

partially reacts by a thermal reaction. In fact the acrylic reaction is exothermic and the heat produced can trigger the polymerisation of epoxydes.[20] When the cationic photoinitiator is added to the mixture together with the radical one (sample C), the polymerisation of the double bond is slower than the polymerisation of samples A and B. The conversion reaches higher levels (90%), in fact the cationic photoinitiator upon irradiation generates radicals. In the presence of the second PI also the opening of the epoxy ring is faster, a higher conversion is reached, up to 70 % after less than 30 seconds. Further investigation on the role of GA is reported in section 2.3.

2.1.2. Swelling study

It was previously observed (see *Chapter V* and *Chapter VI Section A* and *B*) that the reinforced GPEs shown until now could not outstand a swelling test. By dipping the membranes in a liquid solution of organic solvent and lithium salt the polymer membrane was detached from the cellulose substrate.

Aiming to verify the influence of Glycidyl Acrylate and considering the possibility to use this kind of monomer for the production of swelled membranes some preliminary and qualitative tests were done.
Membranes reinforced by handsheets SW40 (35SR, 51gm^{-2}) and prepared by using the formulations reported in Table IV.C. 1 were prepared, immersed in 20 ml of an organic solution composed by Ethylene Carbonate, Diethyl Carbonate (EC:DEC 50:50) and checked every 15 minutes. Figure IV.C. 2 shows the state of the 3 samples after different times of swelling, the samples will be labeld A-cel, B-cel and C-cel.

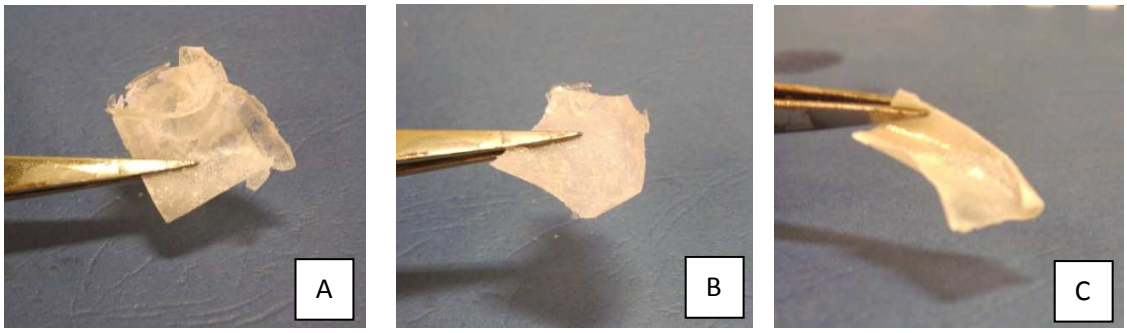

Figure IV.C. 2 A SampleA-cel after 5minutes of swelling; B SampleB-cel after 1hour of swelling; C SampleC-cel after 2hours of swelling.

As visible sample A-cel, which does not contain Glycidyl Acrylate, is no more integer after only 15 minutes of swelling, sample B-cel, which contains GA but only in the presence of the radical photointiator, after 1 hour starts deteriorating, while sample C-cel which contains GA and the two photoinziators, is still integer after 2 hours of swelling. A prolonged test showed that this sample can be left even 24 hours in the organic solution without compromising its structure. These observations demonstrate that the presence of GA can really improve the stability of a membrane submitted to the swelling process. The complete stability of sample C-cel, which was not observed for the other samples, demonstrated also the need of the cationic photoinitiator for the grafting of the polymer to the cellulose substrate.

The swelling percentage as a function of time was also studied (from 15 minutes to 3 h) for sample C-cel, showing a negligible increase in weight of the polymer membrane with time. Figure IV.C.3 shows the variation of the swelling percent as a function of the time of swelling in an EC:DEC (1:1) solution without lithium salt.

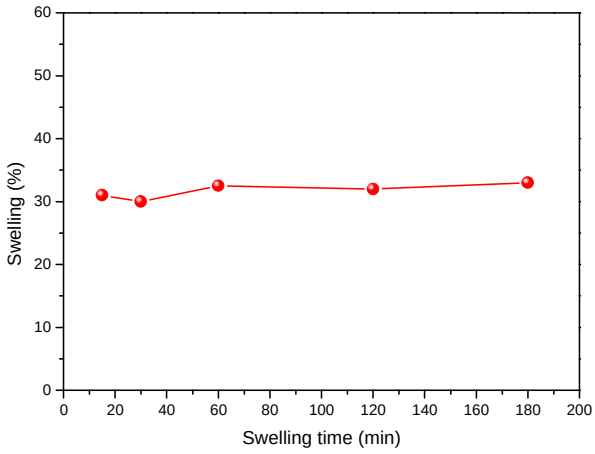

Figure IV.C. 3 Swelling (%) vs swelling time of sample C-cel in an EC:DEC solution

According to this observation the swelling time was chosen of 15 minutes. Aiming to increase the swelling percentage and thus the quantity of electrolyte present in the membrane a further sample (named D-cel) was prepared and tested by means of swelling test. The new formulation contained a percentage of EC:DEC solution directly added in the photocurable mixture. Mantaining the same BEMA:PEGMA ratio the in situ addiction of a plasticizer, such as EC:DEC, allows to obtain polymers with lower Tg and a higher swelling ability[21]. The exact composition is reported in Table IV.C.2. Figure IV.C. 4 gives an indication of the improvement of the swelling percentage.

Sample	BEMA (%)	PEGMA1100 (%)	GA(%)	EC/DEC (%)	Radical PI (%) Darocure (%)	Cationic PI (%)
D-cel	25	25	5	45	+3	+2

Table IV.C. 2 Composition of sample D-cel. The handsheets used was SW40 (35SR, 51gm^{-2}) The EC/DEC solution was directly added to the reactive mixture

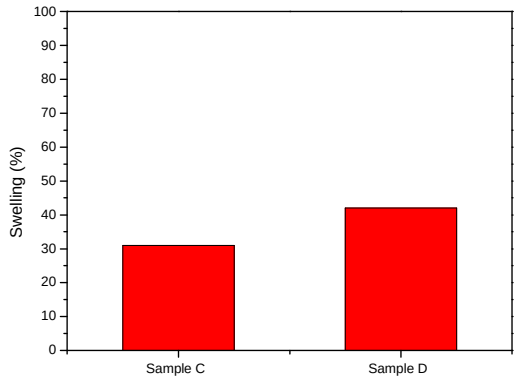

Figure IV.C. 4 Increase of the swelling percentage when the EC/DEC is added to the reactive formulation during sample preparation (Sample D-cel)

As the swelling tests indicated that GA in the presence of radical and cationic PI, assured good adhesion between the polymer and the handsheet and that the in situ addition of a plasticizer can improve the swelling behavior, it was chosen to prepare swelled gel polymer electrolytes following the tested procedure, i.e. using BEMA, PEGMA, GA in the presence of radical and cationic photoinitiators and EC/DEC. As the procedure of swelling multilayered membranes in the presence of GA was successful, various reinforced swelled membranes were prepared. The formulations chosen fulfil these criteria:

- Contains 45% of organic solvent (EC:DEC)
- Contains 5% of GA

PEGMA M_n1100 was chosen since it was demonstrated[21] that its use can increase the mobility of the chains helping the ionic conductivity. The sample prepared are summarized in Table IV.C. 3.

Sample	Handsheet SW40 SR35 51 g/m^2	BEMA (%)	PEGMA 1100 (%)	GA (%)	EC:DEC (%)	Radical PI Darocure1173 (%)	Cationic PI (%)	Swelling (%)
D	no	25	25	5	45	+3	+2	36.1
D-cel	yes	25	25	5	45	+3	+2	42.5
GPE-sw-GA	yes	35	15	5	45	+3	+2	38.4

Table IV.C. 3 Compositions of the membranes prepared. The handsheets used were SW40 (SR35 51g/m^2). In the last column the swelling percentage is indicated.

2.2 Characterisation of the GPEs

The membranes presented in Table IV.C. 3. were firstly tested in terms of ionic conductivity, sample D was prepared with and without the cellulose reinforcement and was also compared to a further membrane named GPE-GA whose formulation is similar to the one of the reference used in previous chapters (*Chapter III*), only GA was added in order to enable the swelling procedure.

The Arrhenius plots obtained are presented in Figure IV.C. 5

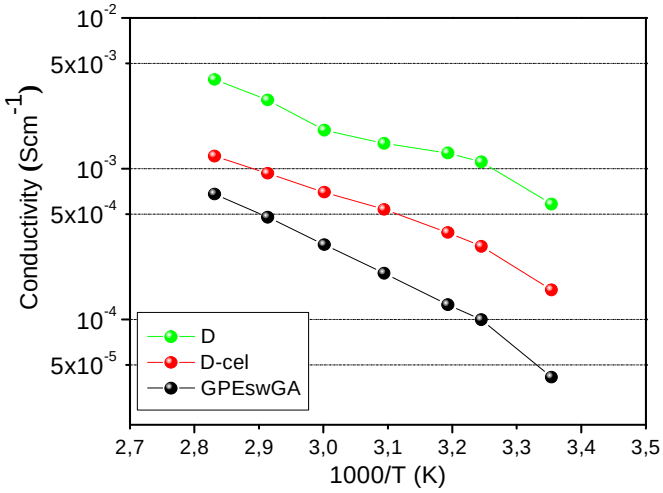

Figure IV.C. 5 Arrhenius plot for membranes D, D-cel and GPE-sw-GA

As already observed and as visible here from the comparison between sample D and sample D-cel the presence of the cellulose reinforcement causes a

decrease of the conductivity which goes from $6*10^{-4}$ to $1,5*10^{-4}$ at room temperature; the values obtained are however satisfacory. When sample D-cel is compared to sample GPE-sw-GA, which contains a lower quantity of monofunctional monomer, it is appreciable the influence of the amount of PEGMA1100 used. The conductivity of sample GPE-sw-GA is evidently lower ($4*10^{-5}$ at room temperature).
However, since PEGMA1100 is solid at ambient temperature and thus hardly workable, formulations containing higher quantities of monufunctional were hard to be prepared. The formulation of sample D-cel resulted to be the best compromise between conductivity and processability.

On the basis of the previous results D-cel was chosen as a membrane for further experiments.
The samples prepared are flexible and easy to handle. The reinforced GPE D-cel presented a Tg of about -60°C, the exact values are reported in Table IV.C.4 together with the thermal stability of the membrane.

Sample	Tg (°C)	T_5 (°C)	T_{10} (°C)	T_{50} (°C)	Residue (%)
D-cel	-58	69	109	375	8

Table IV.C. 4 Thermal properties of sample D-Cel reinforced with handsheets SW40 (SR35, 51g/m^2) compared with the same membrane after swelling in a 1Msolution of LiTFSI in EC:DEC.

The thermal stability of the membrane was accessed by TGA measurements; the Table IV.C.4 reports the values of T_5, T_{10} and T_{50}, which indicate the temperatures for 5%, 10% and 50% weight loss. Figure IV.C.6 shows the weight loss vs temperature plot for the reinforced membrane D-cel. The first big decomposition step is linked to the presence of the organic solvent that evaporates at relatively low temperatures. The presence of the lithium salt is noticed in the residual found over 450°C, temperature at which all the organic components of the membrane are completely degraded.

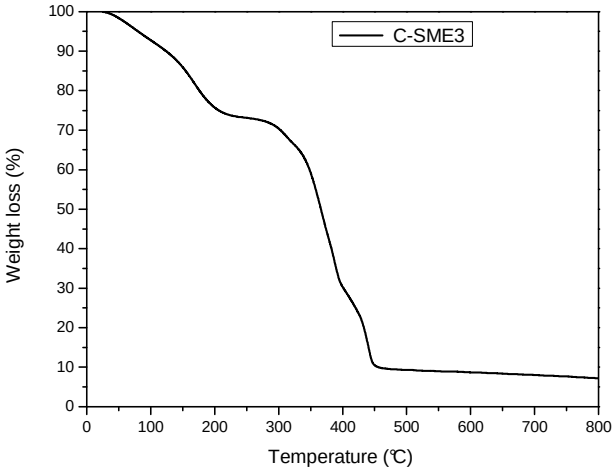

Figure IV.C. 6 TGA plot of sample D-cel reinforced with handsheet SW40 SR35, 51g/m^2

The mechanical behavior of the reinforced membrane was evaluated by means of tensile test. Young's modulus of the membrane D-Cel reinforced with an handsheet SW40, (SR35, 51g/m^2) resulted to be 370 MPa and the tensile resistance 15,6 MPa. These values are satisfactory for the desired application. To verify the handability of the membrane even after swelling a bending test has been performed, the swelled membrane have been rolled up on cylinders with different diameters, no cracks or damage was observed on the GPE even when rolled on the smallest cylinder available (diameter = 3 mm). Figure IV.C. 7 shows the bended membrane.

Figure IV.C. 7 Bending test on D-Cel swelled membrane

The observation of the bendability of the membrane is really satisfactory above all considering that the not reinforced membrane (sample D) prepared

by swelling resulted fragile, hardly handable, it broke when bent on a cilnder of 10mm of diameter.

As shown in the previous paragraph sample D-Cel presents a conductivity of 1.6 10^{-4}s/cm at room temperature and reaches values over 10^{-3} s/cm at 80 °C, these good values encourage the investigation of other electrochemical properties such as electrochemical stability, and cyclability.

The first tests regarding the electrochemical stability were carried out at room temperature. The current–voltage curves, reported in Figure IV.C.8, were obtained for a working acetylene black electrode swept in a cell using the gel electrolyte membranes and a Li metal counter electrode for the anodic scan and for a copper electrode together with the GPE and the Li metal electrode for the cathodic scan.

In the anodic part, the onset of the current which is representative of the decomposition of the electrolyte indicates an anodic breakdown voltage. For this test it can be considered at approx. 4.5 V versus Li. The first scan presents only a small peak at the voltage of 4,2V that in the subsequent scans results in a small increase of the residual current. This behaviour could be occasional and it could be due to the small presence of impurities either in the handsheet used or in the monomers, or it could be due to a side reaction linked to the liquid electrolyte or to one of the components of the membrane. Nevertheless the peak at 4,2 V is small and the main current increase is visible at about 4,5 V vs Li. Furthermore at voltages lower than 4,2 V the anodic scan showed very low residual current, confirming the fact that the membrane can be safely used in its usual working limits.

The cathodic scan presents a low current in all the scan range, a reversible peak at about 0,7 V and clear lithium plating and stripping peaks indicating the correct working of the membrane that allows a reversible passage of lithium ions and their deposition on the electrode.

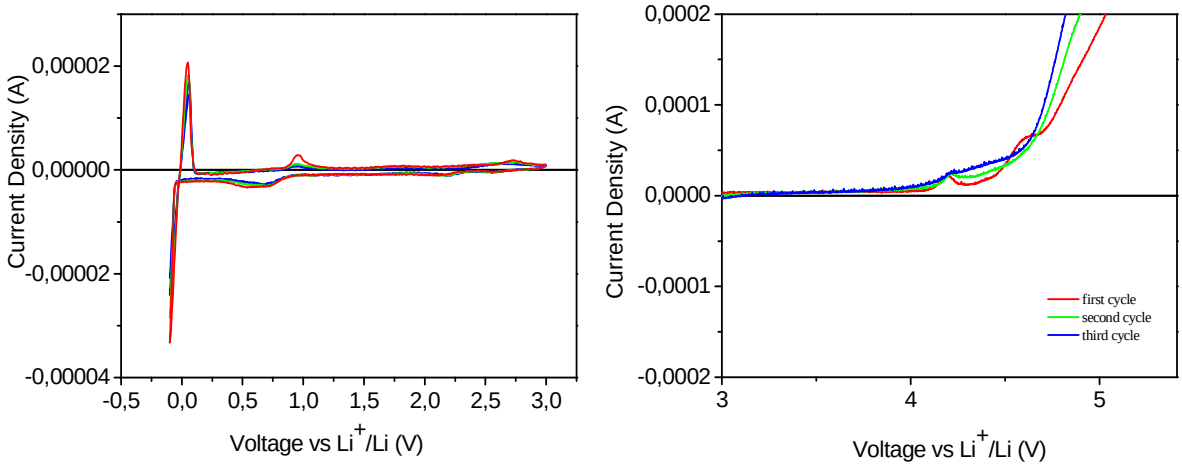

Figure IV.C. 8 Electrochemical stability window (ESW) of GPE at 25 °C; potential scan rate of 0.100 mV s^{-1}.

Finally, the D-Cel reinforced polymer electrolyte membrane was assembled in a complete lithium polymer cell laboratory prototype, and its electrochemical behavior was investigated by means of galvanostatic charge/discharge cycling.

The response of the prototype, assembled by combining a lithium metal anode with a $LiFePO_4$/C composite cathode and the D-Cel as separator, is reported in Figure IV.C. 9 which shows the specific capacity of the cell as a function of the cycle number at room temperature and at different C-rates ranging from C/20 to 1C.

The cell delivers a specific discharge capacity higher than 110 mAh g–1 during the initial cycles, when using a low current density of C/20. As the current density increases, the specific discharge capacity decreases only slightly. Actually, at a high discharge rate of 1C, the cell is able to deliver a discharge capacity of about 90 mAh g^{-1}. Good performance at high current rate may be ascribed to the efficient ionic conduction in the polymer separator and the favorable interfacial charge transport between electrodes and electrolyte in the cell.

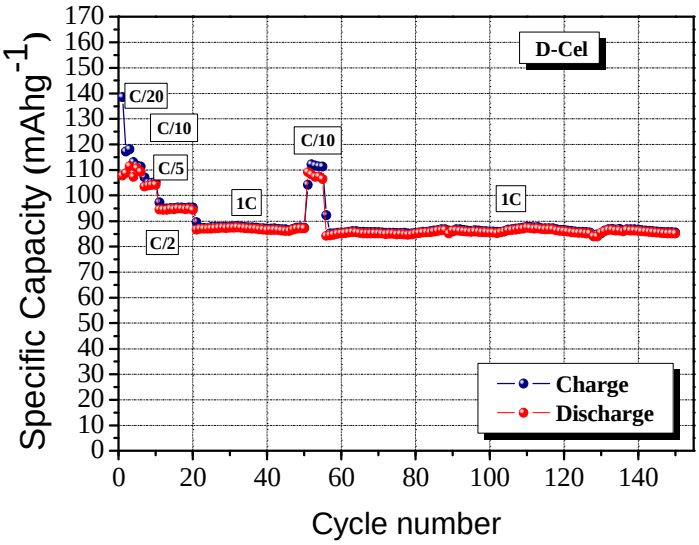

Figure IV.C. 9 Room temperature galvanostatic charge-discharge cycling test of the lithium polymer cell, assembled by sandwiching the GPE between a LiFePO4/C cathode and a Li metal anode, at different C-rates (from C/20 to 5C)

The coulombic efficiency is quite low during the initial cycles; then, after few cycles it is 95 % and it is maintained to ~ 99 % after the 10th cycle, at C-rates higher than C/10. An increase of coulombic efficiency can be associated with an improved interfacial property during charge-discharge cycles of the cell. The extraction and insertion of lithium ions into the structure of $LiFePO_4$ is reversible on repeated cycling; the capacity is highly stable even after long time cycling and, moreover, reducing the C-rate it is completely restored the (see, in Figure IV.C.9, the restoring of the specific capacity values from 1C to C/10 after the 50th cycle).

2.3 Study on the grafting of GA

Glycidyl Acrylate was used with the primary intention of bonding the polymer matrix to the cellulose reinforcement. The practical proof of its efficiency was given by the swelling test.

Accordingly to literature the GA (or GMA) monomer[15-18, 22] is usually used to modify polymeric surfaces by a radical mechanism. Free radical initiators are used to graft the acrylic group onto the surface leaving the pendant glycidyl group for effecting a polymerization in the presence of other oligomers in a subsequent step.

2.3.1 Reactivity of GA

At first a study on the reactivity of Glycidyl Acrylate was developed. An investigation of the kinetic of the reaction of the acrylic and the epoxy groups of GA was done by FT-IR spectroscopy in real time and the influence of the radical and the cationic photoinitiator was evaluated. The instrument used collected the IR spectra while the sample was irradiated by UV light, the kinetic of the conversions was determined by following the decrease of the band attributable to the double bond of the acrylate groups at 1630 cm^{-1} and the one of the epoxy group at 760 cm^{-1}. The C=O bond at 1730 was used as an internal standard. The conversion of the reactive functions is calculated as follows:

$$\eta\% = 1 - \frac{(A_{\text{reactive f, t}} / A_{\text{ref,t}})}{(A_{\text{reactive f, 0}} / A_{\text{ref,0}})} * 100$$

Where $A_{\text{reactive f.t}}$ represent the peak areas under the reactive functionality bands at the at time t, $A_{\text{reactive f.0}}$ is the area at the beginning of the reaction and A_{ref} represents the area under the band of the internal reference at a time = t and at the beginning of the reaction (this area should be unvaried).

In Figure IV.C.10 the rate of reaction and the conversion of GA to polymer with different kinds of photoinitiators is reported.

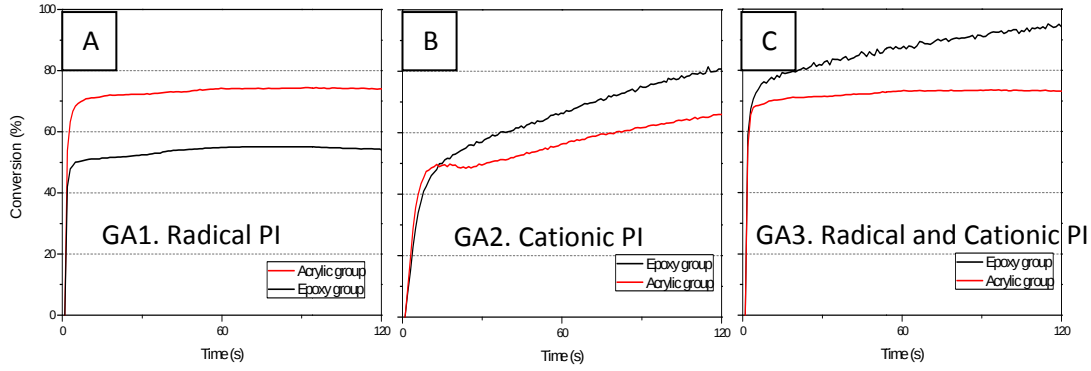

Figure IV.C. 10 Kinetic plots of the conversion of the acrylic and epoxy groups in GA in 3 different samples: GA1 GA + Darocure 1173 (97:3); GA2- GA + Cationic PI (97:3) in the middle; GA3- GA + Darocure 1173 + Cationic PI (95:3:2) on the right.

Figure IV.C.10. A refers to the conversion of the double bond of the acrylate and to the ring opening reaction of the epoxy group of GA in the presence of

the radical PI. It is possible to observe that both functionalities react. The acrylic double bond polymerization is initiated by the radicals formed by the photodissociation of the PI and by explition the exotermicity of the radical double bonds addition, the conversion of the epoxy group is activated by a thermal process. Both processes are fast and reach their maximum in a few second, nevertheless the conversion of the groups is not complete reaching the 70 % for the acrylic group and the 50% for the epoxy one.

By using only the cationic photoinitiator it is possible to see (Figure IV.C.10. B) that both the epoxy and the acrylic group react. The epoxy ring polymerises by the presence of protons generated by the onium salt after photodissociation. In this reaction also radicals are genated and can initiate the polymerization of the acrylate functionality. However in Figure IV.C.10. C it is visible that the faster reaction and higher conversion is reached by using the two initiators together, as a matter of fact both the acrylic and the epoxy groups reach in a few seconds a conversion of about 70%. The percentage of conversion remains constant at 70% for the double bond even after 3 minutes of UV irradiation while for the epoxy ring it continues growing reaching the 98% after 3 minutes of irradiation.

This test further confirms that both the radical and the cationic PIs are necessary for the best reaction of the two GA functionalities.

2.3.2 UV-grafting of GA to cellulose

The grafting of cellulose by GA was studied by surface spectroscopies (FT-IR ATR and XPS analysis).

To mimic the process happening during the preparation of the GPE membranes, grafting experiments were conductied as follows:

- A 20 ml acetone solution was prepared containing the 5% of GA, (i.e. the quantity of GA present in the membrane formulation) and added of 2% of radical PI and 1% of cationic PI.
- The handsheet used was immersed in the mixture and irradiated 1,5 minutes each side.

- The sample, named GA5, was washed in acetone and dried till constant weight.

An untreated hansheet and a sample composed of pure GA UV irradiated for 3 minutes in the presence of the radical and the cationic PIs (named GA100) were used as references.

The three samples were left under vacuum condition at 80°C overnight.

The grafting was first monitored measuring the increase of weight of the handsheet treated with GA. The weight gain measured was about 5%. The grafting yeld can then be calculated:

Weight of GA /1g of paper (51gm^{-2}) = 0,05 g (weight gain 5%)

Moles of GA / 1g of paper = 0,39 mmol (BP Mw = 128 gmol^{-1})

FT-IR ATR analysis spectra were collected on sample GA 5 and compared to the spectra of paper, and of pure GA before polymerization. The spectra obtained are reported and compared to each other in Figure IV.C. 11 (unpolymerized Glycidyl Acrylate, top, neat paper, middle, paper impregnated by GA after polymerisation, bottom).

The main peaks present in the GA spectrum (top) are due to the acrylic group (1735, 1640 cm^{-1}) vibrations and to the asymmetric and symmetric epoxyde ring stretches (913- 844-760 cm^{-1})[23]. They correspond to wave numbers where paper does not show absorption bands (middle), the cellulose, due to its structure, presents several characteristics absorption bands which are: 1162, 1130, 1098, 900 cm^{-1} linked to the anti-symmetric out-of-plane ring stretch of amorphous cellulose; C-O stretching and 1500-1300 for the C-H bending.[24]

In the bottom spectrum concerning the grafted paper, it is possible to observe the disappearance of the peaks related to the epoxy ring at 913- 844-760 cm^{-1} and the simultaneous disappearance of the peak due to the double bond in the acrylic group (1640 cm^{-1}). This evidence confirms that the reaction of both groups has occurred, as expected from the FT-IR analysis previously shown. The presence of the peak at 1735 cm^{-1} that is linked to the ester group of GA also after irradiation confirms the effective presence of the monomer on the

paper surface. However homopolymerisation can occour and extraction of the homopolymer is difficult.

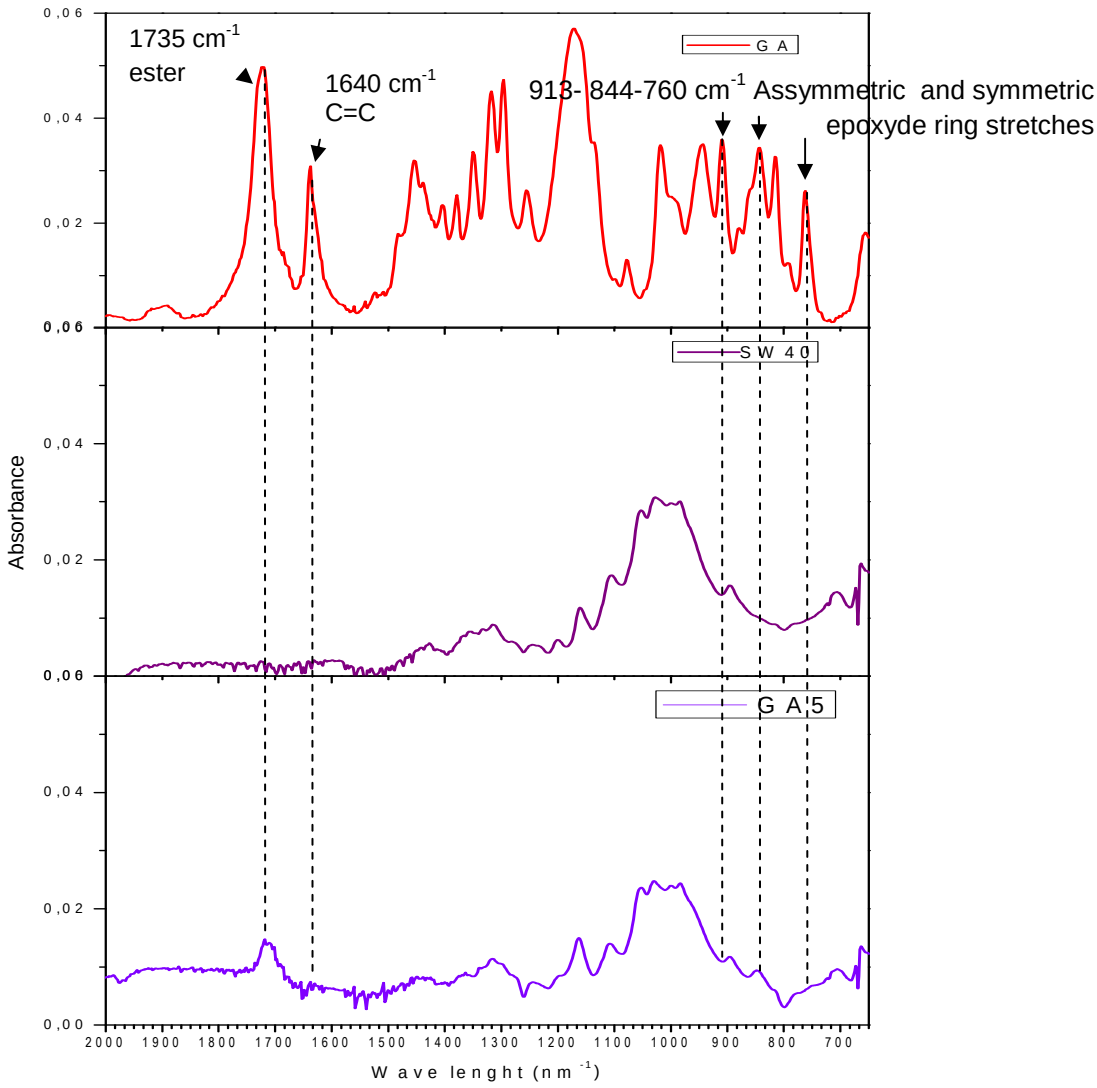

Figure IV.C. 11 FT-IR-ATR analysis performed on pure GA (higher plot); paper (middle plot); sample GA5 after 3 minute UV irradiatiation and washing in acetone (lower plot).

Further analysis for the evaluation of the GA grafting on cellulose has been an XPS investigation[23]. XPS has been performed on sample GA5 and the results obtained were compared to those obtained for unmodified paper and for pure GA after irradiation (GA100). Figure IV.C.12 compares the survey spectra obtained by scanning the binding energies between 0 and 1200 eV for

the tree samples. Oxygen (peak at 531 eV) and Carbon (peak at 285 eV) are the two species detected in all samples.

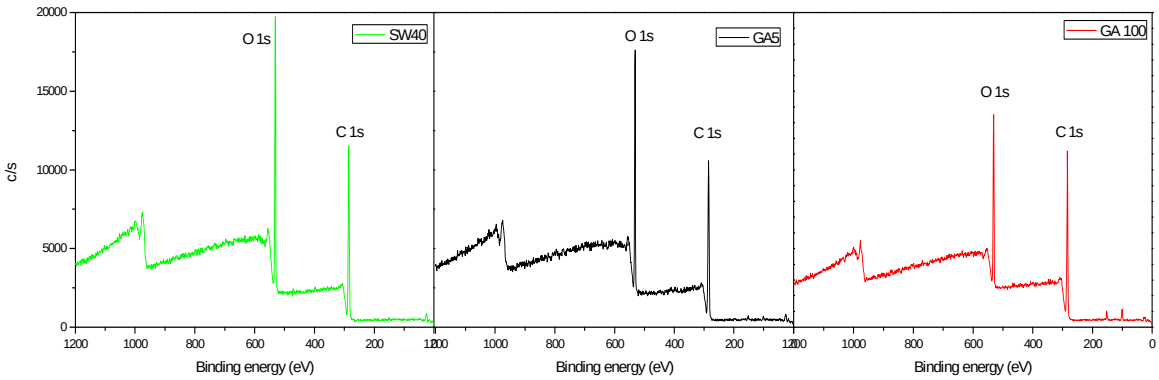

Figure IV.C. 12 XPS survey spectra obtained for sample SW40 (left), GA5 (middle) GA100 (right)

Table IV.C.5 reports the atomic concentration relative to the peaks O1s ans C1s and their ratio, together with the values calculated on the basis of the molecular formula. The structure of the glucose ring in cellulose was considered for sample SW40 while the structure of GA was considered for sample GA100.

Sample	C 1s	O 1s	O/Cmeasured	O/C calculated
SW40	63,5	36,5	0,57	0,83 (pure cellulose)
GA5	66,5	33,5	0,50	-
GA100	71,0	29,0	0,41	0,50

Table IV.C. 5 Carbon and Oxygen content in the three samples anlyzed by XPS. The O/C ratios measured and calculated on the basis of the chemical structure are reported

The relative intensity of the Oxygen signal and thus the measured O/C ratio decreases when GA is grafted to the paper. Comparing the experimental values with those calculated on the basis of the molecular formulae, one can observe that the O/C values obtained from the measurement are lower than expected. This is unusual as the outer surfaces of materials normally can be easily oxidised, nevertheless, considering sample SW40, which shows the major difference between the experimental and the calculated value, it must be considered that, being the handsheet a material of natural origin its

composition is variable, the O/C value in fact has been calculated by considering the structure of pure cellulose, nevertheless it is know from literature[25-27] that lower values of this ratio can be attributed to the presence of lignin.

The core line spectra of Carbon were then analyzed. The binding energy of the carbon 1s depends on the number of bonds between the carbon and oxygen. Figure IV.C.13 shows the C1s peaks of the three samples at high resolution and gives an indication of the kind of bonds relative to each peak. Generally, in fact carbon signal can be resolved into four different peaks: C1 (283 eV), that originates from carbons bonded only to other carbon atoms or to hydrogen and the C2 (285 eV), C3 (286 eV) and C4 (287 eV) peaks that originate from carbon atoms with one, two (or one double) and three oxygen bonds, respectively[23].

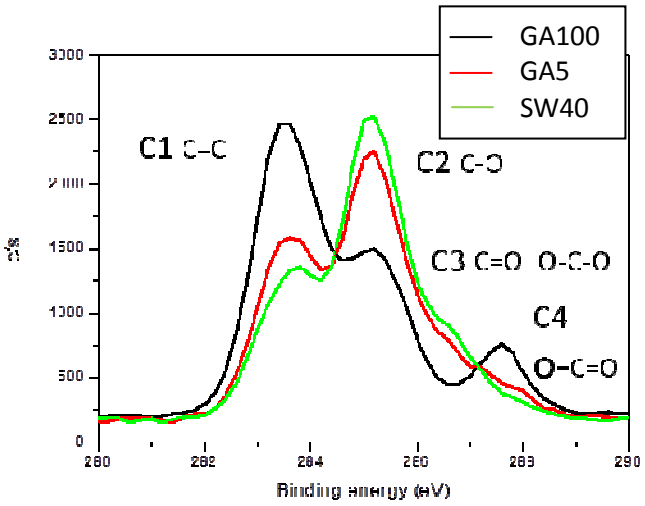

Figure IV.C. 13 Comparison of the C1s spectra of the different samples

Figure IV.C. 14 A, B, C shows the same spectra with the deconvolution of the C signal and the fitting related to each peak. The relative intensities measured from the area of the peaks observed for each sample are reported in Table IV.C.6.

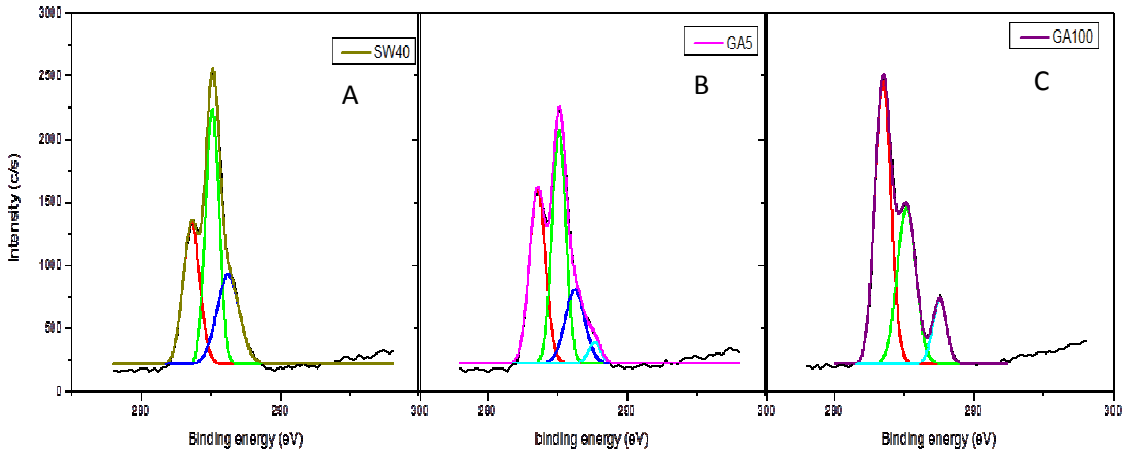

Figure IV.C. 14 A, B, C, High resolution XPS spectra of the C1s peaks of pure paper, sample GA5 and sample GA100. D

	SW40 Exper. (%)	GA5 Exper. (%)	GA100 Exper. (%)	Cellulose Calculated (%)	GA Calculated (%)	GA5 Calculated (%) (based on grafting yeld and exp data)
Peak - C1 283eV	30	36	54		33	31,4
Peak -C2 285eV	44	42	35	83	50	43,5
Peak -C3 286eV	26	19	---	17		24,4
Peak- C4 287eV	---	3	11	--	17	0,7

Table IV.C. 6 Relative areas of the C1, C2, C3 and C4 peaks

If we represent cellulose as made of glucose rings we can see that all the carbon atoms are linked both to other carbons and to oxygens; the bonds with oxygen are ether- ether bonds (-O-C-O-) or involve hydroxyl groups (-C-O-H). There are no ester bonds.

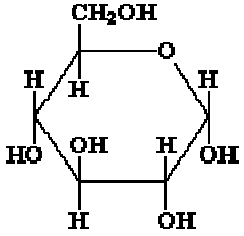

Figure IV.C. 15 Glucose ring molecular structure

Referring to the formula reported above and according to the values found in literature[25-27] for pure cellulose, one can establish the ratios among the signals as 83% for C-O bonds (C2) and 17% for the –C-O-C- bonds (C3). As shown in Figure IV.C.14 A, the sample SW40 (the untreated handsheet) shows C1, C2 and C3 peaks, while C4 is not detectable. Even if the C1 peak is not expected a trimodal C(1s) peak with a C1 component in addition to C2 and C3 contributions is universally observed. When pure cellulose is analyzed the presence of this peak is often associated with hydrocarbon contamination on the sample surface or radiation damage of the cellulose surface[27]. Alternatively, Hua et al.[28] also suggested that part of the C1 peak intensity arises from C–C–O contributions that have a smaller binding energy than the hydroxylic carbon.

In our case the presence of the C1 peak could also be attributed to the possible presence of ligning in the handsheet as already supposed from the analysis of the survey spectra.

In Figure IV.C.14 C, the spectrum obtained from sample GA100 (pure glycidyl acrylate) shows C1, C3 and C4 peaks, while this time C3 is not detectable. Also for GA the peaks can be correlated to its molecular structure.

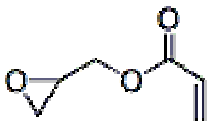

Figure IV.C. 16 Glycidyl acrylate molecular structure

Firstly it is visible that GA presents an ester bond (O-C=O) while no ether-ether bonds and hydroxyl groups are present. Two carbon atoms only linked to other carbon are also present (C-C bond). Referring to the formula reported above one can calculate the ratios among the signals as 33% for C-C bonds (C1), 50% for C-O bonds (C2) and 17% for the –O-C=O bonds (C4). Also in this case the relative intensity of the C1 peak experimentally obtained is higher than expected, the presence of contaminations can be supposed.

When GA is grafted onto the handsheet surface (Figure IV.C.14.B) an intermediate spectrum is obtained; in fact one can find signals corresponding

to C1, C2, C3 and C4. Considering the structure of GA, it is expected an increase of the C1 and C4 peaks while the relative intensity of the C2 and C3 peaks is expected to decrease when compared to the cellulose spectum. The experimental data confirms these trends.

By considering the grafting yield previously calculated (0,39mmol of GA/1g of cellulose, corresponding to 6 mol%) a prediction of the intensity of the peaks of sample GA5, based on a weighted mean of the values experimentally obtained for samples SW40 and GA100 was done. The results obtained are reported in the last column of Table IV.C.6. It is visible that the experimental data indicate the presence of a major quantity of GA being C1 and C4 peaks higher than expected. The difference can be due to the inhomogeneity of the grafting on the sample or to an error in the weight gain measurement due to the manual procedure.

Nevertheless the presence of the peak related to the ester group (C4 peak) in sample GA5 demonstrates the effective presence of the monomer on the paper surface, giving the indication of a probable grafting. However during sample preparation homopolymerisation can occur and the complete extraction of the homopolymer can be difficult.

2.3.3 Results discussion

When the system composed of cellulose, GA and the two PIs is studied it must be considered that many reactions take place at the same time. Firstly the simple irradiation of the cellulose substrate can create active sites (radicals) at the surface of the handsheet[22] that can attack the double bonds of the acrylic group of GA creating a "grafted radical" at the cellulose surface.

The radical initiator, upon irradiation, will create free radicals that can attack the double bonds of the acrylic part in GA promoting their reaction with other free GA molecules forming a homopolymer or with the "grafted radical" previously described, anchoring the GA molecule at the cellulose surface.

At the same time the cationic initiator, after irradiation, will create Brönsted acids and free radicals. The lasts will act as those generated by the other

initiator while the acid will act on the epoxy ring by promoting its opening; in this way the epoxy functionality will have the possibility to react by creating homopolymers or by attacking the OH groups of the cellulose surface, grafting the molecule on it by a chain transfer reaction described in Figure IV.C.17.

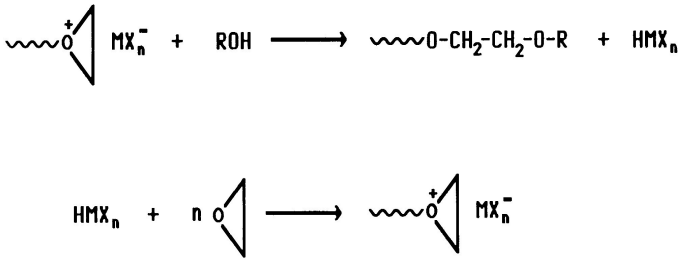

Figure IV.C. 17 Scheme of the chain transfer reaction

The homopolymer created during the preparation of the samples used for the evaluation of the grafting was eliminated during the washing step.

When the oligomers BEMA and PEGMA are added, the system becomes more complicated. The concurrent reactions of grafting and polymerization (not only the formation of homopolymer of the GA) will take place creating a complex network.

In conclusion, from the observations done and the results obtained, one can say that the use of both photoinitiators in the presence of GA helps the formation of a grafted copolymer. Considering the fact that, when GA and the cationic PI are not contemporary used, a good grafting can not be achieved, it is possible to deduce that the chain transfer reaction occurring only in the presence of the two mentioned components, must play the most important role in the grafting actuation.

VI.C.3 Conclusion

The aim of the study reported in this chapter was to develop new polymer membranes reinforced by handsheets having good electrochemical performances, good mechanical properties and suitable to be prepared by a process where the introduction of the electrolyte could be made by swelling.

In this section it has been demonstrated that by the addition of Glycidyl Acrylate to the reactive mixture the swelling process can be enabled. It has been demonstrated that both the reactive groups of GA can react in presence of the appropriate photoinitiators, a grafting reaction of the epoxy group via chain-transfer has been supposed. The reactivity of the monomers has been studied by FT-IR in real time measurements and the grafting has been evaluated by surface spectroscopies.

The polymer membranes prepared, thanks to the cellulose handsheet reinforcement, show high elastic modulus and tensile resistance maintaining high flexibility. Furthermore the mechanical properties are maintained also after swelling in the liquid electrolyte.

It has been shown that the swelling procedure allows to get satisfactory values of conductivity. The thorough analysis of the electrochemical behaviour highlighted a number of good results not only regarding performance, which is in any case appreciable, but also the capacity retention, cycling durability and coulombic efficiency.

Besides these, the system shows attractive features such as intrinsic safety, eco-compatibility, and low production cost and industrialization potentials, highly suitable in the field of Li-based thin flexible batteries.

References

(1) G. Meligrana, C. Gerbaldi, A, Tuel, S. Bodoardo, N. Penazzi, J.Power Sources (2006) 16 p.516.

(2) J. Nair, C. Gerbaldi, G. Meligrana, R .Bongiovanni, S .Bodoardo, N. Penazzi, P. Reale, V. Gentili. J Power Sources (2008) 178 p.751.

(3) C. Decker. Prog Polym Sci (1996) 21 p.593

(4) M. Stephan. European Polymer Journal (2006) 42 p.21

(5) Y. Aihara S. Arai, K. Hayamizu. Electrochimica Acta (2000),8-9 p. 1321

(6) A. Reiche, T. Steurich, B. Sandnix, P. Lobitz, G. Fleschier. Elecrtrochimica acta (1995) 4 0, 13-14 p.153

(7) E.H. Cha D.R. Macfarlane, M. Forsyth, C.W. Lee. Electrochimica Acta (2004), 50, 2–3, p.335

(8) K. Allmer, A. Hult, B. Ranby. J Polym Sci, Polym Chem (1988) 26 p.2099

(9) B. Ranby N.S Allen. M. Edge; J.R. Bellobono; E.Selli (Eds.); Current Trends in Polymer Photochemistry, Ch. 2, Ellis Horwood, New York, 1995

(10) A. Manuel Stephan, K.S. Nahm / Polymer 47 (2006) p.5952

(11) W. Wieczorek, J.R. Stevens, Z. Florjanczyk, Solid State Ionics (1996) 85 p. 76

(12) K. Hayamizu, Y. Aihara, S. Arai, and C. Garcia Martinez J. Phys. Chem. B, (1999), 103, 3, p. 519

(13) T.B. Stachowiak, F. Svec, J.M.J. Fréchet, Chem. Mater. (2006) 18 p.5950

(14) H. Ma, RH Davis, CN Bowman.(2000) 33,2 p.331

(15) K. Kato, E. Uchida, E.T. Kang, Y. Uyama, Y. Ikada;, Prog. Polym. Sci. (2003) 28 p.209

(16) H. Kubota, S. Ujita. Journal of Applied Polymer Science,(1995) 56, 1 p.25

(17) K. Allmer, A. Hult, B.Ranby. J Polym Sci, Polym Chem (1989) 27 p.1641

(18) K. Allmer, J. Hilborn, P.H. Larsson, A. Hult, B. Ranby. J Polym Sci, Polym Chem (1990) 28 p.173

(19) H. A. Krässig and V. Stannett. Advances in Polymer Science (1965), 4,1 p.111

(20) E. Andrzejewska. Prog.Pol. Science (2001) 26, p.605

(21) C. Gerbaldi, J. R. Nair, G. Meligrana, R.Bongiovanni, S. Bodoardo, N. Penazzi. J Appl Electrochem (2009) 39 p.2199

(22) A. Bhattacharya, B.N. Misra Prog. Polym. Sci. (2004) 29 p.767

(23) P. Stenstad, M.Andresen, B. Tanem, , P. Stenius. Cellulose (2008) 15 p.35

(24) P. Yu, H. Block, Z. Niu, K. Doiron. Journal of Synchrotron Radiation (2007)14 p.382

(25) L. Fras, L.-S. Johansson, P. Stenius, J. Laine, K. Stana-Kleinschek, V. Ribitsch. Colloids and Surfaces A: Physicochemical and Engineering Aspects (2005) 260, 1–3, p. 101

(26) J. Gustafsson, L. Ciovica, J.Peltonen. Polymer (2003), 44 p.661

(27) J. C. Bastidas, R. Venditti, J. Pawlak, R. Gilbert, S. Zauscher, J. F. Kadla. Carbohydrate Polymers (2005), 62 p.369

(28) Hua, Z. Q., Situaru, R., Dennes, F., & Young, A. Plasmas and Polymers(1997), 2, 3, p.199

Conclusions

The work presented aimed to develop innovative polymer-based UV cured electrolytes to be used in lithium batteries.
With the goal to prepare self standing electrolytes also for flexible devices the exploitation of cellulose as a reinforcing material and at the same time the exploitation of the papermaking and printing techniques was considered.

Two research lines were followed:

Development of composite membranes based on cellulose microfibrils (MFC) and a polymeric matrix obtained by photopolymerisation of reactive oligomers.

Development of multilayered membranes made of cellulose handsheet and polymeric layers obtained by photopolymerisation of reactive oligomers.

The first part of the work demonstrated the possibility to produce polymer-based electrolytes either in the form of gel polymer or solid polymer with mechanical properties extremely improved by the use of cellulose microfibrils.
The gel polymer electrolytes prepared presented conductivity values that were almost unvaried by the presence of the reinforcing agent, an excellent electrochemical behavior together with outstanding flexibility and handability.
The solid polymer electrolytes showed the possibility to avoid the use of liquid solvent at least when an high temperature application is envisaged and also in this case the use of MFC did not affect the performances of the electrolyte allowing a substantial increase in module and tensile resistance.

The second research line was divided in two parts; in the first one the feasibility of gel-polymer membranes reinforced by cellulose handsheets was shown, and the impact of paper was assessed. The production of these membranes was done by a fast method called "One Shot" implying the introduction of the lithium salt in the photopolymerisable mixture that was drown on the handsheet and UV irradiated. Such a process could be implemented at industrial scale, by using conventional technologies, known in papermaking. It was shown that the use of paper allowed to produce self-sanding and easy to handle electrolytes, with excellent mechanical properties, close to that of paper.

The major drawback of this approach resulted to be the reduction of the ionic conductivity of the final membrane.

Some strategies to counteract this negative effect were studied, and some solutions were provided i.e. the reduction of the grammage and refining degree, the choice of an appropriate fibers mixture (HW:SW 60:40) and use of additives such as alumina and calcium phosphate. Nevertheless, it was also shown that the most influencing component results to be the polymer.

In addition, the specific structure of such membranes (bi-layer) suggested to further investigate the adhesion between the polymer matrix and the cellulose fibres, and namely the grafting of the polymer on the cellulose fibres. Furthermore thinking to the real possibility to industrialize the production process the presence of the lithium salt, which requires inert ambient should be reduced as much as possible and this could be done by swelling a composite polymer-cellulose membrane by a liquid electrolyte in a dedicated step. Also for this reason the adhesion between cellulose and polymer had to be improved, different kind of UV grafting were then proposed in the last chapter.

Two of the three strategies tested proposed the use of benzophenone as anchoring agent; the studies developed demonstrated the occurrence of a grafting of the polymer to the cellulose substrate with an improvement of the stability of the layered structure of the electrolyte. Those kinds of grafting

however did not allow the use of the swelling process. One shot membranes were prepared and tested showing satisfying performances.
A third kind of grafting was at last proposed using Glycidyl Acrylate as grafting molecule, this time the swelling of the composite membrane was enabled resulting in a reinforced-swelled-gel polymer electrolyte presenting high flexibility and mechanical properties and excellent electrochemical performances both in terms of conductivity and behavior in a complete cell.

To conclude the general results obtained show for all the electrolytes presented attractive features such as good conductivity, adapt electrochemical stability and appreciable behavior in a laboratory scale cell in terms of cyclability, culombic efficiency and reversibility added to an extremely improved mechanical behavior with high flexibility and handability which enable their use for flexible devices. Furthermore other positive aspects of these reinforced electrolytes are the intrinsic safety, the eco-compatibility, and the low production cost and industrialization potentials.

Those studies can open the way for the development of an “all paper” device using cellulosic substrates and paper technologies.
Next future perspective can then be the assembly of a cellulose- based, thin, flexible, eco-designed, low cost and safe battery consisting in:

- A polymeric electrolyte with increased mechanical properties, good electrochemical behaviour
- cellulose based electrodes

both to be assembled with low cost and large scale processes by using roll to roll technologies as described in the following figure.

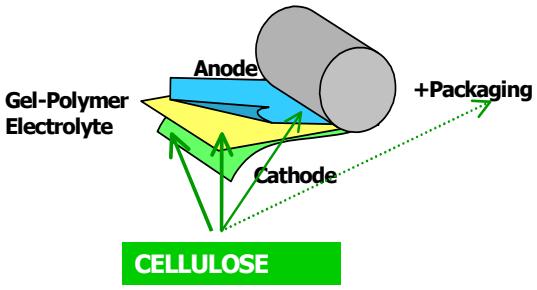

For a further future the possibility to develop a battery completely printed on a cellulose substrate and UV cured can also be envisaged.